

# STUDIES IN OPTIMAL DESIGN OF NONHOMOGENEOUS COLUMNS AND BEAMS

By

VINOD KUMAR GUPTA

✓  
Thesis  
624.1772  
G9595

TH  
AE/ 1976/D  
G9595



DEPARTMENT OF AERONAUTICAL ENGINEERING

INDIAN INSTITUTE OF TECHNOLOGY KANPUR

AUGUST, 1976

AE  
1976  
D  
GUP  
STU

# **STUDIES IN OPTIMAL DESIGN OF NONHOMOGENEOUS COLUMNS AND BEAMS**

**A Thesis Submitted  
in Partial Fulfilment of the Requirements  
for the Degree of  
DOCTOR OF PHILOSOPHY**

**By**  
**VINOD KUMAR GUPTA**

01201

**to the**  
**DEPARTMENT OF AERONAUTICAL ENGINEERING**  
**INDIAN INSTITUTE OF TECHNOLOGY KANPUR**  
**AUGUST, 1976**

AE-1976-D-SUP-

L. L. FANFUR  
**CENTRAL LIBRARY**

Acc. No. **A 50819.**

16 AUG 1977

Thesis  
G24.1772  
G9598

CERTIFICATE

This is to certify that the work STUDIES IN  
OPTIMAL DESIGN OF NONHOMOGENEOUS COLUMNS AND BEAMS has  
been carried out under my supervision and has not been  
submitted elsewhere for a degree.

*P.N. Murthy*  
(P.N. MURTHY)

Professor and Head  
Deptt. of Aeronautical Engineering  
Indian Institute of Technology  
Kanpur, India

**POST GRADUATE OFFICE**

This thesis has been approved  
for the award of the Degree of  
Doctor of Philosophy (Ph.D.)  
in accordance with the  
regulations of the Indian  
Institute of Technology Kanpur

Dated: 27/2/77 *Pz*

### ACKNOWLEDGEMENTS

The author considers it a privilege and a pleasant duty to express his deep sense of gratitude to Prof. P.N.Murti for providing inspiring guidance, critical comments and constant encouragement throughout this investigation.

Author takes this opportunity to acknowledge his gratitude to Prof. E.F. Masur, University of Illinois, for his invaluable comments, especially, on the solution of column-problems. The author is also thankful to Dr. N.G.R. Iyengar for many useful discussions.

The author is thankful to many friends and colleagues who helped directly or indirectly during the course of investigation and the preparation of manuscript. Thanks are also due to Mr. R.N. Srivastava for his excellent typing.

Last but most important of all, the author is highly thankful to his wife and young kids, though they know it not, for so arranging their lives to make this investigation possible.

# TABLE OF CONTENTS

	Page
LIST OF TABLES	vii
LIST OF FIGURES	ix
SYMBOLS AND ABBREVIATIONS	xii
SYNOPSIS	xv
CHAPTER 1 INTRODUCTION	1
1.1 Brief Review of Optimal Tapered Columns	1
1.2 Brief Review of Optimal Tapered Beams	6
1.3 Object and Scope of Present Work	8
CHAPTER 2 GENERAL PROBLEM OF OPTIMIZATION AND ITS FORMULATION	13
2.1 Statement of the General Problem	13
2.2 A Multiplier Rule	16
2.3 Necessary Conditions for the Bolza Problem	17
2.4 Necessary Conditions for Fixed End Points	20
CHAPTER 3 UNIFORM-NONHOMOGENEOUS COLUMNS	22
3.1 Introduction	22
3.2 Formulation of Buckling Problem	23
3.2.1 Derivation of boundary conditions	26
3.3 Modulus Constraint	29
3.4 Statement of the Problem	32
3.5 Different Approaches for Formulation	34
3.6 Necessary Conditions	37
3.7 Boundary Conditions on Multipliers	39
3.7.1 Hinged-Hinged	39
3.7.2 Clamped-Clamped	40
3.7.3 Clamped-Hinged	41
3.8 Optimality Condition and Governing Equation	42
3.9 Analytical Solutions	46
3.9.1 Hinged-Hinged column	47
3.9.2 Free-Clamped column	49
3.9.3 Clamped-Clamped column	50
3.9.4 Clamped-Hinged Column	53

CHAPTER 4	NUMERICAL SOLUTIONS FOR UNIFORM COLUMNS ( $p \neq 1$ )	57
4.1	Introduction	57
4.2	Singular Behaviour	58
4.2.1	Contribution ( $\Delta$ ) due to peak	59
4.3	Hinged-Hinged Column	61
4.4	Free-Clamped Column	64
4.5	Clamped-Clamped Column	65
4.5.1	Partial Integration	65
4.5.1.1	Newton-Raphson for $x_0$ determination	71
4.5.1.2	Incremental steps	71
4.5.1.3	Comments on the method of partial integration	72
4.5.2	Runge-Kutta method	73
4.5.2.1	Comments on the method	76
4.5.3	Method of successive iterations	76
4.5.3.1	Comments on the method	80
4.6	Clamped-Hinged Column	81
CHAPTER 5	TAPERED-NONHOMOGENEOUS COLUMNS	88
5.1	Introduction	88
5.2	Statement of the Problem	89
5.3	Necessary Conditions and the Governing Equation	90
5.4	Analytical Solutions	96
5.4.1	Hinged-Hinged column	100
5.4.2	Free-Clamped column	103
5.4.3	Clamped-Clamped column	103
5.4.4	Clamped-Hinged column	107
5.5	Numerical Solution	111
5.6	Interpretation of $e$ and $\eta$ Distributions	113
5.7	Results and Discussion	116
5.7.1	Tables	117
5.7.2	Curves	118
5.7.3	Important observations	119
5.8	Comments on Efficiency of Method of Successive Iterations	125
CHAPTER 6	UNIFORM-NONHOMOGENEOUS BEAMS	165
6.1	Introduction	165
6.2	Equation of Equilibrium for Transverse Vibrations of a Tapered-Nonhomogeneous Beam	167

		Page
6.2.1	Boundary conditions	168
6.2.2	Equilibrium equation and boundary conditions for uniform beam	169
6.3	Statement of the Problem of Optimization	170
6.4	Necessary Conditions and the Governing Equations	171
6.5	Solution for $p = 1$	177
6.5.1	Hinged-Hinged beam	179
6.5.2	Free-Clamped beam	181
6.5.3	Clamped-Clamped beam	182
6.5.4	Clamped-Hinged beam	184
6.6	Solution for $p \neq 1$	187
6.6.1	Singular behaviour	188
6.6.2	Hinged-Hinged beam	191
6.6.3	Free-Clamped beam	195
6.6.4	Clamped-Clamped beam	196
6.6.5	Clamped-Hinged beam	203
6.7	Comments on the Method of Successive Iterations	206
6.8	Results and Discussion	209
CHAPTER 7	TAPERED-NONHOMOGENEOUS BEAMS	221
7.1	Introduction	221
7.2	Statement of the Problem	222
7.3	Necessary Conditions and Governing Equations	223
7.4	Singular Behaviour	231
7.5	Hinged-Hinged Beam	238
7.5.1	Comments on Numerical Computations	239
7.5.2	Results, Discussion and Comments	243
7.6	Free-Clamped Beam	248
7.6.1	Comments and discussion	257
CHAPTER 8	APPROXIMATE SOLUTIONS	280
8.1	Introduction	280
8.2	Approximating Polynomials and Corresponding Results	280
8.3	Comments and Discussion	284
CHAPTER 9	CONCLUSIONS AND RECOMMENDATIONS	287
9.1	Conclusions	287
9.2	Recommendations for Further Study	292
	REFERENCES	293

LIST OF TABLES

<u>Table</u>		<u>Page</u>
5.1	Variation of $\lambda$ and percent increase in buckling load with $p$ for hinged-hinged and free-clamped columns	126
5.2	Variation of $\lambda$ and percent increase in buckling load with $p$ for clamped-clamped columns	126
5.3	Variation of $\lambda$ and percent increase in buckling load with $p$ for clamped-hinged columns	127
5.4	Inflexion point location $x_0$ for different values of $p$ for clamped-hinged columns	127
5.5	Variation of $e$ along the axis for hinged-hinged and free-clamped uniform columns	128
5.6	Variation of $e$ along the axis for clamped-clamped uniform columns	128
5.7	Variation of $e$ along the axis for clamped-hinged uniform columns	129
5.8	Variation of $e$ along the axis for hinged-hinged and free-clamped tapered columns	129
5.9	Variation of $\eta$ along the axis for hinged-hinged and free-clamped tapered columns	131
5.10	Variation of $e$ along the axis for clamped-clamped tapered columns	132
5.11	Variation of $\eta$ along the axis for clamped-clamped tapered columns	134
5.12	Variation of $e$ along the axis for clamped-hinged tapered columns	135
5.13	Variation of $\eta$ along the axis for clamped-hinged tapered columns	137

6.1	Variation of frequency $\omega$ , percent increase in $\omega$ , and inflexion point location $x_0$ with $p$	213
6.2	Variation of $e$ along the axis for hinged-hinged uniform beams	214
6.3	Variation of $e$ along the axis for free-clamped uniform beams	214
6.4	Variation of $e$ along the axis for clamped-clamped uniform beams	215
6.5	Variation of $e$ along the axis for clamped-hinged uniform beams	215
7.1	Variation of frequency $\omega$ , percent increase in $\omega$ , $\eta_{\max}$ , and location $x^*$ of $\eta_{\max}$ with $p$ for hinged-hinged tapered beams	259
7.2	Variation of $e$ , $\eta$ , and $s$ along the axis for hinged-hinged tapered beams with $q = 1$	260
7.3	Variation of $e$ , $\eta$ , and $s$ along the axis for hinged-hinged tapered beams with $q = 2$	262
7.4	Variation of $e$ , $\eta$ , and $s$ along the axis for hinged-hinged tapered beams with $q = 3$	264
7.5	Variation of frequency $\omega$ and percent increase in $\omega$ with $p$ for free-clamped tapered beams	266
7.6	Variation of $e$ and $\eta$ along the axis for free-clamped tapered beams with $q = 2$	267
7.7	Variation of $e$ and $\eta$ along the axis for free-clamped tapered beams with $q = 3$	268
8.1	Percent increase in $\lambda$ and the associated $e_0$ for $x_0 = 0$ , for hinged-hinged columns with $p = 1$	285
8.2	Variation of percent increase in $\lambda$ with $x_0$ for $e_0 = 0.5$ , for hinged-hinged columns with $q = 1$	285

LIST OF FIGURES

<u>Fig.</u>		Page
3.1	Columns considered in the thesis	139
4.1	Singular behaviour for H-H, C-C and C-H end conditions	140
5.1a	Variation of percent increase in buckling load with $p$ for hinged-hinged, free-clamped and clamped-clamped columns	141
5.1b	Variation of percent increase in buckling load with $p$ for clamped-hinged columns	142
5.2	Variation of $e$ along the axis for hinged-hinged uniform columns ( $q = 0$ )	143
5.3	Variation of $e$ along the axis for clamped-clamped uniform columns ( $q = 0$ )	144
5.4	Variation of $e$ along the axis for clamped-hinged uniform columns ( $q = 0$ )	145
5.5a	Variation of $e$ along the axis for hinged-hinged tapered columns with $q = 1$	146
5.5b	Variation of $e$ along the axis for hinged-hinged tapered columns with $q = 2$	147
5.5c	Variation of $e$ along the axis for hinged-hinged tapered columns with $q = 3$	148
5.6a	Variation of $\eta$ along the axis for hinged-hinged tapered columns with $q = 1$	149
5.6b	Variation of $\eta$ along the axis for hinged-hinged tapered columns with $q = 2$	150
5.6c	Variation of $\eta$ along the axis for hinged-hinged tapered columns with $q = 3$	151
5.7a	Variation of $e$ along the axis for clamped-clamped tapered columns with $q = 1$	152

5.7b	Variation of $e$ along the axis for clamped-clamped tapered columns with $q = 2$	153
5.7c	Variation of $e$ along the axis for clamped-clamped tapered columns with $q = 3$	154
5.8a	Variation of $\eta$ along the axis for clamped-clamped tapered columns with $q = 1$	155
5.8b	Variation of $\eta$ along the axis for clamped-clamped tapered columns with $q = 2$	156
5.8c	Variation of $\eta$ along the axis for clamped-clamped tapered columns with $q = 3$	157
5.9a	Variation of $e$ along the axis for clamped-hinged tapered columns with $q = 1$	158
5.9b	Variation of $e$ along the axis for clamped-hinged tapered columns with $q = 2$	159
5.9c	Variation of $e$ along the axis for clamped-hinged tapered columns with $q = 3$	160
5.10a	Variation of $\eta$ along the axis for clamped-hinged tapered columns with $q = 1$	161
5.10b	Variation of $\eta$ along the axis for clamped-hinged tapered columns with $q = 2$	162
5.10c	Variation of $\eta$ along the axis for clamped-hinged tapered columns with $q = 3$	163
5.11	Variation of number of iterations ( $n$ ) with $p$	164
6.1	Variation of percent increase in frequency with $p$ for uniform beams	216
6.2	Variation of $e$ along the axis for hinged-hinged uniform beams	217
6.3	Variation of $e$ along the axis for free-clamped uniform beams	218
6.4	Variation of $e$ along the axis for clamped-clamped uniform beams	219

6.5	Variation of $e$ along the axis for clamped-hinged uniform beams	220
7.1	Variation of percent increase in frequency with $p$ for hinged-hinged tapered beams	269
7.2a	Variation of $e$ along the axis for hinged-hinged tapered beams with $q = 1$	270
7.2b	Variation of $e$ along the axis for hinged-hinged tapered beams with $q = 2$	271
7.2c	Variation of $e$ along the axis for hinged-hinged tapered beams with $q = 3$	272
7.3a	Variation of $\eta$ along the axis for hinged-hinged tapered beams with $q = 1$	273
7.3b	Variation of $\eta$ along the axis for hinged-hinged tapered beams with $q = 2$	274
7.3c	Variation of $\eta$ along the axis for hinged-hinged tapered beams with $q = 3$	275
7.4	Variation of percent increase in frequency with $p$ for free-clamped tapered beams	276
7.5a	Variation of $e$ and $\eta$ along the axis for free-clamped tapered beams with $q = 2$	277
7.5b	Variation of $e$ and $\eta$ along the axis for free-clamped tapered beams with $q = 3$	278
7.6	Variation of number of iterations ( $n$ ) with $p$ for hinged-hinged beams	279
8.1	Approximate curves for the variation of $e$ along the axis	286

# SYMBOLS AND ABBREVIATIONS

$A$	area of cross-section
$a$	dimensionless area of cross-section
$E$	modulus
$E_0$	reference modulus
$\tilde{E}$	dimensionless modulus, $E/E_0$
$e$	dimensionless modulus, $\tilde{E}/\rho^q$
$G$	function as defined by equation (2.3.9)
$H$	function as defined by equation (2.3.10)
$g_i$	boundary conditions
$I$	second moment of area
$J$	functional
$\bar{J}$	augmented functional
$K$	constant used in various equations
$L$	length
$m$	mass
$m_0$	reference mass
$\bar{m}$	dimensionless mass, $m/m_0$
$p$	positive constant
$P$	critical load
$q$	positive integer constant
$s$	dimensionless stiffness, $e\eta^q$
$u$	dimensionless deflection for beams

$w$	deflection
$x$	dimensionless length
$x_0$	location of inflexion point
$y$	dimensionless deflection for columns
$\alpha$	proportionality factor, characteristic of cross-section
$\lambda$	dimensionless eigen value
$\lambda_E$	dimensionless critical load for Euler column
$\lambda_0$	constant multiplier
$\lambda_i$	variable multiplier
$\gamma_i$	constant multiplier
$\rho$	density
$\rho_0$	reference density
$\tilde{\rho}$	dimensionless density, $\rho/\rho_0$
$\eta$	dimensionless mass per unit length, $\tilde{\rho} a$
$\emptyset$	dimensionless bending moment, $e\eta^q y''$
$\beta$	dimensionless bending moment for column defined in various equations
$\omega$	frequency
$\omega_0$	dimensionless frequency
$E$	dimensionless frequency for Euler beam
$\epsilon$	small positive parameter

## Subscripts:

$E$	Euler
$\max$	maximum
$\min$	minimum

$\xi$	first derivative with respect to $\xi$
$\xi\xi$	second derivative with respect to $\xi$
0	refers to reference column or beam
1	region 1
2	region 2

## Superscripts:

T	transpose of a matrix
'	first derivative with respect to x
"	second derivative with respect to x
'''	third derivative with respect to x
iv	fourth derivative with respect to x

## Abbreviations:

B.C.	boundary conditions
B.C.'s	boundary conditions
H-H	hinged-hinged
F-C	free-clamped
C-C	clamped-clamped
C-H	clamped-hinged
Eqn.	equation
Eqns.	equations
L.H.S.	left hand side
Ref.	reference
R.H.S.	right hand side
w.r.t.	with respect to

## SYNOPSIS

Problems of optimal design of simple elements such as columns and beams have received considerable attention in recent years. Usually length, cross-sectional shape and material are preselected and area is allowed to vary along the length for a given weight of the element. The optimized eigen value is either the buckling load or the natural frequency. Tadjbaksh and Keller have considered the problem of strongest columns while Niordson and his group have studied the stiffest beams also.

Two basic approaches are used in the above studies. In one case the problem is formulated as a classical Bolza problem. The resulting Euler equations yield the optimality criterion. In the other using a perturbation parameter ( $\epsilon$ ), a direct variational approach is used to make the eigen value, written as Rayleigh's quotient, stationary. The equilibrium equation is then solved along with the derived optimality condition.

These studies have established that considerable increases in the eigen values can be achieved by an optimal distribution of stiffness. In this thesis, these studies are extended to examine whether further gains are possible by allowing the material to be nonhomogeneous. This essentially

means variation of stiffness with both modulus and area changing independently. Normally variation of  $E$  can also mean variation of density  $\rho$ . While this is generally true, no explicit relationship between the two is now available in the literature. Even so, with the advent of composite materials and the development of high specific modulus fibers, one can conceive of situations where modulus can vary without any change in density. Thus in the problems studied here, only area and modulus appear as the design variables. The results, however, for a tapered-nonhomogeneous element can be applied in the presence of density variation also by replacing the design variables by their suitable combinations.

To consider a variety of cross-sectional geometries, nondimensional second area moment is considered proportional to  $\eta^q$  where  $\eta$  refers to nondimensional area and  $q$  is an integer. Most of the sections of interest can be described by  $q$  varying from 1 to 3. Modulus variation has been considered in the following form

$$\bar{e} = \int_0^1 e^p dx ; \quad p > 0$$

where  $e$  is a nondimensional modulus when  $\rho$  is constant and is equal to  $\tilde{E}/\tilde{\rho}^q$  if  $\rho$  is a variable. Here  $\tilde{E}$  and  $\tilde{\rho}$  are nondimensional modulus and density respectively. Nondimensionalization is done in such a way that  $\bar{e} = 1$  for a homogeneous-uniform element.

As stated earlier, the problem has been formulated as a Bolza problem in the language of optimal control theory. The necessary conditions for optimality are therefore similar to the statement of Pontryagin's maximum principle. Fortunately adjoint equations in the multipliers can be solved independently in terms of the state variables, thereby yielding simple optimality equations. Using some simple transformations and the optimality conditions, a second order nonlinear equation for a column and fourth order nonlinear equation for a beam are obtained. The equations are numerically integrated. Due to non-imposition of any constraint on the minimum and maximum values of the area and modulus, difficulties in numerical integration, caused by singular behaviour of the function, have been encountered. It was found that an accurate knowledge of the behaviour of the function in the neighbourhood of a singularity is essential for any convergence to right results.

Uniform and tapered ( $q = 1, 2, 3$ ) columns are investigated for various values of  $p$  and for the boundary conditions - hinged-hinged (H-H), free-clamped (F-C), clamped-clamped (C-C), and clamped-hinged (C-H). Analytical solutions are obtained for  $p = 1$ . For  $p \neq 1$ , numerical integration is attempted using three different approaches - successive iterations, Runge Kutta, and the one employing successive iterations after the governing equation is integrated once

analytically. It is found that only the method of successive iterations is successful in determining the solutions in all the cases. The region of integration is divided into hundred or more divisions and integration is done by trapezoidal rule. Solutions for C-C and C-H boundary conditions offer considerable numerical difficulties because of the appearance of singularities at the points of contraflexure. Location of these points is also to be determined from the solutions.

It is interesting to note from the results that the curve of percentage increase in buckling load over the corresponding Euler column versus  $p$  is monotonic, load increasing with decreasing  $p$ . Virtually it appears that for both the uniform and tapered columns, any increase in load can be achieved provided the corresponding modulus variations, which become impractical for very high loads, can be achieved. It is found that for  $e_{\max} = 2.133$ , 63.57 percent increase in load can be achieved for a H-H tapered column of geometrically similar cross-sections ( $q = 2$ ), whereas the corresponding increase for the homogeneous column is 33.3 percent.

Both the uniform and tapered beams have been investigated for various values of  $p$ . Uniform beam problem has been solved for four boundary conditions - H-H, F-C, C-C and C-H. Analytical solutions are obtained for  $p = 1$ . Results indicate that **practically** any increase in frequency

can be achieved by modulus variation alone. The required modulus variations seem to become impractical for very high increases. However, within feasible variations of modulus, substantial increase in frequency over a uniform homogeneous beam is achieved. For a H-H beam it is 19.41 percent with  $e_{\max} = 2.09$ , whereas the increase for the corresponding tapered-homogeneous beam is 6.6 percent.

The solutions for the tapered beams have been obtained for H-H and F-C cases only. For a H-H beam, the solution is obtained for  $q = 1, 2, 3$  and  $p > 0$ . Theoretically, any increase in frequency can be obtained by selecting  $p$  to be small and using corresponding modulus and area distributions. However, area distributions become impractical for small values of  $p$ . Still, it is found that for feasible values of  $p$  a substantial increase in frequency is obtained. Investigation of singular behaviour indicates that the singularity occurs only in curvature.

Nature of the singularity for free-clamped beam is quite different from the H-H beam. Deflection, slope, and curvature simultaneously are singular at the free-end. Singularity is very strong and is controlled by the value of  $q$  only. It does not depend on  $p$ . The solution is obtained for  $q = 2$  and  $3$ . For  $q = 1$ , necessary conditions do not seem to have any meaningful solution. It is further concluded that the effect of modulus variation is not significant as the

increase in frequency through area variation alone is very high, e.g., 5.78 times the frequency of uniform-homogeneous beam as obtained by Niordson.

Since there is no constraint on minimum area and modulus, optimal solutions contain points of zero modulus and area. This is physically unrealistic. Besides, exact physical reproduction of the numerical curves for modulus and area distributions is difficult in practice. So an attempt is made to investigate the sensitivity of eigen value to small changes in these distributions. These have been approximated by simple polynomials with some minimum value of area and modulus. Using these, the eigen value is determined. It is shown through the example of H-H columns with  $p = 1$ , that the critical load is very close to the load for the unconstrained column. It thus appears that the eigen value is not very sensitive to small perturbations in the optimum numerical results. Besides, using the results of the unconstrained problem, it seems possible to prescribe a good approximation to the design variables for the constrained problem.

The results indicate that modulus variation can result in a substantial gain in the eigen values. For structures where minimum weight is of utmost consideration, suitable modulus variation offers the possibility of great improvements provided the proper materials can be developed.

## CHAPTER - 1

### INTRODUCTION

Problems of optimal design of simple elements such as columns and beams have received considerable attention in recent years. Usually length, cross-sectional shape and material are preselected and area is allowed to vary along the length of a given weight of the element. Optimized eigen value is either the buckling load or natural frequency. Realistic designs may involve some additional constraints on the design and state variables.

Since strongest-homogeneous-columns and stiffest-homogeneous beams have been thoroughly investigated in the literature, corresponding non-homogeneous elements are studied in this thesis. A brief review of optimal tapered columns is presented in Section 1.1. Optimal beams with constraint on fundamental frequency of transverse oscillations are reviewed in Section 1.2. Object and scope of the present work is then stated in Section 1.3.

#### 1.1 Brief Review of Optimal Tapered Columns

Interest in problems related to optimal design of columns really started with the treatment, by Keller<sup>5</sup>

and Tadjbaksh and Keller<sup>6</sup>, of the strongest column problem, stated as the determination of the shape of a column of given length and volume of material for which the Euler buckling load is a maximum. It is shown in [5] that of all untwisted columns, hinged at the end points with arbitrary convex cross-sections, the one with cross-sections of equilateral triangles and variation of area like that of the strongest circular column, is the strongest. Triangularization alone results in an increase of 20.9 percent in load and this coupled with optimum tapering, yields an overall increase of 61.2 percent over that of the uniform circular cylinder. It is further shown that these results are applicable to initially twisted columns also, in the absence of any applied couples.

Authors in [6] determine the optimum shape of columns which have similar-cross-sections and are clamped at one end and clamped, free or hinged at the other end. The analysis is based upon the fourth-order homogeneous differential equation (with homogeneous boundary conditions), which describes the equilibrium of an elastic rod in the buckled state. With a suitable change of variables, this equation is reduced to a second-order-self adjoint equation with homogeneous but mixed boundary conditions. Application of direct variational technique along with the theory of

self-adjoint-second order differential equations, produces optimality condition which is a nonlinear relationship between the "shape function" and the eigen function. Incorporating this in the equilibrium equation, the problem reduces to the solution of a nonlinear second order equation in the eigen function. It is solved exactly to produce the critical load and the associated area distribution for the given boundary conditions. Since the obtained eigen value is only stationary, it is shown through the use of integral inequalities, that it is maximum of the lowest eigen values for any shape with the given volume. It is found that in the hinged-hinged, clamped-clamped and clamped-free cases the buckling load is increased by one third over that of a uniform column and in the clamped-hinged case the increase is slightly more - about 35.1 percent. It is further shown that the results may be interpreted as isoperimetric inequalities for eigen values of certain second order differential equations.

Taylor<sup>7</sup> has presented an alternative energy approach by minimizing the total potential energy in the buckled state, treating the given volume as constraint. Governing equations are obtained by the application of direct variational technique. Furthermore, an alternate approach for a proof that the solution of these equations is a maximum of the lowest eigen values, is also presented.

Later, this approach is applied by Taylor and Liu<sup>8</sup> for optimal design of columns, characterized by a linear dependence of stiffness on the volume of the material per unit length, with an inequality constraint on cross-sectional area. Solutions are obtained for clamped-free and clamped-hinged columns. Besides, a proof for the optimality of the designs, is also presented. Method, however, can be easily extended to other types of cross-sectional shapes, but generalization for the proof of optimality of constrained designs is yet to be obtained.

Pragor and Taylor<sup>9</sup> have presented a uniform method, along with the proof of optimality, of treating a variety of problems of optimal design of sandwich structures characterized by the linear dependence of specific stiffness on specific structural weight. Application of the principle of minimum potential energy leads to the optimality condition, which stipulates that a certain specific energy (or power) or the difference between certain specific energies per unit specific stiffness has a constant value throughout the structure. Design problem then reduces to the integration of an optimality condition, which is a differential equation for the optimal displacement field that does not involve any design parameters. Subsequently, the variable specific stiffness of the optimal structure is determined

from the usual differential equations of the structure. The method is later applied to a hinged-hinged sandwich column.

Frauenthal<sup>10</sup> has obtained analytical solution for hinged-hinged optimal columns of various cross-sectional shapes, characterized by a constraint upon the maximum allowable prebuckling stress. This constraint is equivalent to the minimum area constraint used in [8]. Frauenthal essentially solves the problem, tackled in [8], which is generalized to account for other sections of practical interest. The approach used for the formulation is also slightly different. Rayleigh quotient is made stationary subject to the constraints on the prescribed volume and maximum prebuckling stress. Relevant necessary conditions are obtained by applying Euler equations to suitably constructed functional. Using the principle of symmetry and dividing the half column into two parts, analytical solutions are obtained. It is later shown that the solution asymptotically approaches to the solution for strongest column obtained in the literature [6, 9, 11]. It may be mentioned that no formal proof of optimality is presented by the author but it is stated that the analytical solutions are in close agreement with the numerical ones obtained by a modified steepest ascent procedure, suggesting the stationary solutions to be in fact optimal.

## 1.2 Brief Review of Optimal Tapered Beams

Problems of optimal design of vibrating elastic homogeneous elements have been largely studied by Niordson and his group. Niordson<sup>12</sup> has considered a simply supported beam, of given length, with geometrically similar cross-sections ( $q = 2$ ) and determines the optimal tapering which maximizes the fundamental frequency of transverse vibrations for the given volume of the material. Frequency written as the Rayleigh quotient, is maximized for the given volume by the application of direct variational technique. Incorporating the resulting optimality condition in the equation of equilibrium, problem finally reduces to the solution of a highly nonlinear fourth-order differential equation in the displacement function with singular boundary conditions. The solution is numerically obtained by the method of successive iterations. It is found that optimal tapering of the beam produces a 6.6 percent increase in frequency.

Brach<sup>13</sup> considers a whole group of Euler-Bernouli beams characterized by ( $q = 1$ ) a linear relationship between second area moment and cross-sectional area and optimizes their shapes with respect to fundamental frequency for all kinds of homogeneous boundary conditions. To consider practical solution, constraints are put on the design

variable. Necessary conditions to make frequency stationary, are obtained from the first variation of a suitably constructed augmented functional with respect to design and state variables. Equations are solved analytically. It is found that in the hinged-hinged case Euler beam is the optimal. Furthermore, optimal solutions do not exist for free-free and clamped-free beams. This result is later confirmed by Karihaloo and Njorndson<sup>14</sup> through more elaborate mathematical and physical reasonings. Shape of a cantilever beam, with and without a tip mass, is optimized with respect to its fundamental frequency for various cross-sectional styles ( $q = 1, 2, 3$ ). In the absence of a tip mass, this results in an increase of 578 percent for beams having similar cross-sections and 325 percent for beams having rectangular cross-sections of given width ( $q = 3$ ) over that of the corresponding Euler beam. It is further seen that tip mass has a substantial effect on the shape of the beam.

Though the general approach in [14] is essentially the same as that in [12], the extension is by no means trivial. Nature of singularity in the cantilever case being quite different from that of the hinged-hinged beam, iterative solution is developed in a different fashion, as discussed in Chapter 7 of this thesis.

Karihaloo and Niordson<sup>15</sup> have further generalized the problem considered in [12]. Essentially employing the same approach, the shape of a simply supported laterally vibrating beam having the highest possible value of the first fundamental frequency under a given axial compressive load, is determined for  $q = 1, 2, 3$ . In the absence of axial compressive load, for  $q = 3$  the increase in frequency over the corresponding uniform beam is 11.9 percent and for  $q = 1$ , as stated by Brach<sup>13</sup>, no increase in frequency is possible.

### 1.3 Object and Scope of Present Work

These studies have established that considerable increases in the eigen values can be achieved by an optimal distribution of stiffness. In this thesis, strongest columns and stiffest beams are examined for further gains by allowing the material to be nonhomogeneous. This essentially means variation of stiffness with modulus and/or area. Normally variation of modulus can also mean variation of density. While this is generally true, no explicit relationship between the two is available in literature. Even so with the recent advances in composite material technology and the development of high specific modulus fibers, one can easily conceive of situations where longitudinal modulus variation can be achieved, keeping the fiber orientation and density

unchanged. Thus in the problem studied here, only area and modulus appear as the design variables. The results for a tapered-nonhomogeneous element can, however, be applied in the presence of density variation also by replacing the design variables by their suitable combinations.

Stiffness variation in a general case as considered here, can be achieved either by varying area or modulus and/or both. An attempt is, therefore, made here to examine the relative gains offered by the uniform-nonhomogeneous and tapered-nonhomogeneous elements. To include a variety of cross-sectional geometries, nondimensional second area moment is considered proportional to  $\eta^q$  where  $\eta$  refers to nondimensional area and  $q$  is an integer. Besides, modulus variation is considered to be constrained by the following relationship

$$\bar{e} = \int_0^1 e^p dx ; \quad p > 0 ,$$

where  $e$  is a nondimensional modulus and  $\bar{e}$  is unity for the corresponding homogeneous uniform element.

Optimization problem is stated as a classical Bolza problem in calculus of variation. The problem is, however, cast in the language of optimal control theory. The necessary conditions for optimality are, therefore, similar to the statement of Pontryagin's maximum principle.

For the class of problems considered, even though this approach does not offer any special advantages over that used by the authors in [6, 8, 11, 12, 13], the derivation of the governing equations and the boundary conditions, specially on the multipliers, comes out in an elegant and simple manner. Besides, this approach has not been widely used for structural applications and offers decisive advantages for complicated problems, involving finite number of discontinuities and equality and inequality constraints on the design and state variables.

Solution of the governing equations, wherever possible, is obtained analytically. Numerical solutions are obtained by the method of successive iterations. Other numerical methods, as ~~stated~~ in Chapter 4, are also attempted but without much success.

In Chapter 2, a general Bolza problem is stated and cast as a problem in optimal control theory. Necessary conditions (which are equivalent to Pontryagin's maximum principle) obtained from the first variation of a suitably defined augmented functional, are presented without proof. These are then further reduced to equations, which can be directly applied to the problems studied in this thesis.

In Chapter 3, problem of strongest uniform-nonhomogeneous column is investigated. Using the necessary conditions stated in Chapter 2, optimality condition and the governing equations are derived. Analytical solution of these equations, for  $p = 1$  is obtained for the classical homogeneous boundary conditions - hinged-hinged, free-clamped, clamped-clamped and clamped-hinged.

Chapter 4 determines the numerical solutions of the equations of Chapter 3 for  $p \neq 1$ , by the method of successive iterations. Some other numerical schemes, which were attempted with a view to save computer time, are also discussed.

In Chapter 5, a tapered-nonhomogeneous column is considered. Analytical as well as numerical solutions are obtained for all the end conditions considered in Chapter 3. It is further shown that the governing equations for the uniform column can be obtained as a special case of the equations for the tapered column.

In Chapter 6, a uniform nonhomogeneous beam element is investigated for the maximum increase in the fundamental frequency of transverse vibrations. Analytical as well as numerical solutions are obtained for four homogeneous end conditions, like hinged-hinged, free-clamped, clamped-clamped and clamped-hinged.

In Chapter 7, a general tapered-nonhomogeneous beam element is considered. Numerical solutions are obtained for hinged-hinged and free-clamped end conditions.

Since there is no constraint on minimum area and modulus, optimal solutions contain points of zero modulus and area. This is physically unrealistic. Besides, exact physical reproduction of the numerical curves for modulus and area distributions is difficult in practices. So an attempt is made to investigate the sensitivity of eigen value to small changes in these distributions. These have been approximated by simple polynomials with some minimum value of area and modulus. Using these, the eigen value is determined. It is shown through the example of H-H columns with  $p = 1$ , that the critical load is very close to the load for the unconstrained column. It, thus, appears that the eigen value is not very sensitive to small perturbations in the optimum numerical results. Besides, using the results of the unconstrained problem, it seems possible to prescribe a good approximation to the design variables for the constrained problem.

The results indicate that modulus variation can result in a substantial gain in the eigen values. For structures where minimum weight is of utmost consideration, suitable modulus variation offers the possibility of great improvements provided the proper materials can be developed.

## CHAPTER - 2

### GENERAL PROBLEM OF OPTIMIZATION AND ITS FORMULATION

#### 2.1 Statement of the General Problem

A realistic optimum design problem is generally characterized by a finite number of control parameters and variables. The parameters are discrete in nature and the variables could be the state or design variables which depend continuously on time or space. These are to be determined such that a functional, mostly an integral, is a minimum. Construction of the functional depends on the criterion selected for the optimal design. For example in structural design, it is generally the cost or weight of the structure. Further, since the system being designed must be capable of performing certain functions, it may have to meet some side conditions on the state and design variables also. These side conditions generally include both the equality and the inequality constraints. As the problems studied later do not have any inequality constraints, the presentation is confined to equality constraints only. The problem, thus, is the classical Bolza problem in calculus of variation. The formulation given below

follows closely the treatment in Ref. [1]. The problem can now be stated as:

Determine  $u(x)$ ,  $b$ ,  $y(x)$ ,  $x^0 \leq x \leq x^\eta$ , which minimize

$$J = g_0(b, x^j, y^j) + \int_{x^0}^{x^\eta} f_0(x, y(x), u(x), b) dx \quad (2.1.1)$$

subject to the conditions:

$$\frac{dy}{dx} = f(x, y, u, b), \quad x^0 \leq x \leq x^\eta \quad (2.1.2)$$

$$g_\alpha(b, x^j, y^j) + \int_{x^0}^{x^\eta} L_\alpha(x, y(x), u(x), b) dx = 0,$$

$$\alpha = 1, \dots, r \quad (2.1.3)$$

$$\phi_\beta(x, y, u, b) = 0, \quad \beta = 1, \dots, q, \quad x^0 \leq x \leq x^\eta \quad (2.1.4)$$

where

$$\begin{aligned} y(x) &= [y_1(x) \dots y_n(x)]^T; \quad u(x) = [u_1(x) \dots u_m(x)]^T; \\ b &= [b_1 \dots b_l]^T; \quad f(x, y, u, b) = [f_1(x, y, u, b) \dots \\ &\quad f_n(x, y, u, b)]^T \end{aligned} \quad (2.1.5)$$

and  $x^0 < x^j < x^\eta$ , where  $(x^j, y^j)$  are intermediate points,  
 $j = 1, \dots, \eta-1$ .

For the problem considered here, it is assumed that the conditions (2.1.4) do not express any component of  $y(x)$  explicitly. In case some constraint function depends only on  $\dot{y}(x)$  and  $x$ , this constraint is called state variable constraint. Such a constraint is not considered here.

The vector variable  $y(x)$  is called the state variable,  $u(x)$  is called the design (or control) variable and  $b$  is called the design parameter. Equations (2.1.3) contain the boundary conditions on the state variable and functions which determine the end points of the interval. Conditions (2.1.2) and (2.1.4) express the constraints which have been separated such that Eqns. (2.1.2) contain the derivatives of the state variable and Eqns. (2.1.4) do not involve any derivatives of  $y$ . In structural problems Eqns. (2.1.2) represent equation of equilibrium and Eqn. (2.1.4) may involve some relations among the design and state variables representing some side constraints. The independent variable  $x$  may be time or space-type variable, depending on the problem being considered.

The functions  $f_0$ ,  $f$ ,  $L_\alpha$  and  $\phi$  are assumed to be continuously differentiable at all points except  $(x^j, y^j)$ ,  $j = 1, \dots, \eta-1$ . At these points the functions may have jump discontinuities. And so in general  $u(x)$  and  $y'(x)$  are piecewise continuous. The allowed discontinuities,

thus, routinely account for sudden changes, in system behaviour, which do occur in realistic problems of optimal control.

## 2.2 A Multiplier Rule

Necessary conditions for the Bolza problem can be obtained from a very powerful theorem, of Liusternik and Sobolev<sup>2</sup>, which states that -

If  $u(x)$ ,  $b$ ,  $x^j$  and  $y(x)$  provide a solution to the Bolza problem stated earlier, then there exist multipliers  $\lambda_0 \geq 0$ ,  $\gamma_\alpha$ ,  $\alpha=1, \dots, r$ ,  $\lambda_i(x)$ ,  $i=1, \dots, n$  and  $\mu_\beta(x)$ ,  $\beta=1, \dots, q$  not all zero, such that

$$\delta \bar{J} = 0 \quad (2.2.7)$$

where

$$\begin{aligned} \bar{J} = & \lambda_0 g_0(b, x^j, y^j) + \sum_{\alpha=1}^r \gamma_\alpha g_\alpha(b, x^j, y^j) + \int_{x^0}^{x^\eta} \{ \lambda_0 f_0(x, y, u, b) \\ & + \sum_{i=1}^n \lambda_i(x) \left[ \frac{dy_i}{dx} - f_i(x, y, u, b) \right] + \sum_{\alpha=1}^r \gamma_\alpha L_\alpha(x, y, u, b) \\ & + \sum_{\beta=1}^q \mu_\beta(x) \phi_\beta(x, y, u, b) \} dx \end{aligned} \quad (2.2.8)$$

Here  $\delta \bar{J}$  represents the first variation of  $\bar{J}$ .

### 2.3 Necessary Conditions for the Bolza Problem

The simplest Bolza problem is the one having all its functions three times continuously differentiable. Even in this case, however,  $u(x)$  may be only piecewise continuous. To include this possibility, let  $x^*$  be a point of discontinuity of any component of  $u(x)$ . Besides, to be more general, let  $x^0$ ,  $x^j$ ,  $x^*$  and  $x^\eta$  be not fixed but must be determined. This means that these special points are to be treated as parameters which are to be determined much as the design parameter  $b$ .

Before enforcing (2.2.7), for convenience in the development which follows, define

$$G = \lambda_0 g_0(b, x^j, y^j) + \sum_{\alpha=1}^r \gamma_\alpha g_\alpha(b, x^j, y^j) \quad (2.3.9)$$

$$H(x, y, u, b, \lambda, \gamma, \mu) = \lambda^\top(x) f(x, y, u, b)$$

$$\begin{aligned} & - \lambda_0 f_0(x, y, u, b) - \sum_{\alpha=1}^r \gamma_\alpha L_\alpha(x, y, u, b) \\ & - \sum_{\beta=1}^q \mu_\beta(x) \phi_\beta(x, y, u, b) \end{aligned} \quad (2.3.10)$$

so that (2.2.8) becomes

$$\begin{aligned} \bar{J} = G + \int_{x^0}^{x^j} [\lambda^T(x) \frac{dy}{dx} - H] dx + \int_{x^j}^{x^*} [\lambda^T(x) \frac{dy}{dx} - H] dx \\ + \int_{x^*}^{x^\eta} [\lambda^T(x) \frac{dy}{dx} - H] dx \end{aligned} \quad (2.3.11)$$

Writing  $\delta \bar{J}$  with respect to arbitrary variations in  $x^i$ ,  $y^i$ ,  $y(x)$ ,  $u(x)$  and  $b$  and equating it to zero, one gets the following necessary conditions<sup>1</sup>.

$$\frac{d\lambda}{dx} = - \frac{\partial H^T}{\partial y}, \quad \text{for } x \neq x_j \quad (2.3.12)$$

$$\frac{\partial H}{\partial u} = 0, \quad \text{for } x \neq x_j \quad (2.3.13)$$

$$\frac{\partial G}{\partial b} - \int_{x^0}^{x^\eta} \frac{\partial H}{\partial b} dx = 0 \quad (2.3.14)$$

$$\frac{\partial G^T}{\partial y^0} - \lambda(x^0) = 0 \quad (2.3.15a)$$

$$\frac{\partial G^T}{\partial y^\eta} + \lambda(x^\eta) = 0 \quad (2.3.15b)$$

$$\frac{\partial G^T}{\partial y^j} + \lambda(x^j - 0) - \lambda(x^j + 0) = 0 \quad (2.3.15c)$$

$$\frac{\partial G}{\partial x^0} + H(x^0 + 0) = 0 \quad (2.3.16a)$$

$$\frac{\partial G}{\partial x^\eta} - H(x^\eta - 0) = 0 \quad (2.3.16b)$$

$$\frac{\partial G}{\partial x^j} - H(x^j - 0) + H(x^j + 0) = 0 \quad (2.3.16c)$$

$$H(x^* - 0) - H(x^* + 0) = 0 \quad (2.3.17)$$

$$\lambda(x^* - 0) - \lambda(x^* + 0) = 0 \quad (2.3.18)$$

It may be noted that the necessary conditions (2.3.12) through (2.3.18) are linear and homogeneous in the multipliers  $\lambda_0$ ,  $\lambda_i(x)$ ,  $\gamma_\alpha$  and  $\mu_\beta(x)$ . It is, therefore, permissible to choose the magnitude of one multiplier so that the remaining multipliers are uniquely determined. It seems reasonable that if the necessary conditions obtained by setting  $\delta \bar{J} = 0$  are to be related to minimization of  $J$ , then  $\lambda_0$  should not be zero. This is indeed the case and if  $\lambda_0$  is required to be zero by the necessary conditions then the Bolza problem is "abnormal" in a sense. Most meaningful problems are normal and require  $\lambda_0 \neq 0$ . In solving problems using the stated necessary conditions, one should first verify that equations (2.3.12) through (2.3.18) have no solution if  $\lambda_0 = 0$ . It is then permissible to put  $\lambda_0 = 1$  so that the remaining multipliers are uniquely determined.

Even though equations (2.3.12) through (2.3.18) are very complicated, it can be easily seen that they provide just the right number of equations to solve for all unknowns. It, however, does not assert that a solution of these equations exists.

The necessary conditions obtained are very nearly the famous Pontryagin maximum principle<sup>3</sup>. The condition which completes the maximum principle is an inequality which follows from the Weierstrass condition of calculus of variations. This condition is stated without proof<sup>4</sup> as -

In addition to the conditions (2.3.12) through (2.3.18), the solution of the Bolza problem must satisfy the condition

$$H(x, y(x), U, b, \lambda(x), \gamma, 0) \leq H(x, y(x), u(x), b, \lambda(x), \gamma, 0) \quad (2.3.19)$$

for all admissible  $U$  and all  $x^0 \leq x \leq x^\eta$ .

#### 2.4 Necessary Conditions for Fixed End Points

If the end points  $x^0$  and  $x^\eta$  are fixed and if there are no points of discontinuities, the equations (2.3.15c), (2.3.16), (2.3.17) and (2.3.18) drop out. Besides in the absence of any constraints (2.1.4) and control parameters  $b$ , equations (2.3.14) and (2.1.4) also drop out.

The problems considered here in this thesis belong to this category. Hence for such problems one needs to determine the solution of Eqns. (2.3.12), (2.3.13) and (2.3.15) along with Eqns. (2.1.2) and (2.1.3). It may be mentioned here that Eqns. (2.3.12), (2.3.13) and (2.3.15) provide respectively the adjoint equations in the multipliers  $\lambda$ , optimality conditions and the boundary conditions on  $\lambda$  respectively.

This formulation will now be applied to the column and beam problems in the following chapters.

## CHAPTER - 3

### UNIFORM-NONHOMOGENEOUS COLUMNS

#### 3.1 Introduction

Uniform columns of given length, cross-sectional shape and mass are investigated in this chapter for maximum increase in the buckling load through optimum longitudinal variation of modulus. To carry out a systematic study, the problem of buckling of a general tapered-nonhomogeneous column is first formulated in Section 3.2. Reduction of the equilibrium equation and the boundary conditions for a uniform column is then straightforward. A constraining relationship, which is similar to the condition of specified mass, to restrain the modulus variation is proposed in Section 3.3. Optimization problem is then stated in Section 3.4. Equivalent statements of the problem along with the several approaches available in the literature for the formulation are given in Section 3.5. Necessary conditions, for the present problem, are derived in Section 3.6. Boundary conditions on the multipliers, used in the formulation, are obtained in Section 3.7. Optimality condition and the governing equation are finally derived in Section 3.8. These can be solved analytically for  $p = 1$ .

Exact solutions are therefore obtained in Section 3.9 for four classical end conditions such as hinged-hinged, free-clamped, clamped-clamped and clamped-hinged. For  $p \neq 1$ , numerical solutions are determined in Chapter 4 for the above set of end conditions.

### 3.2 Formulation of Buckling Problem

Consider a column of length  $L$ , volume  $V$ , mass  $m$  and cross-sectional area  $A(\xi)$ . Under axial compressive load  $P$ . Neglecting the shear effects, the equation of equilibrium in the buckled state is written as

$$- M_{\xi\xi} + P w_{\xi\xi} = 0 \quad (3.2.1)$$

where, as shown in Fig. 3.1,  $w(\xi)$  is the lateral deflection from the straight position and  $M(\xi)$  is the bending moment, given by:

$$M(\xi) = - E(\xi) I(\xi) w_{\xi\xi} \quad (3.2.2)$$

In equation (3.2.2)  $E(\xi)$  is the Young's modulus of the column material which is isotropic and  $I(\xi)$  is the second moment of area. For the class of columns under consideration, it is related to the area by the relationship

$$I(\xi) = \alpha A^q(\xi) \quad (3.2.3)$$

where  $q$  is an integer and  $\alpha$  is a proportionality factor determined by sectional geometry. It may be noted that  $\alpha$  is not necessarily dimensionless. If  $L$  represents a typical length dimension then the quantity  $\alpha L^{2q-4}$  is dimensionless.

Most of the sections of interest can be represented by varying  $q$  from 1 to 3. For example, as pointed out by Frauenthal<sup>10</sup>,  $q = 1$  represents a sandwich column of fixed width, fixed core thickness (of negligible stiffness) and variable, equal face sheet thickness. Besides,  $q = 1$  also represents a solid rectangular section of fixed depth and variable width. A solid column of geometrically similar cross-sections, used by Tadjbaksh and Keller<sup>6</sup>, is represented by  $q = 2$ . For a solid column of rectangular cross-section of fixed width and variable depth,  $q$  equals 3. Other shapes of practical interest can also be approximately represented by suitable choices of  $q$  and corresponding  $\alpha$ .

Using (3.2.2) and (3.2.3), equation (3.2.1) can be written, in terms of the variables  $E$ ,  $A$  and  $w$ , as:

$$\frac{d^2}{d\xi^2} (E A^q w_{\xi\xi}) + \frac{P}{\alpha} w_{\xi\xi} = 0 \quad (3.2.4)$$

This can be further written as:

$$\frac{d^2}{d\xi^2} \left[ \left( \frac{E}{\rho^q} \right) \cdot (\rho A)^q w_{\xi\xi} \right] + \frac{P}{\alpha} w_{\xi\xi} = 0 \quad (3.2.5)$$

where  $\rho(\xi)$  represents the density. The motivation behind introducing  $\rho$  in the above equation is explained in the next section. It is related to mass  $m$  of the column through the relation:

$$\int_0^L \rho(\xi) A(\xi) d\xi = m \quad (3.2.6)$$

Now, the following nondimensional quantities may be defined

$$\begin{aligned} x &= \frac{\xi}{L}, \quad y = \frac{w}{L}, \quad \tilde{\rho} = \frac{\rho}{\rho_0}, \quad \tilde{E} = \frac{E}{E_0}, \quad a(x) = \frac{A}{A_0} \\ I_0 &= \alpha A_0^q, \quad \lambda = \frac{P \rho_0^q L^{2+q}}{\alpha e_0 m_0^q}, \quad e(x) = \frac{\tilde{E}}{\tilde{\rho}^q}, \quad \eta(x) = \tilde{\rho} a \\ \phi(x) &= e \eta^q y'', \quad m_0 = \rho_0 A_0 L, \quad \bar{m} = \frac{m}{m_0} \end{aligned} \quad (3.2.7)$$

where  $E_0$ ,  $\rho_0$ ,  $A_0$ ,  $I_0$ ,  $m_0$  are the reference modulus, density, cross-sectional area, second moment of the area of cross-section and mass respectively of the corresponding Euler column. Prime here denotes differentiation with respect to  $x$ . It may also be noted that  $\tilde{E}, \tilde{\rho}, \lambda, a(x), \eta$  and  $\phi$  respectively are nondimensional modulus, density, critical load, cross-sectional area, mass per unit length and bending moment.

Introducing, now, the above dimensionless quantities in equations (3.2.5) and (3.2.6), one easily gets:

$$\phi'' + \lambda e^{-1} \eta^{-q} \phi = 0 \quad (3.2.8)$$

$$\int_0^1 \eta(x) dx = \frac{m}{m_0} = 1 \quad (3.2.9)$$

Thus the equation of equilibrium, (3.2.4), which is originally of fourth order in  $w$  reduces to a second order equation (3.2.8) in  $\phi$ . Its solution requires two boundary conditions written in terms of  $\phi$  and  $\phi'$ . These are now derived for various end conditions.

### 3.2.1 Derivation of boundary conditions

Considering a column element at any station  $\xi$ , as shown in Fig. 3.1b, shear force  $S$ , bending moment  $M$  and the applied axial compressive load  $P$  are related as:

$$\frac{d}{d\xi} (EI \frac{d^2 w}{d\xi^2}) + P \frac{dw}{d\xi} + S = 0 \quad (3.2.10)$$

$$\text{or} \quad \phi' + \lambda y' + S_0 = 0 \quad (3.2.11)$$

$$\text{where} \quad S_0 = \frac{S_0 e^q L^{2+q}}{\alpha e_0 m_0^q} \quad (3.2.12)$$

Using equation (3.2.11) and physical conditions associated with a particular type of end fixity, boundary conditions in terms of  $\phi$  and  $\phi'$  can now be easily stated. Based upon the known solutions for the strongest homogeneous tapered columns<sup>6</sup> and being interested in the first mode of buckling only, conditions of symmetry will be employed to derive the boundary conditions for the hinged-hinged and clamped-clamped columns. For such columns, only the interval  $0 \leq x \leq 1/2$  will be considered for determining solution and hence the boundary conditions.

### Hinged-Hinged

Physical conditions along with the conditions of symmetry for such a column are:

$$M(0) = y'(1/2) = S_0(1/2) = 0 \quad (3.2.13)$$

Incorporating the last two conditions in (3.2.13) into (3.2.12), and knowing that  $\phi$  represents bending moment, the following boundary conditions can be stated.

$$\phi(0) = 0 \quad (3.2.14)$$

$$\phi'(1/2) = 0 \quad (3.2.15)$$

Free-Clamped

Physical conditions in this case are (Fig. 3.1c):

$$M(0) = y'(1) = S_0(1) = 0 \quad (3.2.16)$$

Hence the boundary conditions are:

$$\phi(0) = 0 \quad (3.2.17)$$

$$\phi'(1) = 0 \quad (3.2.18)$$

Clamped-Clamped

In this case (Fig. 3.1d), physical conditions along with conditions of symmetry are:

$$y'(0) = S_0(0) = y'(1/2) = S_0(1/2) = 0 \quad (3.2.19)$$

Equation (3.2.11), therefore, easily yields:

$$\phi'(0) = 0 \quad (3.2.20)$$

$$\phi'(1/2) = 0 \quad (3.2.21)$$

Clamped-Hinged

Considering the Fig. (3.1e), one easily gets

$$S_0 = -M_0 = \phi(0) \quad (3.2.22)$$

Inserting  $S_0$  from (3.2.22) into (3.2.11) along with the condition of zero slope at the clamped end  $x = 0$ , boundary conditions for the clamped-hinged column can be easily written as:

$$\phi'(0) + \phi(0) = 0 \quad (3.2.23)$$

$$\phi(1) = 0 \quad (3.2.24)$$

where (3.2.24) states the condition of zero moment at the hinged end.

Boundary conditions derived above for different types of end conditions are similar to those obtained by Tadjbaksh and Keller<sup>6</sup>. The only difference being in the statement of conditions for hinged-hinged and clamped-clamped columns. Besides, the boundary conditions obtained here are simply homogeneous whereas those obtained in Ref.[6] are homogeneous and mixed.

### 3.3 Modulus Constraint

In the problems tackled in this thesis,  $E(\xi)$  is considered as an independent design variable. It can be seen that, if this is allowed to vary unrestrained, the critical load can be increased indefinitely, as evident in the Euler column, where the load is proportional to modulus. Therefore, modulus must be constrained in some fashion.

In the case of strongest homogeneous columns cross-sectional area distribution is determined for the given buckling load, such that mass of the column is a minimum. The solution results in a saving in mass relative

to the corresponding Euler column carrying the same load. The same problem is equivalent to determining the area for the given mass, such that the critical load for the buckling in the first mode is a maximum. Mathematically, the relationship of area to mass can be considered as a constraint on the allowed variation of area, such that

$$\int_0^L A^q(\xi) d\xi = \text{Constant} \quad (3.3.25)$$

where the constant could be proportional to mass. In a similar fashion, we propose the following relationship for the modulus

$$\bar{e} = \int_0^1 e^p(x) dx = 1 ; \quad p > 0 \quad (3.3.26)$$

where  $e$  as defined in (3.2.7) is the nondimensional quantity  $(\tilde{E}/\tilde{\rho}^q)$  and  $p$  is a positive parameter.

Since one is interested in having a relationship which should be simple and should be valid for the corresponding Euler column: also, it can be easily seen that the relation (3.3.26) satisfies these conditions.

In order to understand the motivation behind this particular choice of the relationship (3.3.26), one may consider a column material which allows modulus variation without any change in density. In such a case

$e$  represents nondimensional modulus. As the nondimensionalization has been done with respect to the reference modulus  $E_0$ ,  $e$  gives directly the variation in modulus relative to it. Interpreting (3.3.26),  $\bar{e}$  can be viewed as the average value of  $e^p$ . It is further evident that for  $p = 1$ , the above relationship amounts to a constraint on the modulus variations such that the average value of the modulus remains the same as that of the Euler column. This restricts wild variations in  $E$ , which in practice cannot be achieved.

Since there is no unique way of constraining  $e$  variation, one can mathematically think of any relationship which is valid for the corresponding Euler column also. Depending on this relationship, one will get a particular optimum load and associated distributions of the design variables. Parameter  $p$  is introduced to give generalized averages covering all possibilities. Associated with each value of  $p$ , there will be an optimum value of  $\lambda$  and corresponding distribution of the variables involved. Since  $p$  is unlikely to have any optimum value,  $p$  versus  $\lambda$  relationship is expected to be monotonic. One will then be able to predict distribution of the design variables to get a particular increase in the eigen value. The distributions predicted, however, may not be realistic to be realised practically. It may be mentioned that  $p$  is assumed to be

greater than zero, because optimality condition (Section 3.8), for negative values of  $p$ , will require very large (theoretically tending to infinity) moduli at the points where moment is zero. This is physically unacceptable.

In the case where density is varying along with the modulus, the problem becomes difficult. Since  $\rho$  does not explicitly occur in the governing equation, it is not possible to treat density, modulus and cross-sectional area as three independent design variables. If a relationship between density and modulus is available in a convenient form, it can be incorporated in the present analysis. Since such a relationship is at present not available, the analysis is restricted to two independent design variables,  $e$  and  $\eta$  only. The optimal process will determine  $e$  and  $\eta$  and it is hoped that one can develop the materials and taper the column such that the desired  $e$  and  $\eta$  distributions are achieved. Using these design variables, the explicit appearance of density in the formulation (Chapter 5) is avoided. This explains, also, the artificial introduction of density in the equation of equilibrium (3.2.5).

### 3.4 Statement of the Problem

The optimization problem can now be stated as determination of modulus distribution, constrained by the

relation (3.3.26), such that the buckling load for a column of given mass and geometry is a maximum. In other words, it amounts to maximizing  $\lambda$  such that

$$\int_0^1 \eta(x) dx = \frac{m}{m_0} = 1 \quad (3.2.9)$$

$$\int_0^1 e^p dx = \bar{e} = 1 \quad (3.3.26)$$

For a uniform column of mass  $m_0$  (mass of the reference Euler column),  $a(x)$  is a constant. The Eqn. (3.2.9) then reduces to

$$\int_0^1 \tilde{\rho} dx = 1/a \quad (3.4.27)$$

Thus modulus variation which is normally associated with density variation must be such that (3.4.27) is satisfied. Mathematically, problem requires determination of  $e$  and  $\tilde{\rho}$ , which are somehow inter-related, as high modulus is normally associated with higher density. Since  $\tilde{\rho}$  does not appear explicitly in the equation (3.2.8),  $\tilde{\rho}$  cannot be considered as an independent variable in the formulation. Furthermore, even if this were possible, it may not be physically feasible to develop materials having, simultaneously, the prescribed modulus and density distributions. However,

with the recent advances in composite material technology and development of high specific modulus fibers, one can conceive of developing a material having the prescribed modulus distribution without any change in density, provided the required variation is not too wild. Apparently one can achieve it by using low modulus fibers in regions where the modulus required is low and high modulus fibers where the modulus requirement is large. The density can be maintained constant by suitably controlling the volume fractions of the fibers and matrix along the length.

With density kept constant, it is assumed that  $\tilde{\rho}$  and  $\alpha$  have such values that  $\eta(x) = 1$ . In such a situation, relation (3.4.27) is identically satisfied and the variable  $e$  ( $\tilde{E}/\tilde{\rho}^q$ ) simply becomes  $\tilde{E}$  when  $\tilde{\rho} = 1$ . The problem now reduces to maximizing  $\lambda$  such that (3.4.27) is satisfied.

### 3.5 Different Approaches for Formulation

Because of the similarity in the mathematical nature of  $\bar{e}$  and  $e$  relationship for a uniform element and area-mass relationship for a homogeneous element, the present problem is similar to the problem of design of the minimum mass structures with constraint on the eigen value. This is stated in two equivalent forms: maximizing eigen

value for fixed mass, or minimizing the mass for a fixed eigen value. It is, therefore, either an isoperimetric problem or a Bolza problem in calculus of variations. Various authors have derived the optimality conditions with marginal difference in the approaches. Some of these are:

1. Express the eigen value<sup>10,12</sup>  $P$  as a Rayleigh's quotient

$$P = \frac{\int_0^L EI w_{\xi\xi}^2 d\xi}{\int_0^L w_{\xi}^2 d\xi} \quad (3.5.28)$$

and maximize it subject to the constraint of given mass.

Usually  $P$  is made stationary and only in some cases proof<sup>6,7,8,9</sup> of optimality, i.e., stationary value being the maximum of the minimum eigen values, is available.

2. Mathematically, making  $P$  stationary is equivalent to making  $J$  stationary for the given mass<sup>13</sup>, where  $J$  is defined as:

$$J = \int_0^L (EI w_{\xi\xi}^2 - P w_{\xi}^2) d\xi \quad (3.5.29)$$

3. Mass is made stationary for the given eigen value<sup>7</sup> which, from (3.2.1), is

$$P = - \frac{\frac{d^2}{d\xi^2} (EI w_{\xi\xi})}{w_{\xi\xi}} \quad (3.5.30)$$

$$\text{or} \quad \frac{d^2}{d\xi^2} (EI w_{\xi\xi}) + P w_{\xi\xi} = 0 \quad (3.2.1)$$

Thus, equation of equilibrium is treated as a constraint.

4. Sometimes, an energy approach is used where the total potential energy<sup>7,8</sup> is minimized for the given mass.

5. A direct variational approach, using parameter  $\epsilon$ , is applied to the equation of equilibrium<sup>5,6</sup> (or  $P$  in Eqn. (3.5.28)<sup>12</sup>) and the constraints. The method is not widely followed, as it does not seem to be convenient to apply, specially in the presence of inequality constraints on the design variables.

Generally the technique used in the above approaches is to make a functional  $J$ , written as an integral including the specified constraints, stationary. For this purpose an augmented functional  $\bar{J}$ , consisting of  $J$  and the constraints is written, using multipliers. It is then made stationary with respect to the variables involved. Corresponding Euler equations provide the necessary conditions. Since the extremising of  $\bar{J}$  implies extremization of  $J$  also, it is immaterial whether one minimizes mass for the given eigen value or maximizes eigen value for the given mass. The necessary conditions obtained in both the cases are the same, since the augmented functional

does not change basically. In view of this the present problem can be stated as:

Minimize

$$\bar{e} = \int_0^1 e^p dx \quad (3.5.31)$$

such that

$$\phi'' + \lambda e^{-1} \phi = 0 \quad (3.5.32)$$

$$g_1(\phi(0), \phi(1), \phi'(0), \phi'(1)) = 0 \quad (3.5.33)$$

$$g_2(\phi(0), \phi(1), \phi'(0), \phi'(1)) = 0 \quad (3.5.34)$$

where,  $\eta$  being unity,

$$e = a^q \hat{E} \quad (3.5.35)$$

$$\phi = e y'' \quad (3.5.36)$$

and  $g_1$  and  $g_2$  are the constraints imposed by the end conditions like H-H, E-C, C-C, C-H, as obtained in Section (3.2).

### 3.6 Necessary Conditions

For applying the equations (2.3.12) to (2.3.18), the problem is now cast in the format of control theory.

Defining

$$y_1 = \emptyset \quad (3.6.37)$$

$$y_2 = \emptyset' \quad (3.6.38)$$

Equation (3.5.32), which is a second order equation, can be represented by two first order equations:

$$y_1' = y_2 = f_1 \quad (3.6.39)$$

$$y_2' = -\lambda e^{-1} y_1 = f_2 \quad (3.6.40)$$

Now, using Eqns. (3.5.33), (3.5.34), (3.6.39) and (3.6.40), the functional  $\bar{J}$  can be written as:

$$\bar{J} = \sum_{i=1}^2 \gamma_i g_i + \int_0^1 [\lambda_0 e^p + \sum_{i=1}^2 \lambda_i(x) (y_i' - f_i)] dx \quad (3.6.41)$$

Functions  $G$  and  $H$  defined in (2.3.9) and (2.3.10) can be now easily written. They are:

$$G = \gamma_1 g_1 + \gamma_2 g_2 \quad (3.6.42)$$

$$\begin{aligned} H &= \lambda_1(x) f_1 + \lambda_2(x) f_2 - \lambda_0 e^p \\ &= \lambda_1 y_2 - \lambda_2 \lambda e^{-1} y_1 - \lambda_0 e^p \end{aligned} \quad (3.6.43)$$

Using (2.3.12) and (2.3.13) one easily gets

$$\lambda_1' = -\frac{\partial H}{\partial y_1} = \lambda_2 \lambda e^{-1} \quad (3.6.44)$$

$$\lambda_2' = - \frac{\partial H}{\partial y_2} = - \lambda_1 \quad (3.6.45)$$

$$\frac{\partial H}{\partial c} = \lambda_2 \lambda e^{-2} y_1 - \lambda_0 p e^{p-1} = 0 \quad (3.6.46)$$

Differentiating  $\lambda_2'$  once, and then substituting  $\lambda_1'$  from (3.6.44), one easily gets:

$$\lambda_2'' + \lambda e^{-1} \lambda_2 = 0 \quad (3.6.47)$$

### 3.7 Boundary Conditions on Multipliers

Applying Eqns. (2.3.15a) and (2.3.15b) to the function  $G$  in (3.6.42), one can easily get expressions for the multipliers  $\gamma_1, \gamma_2$  and B.C.'s for  $\lambda_2(x)$ . We shall now derive these for the end conditions - H-H, C-C, C-H. Free-clamped case is not considered, as one can see from (3.2.14)-(3.2.15) and (3.2.17)-(3.2.18), that the boundary conditions for H-H and F-C cases are similar.

#### 3.7.1 Hinged-Hinged

Using relevant boundary conditions and applying Eqns. (2.3.15a) and (2.3.15b), one can easily get:

$$g_1 = \phi(0) = y_1(0) = 0 \quad (3.7.48)$$

$$g_2 = \phi'(1/2) = y_2'(1/2) = 0 \quad (3.7.49)$$

$$\therefore G = \gamma_1 y_1(0) + \gamma_2 y_2(0) \quad (3.7.50)$$

$$\frac{\partial G}{\partial y_1(0)} = \gamma_1 - \lambda_1(0) = 0 \quad (3.7.51)$$

$$\frac{\partial G}{\partial y_2(0)} = 0 - \lambda_2(0) = 0 \quad (3.7.52)$$

$$\frac{\partial G}{\partial y_1(1/2)} = 0 + \lambda_1(1/2) = 0 \quad (3.7.53)$$

$$\frac{\partial G}{\partial y_2(1/2)} = \gamma_2 + \lambda_2(1/2) = 0 \quad (3.7.54)$$

Equations (3.7.51) and (3.7.54) determine constant multipliers  $\gamma_1$  and  $\gamma_2$ , and (3.7.52)-(3.7.53) provide boundary conditions for  $\lambda_1$  and  $\lambda_2$ . Writing  $\lambda_1$  in terms of  $\lambda_2'$  from (3.6.45), boundary conditions on  $\lambda_2$  can easily be written. These are:

$$\lambda_2(0) = 0 \quad (3.7.55)$$

$$\lambda_2'(1/2) = 0 \quad (3.7.56)$$

### 3.7.2 Clamped-Clamped

Using appropriate B.C.'s (3.2.20) and (3.2.21) and following the steps for the H-H case, following relations are obtained.

$$g_1 = \phi'(0) = y_2(0) = 0 \quad (3.7.57)$$

$$g_2 = \phi'(1/2) = y_2(1/2) = 0 \quad (3.7.58)$$

$$G = \gamma_1 y_2(0) + \gamma_2 y_2(1/2) \quad (3.7.59)$$

$$\frac{\partial G}{\partial y_1(0)} = 0 + \lambda_1(0) = 0 \quad (3.7.60)$$

$$\frac{\partial G}{\partial y_2(0)} = \gamma_1 + \lambda_2(0) = 0 \quad (3.7.61)$$

$$\frac{\partial G}{\partial y_1(1/2)} = 0 + \lambda_1(1/2) = 0 \quad (3.7.62)$$

$$\frac{\partial G}{\partial y_2(1/2)} = \gamma_2 + \lambda_2(1/2) = 0 \quad (3.7.63)$$

Equations (3.7.60) and (3.7.62) easily give the B.C.'s on  $\lambda_2$ .

$$\lambda_2'(0) = 0 \quad (3.7.64)$$

$$\lambda_2'(1/2) = 0 \quad (3.7.65)$$

### 3.7.3 Clamped-Hinged

Using B.C.'s (3.2.23) and (3.2.24) and following above steps:

$$g_1 = \phi(0) + \phi'(0) = y_1(0) + y_2(0) = 0 \quad (3.7.66)$$

$$g_2 = \phi(1) = y_1(1) = 0 \quad (3.7.67)$$

$$G = \gamma_1 [y_1(0) + y_2(0)] + \gamma_2 y_1(1) \quad (3.7.68)$$

$$\frac{\partial G}{\partial y_1(0)} = \gamma_1 + \lambda_1(0) = 0 \quad (3.7.69)$$

$$\frac{\partial G}{\partial y_2(0)} = \gamma_1 + \lambda_2(0) = 0 \quad (3.7.70)$$

$$\frac{\partial G}{\partial y_1(1)} = \gamma_2 + \lambda_1(1) = 0 \quad (3.7.71)$$

$$\frac{\partial G}{\partial y_2(1)} = 0 + \lambda_2(1) = 0 \quad (3.7.72)$$

Eliminating  $\gamma_1$  from (3.7.69) and (3.7.70), the B.C.'s on  $\lambda_2$  can easily be written. They are:

$$\lambda_2(0) + \lambda_2'(0) = 0 \quad (3.7.73)$$

$$\lambda_2(1) = 0 \quad (3.7.74)$$

### 3.8 Optimality Condition and Governing Equation

Comparing the Eqn. (3.6.47) for  $\lambda_2$  and the associated boundary conditions derived above for each set of the end conditions, with the Eqn. (3.5.32) for  $\phi$  and corresponding boundary conditions, it is evident that  $\lambda_2$  and  $\phi$  are governed by the same differential equation and boundary conditions. One can therefore easily write  $\lambda_2$  in terms of  $\phi$  as:

$$\lambda_2 = K\phi \quad (3.8.75)$$

where K is a constant. Substituting this in (3.6.46) and replacing  $y_1$  by  $\phi$ , one gets:

$$K\phi^2 e^{-2\lambda} - \lambda_0 p e^{p-1} = 0 \quad (3.8.76)$$

$$\text{or} \quad e^{p+1} = \left( \frac{K\lambda}{\lambda_0 p} \right) \phi^2 \quad (3.8.77)$$

Eqn. (3.8.77) is a relationship which must exist between  $e$  and  $\phi$  for  $\bar{e}$  to be a minimum. It, therefore, can be interpreted as the optimality condition. Since modulus must be positive, the constant K must be positive because  $\lambda_0 > 0$  from the multiplier rule.

Substituting for  $e$  from (3.8.77), the equation of equilibrium (3.5.32) reduces to:

$$\phi'' + \lambda \frac{\phi}{\left( \frac{1}{p+1} \right)} = 0 \quad (3.8.78)$$

$$\left( \frac{K\lambda}{\lambda_0 p} \phi^2 \right)$$

It may be commented that variable  $\phi$  in Eqn. (3.8.78) has been put in the above form to facilitate the integration of this equation for clamped-clamped and clamped-hinged end conditions, where  $\phi$  changes sign at the point of inflexion. If the above form is not used, one is highly susceptible

to commit mistake in determining the solution, specially when  $p$  is an odd integer.

The original optimal problem, thus, reduces to the solution of a second order nonlinear equation (3.8.78) in  $\phi$  with appropriate boundary conditions. As stated in Chapter 2, if the optimal problem is a normal problem,  $\lambda_0$  is then an arbitrary positive constant which is generally taken as unity to normalize the other multipliers, e.g.,  $\lambda_1$ ,  $\lambda_2$ ,  $\gamma_1$  and  $\gamma_2$  used here. This evidently means that for a normal problem which is assumed here, the solution must be independent of  $\lambda_0$ . It may be mentioned that  $\gamma_1$  and  $\gamma_2$  were determined while deriving the B.C.'s on multipliers and  $\lambda_1$  is linearly related to  $\lambda_2'$  which is itself linearly related to  $\phi'$ . For a fixed value of  $\bar{e}$  which is unity here, the number of unknowns is essentially four -  $K$ ,  $e$ ,  $\phi$  and  $\lambda$ . But the number of available equations is only three - Eqns. (3.3.26), (3.8.77) and (3.8.78). One is thus short of one equation. This is really not true, as  $\phi$  is governed by a homogeneous equation and homogeneous B.C.'s. It is an eigen value problem and  $\phi$ , therefore, represents mode shape which remains undetermined within a scalar. Identifying  $K$  as this constant and defining

$$\psi = \left( \frac{K}{\lambda_0^p} \right)^{\frac{1}{2}} \phi \quad (3.8.79)$$

Eqns. (3.8.77) and (3.8.78) reduce to:

$$e = (\lambda \psi^2)^{(1/p+1)} \quad (3.8.80)$$

$$\psi'' + \frac{\lambda \left(\frac{p}{p+1}\right) \psi}{(\psi^2)^{(1/p+1)}} = 0 \quad (3.8.81)$$

These can be further simplified by redefining  $\psi$ . Doing this one easily gets:

$$e = \lambda (\beta^2)^{\frac{p}{p+1}} \quad (3.8.82)$$

$$\beta'' + \frac{\beta}{(\beta^2)^{\frac{p}{p+1}}} = 0 \quad (3.8.83)$$

where

$$\psi = \lambda^{(p/2)} \beta \quad (3.8.84)$$

It may be cautioned here that the transformation (3.8.79) is valid only when  $K \neq 0$ , which in other words, implies that any of the multipliers used in the problem is not equal to zero. If such is the case, care has to be observed while defining a relationship of the form (3.8.79).

One now needs to solve the Eqn. (3.8.83) along with the associated boundary conditions, which being homogeneous, remain the same in terms of  $\beta$ . Eigen value  $\lambda$

can then be determined from (3.3.26). Using expression for  $e$  from (3.8.82) one easily gets

$$\int_0^1 e^p dx = \lambda^p \int_0^1 (\beta^2)^{\left(\frac{p}{p+1}\right)} dx = 1 \quad (3.8.85)$$

or 
$$\lambda = \left[ \frac{1}{\int_0^1 (\beta^2)^{\left(\frac{p}{p+1}\right)} dx} \right]^{1/p} \quad (3.8.86)$$

The nondimensional modulus distribution,  $e(x)$ , is then obtained from (3.8.82).

The solutions, now, will be obtained for each of the end conditions (H-H, F-C, C-C, C-H) for various values of  $p$ . Exact solutions can be obtained for  $p = 1$  and the governing equation has to be integrated numerically for other values. The solutions, therefore, are discussed separately for  $p = 1$  and  $p \neq 1$ .

### 3.9 Analytical Solutions

Equations (3.8.83), (3.8.86) and (3.8.82) respectively reduce to the following equations for  $p = 1$

$$\beta'' + \frac{\beta}{|\beta|} = 0 \quad (3.9.87)$$

$$\lambda = \frac{1}{\int_0^1 |\beta| \, dx} \quad (3.9.88)$$

$$e(x) = \lambda |\beta| \quad (3.9.89)$$

Equation (3.9.89) can be interpreted alternatively. Substituting for  $e(x)$  in terms of  $\beta$  and  $y''$  one easily gets:

$$y'' = \pm C_0 \quad (3.9.90)$$

where  $C_0$  is a constant. Thus the optimality condition requires buckling to take place such that the magnitude of curvature remains constant. This is a familiar result which Prager and Taylor<sup>9</sup> obtained for homogeneous columns with stiffness proportional to mass per unit length. For the problem considered here, stiffness is proportional to  $e$  because cross-sectional area is constant. Mathematically both the problems are the same if modulus and area are interchanged, and hence the same optimality condition.

### 3.9.1 Hinged-Hinged column

The governing Eqn. (3.9.87) is to be solved for the following B.C.'s.

$$\beta(0) = 0 \quad (3.9.91)$$

$$\beta'(1/2) = 0 \quad (3.9.92)$$

For a H-H column the curvature, hence the bending moment represented by  $\beta$ , does not change sign for the lowest critical load. The Eqn. (3.9.87) reduces to

$$\beta'' + 1 = 0 \quad (3.9.93)$$

Integration of the above equation gives

$$\beta = -\frac{1}{2}x^2 + c_1x + c_2 \quad (3.9.94)$$

Determining the constants  $c_1$  and  $c_2$ , using the B.C.'s (3.9.91) and (3.9.92), the following solution is easily obtained.

$$\beta = \frac{1}{2}(x - x^2) \quad (3.9.95)$$

Substituting, now,  $\beta$  in Eqn. (3.9.88) one easily gets:

$$\lambda = \frac{1}{2 \int_0^{1/2} \frac{1}{2}(x - x^2)dx} = 12 \quad (3.9.96)$$

Substitution of  $\lambda$  and  $\beta$ , obtained above, in Eqn. (3.9.89) yields:

$$e(x) = 6(x - x^2) \quad (3.9.97)$$

It may be noted that Eqn. (3.9.97) gives the required nondimensional modulus distribution and Eqn. (3.9.96)

gives the nondimensional critical load, which for the corresponding Euler column is  $\pi^2$ . Denoting this by  $\lambda_E$ , one gets:

$$\frac{\lambda}{\lambda_E} = \frac{12}{\pi^2} = 1.216 \quad (3.9.98)$$

Thus modulus variation produces a 21.6 percent increase in critical load over the Euler column. Further, from Eqn. (3.9.97), it is obvious that the minimum value of  $e$  is zero at  $x = 0$  and its maximum value is 1.50 at  $x = 1/2$ . The corresponding  $e$  distribution is shown in Figure 5.2.

### 3.9.2 Free-Clamped column

The B.C.'s for a free-clamped column from Eqns. (3.2.17) and (3.2.18) are:

$$\beta(0) = 0 \quad (3.9.99)$$

$$\beta'(1) = 0 \quad (3.9.100)$$

If the nondimensionalization of  $w$  and  $\xi$  in this case is carried out with respect to  $2L$  instead of  $L$ , then it is easily seen that the governing equation and the B.C.'s for H-H and F-C are identical, and hence the solution for  $\beta$ ,  $\lambda$  and  $e(x)$ . But the actual critical load for the F-C column will be one fourth the load for the H-H column, as

the eigen value  $\lambda$  is nondimensionalized with respect to  $(E_0 I_0 / L^2)$  and in this case  $L$  is to be replaced by  $2L$ . Since a similar result holds for the Euler column also, the increase in load for the E-C column is also 21.6 percent, as obtained for H-H column. First half of the Figure 5.2a, which shows modulus distribution for a H-H column, provides the corresponding distribution for the E-C case also. Distribution is therefore not shown separately.

### 3.9.3 Clamped-Clamped column

In this case the optimality condition (3.9.90) can be satisfied only when curvature changes sign at some station  $x_0$ . This obviously means that  $\beta$  must change sign at  $x_0$ . Since the bending moment and shear force must be continuous,  $\beta$  must vanish at  $x_0$ . Now the interval  $0 \leq x \leq 1/2$  is divided into two parts -  $0 \leq x \leq x_0$  and  $x_0 \leq x \leq 0.5 - x_0$ . Let the running coordinate in these regions be  $x_1$  and  $x_2$  and corresponding  $\beta$  be denoted by  $\beta_1$  and  $\beta_2$ . Using the relevant B.C.'s (3.2.20) and (3.2.21) and the continuity conditions on  $\beta$  and  $\beta'$ , the following five conditions can be stated to determine  $\beta_1$ ,  $\beta_2$  and  $x_0$ .

$$\beta_1'(0) = 0 \quad (3.9.101)$$

determined. This is easily done by using conditions (3.9.101) to (3.9.105). The values obtained are:

$$x_0 = 0.25; \quad c_1 = 0; \quad c_2 = \frac{x_0^2}{2} = \frac{1}{32} \quad (3.9.110)$$

$$d_1 = -x_0 = -\frac{1}{4}; \quad d_2 = 0$$

Using these values,  $\beta_1$  and  $\beta_2$  are easily written as:

$$\beta_1 = \frac{1}{2}\left(\frac{1}{16} - x_1^2\right); \quad 0 \leq x_1 \leq 1/4 \quad (3.9.111)$$

$$\beta_2 = -\frac{1}{2}\left(\frac{x_2}{2} - x_2^2\right); \quad 0 \leq x_2 \leq 1/4 \quad (3.9.112)$$

Now, using (3.9.88) and the above expressions for  $\beta_1$  and  $\beta_2$ ,  $\lambda$  can be written as:

$$\lambda = \frac{1}{2\left[\int_0^{1/4} \frac{1}{2}\left(\frac{1}{16} - x_1^2\right)dx_1 + \int_0^{1/4} \frac{1}{2}\left(\frac{x_2}{2} - x_2^2\right)dx_2\right]} \quad (3.9.113)$$

Carrying out the integration in (3.9.113) one gets

$$\lambda = 48 \quad (3.9.114)$$

The expressions then for the moduli  $e_1$  and  $e_2$  in the two regions are

$$e_1(x_1) = 24\left(\frac{1}{16} - x_1^2\right) \quad (3.9.115)$$

$$e_2(x_2) = 24\left(\frac{x_2}{2} - x_2^2\right) \quad (3.9.116)$$

The above expressions thus provide the required modulus distribution. It is easily seen that the maximum value of  $e$  which is 1.5, occurs at the clamped end, and at the point of symmetry (middle) where  $x_2 = 1/4$ , while  $e_{\min}$  which is zero occurs at the point of contraflexure  $x_0$ , where the bending moment is zero and curvature changes sign.

Equation (3.9.114) gives the value of nondimensionalized load which, obviously, is four times that for the H-H column. Since this is true for the Euler column also, the increase in the critical load for C-C ends is also 21.6 percent. Corresponding modulus distribution is shown in Figure 5.3.

#### 3.9.4 Clamped-Hinged column

This column, as in the case of C-C ends, is also characterized by a point of inflexion at  $x = x_0$ . Dividing the interval  $0 \leq x \leq 1$  into two parts as done for the C-C ends, following the same notation and using the relevant B.C.'s (3.2.23) and (3.2.24) the following conditions can be stated.

$$\beta_1(0) + \beta_1'(0) = 0 \quad (3.9.117)$$

$$\beta_1(x_0) = 0 \quad (3.9.118)$$

$$\beta_2(0) = 0 \quad (3.9.119)$$

$$\beta_2(1 - x_0) = 0 \quad (3.9.120)$$

$$\beta_1'(x_0) = \beta_2'(0) \quad (3.9.121)$$

where  $\beta_1$  and  $\beta_2$  are governed by the Eqns. (3.9.106) and (3.9.107) and corresponding general solutions are given by (3.9.108) and (3.9.109). Using the conditions (3.9.117) to (3.9.121), following values of the undetermined constants are obtained.

$$x_0 = 1 - \frac{1}{\sqrt{2}} = 0.29289 \quad (3.9.122a)$$

$$c_1 = - \frac{x_0^2}{2(1 - x_0)} = - 0.06066 \quad (3.9.122b)$$

$$c_2 = - c_1 = 0.06066 \quad (3.9.122c)$$

$$d_1 = - \frac{(1 - x_0)}{2} = - 0.35355 \quad (3.9.122d)$$

$$d_2 = 0 \quad (3.9.122e)$$

With these values and following the same steps as in C-C case, the solution is easily obtained as:

$$\beta_1 = 0.06066(1 - x_1) - \frac{x_1^2}{2}; \quad 0 \leq x_1 \leq x_0 \quad (0 \leq x \leq x_0) \quad (3.9.123)$$

$$\beta_2 = \frac{x_2^2}{2} - 0.35355x_2; \quad 0 \leq x_2 \leq 1-x_0 \quad (x_0 \leq x \leq 1-x_0) \quad (3.9.124)$$

$$\begin{aligned} \lambda &= \frac{1}{\int_0^{x_0} [0.06066(1-x_1) - \frac{x_1^2}{2}] dx_1 + \int_0^{1-x_0} (0.35355x_2 - \frac{x_2^2}{2}) dx_2} \\ &= 24.73 \end{aligned} \quad (3.9.125)$$

$$e_1(x_1) = \lambda [0.06066(1 - x_1) - \frac{x_1^2}{2}] \quad (3.9.126)$$

$$e_2(x_2) = \lambda [0.35355x_2 - \frac{x_2^2}{2}] \quad (3.9.127)$$

Equations (3.9.126) and (3.9.127) provide the optimum modulus distribution. It can be shown that the maximum value of  $e$  is 1.5455 occurring at  $x_2 = 0.35355$  while minimum value is zero, occurring at the point of contraflexure ( $x = x_0$ ) and the hinged end ( $x = 1$ ). However, the value of  $e$  at the clamped end ( $x = 0$ ) is 1.5 which is the maximum value for all other B.C.'s. Modulus distribution is plotted and is shown in Figure 5.4.

Equation (3.9.125) gives the nondimensional load which ( $\lambda_E$ ) for the corresponding Euler column is 20.19.<sup>16</sup>

This gives

$$\frac{\lambda}{\lambda_E} = \frac{24.73}{20.19} = 1.2248 \quad (3.9.128)$$

Thus, the percentage increase in load is 22.48 which is slightly more than the increase (21.6) for other end conditions.

## CHAPTER - 4

### NUMERICAL SOLUTIONS FOR UNIFORM COLUMNS ( $p \neq 1$ )

#### 4.1 Introduction

The governing Eqn. (3.8.83) which is rewritten here for convenience as

$$\beta'' + \beta^{\frac{p-1}{p+1}} = 0 \quad (4.1.1)$$

for  $\beta > 0$ , will be solved numerically for  $p \neq 1$  in this chapter. The solutions will be obtained for the same set of end conditions as considered in Chapter 3. Eqn. (4.1.1) is evidently singular for  $p < 1$  at points where  $\beta = 0$  i.e. at the ends which are hinged or free and at the points of contraflexure. Experience reveals that the numerical integration around singularity needs to be done carefully.

Section 4.2, therefore, discusses the nature and effect of singular behaviour. It presents a method of numerical approximation around the singularity. This is then applied in Sections 4.3 to 4.6, where solutions are obtained for four end conditions - H-H, F-C, C-C and C-H - by the method of successive iterations. Other numerical techniques such as partial integration and

Runge-Kutta were also attempted to improve the efficiency and are discussed in Section 4.5.

#### 4.2 Singular Behaviour

Numerical integration of (4.1.1) reveals that for small values of  $p$ , specially for those less than 0.1, the results are highly susceptible to the approximations made in integration near the singularity. Here even though iterative process for the integration converges the results may still be erroneous. The effect of peak, at the singularity, therefore, cannot be ignored and has to be determined very carefully. This requires investigation of analytical behaviour of  $\beta''$  in the neighbourhood of the singularity.

Let the singularity occur at  $x = 0$ . As in Ref. [12], near this point  $\beta$  can be expanded in a power series given by

$$\beta \sim a_0 x + a_1 x^\alpha + a_2 x^2 + \dots \quad (4.2.2)$$

where  $\alpha$  is a fractional power which should have a value  $1 < \alpha < 2$ . This will make  $\beta''$  singular at  $x = 0$ .  $\beta'$ , which represents shear force at points where slope is zero, will however remain finite as expected from the physical behaviour of the problem. Eqn. (4.1.1) can now be expanded in terms of  $x$  near  $x = 0$  by using (4.2.2). As the equation

involves  $\beta''$ , one needs to consider only the leading term ( $x^\alpha$ ) in (4.2.2). Exponent  $\alpha$  can then be determined from the fact that Eqn. (4.1.1) must be satisfied at  $x = 0$ . This necessitates that both the terms  $\beta''$  and  $\beta^{(p-1)/(p+1)}$  of this equation must have similar behaviour in  $x$ . Following this one gets

$$\beta \sim x^\alpha \quad (4.2.3)$$

$$\beta^{\frac{p-1}{p+1}} \sim x^{\alpha \frac{(p-1)}{p+1}} \quad (4.2.4)$$

$$\beta'' \sim x^{\alpha-2} \quad (4.2.5)$$

Equating powers of  $x$  in (4.2.4) and (4.2.5)

$$\alpha \frac{(p-1)}{(p+1)} = \alpha - 2 \quad (4.2.6)$$

$$\text{or} \quad \alpha = 1 + p \quad (4.2.7)$$

Since  $0 < p < 1$ , evidently  $1 < \alpha < 2$ .

#### 4.2.1 Contribution ( $\Delta$ ) due to peak

As already stated, the results become sensitive to the effect of the peak for small values of  $p$ . This can be studied in the following manner.

In the small interval  $0 \leq x \leq \epsilon$  where  $\epsilon$  is small and for small value of  $p$ ,  $\beta$  can be assumed to vary linearly with  $x$  and written as:

$$\beta = ax \quad (4.2.8)$$

where  $a$  is a constant. One can then approximate the contribution ( $\Delta$ ) of the peak (Figure 4.1) as:

$$\Delta = \int_0^{\epsilon} \beta^{\frac{p-1}{p+1}} dx = a^{\frac{p-1}{p+1}} \cdot \frac{\epsilon^{\frac{2p}{p+1}}}{(2p/p+1)} \quad (4.2.9)$$

Here the constant  $a$  was approximated in two ways - by matching either  $\beta'$  or  $\beta''$  at  $x = \epsilon$ . By matching  $\beta'$  one easily gets,

$$\Delta = \frac{|\beta'(\epsilon)|^{\frac{p-1}{p+1}} \cdot \epsilon^{\frac{2p}{p+1}}}{(2p/p+1)} \quad (4.2.10)$$

and by matching  $\beta''$  one gets

$$\Delta = \frac{|\beta''(\epsilon)| \epsilon}{(2p/p+1)} \quad (4.2.11)$$

Since  $\beta''$  curve is to be approximated around  $x = 0$ , to compute  $\beta'$  at  $x = 0$ , it seems logical to use relation (4.2.11) which employs continuity in  $\beta''$  at  $x = h$ . This relation, therefore, is used in the computations done in this thesis. It is found that the use of (4.2.10) yields erroneous

results if  $p \leq 0.1$ . However for  $p \geq 0.1$  both (4.2.10) and (4.2.11) lead to same solutions. The Eqn. (4.1.1) will now be integrated for various end conditions.

### 4.3 Hinged-Hinged Column

This requires determination of solution of Eqn. (4.1.1), which is rewritten here as:

$$\beta'' + \beta^{-r} = 0 \quad (4.3.12)$$

where

$$r = \frac{1-p}{1+p} \quad (4.3.13)$$

for the boundary conditions

$$\beta(0) = 0 \quad (3.9.91)$$

$$\beta'(1/2) = 0 \quad (3.9.92)$$

Eqn. (4.3.12) is numerically integrated for various values of  $p$  ranging from 0.02 to 5 by the method of successive iterations. Integrating (4.3.12) with respect to  $x$  between the limits  $x$  to  $1/2$  one gets:

$$\int_x^{1/2} \beta'' dx + \int_x^{1/2} \beta^{-r} dx = 0 \quad (4.3.14)$$

using (3.9.92), this reduces to:

$$\beta' = \int_x^{1/2} \beta^{-r} dx \quad (4.3.15)$$

Integrating this between the limits 0 to x, satisfying the B.C. (3.9.91),  $\beta(x)$  can be obtained as:

$$\beta = \int_0^x \int_x^{1/2} \beta^{-r} dx^2 \quad (4.3.16)$$

With the help of (4.3.15) and (4.3.16), one can then establish the following iterative scheme.

$$\beta'_{n+1} = \int_x^{1/2} \beta_n^{-r} dx \quad (4.3.17)$$

$$\beta_{n+1} = \int_0^x \beta'_{n+1} dx = \int_0^x \int_x^{1/2} \beta_n^{-r} dx^2 \quad (4.3.18)$$

Thus the steps involved in the above iteration are:

1. Start with some initial function  $\beta_n(x)$  and carry out the integration in (4.3.17) to determine  $\beta'_{n+1}$ .
2. Using  $\beta'_{n+1}$  carry out the integration in (4.3.18) to determine  $\beta_{n+1}$ .
3. Repeat the iteration described in the above steps till  $\beta$  converges.

Starting with practically any initial function, which may or may not satisfy the B.C.'s, the convergence takes place in few iterations. However it is found that

the convergence gets slow with decreasing values of  $p$ . It may be noted that even though the initial function does not satisfy the B.C.'s, the function  $\beta$  obtained after each cycle of iteration satisfies all the B.C.'s of the problem. The iteration is developed in such a way that after each integration the highest derivative is separated and put on the L.H.S. of the equation obtained. It may be noted that each integration satisfies one of the boundary conditions and hence two integrations are necessary to satisfy two boundary conditions.

Integration is done by using trapezoidal rule and the region of integration is divided into hundred equal parts. Sufficiently small interval was taken for proper rapid convergence and computations are done in double precision.

Convergence of  $\beta$  is ensured not only by checking the convergence on  $\beta$  distribution but also by checking the convergence of the nondimensional eigen value  $\lambda$  which is determined from Eqn. (3.8.86). This is important to avoid premature termination. Computations reveal that convergence for  $\beta$  is in general more rapid than the convergence of  $\lambda$ .

Having determined  $\beta$  and associated  $\lambda$ , corresponding modulus distribution  $e(x)$  is obtained from Eqn. (3.8.82).

The solution shows a monotonic increase in  $\lambda$  with decreasing  $p$ . The associated maximum modulus also increases with smaller values of  $p$ . However, as  $p$  increases and becomes large, eigen value  $\lambda$  tends to the Euler load and modulus distribution becomes flat i.e.  $e(x)$  is nearly one. This is an expected result, because  $e$  is given by

$$\int_0^1 e^p dx = 1 \quad (3.3.26)$$

The above relationship for large values of  $p$  can obviously be satisfied when  $e(x)$  is close to unity, which refers to Euler column for  $\lambda = 1$ .

All the results are discussed and presented, later, in Section 5.7.

#### 4.4 Free-Clamped Column

As stated in Section (3.9.2) the solution for a free-clamped column can be easily obtained from the solution for the H-H column. The critical load is one fourth of the load for the H-H case and the value  $e(x)$  of the modulus at any station  $x = \xi$  for the free-clamped case equals the value of  $e(x)$  at  $x = \xi/2$  for the H-H boundary condition.

#### 4.5 Clamped-Clamped Column

This column, as stated in Section (3.9.3), is characterized by the existence of an inflexion point  $x_0$  whose location is also to be determined along with the solution of the governing Eqn. (4.1.1). Since singularity occurs at  $x = x_0$  (in this case for  $p < 1$ ) the effect of peak is to be estimated on the left as well as on the right hand side of the singularity (Figure 4.1). The position of  $x_0$  being unknown, serious difficulties are encountered in arriving at the convergence. In order to reduce the computation time, three different numerical schemes - (i) partial numerical integration, (ii) Runge-Kutta and (iii) successive iterations - were attempted.

##### 4.5.1 Partial integration

Problem involves the determination of the solution of Eqn. (4.1.1) for the B.C.'s stated in (3.9.101)-(3.9.105). Multiplying (4.1.1) by  $2\beta'$  and rewriting one gets

$$2\beta'\beta'' + 2\beta^{\frac{p-1}{p+1}}\beta' = 0 \quad (4.5.19)$$

or

$$\frac{d}{dx}(\beta'^2) + 2\beta^{\frac{p-1}{p+1}}\frac{d\beta}{dx} = 0 \quad (4.5.20)$$

Now integration of this equation once w.r.t.  $x$  yields:

$$\beta'^2 + \left(\frac{p+1}{p}\right) \beta^{\frac{2p}{p+1}} = \frac{p+1}{p} C_0^2 \quad (4.5.21)$$

where  $C_0$  is constant of integration. Defining

$$\beta^{\frac{2p}{p+1}} = C_0^2 \cos^2 \theta(x); \quad C_0 > 0 \quad (4.5.22)$$

$$\text{or} \quad \beta^{\frac{p}{p+1}} = \pm C_0 \cos \theta(x) \quad (4.5.23)$$

where  $\theta(x)$  is a variable to be determined as the solution of the present problem. Eqn. (4.5.21) gives

$$\beta'^2 = \left(\frac{p+1}{p}\right) C_0^2 \sin^2 \theta(x) \quad (4.5.24)$$

$$\text{or} \quad \beta' = \pm \left(\frac{p+1}{p}\right)^{1/2} C_0 \sin \theta(x) \quad (4.5.25)$$

Now using (4.5.22) and (4.5.24) and setting conditions (3.9.101), (3.9.102) and (3.9.104), these boundary conditions can be restated in terms of  $\theta$ .

$$\theta(0) = 0 \quad (4.5.26)$$

$$\theta(x_0) = \pi/2 \quad (4.5.27)$$

$$\theta(1/2) = \pi \quad (4.5.28)$$

Thus  $\theta(x)$  varies from 0 to  $\pi/2$  for  $0 \leq x \leq x_0$  and from  $\pi/2$  to  $\pi$  for  $x_0 \leq x \leq 1/2$ . Assuming, without any loss in generality,  $\beta > 0$  for  $0 \leq x \leq x_0$  and  $\beta < 0$  for  $x_0 \leq x \leq 1/2$ , the negative (-) sign in (4.5.23) can be dropped. Now since  $\beta$  goes on decreasing from a positive value to zero at  $x_0$  and from zero to the maximum negative value at  $x = 1/2$ ,  $\beta'$  is negative throughout the domain of integration. Because  $1 \geq \sin\theta(x) \geq 0$  for  $0 \leq \theta(x) \leq \pi$ , positive (+) sign in (4.5.25) can be dropped. Expressions for  $\beta$  and  $\beta'$  can now be written as

$$\beta = [C_0 \cos\theta(x)]^{\frac{p+1}{p}} \quad (4.5.29)$$

$$\beta' = - \left(\frac{p+1}{p}\right)^{1/2} C_0 \sin\theta(x) \quad (4.5.30)$$

To determine  $\theta(x)$ , differentiation of (4.5.22) yields:

$$\frac{2p}{p+1} \cdot \beta^{\frac{2p}{p+1}} \cdot \frac{\beta'}{\beta} = - 2C_0^2 \cos\theta \sin\theta \theta' \quad (4.5.31)$$

Using Eqns. (4.5.22), (4.5.29) and (4.5.30), this reduces to:

$$\theta' = \left(\frac{p}{p+1}\right)^{1/2} C_0^{-1/p} (\cos\theta)^{-1/p} \quad (4.5.32)$$

Integrating this w.r.t.  $x$  between the limits  $x = 0$  and  $x = x_0$  along with condition (4.5.26),  $\theta(x)$  can be written as:

$$\theta(x) = \left(\frac{p}{p+1}\right)^{1/2} C_0^{-1/p} \int_0^x (\cos\theta)^{-1/p} dx; \quad 0 \leq x \leq x_0 \quad (4.5.33)$$

constant  $C_0$  can be determined using the condition (4.5.27) which yields:

$$\left(\frac{p}{p+1}\right)^{1/2} C_0^{-1/p} = \frac{\pi}{2 \int_0^{x_0} (\cos\theta)^{-1/p} dx} \quad (4.5.34)$$

Substituting this in Eqns. (4.5.32) and (4.5.33), following expressions for  $\theta'$  and  $\theta(x)$  can be written.

$$\theta' = \frac{\pi}{2} \frac{(\cos\theta)^{-1/p}}{\int_0^{x_0} (\cos\theta)^{-1/p} dx} \quad (4.5.35)$$

$$\theta(x) = \frac{\pi}{2} \frac{\int_0^x (\cos\theta)^{-1/p} dx}{\int_0^{x_0} (\cos\theta)^{-1/p} dx}; \quad 0 \leq x \leq x_0 \quad (4.5.36)$$

Eqn. (4.5.36) thus determines  $\theta(x)$  for  $0 \leq x \leq x_0$  for a given value of  $x_0$ . Now,  $\theta(x)$  in the region  $x_0 \leq x \leq 1/2$  is obtained by integrating (4.5.35). The expression obtained is:

$$\theta(x) = \frac{\pi}{2} - \frac{\pi}{2} \frac{\int_{x_0}^x (\cos\theta)^{-1/p} dx}{\int_0^{x_0} (\cos\theta)^{-1/p} dx}; \quad x_0 \leq x \leq 1/2 \quad (4.5.37)$$

It may be noted that by the use of (4.5.35) to get (4.5.37) continuity of  $\theta$  and  $\theta'$  is ensured at  $x = x_0$ . This implies continuity of  $\beta$  and  $\beta'$  also. Now the Eqn. (4.5.37) determines  $\theta(x)$  in the region  $x_0 \leq x \leq 1/2$  for a given value of  $x_0$ . The only quantity which still remains to be determined is  $x_0$ . This is to be determined from the condition (4.5.28) which is still to be fulfilled. This gives

$$\theta(1/2) = \pi = \frac{\pi}{2} - \frac{\pi}{2} \frac{\int_{x_0}^{1/2} (\cos\theta)^{-1/p} dx}{\int_0^{x_0} (\cos\theta)^{-1/p} dx} \quad (4.5.38)$$

$$\text{or } \int_0^{x_0} (\cos\theta)^{-1/p} dx + \int_{x_0}^{1/2} (\cos\theta)^{-1/p} dx = 0 \quad (4.5.39)$$

since  $0 \leq \theta \leq \pi/2$  for  $0 \leq x \leq x_0$  and  $\pi/2 \leq \theta \leq \pi$  for  $x_0 \leq x \leq 1/2$ , first term in (4.5.39) is positive and the second is negative. We have thus obtained all the relevant relations (4.5.36), (4.5.37) and (4.5.39) to set up iterative scheme to determine  $\theta$  and hence  $\beta$ ,  $\lambda$  and  $e(x)$ . The steps involved, therefore, are:

1. Choose an initial value for  $x_0$ , say, 0.25. This appears to be a reasonable value as the location of the point of inflexion is not expected to vary considerably with  $p$ .

2. Select an initial function  $\theta_n(x)$  such that it varies from 0 to  $\pi/2$  for  $0 \leq x \leq x_0$  and is greater than  $\pi/2$  in the region  $x_0 \leq x \leq 1/2$ . This ensures  $\theta > \pi/2$  for  $x_0 \leq x \leq 1/2$  in all the subsequent iterations.
3. Determine  $\theta_{n+1}(x)$  for the next cycle of iteration from the following expressions which are written from (4.5.36) and (4.5.37)

$$\theta_{n+1}(x) = \frac{\pi}{2} \frac{\int_0^x (\cos \theta_n)^{-1/p} dx}{\int_0^{x_0} (\cos \theta_n)^{-1/p} dx}; \quad 0 \leq x \leq x_0 \quad (4.5.40)$$

$$\theta_{n+1}(x) = \frac{\pi}{2} \left( 1 - \frac{\int_{x_0}^x (\cos \theta_n)^{-1/p} dx}{\int_0^{x_0} (\cos \theta_n)^{-1/p} dx} \right); \quad x_0 \leq x \leq 1/2 \quad (4.5.41)$$

4. Using the new value of  $\theta(x)$  i.e.  $\theta_{n+1}(x)$ , repeat the step 3, till convergence on  $\theta$  is attained.
5. Now check if the determined value of  $\theta$  satisfies Eqn. (4.5.39). If it is not satisfied, suitably select another value of  $x_0$  and repeat the steps 2 to 4 till the simultaneous convergence on  $\theta$  and  $x_0$  is obtained.

### Selection of initial $x_0$

To select this suitable value of  $x_0$ , two methods (a) Newton-Raphson and (b) successive increments, were employed.

#### 4.5.1.1 Newton-Raphson

Denoting L.H.S. of (4.5.39) by  $F(x_0^j)$  for the  $j^{\text{th}}$  value of  $x_0$ ,  $x_0^{j+1}$  can be determined from the following

$$x_0^{j+1} = x_0^j - \frac{F(x_0)}{\left. \frac{d}{dx} F(x_0) \right|_{x_0 = x_0^j}} \quad (4.5.42)$$

where

$$F(x_0^j) = \int_0^{x_0^j} (\cos \theta)^{-1/p} dx + \int_{x_0^j}^{1/2} (\cos \theta)^{-1/p} dx \quad (4.5.43)$$

It was however discovered that some times  $x_0^{j+1} - x_0^j$  is so large that the convergence on the value of  $x_0$  does not take place. This scheme finally did not work for the present problem and so was abandoned.

#### 4.5.1.2 Incremental steps

In this method, starting with some initial value of  $x_0$ ,  $F(x_0)$  defined in (4.5.43), is computed. Value of

$x_0$  is then increased or decreased by suitably fixed intervals  $\Delta x_0$  and at each stage  $F(x_0)$  is determined. This is carried out till, for two successive values of  $x_0$ ,  $F(x_0)$  changes sign. Using linear interpolation the new value of  $x_0$  is determined. The value of  $F(x_0)$  is checked to see if it meets termination criterion. Mostly it does. If termination criterion is not met by this value of  $x_0$ , another value is determined in the manner explained. The process is repeated, till the convergence on  $x_0$  is reached.

#### 4.5.1.3 Comments on the method of partial integration

The method involves, unlike the method of successive iterations, only one integration in the iterative process and so is expected to be faster from the convergence point of view. However it does not happen. This is perhaps due to the existence of singularity at the inflexion point. No matter how carefully, the approximations are made in the region around singularity, Eqn. (4.5.39) could not be satisfied within reasonable limits. From academic point of view, the method was applied to the hinged-hinged B.C.'s also. It was found that it miserably failed, whereas the method of successive iterations, as already shown, works pretty well. Thus this innocent looking method had to be abandoned.

#### 4.5.2 Runga-Kutta method

Dividing the region of integration into two parts as done in Section (3.9.3) and using the same notation, the governing equation and the B.C.'s in the two regions can be restated as:

$$\beta_1'' + \beta_1^{\frac{p-1}{p+1}} = 0; \quad 0 \leq x \leq x_0 \quad (0 \leq x_1 \leq x_0) \quad (4.5.44)$$

$$\beta_2'' + \beta_2^{\frac{p-1}{p+1}} = 0; \quad x_0 \leq x \leq 0.5 \quad (0 \leq x_2 \leq 0.5 - x_0) \quad (4.5.45)$$

$$\beta_1'(0) = 0 \quad (3.9.101)$$

$$\beta_1(x_0) = 0 \quad (3.9.102)$$

$$\beta_2(0) = 0 \quad (3.9.103)$$

$$\beta_2'(0.5 - x_0) = 0 \quad (3.9.104)$$

$$\beta_1'(x_0) = \beta_2'(0) \quad (3.9.105)$$

Eqns. (4.5.44) and (4.5.45) are integrated by using **quartic** Runga-Kutta method. Since only one initial condition is specified for  $\beta_1$ , the other initial condition is obtained by using Newton-Raphson technique which involves integration of one more equation. The method is a standard one and is given below.

Let the unknown initial condition on  $\beta_1$  be

$$\beta_1(0) = \alpha \quad (4.5.46)$$

Differentiating Eqns. (4.5.44), (4.5.46) and (3.9.101)

partially with respect to  $\alpha$ , one gets:

$$\beta_{1\alpha}'' + \left(\frac{p-1}{p+1}\right) \beta_1' \frac{2}{p+1} \beta_{1\alpha} = 0 \quad (4.5.47)$$

$$\beta_{1\alpha}(0) = 1 \quad (4.5.48)$$

$$\beta_{1\alpha}'(0) = 0 \quad (4.5.49)$$

where  $\beta_{1\alpha}$  denotes partial derivative of  $\beta_1$  w.r.t.  $\alpha$ .

Now for the given value of  $x_0$ ,  $\alpha$  is to be determined such that the condition (3.9.102) is satisfied. This is obtained from Newton-Raphson technique. If  $\alpha_n$  and  $\alpha_{n+1}$  are the values of  $\alpha$  for the  $n^{\text{th}}$  and  $n+1^{\text{th}}$  iteration, then

$$\alpha_{n+1} = \alpha_n - \frac{\beta_1(x_0)}{\beta_{1\alpha}(x_0)} \quad (4.5.50)$$

Now, once  $\alpha$  is determined, the solution for  $\beta_2$  is obtained in one step as the initial conditions for  $\beta_2$  are known from the conditions (3.9.103) and (3.9.105). Inflexion point location,  $x_0$ , is then obtained by satisfying the condition (3.9.104).

The steps of iteration can now be outlined as:

1. Assume a suitable value of  $x_0$  which was taken to be  $1/4$ .
2. Choose a value of  $\alpha$  (say  $\alpha_n$ ) and integrate the Eqn. (4.5.44) using the condition (3.9.101).
3. Using the solution for  $\beta_1$  obtained in step 2, integrate the Eqn. (4.5.47) for  $\beta_{1\alpha}$  for the initial conditions (4.5.48) and (4.5.49).
4. Now determine  $\alpha_{n+1}$  from (4.5.50).
5. Repeat the steps 2 to 4, with this new value of  $\alpha$ , till  $\alpha$  converges.
6. Using the value of  $\beta_1'(x_0)$  from step 2 and using the initial conditions (3.9.103) and (3.9.105) integrate the Eqn. (4.5.45) for  $\beta_2$ .
7. Now check if the condition (3.9.104) is satisfied. If not, using the method of incremental steps outlined in Section (4.5.1), determine new  $x_0$  and repeat the above steps.
8. The process is to be continued till convergence on  $x_0$  is achieved.

Having determined  $\beta$  and  $x_0$ ,  $\lambda$  and  $e$  are determined from Eqns. (3.8.86) and (3.8.82).

#### 4.5.2.1 Comments on the method

The method worked quite satisfactorily for  $p > 1$ . Convergence is very fast and the results agree with those obtained by the method of successive iterations. However the method fails for  $p < 1$ . Specially for  $p \leq 0.4$ , the method completely breaks down. This happens perhaps due to the fact that the governing Eqns. (4.5.44), (4.5.45) and (4.5.47) for  $\beta_1$ ,  $\beta_2$  and  $\beta_{1\alpha}$  respectively are singular. Despite approximating  $\beta_1$ ,  $\beta_2$  and  $\beta_{1\alpha}$  in various ways near the singularity, the method did not work. And hence, this method was also abandoned. Finally, the method of successive iterations, which is discussed now, worked and has been used in all the problems treated in this thesis.

#### 4.5.3 Method of successive iterations

Integrating Eqn. (4.5.44) once w.r.t.  $x_1$  between the limits 0 to  $x_1$  and using the condition (3.9.101), one gets:

$$\beta_1' = - \int_0^{x_1} \beta_1^{-r} dx_1 \quad (4.5.51)$$

where  $r$  is defined in (4.3.13). At  $x = x_0$ , Eqn. (4.5.51), therefore, yields:

$$\beta_1'(x_0) = - \int_0^{x_0} \beta_1^{-r} dx_1 \quad (4.5.52)$$

Now integration of (4.5.51) between the limits  $x_1$  to  $x_0$ , along with the condition (3.9.102), yields the following expression for  $\beta_1$ .

$$\beta_1 = \int_{x_1}^{x_0} \int_0^{x_1} \beta_1^{-r} dx_1^2 ; \quad 0 \leq x_1 \leq x_0 \quad (4.5.53)$$

Integrating Eqn. (4.5.45) w.r.t.  $x_2$  between the limits 0 to  $x_2$  and using Eqns. (3.9.105) and (4.5.52),  $\beta_2'$  is obtained as:

$$\beta_2' = - \int_0^{x_0} \beta_1^{-r} dx_1 - \int_0^{x_2} \beta_2^{-r} dx_2 \quad (4.5.54)$$

Integrating the above equation again between the limits 0 to  $x_2$  and using the condition (3.9.103), expression for  $\beta_2$  is obtained as:

$$\beta_2 = - \left[ x_2 \int_0^{x_0} \beta_1^{-r} dx_1 + \int_0^{x_2} \int_0^{x_2} \beta_2^{-r} dx_2^2 \right] ;$$

$$0 \leq x_2 \leq 0.5 - x_0 \quad (4.5.55)$$

The condition (3.9.104), which has not been satisfied so far can be incorporated in (4.5.54) to determine  $x_0$ .

$$\int_0^{x_0} \beta_1^{-r} dx_1 + \int_0^{0.5 - x_0} \beta_2^{-r} dx_2 = 0 \quad (4.5.56)$$

All the relevant expressions which take care of all the B.C.'s of the problem are thus established. The iteration can now be outlined.

### Steps in Iteration

1. Select a suitable value of  $x_0$ .
2. Choose initial starting functions  $\beta_1$  and  $\beta_2$ . The functions corresponding to  $p = 1$ , for which the analytical solution is obtained in Section (3.9.3), are selected as the initial functions. This ensures that  $\beta_1 > 0$  and  $\beta_2 < 0$ .
3. Determine new values of  $\beta_1$  and  $\beta_2$  from (4.5.53) and (4.5.55).
4. With these new values of  $\beta_1$  and  $\beta_2$  repeat the step 3 until  $\beta_1$  and  $\beta_2$  converge. To check the convergence compute  $\lambda$  in each cycle of iteration. Stop iteration when the percentage difference in the values of  $\lambda$  for two consecutive cycles falls below a preassigned small value  $\epsilon$ . One thus gets the solution of the problem for a given  $x_0$  which is still to be determined.

5. Check, now, if the Eqn. (4.5.56) is satisfied. If not, use method of incremental steps to determine  $x_0$  i.e. take a new value of  $x_0$  and repeat the steps 2 to 4 till the simultaneous convergence on  $\beta$  and  $x_0$  is achieved. One then gets a numerical solution of the governing equation for the prescribed B.C.'s.

#### Expressions for $\lambda$ and $e(x)$

Equations to determine the eigen value  $\lambda$  and the modulus  $e(x)$  can now be easily written from (3.8.86) and (3.8.82).

$$\lambda = \left[ 2 \int_0^{x_0} (\beta_1^2)^{\frac{p}{p+1}} dx_1 + 2 \int_0^{0.5-x_0} (\beta_2^2)^{\frac{p}{p+1}} dx_2 \right]^{-\frac{1}{p}} \quad (4.5.57)$$

$$e_1(x_1) = \lambda (\beta_1^2)^{\frac{p}{p+1}} ; \quad 0 \leq x_1 \leq x_0 \quad (0 \leq x \leq x_0) \quad (4.5.58)$$

$$e_2(x_2) = \lambda (\beta_2^2)^{\frac{p}{p+1}} ; \quad 0 \leq x_2 \leq 0.5-x_0 \quad (x_0 \leq x \leq 0.5-x_0) \quad (4.5.59)$$

where  $e_1(x_1)$  and  $e_2(x_2)$  correspond to modulus distribution  $e(x)$  in the regions governed by  $x_1$  and  $x_2$  respectively.

#### 4.5.3.1 Comments on the method

The method is very efficient. Convergence is rapid for  $p$  having values close to unity. Number of iterations increases considerably as  $p$  is reduced from 1 to 0.05. In all the cases termination condition (4.5.56) could be met practically to any degree of accuracy. The method is thus definitely superior to the method of partial integration where it becomes very difficult to satisfy similar termination criterion.

It may be stated here that, in all the cases, the inflexion point location  $x_0$  remains fixed at  $x_0 = 1/4$ . In other words, inflexion point location for optimal columns considered here, is invariant irrespective of the values of  $p$  and  $q$ . They occur at a distance of  $L/4$  from each of the clamped ends. Since this is not known apriori, one is likely to determine  $x_0$  numerically by initially selecting a value which is not exactly  $1/4$ . Numerical experience reveals that it is practically impossible to reach this value by starting from any other value of  $x_0$ . Numerical instabilities are encountered and it is very hard to satisfy termination criterion. Unfortunately the method of partial integration and Runge-Kutta method discussed in Sections 4.5.1 and 4.5.2 did not work even with  $x_0 = 1/4$ .

Runga-Kutta method, though worked for  $p > 0$  but did not meet the termination criterion as accurately as the method of successive iterations.

All the computations have been performed in double precision by dividing the region of integration into two hundred parts. The general nature of the solution is the same as that obtained for  $p = 1$  in Section 3.9.3. Results are discussed and presented in Section 5.7 where uniform and tapered columns are discussed simultaneously.

#### 4.6 Clamped-Hinged Column

Since a clamped-hinged column is also characterized by an inflexion point,  $x_0$ , Eqns. (4.5.44) and (4.5.45) are to be solved in this case for the B.C.'s stated in (3.9.117) to (3.9.121). Method of successive iterations is now applied to determine  $\beta_1$  and  $\beta_2$ .

Integration of (4.5.44) between the limits 0 to  $x_1$  yields:

$$\beta_1'(x_1) - \beta_1'(0) + \int_0^{x_1} \beta_1^{-r} dx_1 = 0 \quad (4.6.61)$$

Integrating this once again between the limits  $x_1$  to  $x_0$  and using (3.9.118), one gets:

$$\beta_1(x_1) = -(x_0 - x_1) \beta_1'(0) + \int_{x_1}^{x_0} \int_0^{x_1} \beta_1^{-r} dx_1^2 \quad (4.6.62)$$

Using condition (3.9.117), this reduces to:

$$\beta_1(x_1) = (x_0 - x_1) \beta_1(0) + \int_{x_1}^{x_0} \int_0^{x_1} \beta_1^{-r} dx_1^2 \quad (4.6.63)$$

and hence

$$\beta_1(0) = -\beta_1'(0) = \frac{\int_0^{x_0} \int_0^{x_1} \beta_1^{-r} dx_1^2}{(1 - x_0)} \quad (4.6.64)$$

Substituting for  $\beta_1(0)$  in (4.6.63), following relation for  $\beta_1$  is obtained.

$$\beta_1(x_1) = \frac{x_0 - x_1}{1 - x_0} \int_0^{x_0} \int_0^{x_1} \beta_1^{-r} dx_1^2 + \int_{x_1}^{x_0} \int_0^{x_1} \beta_1^{-r} dx_1^2 \quad (4.6.65)$$

### Expression for $\beta_2(x_2)$

Integrating (4.5.45) between 0 to  $x_2$  and using (3.9.121) and (4.6.64),  $\beta_2'(x_2)$  is obtained as:

$$\beta_2'(x_2) = -\frac{\int_0^{x_0} \int_0^{x_1} \beta_1^{-r} dx_1^2}{(1 - x_0)} - \int_0^{x_2} \beta_2^{-r} dx_2 \quad (4.6.66)$$

This together with (3.9.119) yields:

$$\beta_2(x_2) = -\frac{x_2}{(1-x_0)} \int_0^{x_0} \int_0^{x_1} \beta_1^{-r} dx_1^2 - \int_0^{x_2} \int_0^{x_2} \beta_2^{-r} dx_2^2 \quad (4.6.67)$$

#### Determination of $x_0$

Eqns. (4.6.65) and (4.6.67) determine  $\beta(x)$  for a specified  $x_0$  which can be determined by satisfying the remaining B.C. (3.9.120). This gives

$$F(x_0) = -\beta_2(1-x_0) = -\int_0^{x_0} \int_0^{x_1} \beta_1^{-r} dx_1^2 + \int_0^{1-x_0} \int_0^{x_2} \beta_2^{-r} dx_2^2 = 0 \quad (4.6.68)$$

Thus Eqns. (4.6.65), (4.6.67) and (4.6.68) define relevant steps to determine the iterative solution for  $\beta(x)$ . This scheme, however, does not work because condition (4.6.68) cannot be met for all values of  $p$ . The method has been developed in such a way that all the equations and conditions except the condition of zero moment, which is used to determine  $x_0$ , at the hinged end are satisfied exactly. During computations  $\beta_1$  and  $\beta_2$  are kept positive and negative respectively. For a particular value of  $x_0$ , in some cases, it is found that  $\beta_2(1-x_0)$  comes out to be positive. This means, singularity which is supposed to occur at the hinged

end occurs earlier. This creates serious numerical problems as one not only needs to determine contributions,  $\Delta_1$ ,  $\Delta_2$ , and  $\Delta_3$ , due to the peaks (Figure 4.1c) but also another contribution,  $\Delta_4$ , at the right hand side of second singularity which should occur exactly at the hinged end. Since it is cumbersome to incorporate  $\Delta_4$  in the iterative process, the above scheme had to be abandoned.

#### 4.6.1 Alternative scheme

This scheme attempts to satisfy the zero moment condition at the hinged end exactly and the condition of continuity of  $\beta'$  at  $x = x_0$  approximately.

Integration of (5.4.45), twice, and use of (3.9.119) gives:

$$\beta_2'(x_2) - \beta_2'(0) + \int_0^{x_2} \beta_2^{-r} dx_2 = 0 \quad (4.6.69)$$

$$-\beta_2'(x_2) - (1 - x_0 - x_2) \beta_2'(0) + \int_{x_2}^{1-x_0} \int_0^{x_2} \beta_2^{-r} dx_2^2 = 0 \quad (4.6.70)$$

Hence the condition (3.9.120) determines  $\beta_2'(0)$  and  $\beta_2(x_2)$ .

$$\beta_2'(0) = \frac{1}{1-x_0} \int_0^{1-x_0} \int_0^{x_2} \beta_2^{-r} dx_2^2 \quad (4.6.71)$$

$$\beta_2(x_2) = - \frac{(1-x_0-x_2)}{(1-x_0)} \int_0^{1-x_0} \int_0^{x_2} \beta_2^{-r} dx_2^2 + \int_{x_2}^{(1-x_0)} \int_0^{x_2} \beta_2^{-r} dx_2^2 \quad (4.6.72)$$

It is evident from (4.6.72) that  $\beta_2(0)$  and  $\beta_2(1-x_0)$  are zero. Thus by choosing  $\beta_2(x_2)$  initially as a negative function, it always remains negative at every stage of iteration.

#### Determination of $x_0$

Condition (3.9.121) will now be applied to determine  $x_0$ . Using (4.6.64) and (4.6.71) it can be restated as:

$$F(x_0) = -\beta_1'(x_0) + \beta_2'(0) = \frac{1}{1-x_0} \left[ \int_0^{x_0} \int_0^{x_1} \beta_1^{-r} dx_1^2 + \int_0^{1-x_0} \int_0^{x_2} \beta_2^{-r} dx_2^2 \right] \quad (4.6.73)$$

It may be noted that  $\beta_1$  being positive and  $\beta_2$  being negative, first integral in (4.6.73) is positive and the second one is negative.

#### 4.6.2 Steps in iteration

Equations (4.6.65), (4.6.72) and (4.6.73) provide the relevant steps in the iterative process to determine the solution for  $\beta(x)$ . These may be stated as:

1. Choose a suitable value of  $x_0$ . The value ( $x_0 = 0.29289$ ) obtained for the case  $p = 1$  serves as a good starting point.
2. Choose initial functions  $\beta_1(x_1)$  and  $\beta_2(x_2)$  such that  $\beta_1 > 0$  and  $\beta_2 < 0$ . Solution for  $p = 1$  provides a good initial guess.
3. Using these functions determine new  $\beta_1(x_1)$  and  $\beta_2(x_2)$  from (4.6.65) and (4.6.72) and continue iteration till the convergence takes place. To avoid premature termination convergence is sought on the eigen value  $\lambda$ .
4. Now check if the Eqn. (4.6.73) is satisfied. This ensures that the chosen value of  $x_0$  and the solution obtained satisfy the condition of continuity of shear force at the inflexion point. If it is so, the iteration is to be stopped. Otherwise a new value of  $x_0$  is selected and above steps are then repeated. Method of incremental steps is used to select  $x_0$ . Besides, to avoid premature termination instead of applying the criterion  $|F(x_0)| < \epsilon$ , the following conditions is used.

$$\frac{|F(x_0)|}{|\beta_1'(x_0)|} < \varepsilon \quad (4.6.74)$$

#### 4.6.3 Expressions for $\lambda$ and $e(x)$

Once the solution for  $\beta$  is determined,  $\lambda$  and  $e(x)$  are easily obtained from (3.8.86) and (3.8.82).

$$\lambda = \left[ \int_0^{x_0} (\beta_1^2)^{\frac{p}{p+1}} dx_1 + \int_0^{1-x_0} (\beta_2^2)^{\frac{p}{p+1}} dx_2 \right]^{-\frac{1}{p}} \quad (4.6.75)$$

$$e_1(x_1) = \lambda (\beta_1^2)^{\frac{p}{p+1}} ; \quad 0 \leq x_1 \leq x_0 \quad (0 \leq x \leq x_0) \quad (4.6.76)$$

$$e_2(x_2) = \lambda (\beta_2^2)^{\frac{p}{p+1}} ; \quad 0 \leq x_2 \leq 1-x_0 \quad (x_0 \leq x \leq 1) \quad (4.6.77)$$

The solution is determined for various values of  $p$  ranging from 0.05 to 5. Eigen value  $\lambda$ , percent increase in load and the inflexion point location are available in Tables 5.3 and 5.4 and Figure 5.1b. Corresponding modulus distribution is given in Table 5.7 and Figure 5.4. A discussion on results is presented later in Section 5.7.

## CHAPTER - 5

### TAPERED-NONHOMOGENEOUS COLUMNS

#### 5.1 Introduction

In the present chapter, tapered columns are investigated for the maximum critical load. Unlike the uniform columns discussed in Chapters 3 and 4, tapered columns are generally characterized by the three design variables - cross-sectional area, modulus and density. As stated earlier in Sections 1.3 and 3.3, it is not feasible to consider these as independent variables. And so, only two independent variables  $e$  and  $\eta$  defined in (3.2.7) are considered here.

Essentially the approach for investigating tapered columns is the same as that for uniform columns, the only difference being the introduction of an additional design variable and a constraint.

The problem is stated in Section 5.2. Optimality conditions and governing equations are derived in Section 5.3. Analytical and numerical results are obtained in Sections 5.4 and 5.5 for various types of end fixities. Section 5.6 provides interpretation of  $e$  and  $\eta$  for tapered columns and Section 5.7 offers discussion and comments on

where the variables  $\phi$ ,  $\eta$  and  $e$  are defined in (3.2.7) and  $g_1$  and  $g_2$  state the boundary conditions.

### 5.3 Necessary Conditions and the Governing Equation

Following the steps in Section 3.6, Eqns. (2.3.12) to (2.3.18) can be easily applied to derive the necessary conditions. Defining

$$y_1 = \phi \quad (5.3.2)$$

$$y_2 = \phi' \quad (5.3.3)$$

equilibrium equation (3.2.8) is represented by the following two first order equations.

$$y_1' = y_2 = f_1 \quad (5.3.4)$$

$$y_2' = -\lambda \eta^{-q} e^{-1} y_1 = f_2 \quad (5.3.5)$$

Now using Eqns. (3.3.26), (3.5.33), (3.5.34), (5.3.4) and (5.3.5), augmented functional  $\bar{J}$  can be written as:

$$\begin{aligned} \bar{J} = & \sum_{i=1}^2 \gamma_i g_i + \int_0^1 \left[ \lambda_0 \eta + \sum_{i=1}^2 \lambda_i(x) (y_i' - f_i) \right. \\ & \left. + \gamma_3 (e^p - 1) \right] dx \end{aligned} \quad (5.3.6)$$

Functions  $G$  and  $H$ , defined in (2.3.9) and (2.3.10) are easily obtained from (5.3.6).

$$G = \gamma_1 g_1 + \gamma_2 g_2 \quad (5.3.7)$$

$$H = \lambda_1 f_1 + \lambda_2 f_2 - \lambda_0 \eta - \gamma_3 (e^p - 1)$$

$$\text{or } H = \lambda_1 y_2 - \lambda_2 \lambda e^{-1} \eta^{-q} y_1 - \lambda_0 \eta - \gamma_3 (e^p - 1) \quad (5.3.8)$$

### Necessary conditions

Applying equations (2.3.12) and (2.3.13) to the function  $H$  defined in (5.3.8), following equations are obtained.

$$\lambda_1' = - \frac{\partial H}{\partial y_1} = \lambda_2 \lambda e^{-1} \eta^{-q} \quad (5.3.9)$$

$$\lambda_2' = - \frac{\partial H}{\partial y_2} = - \lambda_1 \quad (5.3.10)$$

$$\frac{\partial H}{\partial \eta} = \lambda_2 q \lambda e^{-1} \eta^{-(1+q)} y_1 - \lambda_0 = 0 \quad (5.3.11)$$

$$\frac{\partial H}{\partial e} = \lambda_2 \lambda e^{-2} \eta^{-q} y_1 - \gamma_3 p e^{p-1} = 0 \quad (5.3.12)$$

Differentiating  $\lambda_2'$  once and then substituting  $\lambda_1'$  from (5.3.9) one easily gets:

$$\lambda_2'' + \lambda e^{-1} \eta^{-q} \lambda_2 = 0 \quad (5.3.13)$$

Now, since the form of function  $G$  defined in (5.3.7) is the same as that in (3.6.42) for the uniform column, the

equations obtained in Section 3.7 are applicable here also. Boundary conditions on  $\lambda_2$  are thus the same as those on  $\phi$  for each set of end conditions. From Eqn. (5.3.13) it is obvious that  $\lambda_2$  and  $\phi$  are governed by the same differential equation also. It thus easily follows that  $\lambda_2$  and  $\phi$  are related through a constant. Hence

$$\lambda_2 = K\phi \quad (5.3.14)$$

#### Optimality condition

Using (5.3.2) and (5.3.14) in (5.3.11) and (5.3.12) following relations are obtained.

$$\frac{\phi^2}{e \eta^{1+q}} = \frac{\lambda_0}{K q \lambda} \quad (5.3.15)$$

$$\frac{\phi^2}{e^{p+1} \eta^q} = \frac{\gamma_3^p}{K \lambda} \quad (5.3.16)$$

Eqns. (5.3.15) and (5.3.16) establish relationships between the design variables  $e$  and  $\eta$  and the state variable  $\phi$ .

These may be termed as the optimality conditions. Eliminating  $\phi$  one gets the following relationship between the variables  $e$  and  $\eta$ .

$$\frac{e^p}{\eta} = \frac{\lambda_0}{\gamma_3^p pq} \quad (5.3.17)$$

Integrating (5.3.17) and using (3.3.26) and (5.2.1) with  $\bar{m} = 1$ , one gets:

$$\int_0^1 e^p dx = \frac{\lambda_0}{\gamma_{3pq}} \int_0^1 \eta dx \quad (5.3.18)$$

or 
$$\frac{\lambda_0}{\gamma_{3pq}} = 1 \quad (5.3.19)$$

Hence (5.3.17) yields:

$$\eta = e^p \quad (5.3.20)$$

Substitution of  $\eta$  from (5.3.20) into (5.3.15), yields:

$$\frac{\phi^2}{e^{1+p+pq}} = \frac{\lambda_0}{Kq\lambda} \quad (5.3.21)$$

or 
$$e^p = \left( \frac{Kq\lambda}{\lambda_0} \phi^2 \right)^{\frac{p}{1+p+pq}} \quad (5.3.22)$$

Now, redefining (assuming  $K \neq 0$ )

$$\psi = \left( \frac{Kq}{\lambda_0} \right)^{\frac{1}{2}} \phi \quad (5.3.23)$$

Eqn. (5.3.22) reduces to

$$e^p = (\lambda \psi^2)^{\frac{p}{1+p+pq}} \quad (5.3.24)$$

Now substituting for  $e$  and  $\eta$  in terms of  $\psi$ , by using Eqns. (5.3.20), (5.3.23) and (5.3.24), the Eqn. (3.2.8) can be rewritten in terms of only one variable  $\psi$ .

$$\psi'' + \lambda \cdot (\lambda \psi^2)^{-\frac{1}{1+p+pq}} \cdot (\lambda \psi^2)^{-\frac{pq}{1+p+pq}} \psi = 0 \quad (5.3.25)$$

$$\text{or } \psi'' + \lambda^{\frac{p}{1+p+pq}} \cdot \frac{\psi}{(\psi^2)^{\frac{1+pq}{1+p+pq}}} = 0 \quad (5.3.26)$$

Eqn. (5.3.26) can be further simplified by making the transformation

$$\psi = \lambda^{\frac{p}{2(1+p)}} \beta \quad (5.3.27)$$

which reduces this to

$$\beta'' + \frac{\beta}{(\beta^2)^{\frac{1+pq}{1+p+pq}}} = 0 \quad (5.3.28)$$

Eqn. (5.3.28) is thus the governing equation in one variable  $\beta$  which is proportional to bending moment. This is to be solved for appropriate boundary conditions, representing the end fixities.

### Expressions for $e$ , $\eta$ and $\lambda$

Substitution of  $\psi$  from (5.3.27) into (5.3.24)

yields

$$e^p = \left( \lambda^{\frac{1+p+pq}{1+pq}} \cdot \beta^2 \right)^{\frac{p}{1+p+pq}} \quad (5.3.29)$$

$$\text{or} \quad \eta = e^p = \lambda^{\frac{p}{1+pq}} \cdot (\beta^2)^{\frac{p}{1+p+pq}} \quad (5.3.30)$$

$$\text{or} \quad e = \lambda^{\left(\frac{1}{1+pq}\right)} \cdot (\beta^2)^{\frac{1}{1+p+pq}} \quad (5.3.31)$$

Integrating (5.3.30) and using (3.3.26), one easily gets:

$$\lambda = \left[ \int_0^1 (\beta^2)^{\frac{p}{1+p+pq}} dx \right]^{-\left(\frac{1+pq}{p}\right)} \quad (5.3.32)$$

Once  $\beta$  is determined from the solution of Eqn. (5.3.28), eigen value  $\lambda$  representing the nondimensional critical load, is determined from (5.3.32). Variable  $e$  is then obtained from (5.3.31), and since  $\eta$  and  $e$  are related,  $\eta$  is determined from the Eqn. (5.3.20).

#### 5.3.1 Special case, $q = 0$

Eqns. (5.3.28), (5.3.32) and (5.3.31) reduce to the following Eqns. for  $q = 0$

$$\beta'' + \frac{\beta}{(\beta^2)^{\frac{1}{1+p}}} = 0 \quad (5.3.33)$$

$$\lambda = \left[ \int_0^1 (\beta^2)^{\left(\frac{p}{1+p}\right)} dx \right]^{-1/p} \quad (5.3.34)$$

$$e = \lambda (\beta^2)^{\frac{1}{1+p}} \quad (5.3.35)$$

It is interesting to note that these equations are the same as those obtained in Section 3.8 for a uniform column.

Hence the governing equations for the tapered columns can be easily applied to get the corresponding equations for the uniform column for which  $q = 0$ . Here it is a fortunate situation. But it may not be true always, since the number of constraints and the variables is not the same for uniform and tapered columns. It will be seen later in Section 7.5, while investigating optimal vibrating beams, that the equations for uniform beam cannot be obtained by putting  $q = 0$  in the Eqns. for the tapered beam.

#### 5.4 Analytical Solutions

Rewriting the governing Eqn. (5.3.28) as:

$$\beta'' + \beta^{\left(\frac{p-1-pq}{1+p+pq}\right)} = 0 \quad (5.4.36)$$

$$\text{or} \quad \beta'' + \beta^{-r} = 0 \quad (5.4.37)$$

where

$$r = \frac{1+pq-p}{1+pq+p} > 0 \quad (5.4.38)$$

It is evident that Eqn. (5.4.37) is singular for all values of  $p$  as  $q \geq 1$ . This singular behaviour as stated in Section (4.2) creates numerical difficulties and is crucial to get the correct results. Still for  $p = 1$ , the singularity is integrable and analytical solutions can be obtained. Substituting  $p = 1$  in (5.4.36), it reduces to:

$$\beta'' + \beta^{-\left(\frac{q}{2+q}\right)} = 0 \quad (5.4.39)$$

Multiplication by  $\beta'$  gives:

$$2\beta'\beta'' + 2\beta^{-\left(\frac{q}{2+q}\right)} \frac{d\beta}{dx} = 0 \quad (5.4.40)$$

$$\text{or} \quad \frac{d}{dx} (\beta'^2) + 2\beta^{-\left(\frac{q}{2+q}\right)} \frac{d\beta}{dx} = 0 \quad (5.4.41)$$

Integration of (5.4.41) between 0 to  $x$  yields

$$\beta'^2 + (q+2) \beta^{\frac{2}{2+q}} = (q+2)c^2 \quad (5.4.42)$$

where  $C$  is the constant of integration. Now it is convenient to express  $\beta$  in terms of a parameter  $\theta(x)$  by the following transformation.

$$\beta^{\frac{2}{2+q}} = C^2 \sin^2 \theta(x) \quad (5.4.43)$$

$$\text{or} \quad \beta = \pm [C \sin \theta(x)]^{q+2} \quad (5.4.44)$$

Introducing  $\beta$  from (5.4.43) in terms of  $\theta$ , Eqn. (5.4.42) reduces to

$$\beta'^2 = (q+2) C^2 \cos^2 \theta(x) \quad (5.4.45)$$

$$\text{or} \quad \beta' = \pm C (q+2)^{\frac{1}{2}} \cos \theta(x) \quad (5.4.46)$$

Differentiation in (5.4.44) yields another expression for  $\beta'$ .

$$\beta' = \pm (q+2) [C \sin \theta(x)]^{q+1} C \cos \theta(x) \frac{d\theta}{dx} \quad (5.4.47)$$

It may be stated here that in Eqns. (5.4.44), (5.4.46) and (5.4.47) only + sign is to be used for odd values of  $q$  and  $\pm$  sign for even values. Besides + sign is to be used in the region before the inflexion point and - sign after the inflexion point. It is necessary to do this to take care of the change in sign of  $\beta$  at the inflexion point for clamped-clamped and clamped-hinged end conditions.

Eliminating  $\beta'$  from (5.4.46) and (5.4.47) following equation in  $\theta$  is obtained,

$$\sqrt{q+2} [C \sin\theta(x)]^{q+1} \frac{d\theta}{dx} = 1 \quad (5.4.48)$$

$$\text{or} \quad (\sin\theta)^{q+1} d\theta = \frac{1}{\sqrt{q+2} C^{q+1}} dx \quad (5.4.49)$$

Integrating this between 0 to x

$$\int_0^x (\sin\theta)^{q+1} d\theta = \frac{1}{\sqrt{q+2} C^{1+q}} x \quad (5.4.50)$$

Eqn. (5.4.50), now has to be integrated separately for different values of  $q$ . Doing this and rewriting (5.4.44) and (5.4.46) for different values of  $q$ , following expressions are obtained.

Case 1:  $q = 1$

$$-\frac{1}{4} \sin 2\theta + \frac{\theta}{2} = -\frac{1}{4} \sin 2\theta(0) + \frac{\theta(0)}{2} + \frac{1}{\sqrt{3} C^2} x \quad (5.4.51)$$

$$\beta = C^3 \sin^3 \theta \quad (5.4.52)$$

$$\beta' = \sqrt{3} C \cos \theta \quad (5.4.53)$$

Case 2:  $q = 2$

$$\cos^3 \theta - 3 \cos \theta = \cos^3 \theta(0) - 3 \cos \theta(0) + \frac{3}{2C^3} x \quad (5.4.54)$$

$$\beta = \pm C^4 \sin^4 \theta \quad (5.4.55)$$

$$\beta' = \pm 2C \cos \theta \quad (5.4.56)$$

Case 3: q = 3

$$\frac{\sin 4\theta}{32} - \frac{\sin 2\theta}{4} + \frac{3\theta}{8} = \frac{\sin 4\theta(0)}{32} - \frac{\sin 2\theta(0)}{4} + \frac{3\theta(0)}{8} + \frac{x}{\sqrt{5} C^4} \quad (5.4.57)$$

$$\beta = C^5 \sin^5 \theta \quad (5.4.58)$$

$$\beta' = \sqrt{5} C \cos \theta \quad (5.4.59)$$

Here  $\theta(0)$  is another constant of integration which may be interpreted as the value of  $\theta$  at  $x = 0$ . Eqns. (5.4.51), (5.4.54) and (5.4.57), thus involve two constants  $C$  and  $\theta(0)$  which are to be determined from the boundary conditions.

Since there is hardly any difference in the approach to get the solution for different values of  $q$ , the detailed solution is therefore presented for  $q = 2$  only.

### Solutions for q = 2

#### 5.4.1 Hinged-Hinged column

The appropriate Eqns. and the B.C.'s for a H-H column are:

$$\cos^3 \theta - 3 \cos \theta = \cos^3 \theta(0) - 3 \cos \theta(0) + \frac{3}{2C^3} x \quad (5.4.54)$$

$$\beta = C^4 \sin^4 \theta \quad (5.4.55)$$

$$\beta' = 2C \cos \theta \quad (5.4.56)$$

$$\beta(0) = 0 \quad (3.9.91)$$

$$\beta'(1/2) = 0 \quad (3.9.92)$$

Boundary conditions (3.9.91) and (3.9.92) evidently imply:

$$\theta(0) = 0 \quad (5.4.60)$$

$$\theta(1/2) = \pi \quad (5.4.61)$$

Eqs. (5.4.54) and (5.4.61) together determine C as:

$$C = (3/8)^{1/3} \quad (5.4.62)$$

and hence  $\beta$  and  $\beta'$  reduce to:

$$\beta = \left(\frac{3}{8}\right)^{4/3} \sin^4 \theta \quad (5.4.63)$$

$$\beta' = 2 \cdot \left(\frac{3}{8}\right)^{1/3} \cos \theta \quad (5.4.64)$$

#### Expressions for $\theta$ , $e$ , $\eta$ and $\lambda$

Substitution of C and  $\theta(0)$  in (5.4.54), yields the following equation to determine  $\theta$ .

$$\cos^3 \theta - 3 \cos \theta = 2(2x - 1) \quad (5.4.65)$$

Rewriting of the Eqns. (5.3.20), (5.3.31) and (5.3.32) for  $p = 1$  and  $q = 2$  gives:

$$\eta = e = \lambda^{1/3} (\beta^2)^{1/4} \quad (5.4.66)$$

$$\lambda = \left[ \int_0^1 (\beta^2)^{1/4} dx \right]^{-3} \quad (5.4.67)$$

Since  $\beta$  is determined in terms of  $\theta$ , (5.4.67) can be rewritten as:

$$\lambda = \left[ 2 \int_{\theta(0)}^{\theta(1/2)} (\beta^2)^{1/4} \frac{dx}{d\theta} \cdot d\theta \right]^{-3} \quad (5.4.68)$$

Substituting for  $\beta$  from (5.4.55) and  $\frac{dx}{d\theta}$  from (5.4.48) in (5.4.68)

$$\lambda = \left[ 4C^5 \int_0^{\pi/2} \sin^5 \theta d\theta \right]^{-3} = \frac{1}{64} \left( \frac{8}{3} \right)^5 * \left( \frac{8}{15} \right)^{-3} = \frac{125}{9} \quad (5.4.69)$$

Expressions for  $\eta$  and  $e$  are now easily obtained from (5.4.63) and (5.4.67)

$$\eta = e = \left( \frac{125}{9} \right)^{1/3} \cdot \left( \frac{3}{8} \right)^{2/3} \sin^2 \theta \quad (5.4.70)$$

$$\text{or} \quad \eta = e = 1.25 \sin^2 \theta \quad (5.4.71)$$

Equation (5.4.71) provides the optimal modulus and cross-sectional area distributions and Eqn. (5.4.69) yields the corresponding critical load. Comparing this with the Euler load which is  $\pi^2$ , the increase in load is 40.8 percent.

Maximum value of  $\eta$  is 1.25 which in the case of tapered homogeneous column<sup>6</sup> is 1.33. This is expected because maximum modulus and area occur at the same station and so the additional stiffness is provided by the increase in modulus. Distribution of  $e$ , which is same as  $\eta$  here, is shown in Figure 5.5b.

#### 5.4.2 Free-Clamped column

As stated in Section (3.9.2)  $e$  and  $\eta$  distributions for a free-clamped column can be easily obtained from the solution for the H-H case. The critical load is one fourth the load for H-H column but the percent increase in the load is the same in both the cases (40.8).

#### 5.4.3 Clamped-Clamped column

Since C-C column is characterized by an inflexion point, where  $\beta$  changes sign, at  $x = x_0$ , the region of integration  $0 \leq x \leq 1/2$  is divided into two parts -  $0 \leq x \leq x_0$  and  $x_0 \leq x \leq 1/2$ . Defining the variables and

the undetermined constants as done in Section 3.9 , the following appropriate equations and the boundary conditions can be stated.

$$\beta_1 = c_1^4 \sin^4 \theta_1 \quad (5.4.72)$$

$$\beta_2 = -c_2^4 \sin^4 \theta_2 \quad (5.4.73)$$

$$\cos^3 \theta_i - 3 \cos \theta_i = \cos^3 \theta_i(0) - 3 \cos \theta_i(0) + \frac{3}{2c_i^3} x_i \quad (5.4.74)$$

$$\beta_1' = -2c_1 \cos \theta_1 \quad (5.4.75)$$

$$\beta_2' = -2c_2 \cos \theta_2 \quad (5.4.76)$$

$$\beta_1'(0) = 0 \quad (3.9.101)$$

$$\beta_1(x_0) = 0 \quad (3.9.102)$$

$$\beta_2(0) = 0 \quad (3.9.103)$$

$$\beta_2'(0.5 - x_0) = 0 \quad (3.9.104)$$

$$\beta_1'(x_0) = \beta_2'(0) \quad (3.9.105)$$

where  $i$  varies from 1 to 2 and the running coordinates  $0 \leq x_1 \leq x_0$  and  $0 \leq x_2 \leq 0.5 - x_0$  in the two regions correspond to  $0 \leq x \leq x_0$  and  $x_0 \leq x \leq 0.5$  respectively. Above equations easily give the following values of  $\theta_i$  at the end points of the two regions.

$$\theta_1(0) = \pi/2 \quad (5.4.77)$$

$$\theta_1(x_0) = \pi \quad (5.4.78)$$

$$\theta_2(0) = \pi \quad (5.4.79)$$

$$\theta_2(0.5-x_0) = 3\pi/2 \quad (5.4.80)$$

Satisfying (5.4.74) at  $x = x_0$  and  $x = 1/2$  and using the continuity condition (3.9.105) on  $\beta'$ ,  $x_0$ ,  $C_1$  and  $C_2$  are easily determined.

$$x_0 = 1/4 \quad (5.4.81)$$

$$C_1 = -C_2 = \left(\frac{3}{16}\right)^{1/3} \quad (5.4.82)$$

It may be stated here that, in a similar way,  $x_0$  was determined for  $q = 2$  and  $q = 3$  also and it was found that it remains the same. In other words, inflexion point location does not change with  $q$ .

Inserting the constants thus determined, in the Eqn. (5.4.74), the following expressions are obtained.

$$\cos^3\theta_1 - 3\cos\theta_1 = 8x_1; \quad 0 \leq x_1 \leq 1/4 \quad (5.4.83)$$

$$\cos^3\theta_2 - 3\cos\theta_2 = 2 - 8x_2; \quad 0 \leq x_2 \leq 1/4 \quad (5.4.84)$$

It may be stated that the above cubic equations can be solved exactly.

Expressions for  $e$ ,  $\eta$  and  $\lambda$

Using (5.4.67),  $\lambda$  can be determined in the following manner.

$$\begin{aligned}
 \lambda^{-1/3} &= 2 \int_0^{1/4} (\beta_1^2)^{1/4} dx_1 + 2 \int_0^{1/4} (\beta_2^2)^{1/4} dx_2 \\
 &= 2 \int_{\pi/2}^{\pi} (\beta_1^2)^{1/4} \frac{dx_1}{d\theta_1} d\theta_1 + 2 \int_{\pi}^{3\pi/2} (\beta_2^2)^{1/4} \frac{dx_2}{d\theta_2} d\theta_2 \\
 &= 4C_1^5 \left[ \int_{\pi/2}^{\pi} \sin^5 \theta_1 d\theta_1 - \int_{\pi}^{3\pi/2} \sin^5 \theta_2 d\theta_2 \right] \\
 &= \frac{64}{15} C_1^5 \quad (5.4.85)
 \end{aligned}$$

Inserting  $C_1$  from (5.4.82), one gets:

$$\lambda = \left(\frac{15}{64}\right)^3 \cdot \left(\frac{16}{3}\right)^5 = \frac{500}{9} \quad (5.4.86)$$

Eqn. (5.4.66) together with (5.4.86), (5.4.83) and (5.4.84) yields desired relations to determine  $e$  and  $\eta$ .

$$e_i = \eta_i = 1.25 \sin^2 \theta_i, \quad i = 1, 2 \quad (5.4.87)$$

Eqn. (5.4.86), here, determines critical load which is four times the load for the H-H column. Since this is true even for the Euler column, the percentage increase in load in this case is also 40.8 as obtained in

Section 5.4.1. Similarly Eqn. (5.4.87) provides the optimal modulus and area distributions whose maximum value is 1.25, which is the same as that for the hinged-hinged column.

Distribution of  $\theta(\eta)$  is shown in Figure 5.7b.

#### 5.4.4 Clamped-Hinged columns

These columns are also characterized by an inflexion point at  $x = x_0$ . Following the steps in Sections (3.9.4) and (5.4.3), it is evident that Eqns. (5.4.72) to (5.4.76) are applicable in this case also. The appropriate boundary conditions are stated in Eqns. (3.9.117) to (3.9.121) which are rewritten below for convenience.

$$\beta_1(0) + \beta_1'(0) = 0 \quad (3.9.117)$$

$$\beta_1(x_0) = 0 \quad (3.9.118)$$

$$\beta_2(0) = 0 \quad (3.9.119)$$

$$\beta_2(1-x_0) = 0 \quad (3.9.120)$$

$$\beta_1'(x_0) = \beta_2'(0) \quad (3.9.121)$$

Boundary conditions (3.9.117) to (3.9.121) when inserted in the expressions for  $\beta_i$  and  $\beta_i'$  give

$$\theta_1(x_0) = \theta_2(0) = \pi \quad (5.4.88)$$

$$\theta_2(1-x_0) = 2\pi \quad (5.4.89)$$

$$C_1 = -C_2 \quad (5.4.90)$$

Satisfying (5.4.74) at  $x_1 = x_0$  and  $x_2 = 1-x_0$ , and writing (3.9.117) in terms of  $\theta_0$ , following Eqns. are obtained to determine  $C_1$ ,  $x_0$  and  $\theta(0)$ .

$$t^3 - 3t + \frac{3}{2C_1^3} x_0 = 2 \quad (5.4.91)$$

$$\frac{x_0}{C_1^3} = \frac{1}{C_1^3} - \frac{8}{3} \quad (5.4.92)$$

$$C_1^3 = -\frac{2t}{1 - 2t^2 + t^4} \quad (5.4.93)$$

where

$$t = \cos\theta_1(0) \quad (5.4.94)$$

Elimination of variables in (5.4.91) to (5.4.93) yields:

$$t^4 - 6t^2 - 24t - 3 = 0 \quad (5.4.95)$$

$$x_0 = \frac{2 - t^3 + 3t}{6 - t^3 + 3t} \quad (5.4.96)$$

Eqns. (5.4.93) to (5.4.96) yield the following values for  $t$ ,  $\theta_1(0)$ ,  $x_0$  and  $C_1$ .

$$t = -0.1292 \quad (5.4.97)$$

$$\theta_1(0) = 1.7003 \quad (5.4.98)$$

$$x_0 = 0.2876 \quad (5.4.99)$$

$$c_1^3 = 0.2671 \quad (5.4.100)$$

Having thus determined the desired constants, the solution can be, now, easily obtained by following the steps in Section (5.4.3).

$$\cos^3 \theta_1 - 3\cos \theta_1 = 5.615 x_1 + 0.3853 \quad (5.4.101)$$

$$\beta_1 = 0.1721 \sin^4 \theta_1 \quad (5.4.102)$$

$$\frac{dx_1}{d\theta_1} = 0.5342 \sin^3 \theta_1 \quad (5.4.103)$$

$$\cos^3 \theta_2 - 3\cos \theta_2 = 5.615 \theta_2 - 2 \quad (5.4.104)$$

$$\beta_2 = -0.1721 \sin^4 \theta_2 \quad (5.4.105)$$

$$\frac{dx_2}{d\theta_2} = -0.5342 \sin^3 \theta_2 \quad (5.4.106)$$

Expressions for  $e$ ,  $\eta$  and  $\lambda$

$$\lambda^{-1/3} = \int_0^{x_0} (\beta_1^2)^{1/4} dx_1 + \int_0^{1-x_0} (\beta_2^2)^{1/4} dx_2 \quad (5.4.107)$$

$$\text{or } \lambda^{-1/3} = 2C_1^5 \left[ \int_{1.7003}^{\pi} \sin^5 \theta_1 d\theta_1 - \int_{\pi}^{2\pi} \sin^5 \theta_2 d\theta_2 \right] \quad (5.4.108)$$

Substituting for  $C_1$  and integrating

$$\lambda = 28.76 \quad (5.4.109)$$

Hence expressions for  $e$  and  $\eta$  are:

$$e_i = \eta_i = 1.273 \sin^2 \theta_i, \quad i = 1, 2 \quad (5.4.110)$$

Equation (5.4.109) determines the buckling load which is 42.43 percent more than the Euler load ( $\lambda_E = 20.19$ ). It is interesting to note that the increase in load for a C-H column is slightly more than the increase (40.8 percent) for other columns. This is observed even for tapered-homogeneous column<sup>6</sup> where the percent increase for C-H B.C. is 35.1 and for other B.C.'s it is 33.3.

Equation (5.4.110) provides the desired optimum distribution of  $e$  and  $\eta$ . Maximum value of these is 1.273 at station  $x_2$  where  $\theta_2(x_2) = 3\pi/2$ . Substitution of  $\theta_1(0)$  in (5.4.110) reveals that the value of  $e(\eta)$  at the clamped end is 1.25 which is the maximum value for other boundary conditions. Distribution of  $e(\eta)$  is shown graphically in Figure 5.9b.

### Solution for $q = 1$ and $q = 3$

Equation (5.4.50) is solved exactly for  $q = 2$  in Sections 5.4.1 to 5.4.4. For  $q = 1$  and  $q = 3$ , the resulting Eqns. (5.4.51) and (5.4.57) in  $\Theta$ , however, have to be solved numerically. The solution, therefore, in these cases is obtained numerically in Section 5.5, along with the solution for  $p \neq 1$ , which anyway cannot be obtained analytically. Corresponding  $e(\eta)$  distributions for various types of end conditions are shown in Figures 5.5 to 5.10.

The results are discussed in Section 5.7.

### 5.5 Numerical Solution

Governing Eqn. (5.4.37) is integrated numerically for  $p \neq 1$ . To check the results in Section 5.4, solution is obtained even for  $p = 1$ . It is found that the two solutions are the same.

Since the equation is singular at points where  $\beta$  is zero, integration around the singularity is to be done carefully. Following the steps in Section 3.7, contribution ( $\Delta$ ) of the peak around the singularity can be approximated by the following

$$\begin{aligned} \Delta &= \int_0^\epsilon \beta^{\left(\frac{p-1-pq}{p+1+pq}\right)} dx \\ &= \frac{|\beta''(\epsilon)| \epsilon}{(2p/1+p+pq)} \end{aligned} \quad (5.5.111)$$

It may be mentioned that the constant  $a$ , in Eqn. (4.2.8), which is used in getting (5.5.111) is obtained by matching  $\beta''$  at  $x = \epsilon$ .

The numerical integration is done by the method of successive iterations. Details of the method for each of the end conditions are discussed in Chapter 4. As mentioned in Section 5.3, uniform column being a special case of tapered column, the form of the governing equation and the boundary conditions in the two cases are the same. The equations for iteration as developed in Chapter 4 can therefore be directly applied here also, the only difference being in the value of the parameter  $r$ . In the present case  $r$  has the value

$$r = \frac{1+pq-p}{1+pq+p}, \quad r > 0 \quad (5.5.112)$$

which for the corresponding uniform column ( $q = 0$ ), as used in Chapter 4, is  $\frac{1-p}{1+p}$ . Therefore, there is hardly any need to rewrite the equations and steps of iteration. These are available for various end condition in Chapter 4.

It is worth mentioning here that computations in the case of clamped-clamped column reveal that the inflexion point location does not change with  $p$  and  $q$ . It always occurs at  $x_0 = 1/4$ . This could be shown analytically

for  $p = 1$ , but cannot be proved in general for any value of  $p$ , as the Eqn. (5.4.36) cannot be integrated analytically. Similar result holds for the Euler and tapered-homogeneous columns<sup>6</sup>.

In the case of clamped-hinged column, it is found that for all values of  $p$  and  $q$ , sum of the values of  $\beta'$  at the inflexion point and at the hinged end is zero. It is found to be exactly true for an Euler column and in the present work, it holds in the cases where analytical results have been obtained. This condition was therefore used as an additional check on numerical results.

## 5.6 Interpretation of $e$ and $\eta$ Distributions

Nondimensional quantities  $e$  and  $\eta$  are related to the physical quantities - modulus ( $E$ ), density ( $\rho$ ) and cross-sectional area ( $A$ ) - by the following relations obtained from (3.2.7).

$$e = \frac{\tilde{E}}{\tilde{\rho}^q} = \frac{(E/E_0)}{(\rho/\rho_0)^q} \quad (5.6.113)$$

$$\eta = \frac{\tilde{\rho}}{\rho_0} a = \frac{\rho A}{\rho_0 A_0} \quad (5.6.114)$$

where  $E_0$ ,  $\rho_0$  and  $A_0$  are modulus, density and cross-sectional area of the corresponding Euler column.

Now, if one can develop the material, such that  $\rho$  is a constant and equals  $\rho_0$ , then  $e$  and  $\eta$  reduce to the following nondimensional modulus and cross-sectional area.

$$e = \tilde{E} = E/E_0 \quad (5.6.115)$$

$$\eta = a = A/A_0 \quad (5.6.116)$$

Thus  $e$  and  $\eta$  distributions obtained in Sections 5.4 and 5.5 provide optimum modulus and area variations along the axis. Besides, since the nondimensionalization has been done with respect to the corresponding quantities for Euler column,  $e$  and  $\eta$  values at any particular station directly give the increase in modulus and area relative to Euler column for which these are unity.

If it is not possible to develop the material with density constant along the axis, then the Eqns. (5.6.113) and (5.6.114) imply that  $\tilde{E}$ ,  $\tilde{\rho}$  and  $a$  must be adjusted so that  $e$  and  $\eta$  obtained numerically remain the same. In other words, the three design variables(modulus, density and area) are in the control of the designer such that they can assume only those values, which yield the obtained distributions of  $e$  and  $\eta$ . From design standpoint it is obvious that one would like to keep one of the variables, which in this case could be cross-sectional area, constant and, if possible, vary modulus and density only, to get the desired

distributions of  $e$  and  $\eta$ . If it is feasible, one would like to have it from fabrication considerations. It is evident from (5.6.113) and (5.6.114) that if  $A$  is kept constant,  $e$  and  $\eta$  directly prescribe  $E$  and  $\rho$  distributions. The two extreme cases,  $p \ll 1$  and  $p \gg 1$ , will now be considered to examine the feasibility of maintaining constant area.

#### 5.6.1 Case 1, $p \ll 1$

Results reveal that in this case  $\eta(x) \approx 1$  and  $e(x)$  controls the increase in load. At stations where  $e$  is large, from (5.6.113),  $\tilde{E}$  should be large and  $\tilde{\rho}$  should be small. This is feasible by using high specific modulus fibers for increasing  $\tilde{E}$  and  $\tilde{\rho}$  can be made small by making  $a$ , which is constant when  $A$  is constant, in (5.6.114)  $> 1$ . This ensures smaller  $\tilde{\rho}$  for  $\eta(x) \approx 1$ .

#### 5.6.2 Case 2, $p \gg 1$

In this case  $e(x) \approx 1$  and  $\eta(x)$  controls the increase in load. Due to keeping constant  $A$ , higher  $\eta$  from (5.6.114) implies higher  $\tilde{\rho}$ . Since  $e(x) \approx 1$ , it implies from (5.6.113), the use of higher modulus fibers (large  $\tilde{E}$ ) where  $\eta$  is large. Magnitude of maximum values can, however, be reduced by making  $a > 1$ .

It thus, theoretically, seems to be feasible to produce, in practice, the numerically obtained distributions of  $e$  and  $\eta$ . Consequently large increases in critical loads can be achieved.

## 5.7 Results and Discussion

As already stated, uniform as well as tapered columns are governed by the same equations. Computations reveal certain features which are common to both. A unified discussion is therefore presented.

Essentially, Eqn. (5.4.36) has been solved for uniform ( $q = 0$ ) and tapered ( $q = 1, 2, 3$ ) columns. For each value of  $q$ ,  $p$  varies from values very close to zero (0.05) to five at appropriate intervals. For each set of the values of the parameters  $p$  and  $q$ , solution is obtained for four boundary conditions - H-H, F-C, C-C, C-H. Fortunately the solution for free-clamped case is easily deducible from the solution for the H-H case, because of the similarity in boundary conditions in the two cases. Computations, therefore, are performed for only three different end conditions.

In each case  $e$ ,  $\eta$  and nondimensionalized stiffness( $s$ ), defined by

$$s = e \eta^q, \quad (5.7.117)$$

distributions are determined along with the eigen value  $\lambda$ . Though  $s$  can be determined from  $c$  and  $\eta$ , still it is computed to check for any anomalies in the numerical results. Since one cannot appreciate the increase in load by looking at the values of  $\lambda$ , the results are presented in the form of percent increase in load.

The results are presented both in the tabular and graphical forms.

#### 5.7.1 Tables

Tables 5.1 to 5.3 provide the variation of the critical load and the percent increase in load with  $p$  for uniform and tapered columns, for all the four end conditions. Location of inflexion point in the case of clamped-hinged column is separately given for different values of  $q$  and  $p$  in Table 5.4.

Tables 5.5 to 5.7 provide the variation along the axis for uniform columns for different values of  $p$  and for all the four end conditions.

Tables 5.8 to 5.13 provide  $e$  and  $\eta$  variations along the axis for tapered columns for various values of  $p$  and all the boundary conditions.

Most of the results have been obtained for  $p \geq 0.05$ . However, for academic interest results were obtained for  $p = 0.02$  also in the case of hinged-hinged column with  $q = 1$ . It was done to test the method and the behaviour of percent increase in load versus  $p$  curve. Computation worked satisfactorily, but was not extended to other cases because of the large computation time and infeasible distributions of  $e$  obtained,  $e_{\max}$  becoming really large.

### 5.7.2 Curves

Figure 5.1 provides variation of percent increase in buckling load-with  $p$  for uniform and tapered columns for each of the four end conditions.

Figures 5.2 to 5.4, provide distribution of  $e$  for uniform columns for various end fixities. These variations, though have been computed for several values of  $p$  and presented in tabular forms, are shown only for three values  $p = 0.1$ ,  $p = 1.0$  and  $p = 5.0$ . These curves largely represent the entire range of variation of  $p$  and typically indicate the trends of variations. Results for  $p = 1.0$  are shown primarily because the governing equation could be integrated analytically. Besides,  $p \ll 1.0$  and  $p \gg 1.0$ , represent the extreme cases. The value  $p = 0.1$ , is selected since the

distributions obtained for this appear to be physically realizable. For  $p < 0.1$ , maximum modulus values could be so high that they may become hard to be achieved.

Figures 5.5 to 5.10 provide  $e$  and  $\eta$  distributions for tapered columns for various end conditions.

Figure 5.11 finally gives variation of number of iterations with  $p$  for various end conditions. Curves are drawn for  $q = 1$  only. These curves reflect on the efficiency of the method of successive iterations.

### 5.7.3 Important observations

The following observations, highlighting the important features of the results can be made from a study of the tables and curves.

#### $p$ versus $\lambda$ curves

Percent increase in load versus  $p$  curves for all values of  $q$  and all end fixities is monotonic, load increasing with decreasing value of  $p$ . Theoretically any increase in load can be achieved by selecting small values of  $p$ . But higher the increase in load, higher is the  $e_{\max}$  required. This physically limits the increase in load. As an example,  $p = 0.02$  results in an increase of 97.73 percent in load with  $e_{\max} = 3.06$  for a hinged-hinged column with  $q = 1$ .

As  $p$  increases, percent increase in load decreases asymptotically to zero for a uniform column and approaches to the value for the corresponding homogeneous columns in the tapered case. For  $q = 2$ , it can be seen that it tends to 33.3 percent in the case of H-H, F-C and C-C end fixities and 35.1 percent for C-H boundary condition. These results were obtained by Tadjbaksh and Keller<sup>6</sup>. This is expected because a large value of  $p$  implies approximately a constant modulus,  $e(x) \approx 1$ , which corresponds to Euler column in uniform case and tapered-homogeneous in the remaining cases.

For a particular value of  $q$ , percent increase in load versus  $p$  curves are identical for H-H, F-C and C-C columns. It is observed that for uniform and as well as tapered columns, the load for a hinged-hinged column is four times the load for free-clamped column, and the load for clamped-clamped case is four times the load for the H-H case. This behaviour is observed for all values of  $p$ . Thus the concept of equivalent length, developed for the Euler column is valid for nonhomogeneous, uniform and tapered columns also. Though this has been shown in Section 3.9.2 analytically for F-C column, it appears to be true for a C-C column also. This is because of the invariant location of inflexion points which occur at a distance of  $L/4$  from either ends. Thus it implies that C-C column is equivalent

to a H-H column of length  $L/2$ . This means that the results including the distributions of  $e$  and  $\eta$  can be deduced from the results for H-H column. This, however, is not obvious from the equations and boundary conditions. One arrives at these conclusions only after the computations are done separately for C-C columns. Besides, since the results in C-C case are obtained by satisfying different B.C.'s, the agreement in the results with those obtained for H-H column provides an indirect check on numerical computations. This is important, specially, when  $p$  is small, which poses numerical problems and may lead to incorrect results. There are hardly any results, available in the literature, with which the obtained results can be compared. The available results, however, correspond to only extreme values of the parameter  $p$  ( $p \gg 1$ ).

Finally it is observed that though the inflexion point location varies with  $p$  and  $q$  for clamped-hinged columns, this variation is very small. Further, the eigen value is not very sensitive to the location of inflexion points. Thus small errors in computing this location, do not affect the critical load appreciably.

### e and $\eta$ distributions

The general trend of  $e$  and  $\eta$  variation along the axis is similar to the variation of bending moment in the column. Thus  $e$  and  $\eta$  assume maximum and minimum values where bending moment is a maximum or minimum.

With increasing  $p$ ,  $e$  curve becomes more and more flat i.e. the column tends to become homogeneous. However,  $\eta$  distribution approaches to the area distribution for an optimum tapered-homogeneous column. Specially for  $q = 2$ , it can be seen to approach the curves in Ref. 6.

With decreasing  $p$ ,  $\eta$  curves become more and more flat. This amounts to the fact that the increase in buckling load is largely contributed by optimum modulus distribution. This is in fact true. The maximum increase that can be obtained by optimum tapering ( $q = 2$ ) only, is 33.3 percent, the additional increase is due to the modulus variation. For an increase in load above sixty percent, modulus plays the major role. Uniform column therefore is to be preferred to a tapered column for higher increases in load to avoid the inconvenience in fabrication of a tapered column. But this increase is limited by the maximum value of the required  $e$  distribution. Since the tapered column for the same  $e_{\max}$  produces a higher increase in load, it is to be recommended in cases where higher load is of utmost importance.

Maximum value of  $\eta$  in all the cases is less than  $\eta_{\max}$  for the corresponding homogeneous column. For  $q = 2$ , it can be seen that it is less than 1.5, obtained by Tadjbaksh and Keller<sup>6</sup> for H-H, F-C and C-C end conditions.

Distributions of  $e$  and  $\eta$  for each half of the C-C column are symmetric about the inflexion point. This permits to deduce the solution from the solution of the hinged-hinged column.

### Comments

Results thus reveal the existence of a tremendous increase in load by suitable variation of modulus. If proper materials can be developed, it is then possible to prescribe distributions of modulus and area to achieve a desired increase in load. The prescribed distributions are optimum in the sense considered in this thesis.

It may be mentioned that both for the uniform and tapered columns, materials may be developed with constant density and prescribed modulus distributions. While developing the material, in practice, the density obtained may or may not be the same ( $\rho_0$ ) as that of the corresponding Euler column. Since the column under consideration must have the same mass ( $m_0$ ) as the corresponding Euler column, **in such a case, it is possible to do so by suitably adjusting**

the cross-sectional area distribution. For example, for a uniform column, if  $\rho < \rho_0$ , then by taking  $A > A_0$  it is possible to have  $\eta(x) = 1$ . Similarly the dimensionless area ( $a(x) = A/A_0$ ) can be suitably adjusted for tapered columns.

Finally, in the solutions obtained in Chapters 3, 4 and 5, eigen value has been made stationary only. In fact, it is optimal also, as shown by Tadjbaksh and Keller<sup>6</sup> who have considered the general problem of determining the stationary eigen value of second order systems with homogeneous boundary conditions, and then through integral inequalities have shown that the obtained stationary value is the maximum of the minimum eigen values of the system for  $n < 1$ , where  $n$  is a constant defined in Eqn. 4, Section 5 of Ref. 6. This depends on the parameters of the system (in our case  $p$  and  $q$ ). Both the uniform and tapered columns, studied here, can be put as a special case of the above general problem. It can be easily shown that

$$n = - \frac{p}{1+pq} \quad (5.7.118)$$

Since  $p > 0$  and  $q \geq 1$ ,  $n$  in our case is negative which is less than one. Hence the solutions obtained are not only stationary but optimal also.

## 5.8 Comments on Efficiency of Method of Successive Iterations

A study of the number of iterations required for the convergence was made, in all the cases including different values of  $p$  and  $q$  and various types of end conditions. Generally, it is found that the convergence occurs in few iterations if the value of  $p$  is around unity. For  $p$  less than or greater than one, number of iterations,  $n$ , required for convergence starts increasing. This increase is not much if  $p > 1$ , but as  $p$  approaches zero, the increase in  $n$  is very high. From academic point of view, solution was obtained for a H-H column with  $q = 1$  and  $p = 0.02$ . Convergence in this case took place after 222 iterations. This is also one of the reasons for determining the solutions in all other cases for  $p \geq 0.05$ .

The general trend of number of iterations ( $n$ ) versus  $p$  curves essentially remaining the same for different values of  $q$  ( $q = 0, 1, 2, 3$ ),  $n$  versus  $p$  curves are therefore drawn for all the end conditions - H-H, C-C and C-H - for  $q = 1$  only. These are shown in Figure 5.11.

Table 5.1: Variation of  $\lambda$  and percent increase in buckling load with  $p$  for hinged-hinged and free-clamped\* columns

p	q = 0		q = 1		q = 2		q = 3	
	$\lambda$	percent increase	$\lambda$	percent increase	$\lambda$	percent increase	$\lambda$	percent increase
0.05	16.97	71.92	17.04	72.66	17.13	73.55	17.21	74.41
0.1	15.86	60.67	16.00	62.11	16.14	63.57	16.26	64.80
0.4	13.56	37.44	14.17	43.59	14.61	48.02	14.94	51.42
0.8	12.35	25.13	13.37	35.47	14.04	42.26	14.51	47.03
1.0	12.00	21.59	13.16	33.37	13.90	40.81	14.41	45.97
3.0	10.76	9.03	12.45	26.21	13.44	36.18	14.08	42.63
5.0	10.41	5.49	12.28	24.46	13.33	35.06	14.00	41.90

$$* \lambda_{F-C} = \frac{\lambda_{H-H}}{4}$$

Table 5.2: Variation of  $\lambda$  and percent increase in buckling load with  $p$  for clamped-clamped columns

p	q = 0		q = 1		q = 2		q = 3	
	$\lambda$	percent increase	$\lambda$	percent increase	$\lambda$	percent increase	$\lambda$	percent increase
0.05	67.87	71.92	68.23	72.82	68.51	73.55	68.86	74.41
0.1	63.43	60.67	64.00	62.11	64.57	63.57	65.06	64.80
0.4	54.24	37.40	56.66	43.51	58.44	48.02	59.78	51.43
0.8	49.40	25.14	53.47	35.45	56.16	42.26	58.01	46.95
1.0	48.00	21.59	52.65	33.36	55.56	40.73	57.62	45.96
3.0	42.98	8.87	49.82	26.20	53.76	36.18	56.32	42.65
5.0	41.64	5.49	49.14	24.46	53.31	35.05	56.05	41.97

Table 5.5: Variation of  $e$  along the axis for hinged-hinged and free-clamped uniform columns

Station	p=0.05	p=0.1	p=0.4	p=0.8	p=1	p=3	p=5
0	0	0	0	0	0	0	0
1	0.1993	0.1892	0.2080	0.2584	0.2850	0.4969	0.6190
2	0.5461	0.5126	0.4906	0.5207	0.5400	0.6934	0.7746
3	0.9414	0.8759	0.7785	0.7617	0.7650	0.8343	0.8779
4	1.339	1.238	1.049	0.9755	0.9600	0.9429	0.9541
5	1.710	1.573	1.291	1.159	1.125	1.028	1.012
6	2.035	1.865	1.496	1.311	1.260	1.094	1.056
7	2.299	2.103	1.660	1.430	1.365	1.144	1.089
8	2.495	2.278	1.779	1.515	1.440	1.178	1.111
9	2.615	2.385	1.851	1.566	1.485	1.198	1.125
10	2.655	2.421	1.875	1.584	1.500	1.205	1.129

(Stations are located at equal intervals along the axis).

Table 5.6: Variation of  $e$  along the axis for clamped-clamped uniform columns

x	p=0.05	p = 0.1	p = 0.4	p = 0.8	p = 1	p = 3	p = 5
0	2.655	2.421	1.875	1.584	1.500	1.205	1.129
0.05	2.495	2.278	1.779	1.515	1.440	1.178	1.111
0.10	2.035	1.865	1.496	1.311	1.260	1.094	1.056
0.15	1.339	1.238	1.049	0.9755	0.9600	0.9429	0.9541
0.20	0.5461	0.5126	0.4906	0.5207	0.5400	0.6934	0.7746
0.25	0	0	0	0	0	0	0
0.30	0.5461	0.5126	0.4906	0.5207	0.5400	0.6934	0.7746
0.35	1.339	1.238	1.049	0.9755	0.9600	0.9429	0.9541
0.40	2.035	1.865	1.496	1.311	1.260	1.094	1.056
0.45	2.495	2.278	1.779	1.515	1.440	1.178	1.111
0.50	2.655	2.421	1.875	1.584	1.500	1.205	1.129

Table 5.7: Variation of  $e$  along the axis for clamped-hinged uniform columns

x	p=0.05	p = 0.1	p = 0.4	p = 0.8	p = 1	p = 3	p = 5
0	2.672	2.475	1.869	1.583	1.500	1.205	1.129
0.1	1.889	1.770	1.416	1.268	1.226	1.085	1.051
0.2	0.7482	0.7184	0.6576	0.6892	0.7054	0.8157	0.8679
0.3	0.0399	0.0380	0.0515	0.0558	0.0615	0.1441	0.2191
0.4	1.021	0.9690	0.8590	0.8012	0.7946	0.8366	0.8760
0.5	2.061	1.931	1.560	1.339	1.280	1.095	1.055
0.6	2.645	2.464	1.928	1.609	1.519	1.208	1.130
0.7	2.608	2.430	1.904	1.597	1.510	1.207	1.130
0.8	1.959	1.835	1.492	1.305	1.254	1.090	1.053
0.9	0.8881	0.8420	0.7599	0.7467	0.7506	0.8249	0.8721
1.0	0	0	0	0	0	0	0

Table 5.8: Variation of  $e$  along the axis for hinged-hinged and free-clamped tapered columns

a) for  $q = 1$

Station	p=0.05	p = 0.1	p = 0.4	p = 0.8	p = 1	p = 3	p = 5
0	0	0	0	0	0	0	0
1	0.2165	0.2209	0.3128	0.4236	0.4687	0.7084	0.8004
2	0.5651	0.5482	0.5999	0.6748	0.7041	0.8476	0.8979
3	0.9495	0.8938	0.8509	0.8671	0.8770	0.9342	0.9557
4	1.328	1.225	1.066	1.020	1.011	0.9952	0.9953
5	1.677	1.525	1.247	1.142	1.116	1.040	1.024
6	1.979	1.782	1.394	1.237	1.197	1.073	1.045
7	2.224	1.988	1.508	1.309	1.258	1.097	1.060
8	2.404	2.139	1.588	1.359	1.300	1.114	1.070
9	2.513	2.230	1.637	1.389	1.325	1.123	1.076
10	2.550	2.261	1.653	1.399	1.333	1.126	1.078

Table 5.8: Continued

b) for  $q = 2$ 

Station	p=0.05	p = 0.1	p = 0.4	p = 0.8	p = 1	p = 3	p = 5
0	0	0	0	0	0	0	0
1	0.2333	0.2514	0.3993	0.5369	0.5858	0.8008	0.8693
2	0.5830	0.5796	0.6739	0.7593	0.7878	0.9036	0.9378
3	0.9568	0.9086	0.8924	0.9147	0.9238	0.9643	0.9768
4	1.318	1.214	1.070	1.032	1.024	1.006	1.003
5	1.647	1.485	1.213	1.121	1.100	1.036	1.022
6	1.930	1.714	1.326	1.190	1.157	1.057	1.035
7	2.157	1.895	1.412	1.240	1.199	1.073	1.045
8	2.323	2.027	1.473	1.275	1.228	1.083	1.051
9	2.424	2.106	1.508	1.296	1.245	1.089	1.055
10	2.458	2.133	1.520	1.303	1.250	1.091	1.056

Table 5.8: Concluded

c) for  $q = 3$ 

Station	p=0.05	p = 0.1	p = 0.4	p = 0.8	p = 1	p = 3	p = 5
0	0	0	0	0	0	0	0
1	0.2499	0.2806	0.4693	0.6159	0.6633	0.8504	0.9040
2	0.5998	0.6076	0.7265	0.8110	0.8366	0.9309	0.9562
3	0.9634	0.9209	0.9184	0.9401	0.9477	0.9773	0.9855
4	1.309	1.205	1.068	1.034	1.027	1.008	1.005
5	1.620	1.451	1.186	1.105	1.086	1.031	1.019
6	1.885	1.657	1.278	1.158	1.130	1.047	1.028
7	2.097	1.818	1.347	1.197	1.162	1.058	1.035
8	2.252	1.935	1.395	1.224	1.184	1.066	1.040
9	2.346	2.005	1.423	1.239	1.196	1.070	1.043
10	2.377	2.029	1.433	1.244	1.201	1.072	1.044

(Stations are located at equal intervals along the axis).

Table 5.9: Variation of  $\eta$  along the axis for hinged-hinged and free-clamped tapered columns

a) for  $q = 1$

Station	$p=0.05$	$p = 0.1$	$p = 0.4$	$p = 0.8$	$p = 1$	$p = 3$	$p = 5$
0	0	0	0	0	0	0	0
1	0.9263	0.8598	0.6282	0.5030	0.4687	0.3554	0.3284
2	0.9719	0.9417	0.8151	0.7300	0.7041	0.6089	0.5835
3	0.9974	0.9888	0.9375	0.8922	0.8770	0.8153	0.7973
4	1.014	1.021	1.026	1.016	1.011	0.9856	0.9769
5	1.026	1.043	1.092	1.112	1.116	1.125	1.126
6	1.035	1.059	1.142	1.185	1.197	1.236	1.245
7	1.041	1.071	1.178	1.240	1.258	1.321	1.337
8	1.045	1.079	1.203	1.278	1.300	1.381	1.403
9	1.047	1.084	1.218	1.300	1.325	1.417	1.442
10	1.048	1.085	1.223	1.308	1.333	1.429	1.455

Table 5.9: Continued

b) for  $q = 2$

Station	$p=0.05$	$p = 0.1$	$p = 0.4$	$p = 0.8$	$p = 1$	$p = 3$	$p = 5$
0	0	0	0	0	0	0	0
1	0.9298	0.8710	0.6927	0.6081	0.5858	0.5136	0.4965
2	0.9734	0.9469	0.8540	0.8023	0.7878	0.7378	0.7252
3	0.9978	0.9905	0.9555	0.9311	0.9238	0.8966	0.8894
4	1.014	1.020	1.027	1.025	1.024	1.017	1.015
5	1.025	1.040	1.080	1.096	1.100	1.110	1.113
6	1.033	1.055	1.120	1.149	1.157	1.182	1.188
7	1.039	1.066	1.148	1.188	1.199	1.235	1.244
8	1.043	1.073	1.167	1.215	1.228	1.271	1.282
9	1.045	1.077	1.179	1.231	1.245	1.293	1.305
10	1.046	1.079	1.182	1.236	1.250	1.300	1.313

Table 5.9: Concluded

c) for  $q = 3$ 

Station	p=0.05	p = 0.1	p = 0.4	p = 0.8	p = 1	p = 3	p = 5
0	0	0	0	0	0	0	0
1	0.9330	0.8807	0.7389	0.6786	0.6633	0.6150	0.6038
2	0.9748	0.9514	0.8800	0.8457	0.8366	0.8068	0.7995
3	0.9981	0.9918	0.9665	0.9518	0.9477	0.9334	0.9298
4	1.015	1.019	1.027	1.027	1.027	1.025	1.025
5	1.024	1.038	1.071	1.083	1.086	1.095	1.097
6	1.032	1.052	1.103	1.124	1.130	1.147	1.151
7	1.038	1.062	1.127	1.155	1.162	1.185	1.190
8	1.041	1.068	1.142	1.175	1.184	1.211	1.217
9	1.044	1.072	1.152	1.187	1.196	1.226	1.233
10	1.044	1.073	1.155	1.191	1.201	1.231	1.238

(Stations are located at equal intervals along the axis).

Table 5.10: Variation of  $e$  along the axis for clamped-clamped tapered columnsa) for  $q = 1$ 

x	p=0.05	p = 0.1	p = 0.4	p = 0.8	p = 1	p = 3	p = 5
0	2.550	2.261	1.653	1.399	1.333	1.126	1.078
0.05	2.404	2.139	1.588	1.359	1.300	1.114	1.070
0.10	1.979	1.782	1.394	1.237	1.197	1.073	1.045
0.15	1.328	1.225	1.066	1.020	1.011	0.9952	0.9953
0.20	0.5651	0.5482	0.5999	0.6748	0.7041	0.8476	0.8979
0.25	0	0	0	0	0	0	0
0.30	0.5651	0.5482	0.5999	0.6748	0.7041	0.8476	0.8979
0.35	1.328	1.225	1.066	1.020	1.011	0.9952	0.9953
0.40	1.979	1.782	1.394	1.237	1.197	1.073	1.045
0.45	2.404	2.139	1.588	1.359	1.300	1.114	1.070
0.50	2.550	2.261	1.653	1.399	1.333	1.126	1.078

Table 5.10: Continued

b) for  $q = 2$ 

x	p=0.05	p = 0.1	p = 0.4	p = 0.8	p = 1	p = 3	p = 5
0	2.458	2.133	1.520	1.303	1.250	1.091	1.056
0.05	2.323	2.027	1.473	1.275	1.228	1.083	1.051
0.10	1.930	1.714	1.326	1.190	1.157	1.057	1.035
0.15	1.318	1.214	1.070	1.032	1.024	1.006	1.003
0.20	0.5830	0.5796	0.6739	0.7593	0.7878	0.9036	0.9378
0.25	0	0	0	0	0	0	0
0.30	0.5830	0.5796	0.6739	0.7593	0.7878	0.9036	0.9378
0.35	1.318	1.214	1.070	1.032	1.024	1.006	1.003
0.40	1.930	1.714	1.326	1.190	1.157	1.057	1.035
0.45	2.323	2.027	1.473	1.275	1.228	1.083	1.051
0.50	2.458	2.133	1.520	1.303	1.250	1.091	1.056

Table 5.10: Concluded

c) for  $q = 3$ 

x	p=0.05	p = 0.1	p = 0.4	p = 0.8	p = 1	p = 3	p = 5
0	2.377	2.029	1.433	1.244	1.201	1.072	1.044
0.05	2.252	1.935	1.395	1.224	1.184	1.066	1.040
0.10	1.885	1.657	1.278	1.158	1.130	1.047	1.028
0.15	1.309	1.205	1.068	1.034	1.027	1.008	1.005
0.20	0.5998	0.6076	0.7265	0.8110	0.8366	0.9309	0.9562
0.25	0	0	0	0	0	0	0
0.30	0.5998	0.6076	0.7265	0.8110	0.8366	0.9309	0.9562
0.35	1.309	1.205	1.068	1.034	1.027	1.008	1.005
0.40	1.885	1.657	1.278	1.158	1.130	1.047	1.028
0.45	2.252	1.935	1.395	1.224	1.184	1.066	1.040
0.50	2.377	2.029	1.433	1.244	1.201	1.072	1.044

Table 5.11: Variation of  $\eta$  along the axis for clamped-clamped tapered columnsa) for  $q = 1$ 

x	p=0.05	p = 0.1	p = 0.4	p = 0.8	p = 1	p = 3	p = 5
0	1.048	1.085	1.223	1.308	1.333	1.429	1.455
0.05	1.045	1.079	1.203	1.278	1.300	1.381	1.403
0.10	1.035	1.059	1.142	1.185	1.197	1.236	1.245
0.15	1.014	1.021	1.026	1.016	1.011	0.9856	0.9769
0.20	0.9719	0.9417	0.8151	0.7300	0.7041	0.6089	0.5835
0.25	0	0	0	0	0	0	0
0.30	0.9719	0.9417	0.8151	0.7300	0.7041	0.6089	0.5835
0.35	1.014	1.021	1.026	1.016	1.011	0.9856	0.9769
0.40	1.035	1.059	1.142	1.185	1.197	1.236	1.245
0.45	1.045	1.079	1.203	1.278	1.300	1.381	1.403
0.50	1.048	1.085	1.223	1.308	1.333	1.429	1.455

Table 5.11: Continued

b) for  $q = 2$ 

x	p=0.05	p = 0.1	p = 0.4	p = 0.8	p = 1	p = 3	p = 5
0	1.046	1.079	1.182	1.236	1.250	1.300	1.313
0.05	1.043	1.073	1.167	1.215	1.228	1.271	1.282
0.10	1.033	1.055	1.120	1.149	1.157	1.182	1.188
0.15	1.014	1.020	1.027	1.025	1.024	1.017	1.015
0.20	0.9734	0.9469	0.8540	0.8023	0.7878	0.7378	0.7252
0.25	0	0	0	0	0	0	0
0.30	0.9734	0.9469	0.8540	0.8023	0.7878	0.7378	0.7252
0.35	1.014	1.020	1.027	1.025	1.024	1.017	1.015
0.40	1.033	1.055	1.120	1.149	1.157	1.182	1.188
0.45	1.043	1.073	1.167	1.215	1.228	1.271	1.282
0.50	1.046	1.079	1.182	1.236	1.250	1.300	1.313

Table 5.11: Concluded

c) for  $q = 3$ 

x	p=0.05	p = 0.1	p = 0.4	p = 0.8	p = 1	p = 3	p = 5
0	1.044	1.073	1.155	1.191	1.201	1.231	1.238
0.05	1.041	1.068	1.142	1.175	1.184	1.211	1.217
0.10	1.032	1.052	1.103	1.124	1.130	1.147	1.151
0.15	1.014	1.019	1.027	1.027	1.027	1.025	1.025
0.20	0.9748	0.9514	0.8800	0.8457	0.8366	0.8068	0.7995
0.25	0	0	0	0	0	0	0
0.30	0.9748	0.9514	0.8800	0.8457	0.8366	0.8068	0.7995
0.35	1.014	1.019	1.027	1.027	1.027	1.025	1.025
0.40	1.032	1.052	1.103	1.124	1.130	1.147	1.151
0.45	1.041	1.068	1.142	1.175	1.184	1.211	1.217
0.50	1.044	1.073	1.155	1.191	1.201	1.231	1.238

Table 5.12: Variation of  $e$  along the axis for clamped-hinged tapered columnsa) for  $q = 1$ 

x	p=0.05	p = 0.1	p = 0.4	p = 0.8	pp = 1	p = 3	p = 5
0	2.561	2.301	1.657	1.379	1.331	1.125	1.076
0.1	1.840	1.693	1.339	1.185	1.168	1.063	1.038
0.2	0.7611	0.7413	0.7463	0.7754	0.8138	0.9087	0.9385
0.3	0.0466	0.0526	1.131	0.2237	0.2300	0.4890	0.6317
0.4	1.023	0.9809	0.9193	0.9263	0.9152	0.9479	0.9648
0.5	1.999	1.838	1.440	1.273	1.219	1.080	1.049
0.6	2.535	2.295	1.687	1.426	1.350	1.131	1.081
0.7	2.501	2.265	1.671	1.415	1.343	1.129	1.080
0.8	1.905	1.753	1.390	1.238	1.195	1.072	1.044
0.9	0.8964	0.8611	0.8347	0.8574	0.8670	0.9294	0.9527
1.0	0	0	0	0	0	0	0

Table 5.12: Continued

b) for  $q = 2$ 

x	p=0.05	p = 0.1	p = 0.4	p = 0.8	p = 1	p = 3	p = 5
0	2.572	2.166	1.529	1.303	1.250	1.088	1.053
0.1	1.887	1.632	1.287	1.164	1.135	1.046	1.028
0.2	0.8454	0.7635	0.8041	0.8527	0.8698	0.9369	0.9592
0.3	0.0239	0.0671	1.759	0.3126	0.3679	0.6785	0.7835
0.4	0.9614	0.9877	0.9485	0.9533	0.9570	0.9809	0.9874
0.5	1.887	1.760	1.359	1.211	1.174	1.065	1.040
0.6	2.396	2.159	1.544	1.317	1.263	1.097	1.059
0.7	2.381	2.133	1.532	1.311	1.257	1.095	1.058
0.8	1.842	1.685	1.322	1.188	1.156	1.057	1.035
0.9	0.8994	0.8767	0.8780	0.9055	0.9160	0.9614	0.9751
1.0	0	0	0	0	0	0	0

Table 5.12: Concluded

c) for  $q = 3$ 

x	p=0.05	p = 0.1	p = 0.4	p = 0.8	p = 1	p = 3	p = 5
0	2.379	2.057	1.442	1.248	1.202	1.072	1.044
0.1	1.757	1.583	1.248	1.114	1.113	1.041	1.025
0.2	0.7839	0.7831	0.8422	0.8899	0.9031	0.9596	0.9744
0.3	0.0613	0.0826	0.2365	0.4003	0.4668	0.7384	0.8281
0.4	1.026	0.9928	0.9655	0.9709	0.9750	0.9879	0.9922
0.5	1.894	1.694	1.304	1.173	1.143	1.051	1.031
0.6	2.354	2.048	1.450	1.255	1.210	1.075	1.046
0.7	2.325	2.025	1.441	1.250	1.205	1.073	1.045
0.8	1.813	1.628	1.274	1.156	1.129	1.045	1.028
0.9	0.9108	0.8896	0.9055	0.9322	0.9411	0.9747	0.9839
1.0	0	0	0	0	0	0	0

Table 5.13: Variation of  $\eta$  along the axis for clamped-hinged tapered columnsa) for  $q = 1$ 

x	p=0.05	p = 0.1	p = 0.4	p = 0.8	p = 1	p = 3	p = 5
0	1.048	1.087	1.224	1.293	1.331	1.425	1.446
0.1	1.031	1.054	1.124	1.146	1.168	1.201	1.205
0.2	0.9864	0.9705	0.8895	0.8159	0.8138	0.7504	0.7280
0.3	0.8579	0.7449	0.4182	0.3018	0.2300	0.1169	0.1006
0.4	1.001	0.9981	0.9669	0.9406	0.9152	0.8516	0.8360
0.5	1.035	1.063	1.157	1.213	1.219	1.259	1.271
0.6	1.048	1.087	1.233	1.328	1.350	1.448	1.477
0.7	1.047	1.085	1.228	1.320	1.343	1.439	1.467
0.8	1.033	1.058	1.141	1.186	1.195	1.233	1.242
0.9	0.9945	0.9852	0.9303	0.8842	0.8670	0.8028	0.7848
1.0	0	0	0	0	0	0	0

Table 5.13: Continued

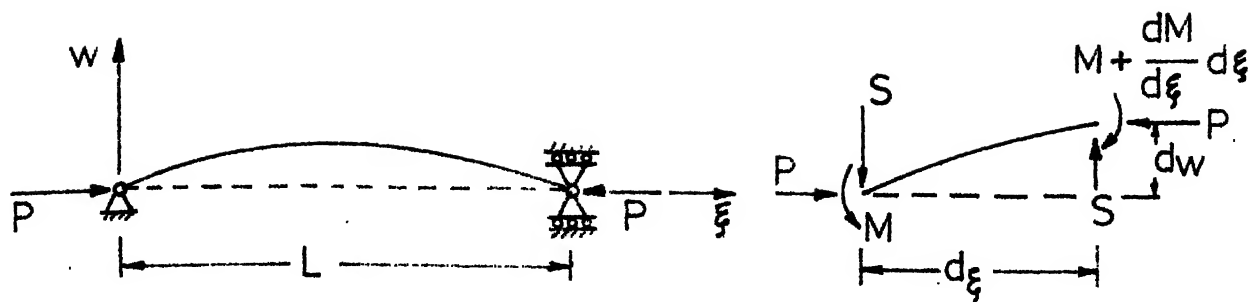
b) for  $q = 2$ 

x	p=0.05	p = 0.1	p = 0.4	p = 0.8	p = 1	p = 3	p = 5
0	1.048	1.080	1.185	1.236	1.250	1.287	1.297
0.1	1.032	1.050	1.106	1.129	1.135	1.144	1.147
0.2	0.9916	0.9734	0.9165	0.8803	0.8698	0.8223	0.8118
0.3	0.8297	0.7633	0.4990	0.3945	0.3679	0.3124	0.2953
0.4	0.9980	0.9988	0.9791	0.9625	0.9570	0.9438	0.9386
0.5	1.032	1.058	1.131	1.165	1.174	1.209	1.216
0.6	1.045	1.080	1.190	1.247	1.263	1.320	1.333
0.7	1.044	1.079	1.186	1.242	1.257	1.312	1.325
0.8	1.031	1.054	1.118	1.148	1.156	1.182	1.188
0.9	0.9947	0.9869	0.9493	0.9237	0.9160	0.8887	0.8813
1.0	0	0	0	0	0	0	0

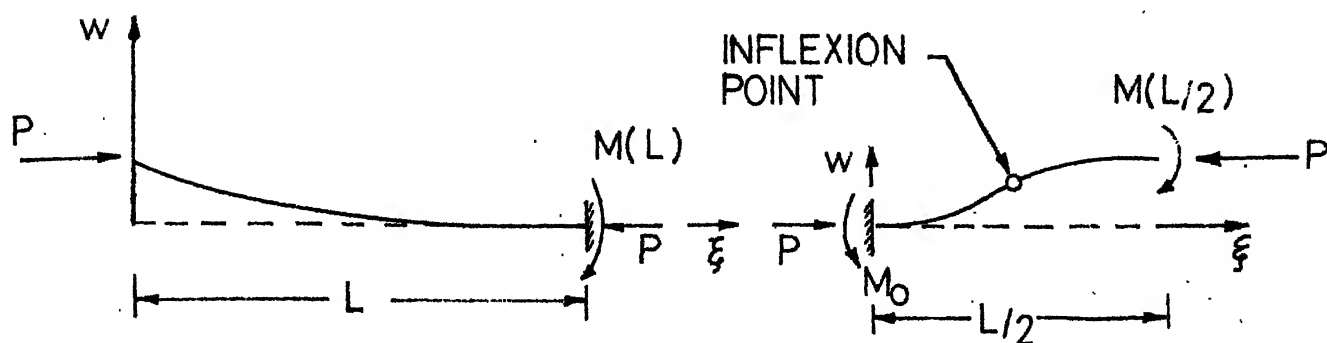
Table 5.13: Concluded

c) for  $q = 3$ 

x	p=0.05	p = 0.1	p = 0.4	p = 0.8	p = 1	p = 3	p = 5
9	1.044	1.075	1.158	1.194	1.202	1.232	1.239
0.1	1.029	1.047	1.093	1.110	1.113	1.127	1.130
0.2	0.9879	0.9758	0.9336	0.9109	0.9031	0.8835	0.8783
0.3	0.8697	0.7793	0.5617	0.4808	0.4668	0.4026	0.3895
0.4	1.001	0.9993	0.9861	0.9767	0.9750	0.9640	0.9615
0.5	1.032	1.054	1.112	1.136	1.143	1.162	1.167
0.6	1.044	1.074	1.160	1.199	1.210	1.242	1.250
0.7	1.043	1.073	1.157	1.195	1.205	1.237	1.245
0.8	1.030	1.050	1.102	1.123	1.129	1.145	1.149
0.9	0.9953	0.9884	0.9611	0.9454	0.9411	0.9260	0.9222
1.0	0	0	0	0	0	0	0

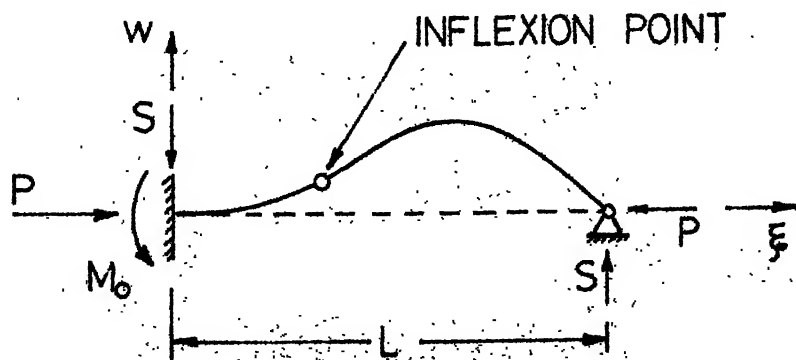


a) HINGED - HINGED

b) FREE BODY OF AN ELEMENT  $d\xi$ 

c) FREE - CLAMPED

d) CLAMPED - CLAMPED



e) CLAMPED - HINGED

FIG.3.1. COLUMNS CONSIDERED IN THE THESIS

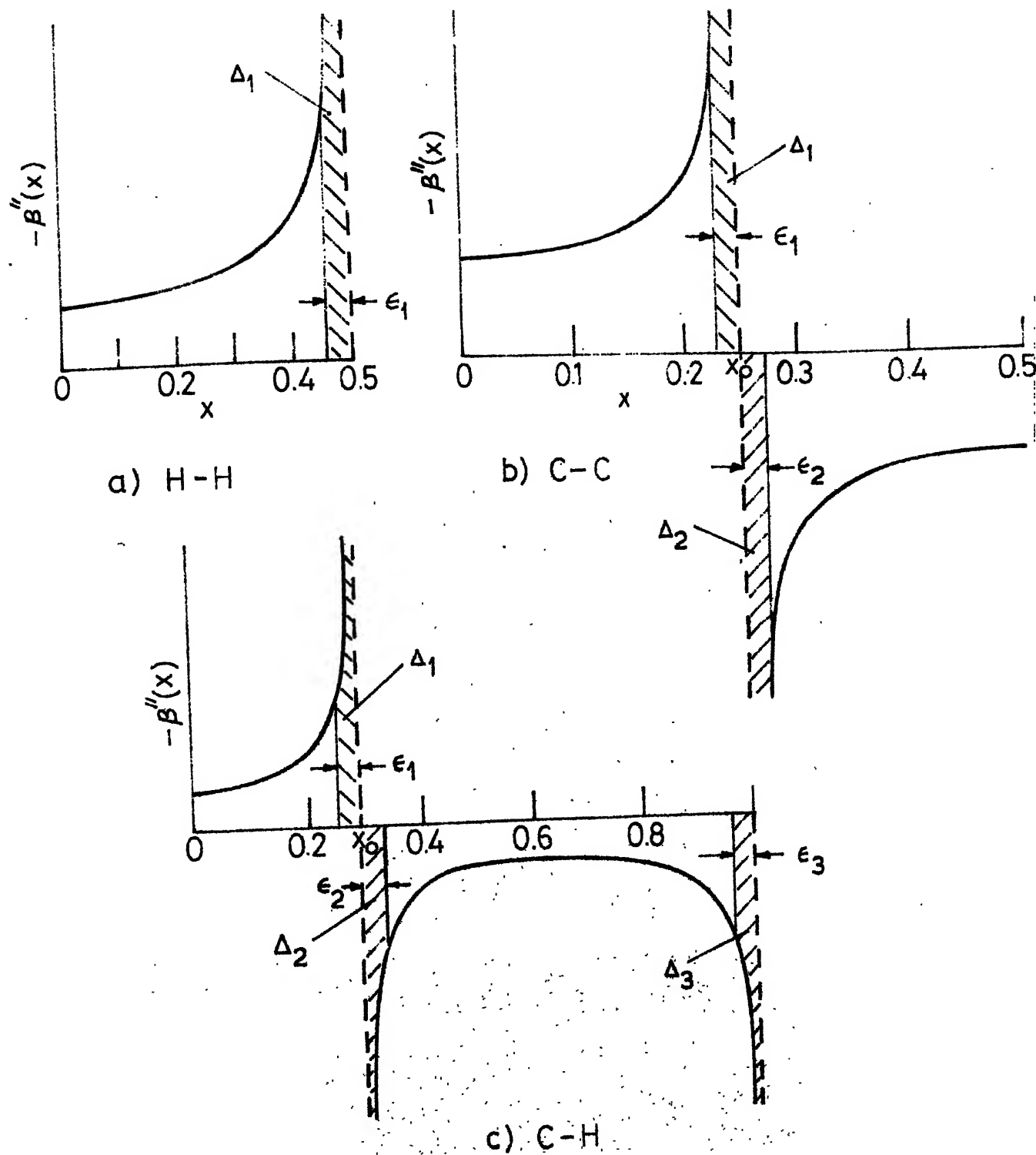


FIG. 4.1 SINGULAR BEHAVIOUR FOR H-H, C-C AND C-H END CONDITIONS

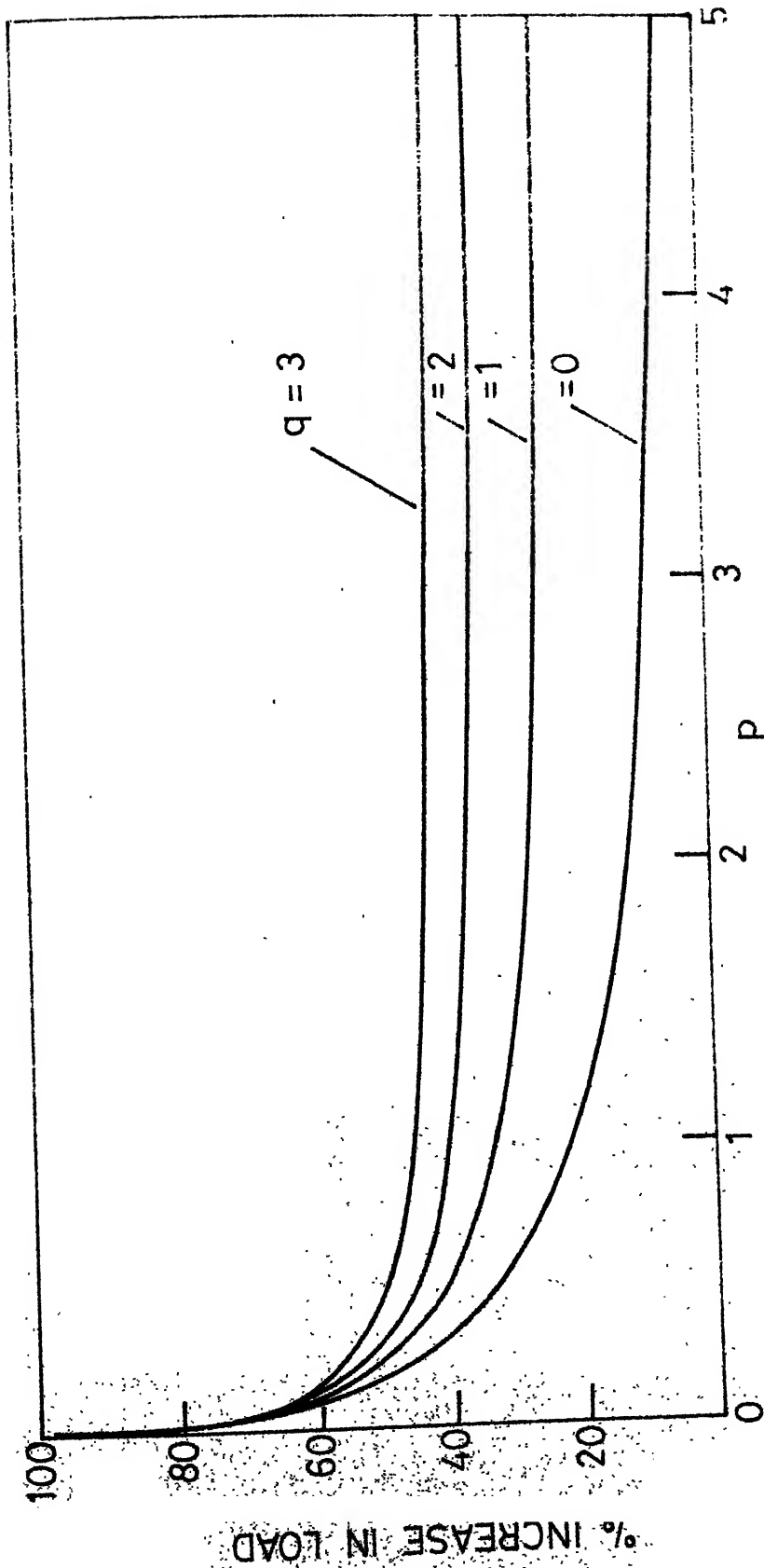


FIG. 5.1a. VARIATION OF PERCENT INCREASE IN BUCKLING LOAD WITH  $p$  FOR HINGED-HINGED, FREE-CLAMPED AND CLAMPED-CLAMPED COLUMNS

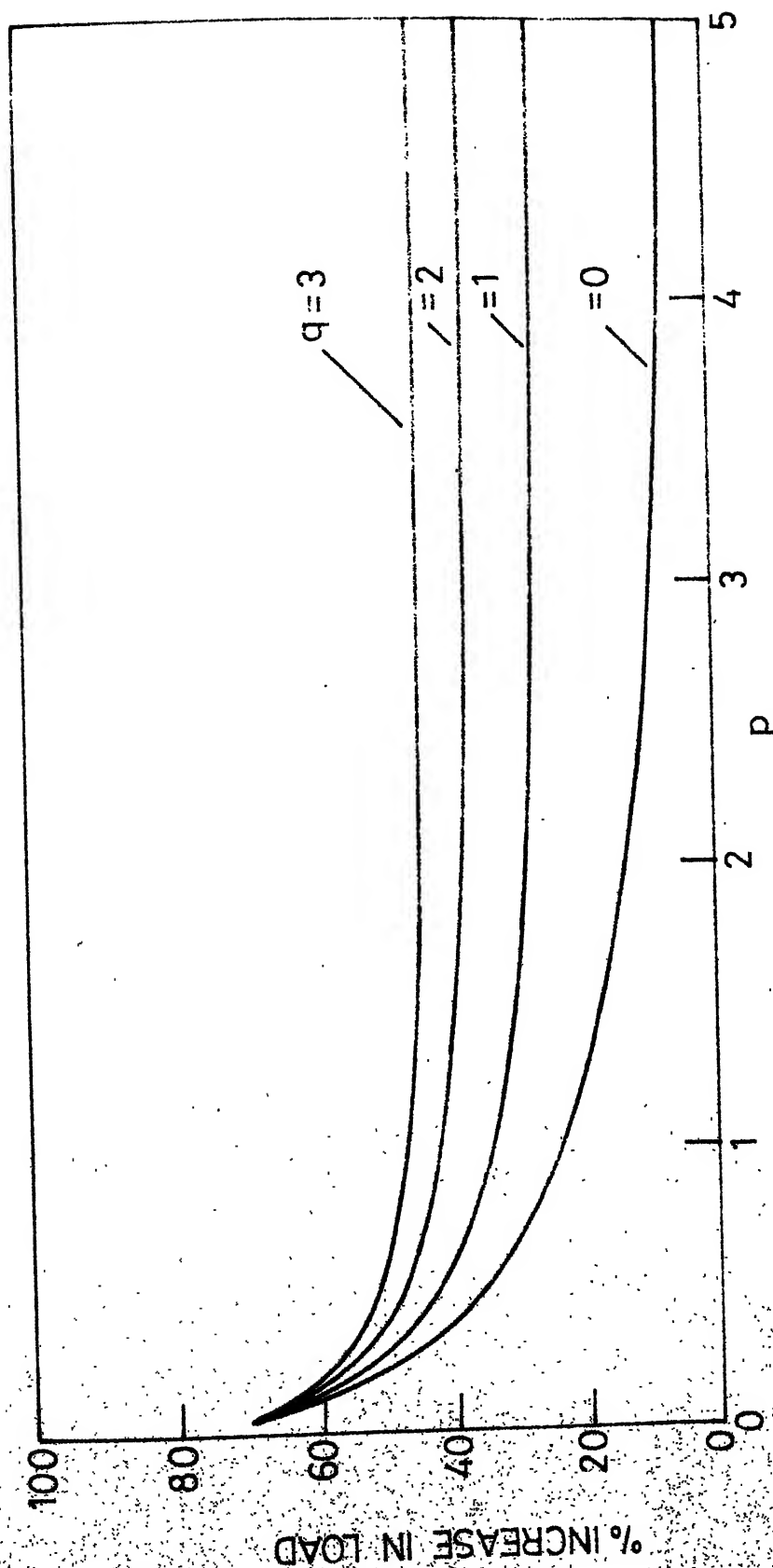


FIG 5.1b. VARIATION OF PERCENT INCREASE IN BUCKLING LOAD WITH  $p$   
FOR CLAMPED - HINGED COLUMNS

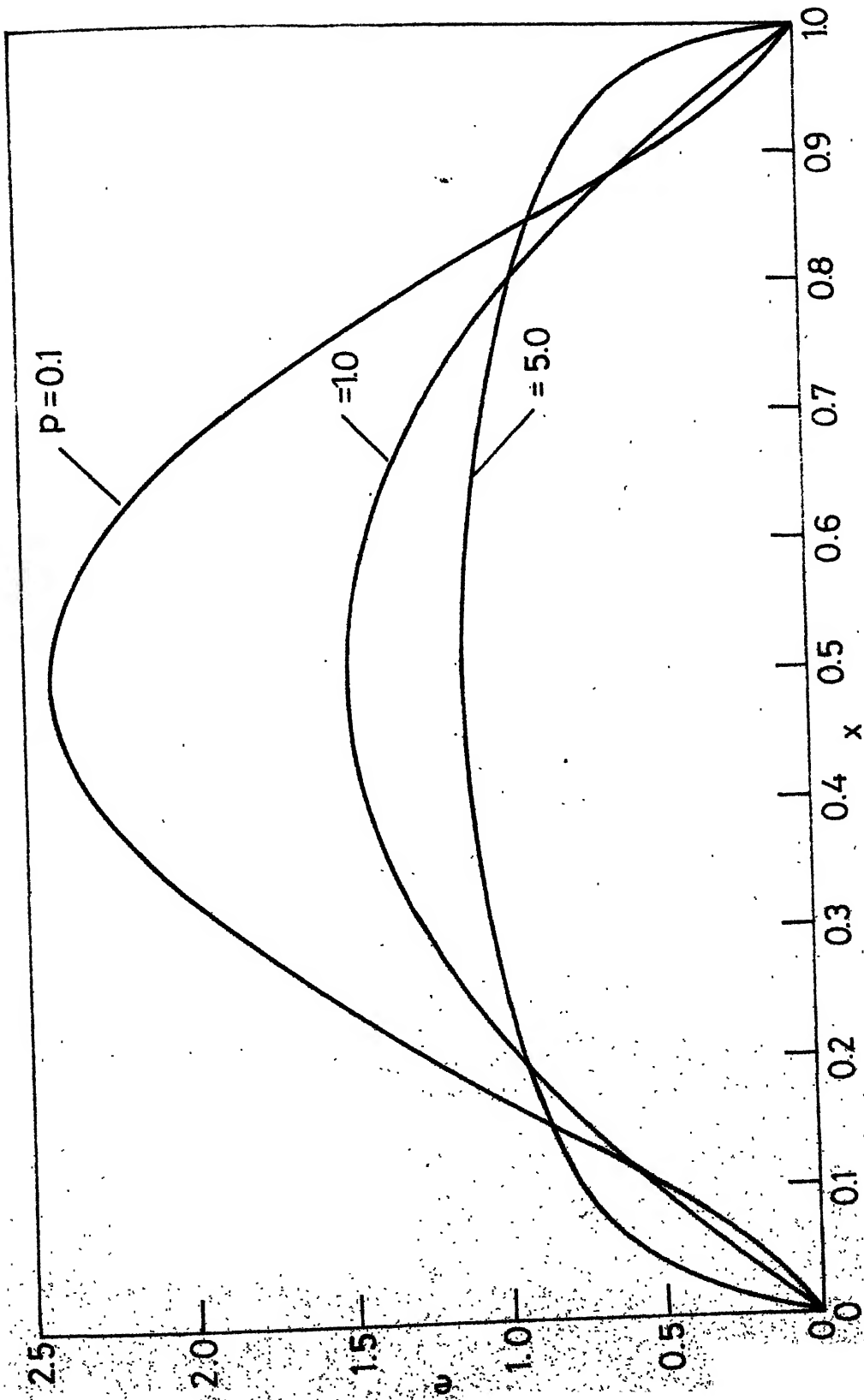


FIG 5.2. VARIATION OF  $e$  ALONG THE AXIS FOR HINGED - HINGED  
UNIFORM COLUMNS ( $q=0$ )

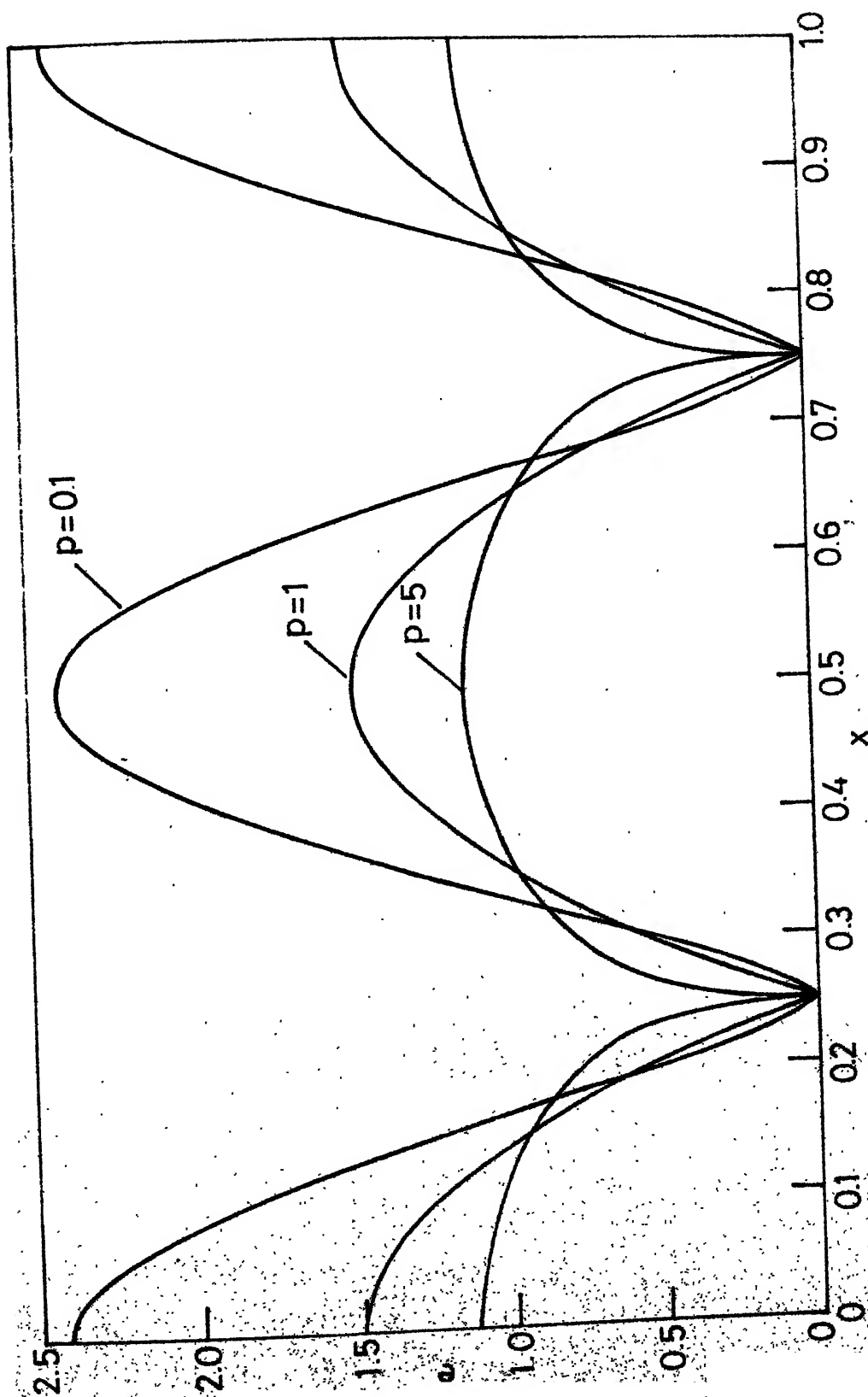


FIG.5.3 VARIATION OF  $e$  ALONG THE AXIS FOR CLAMPED - CLAMPED  
UNIFORM COLUMNS ( $q=0$ )

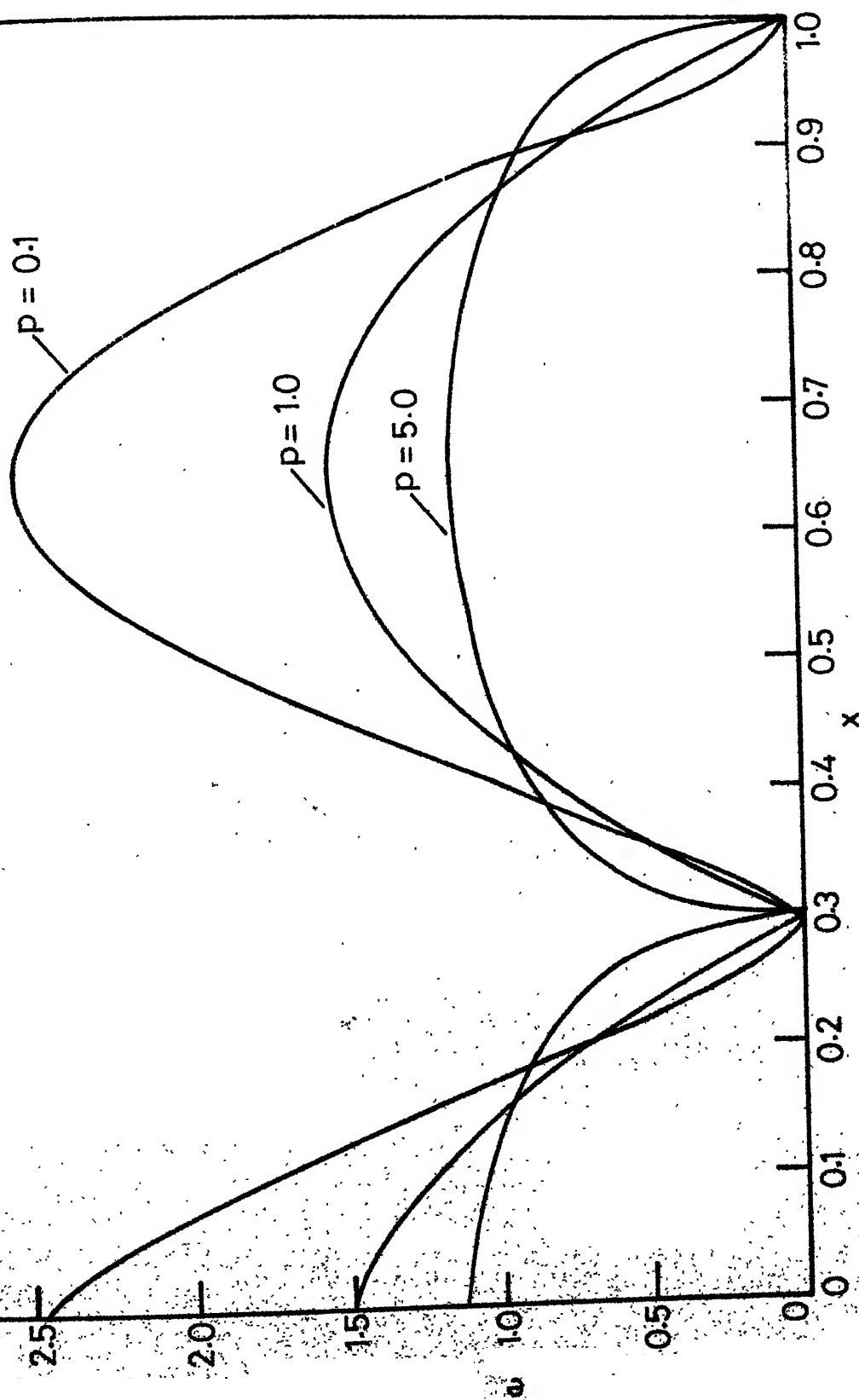


FIG. 5.4. VARIATION OF  $e$  ALONG THE AXIS FOR CLAMPED-HINGED UNIFORM COLUMNS ( $q=0$ )

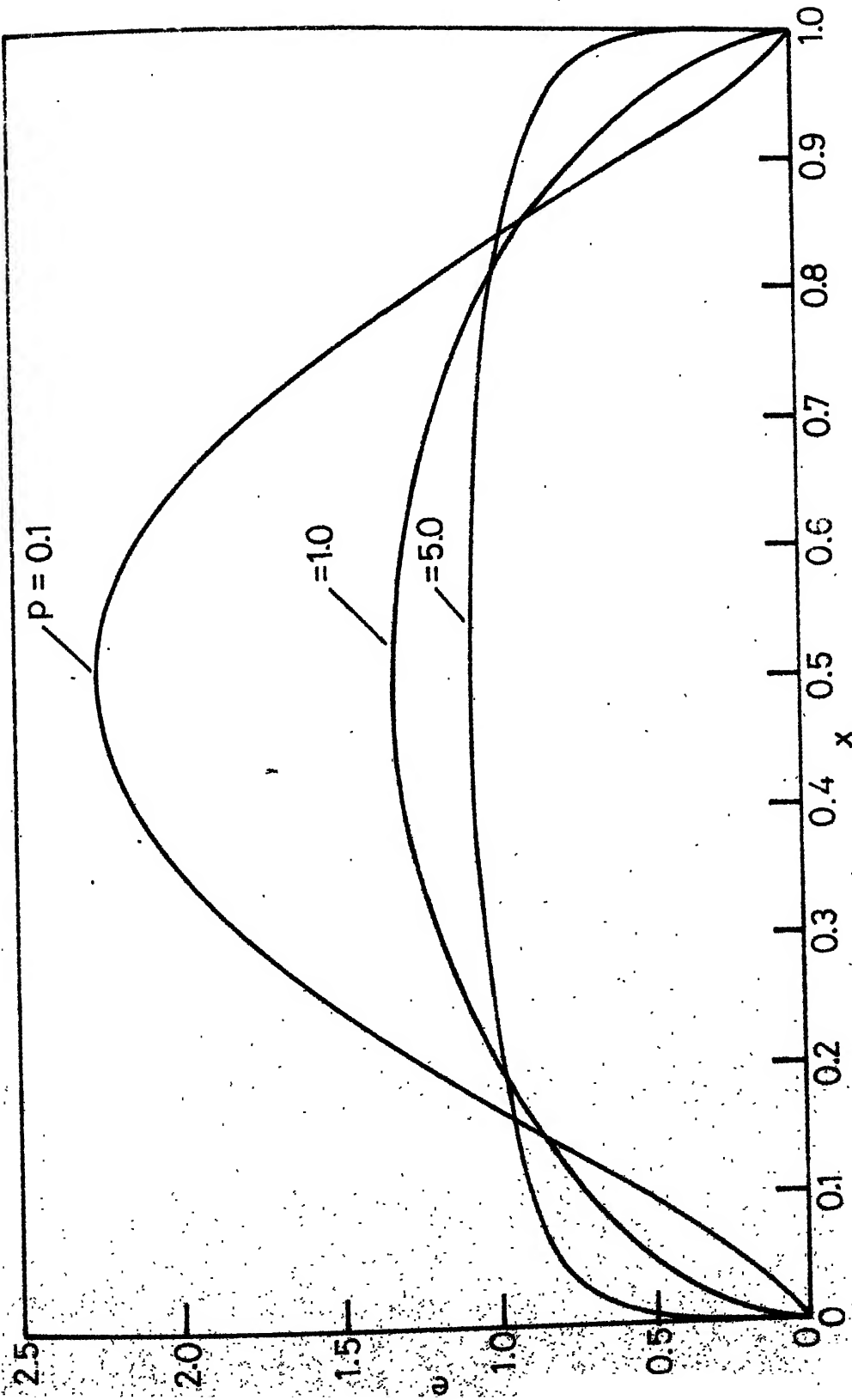


FIG. 5.5.a. VARIATION OF  $e$  ALONG THE AXIS FOR HINGED - HINGED TAPERED COLUMNS WITH  $q=1$

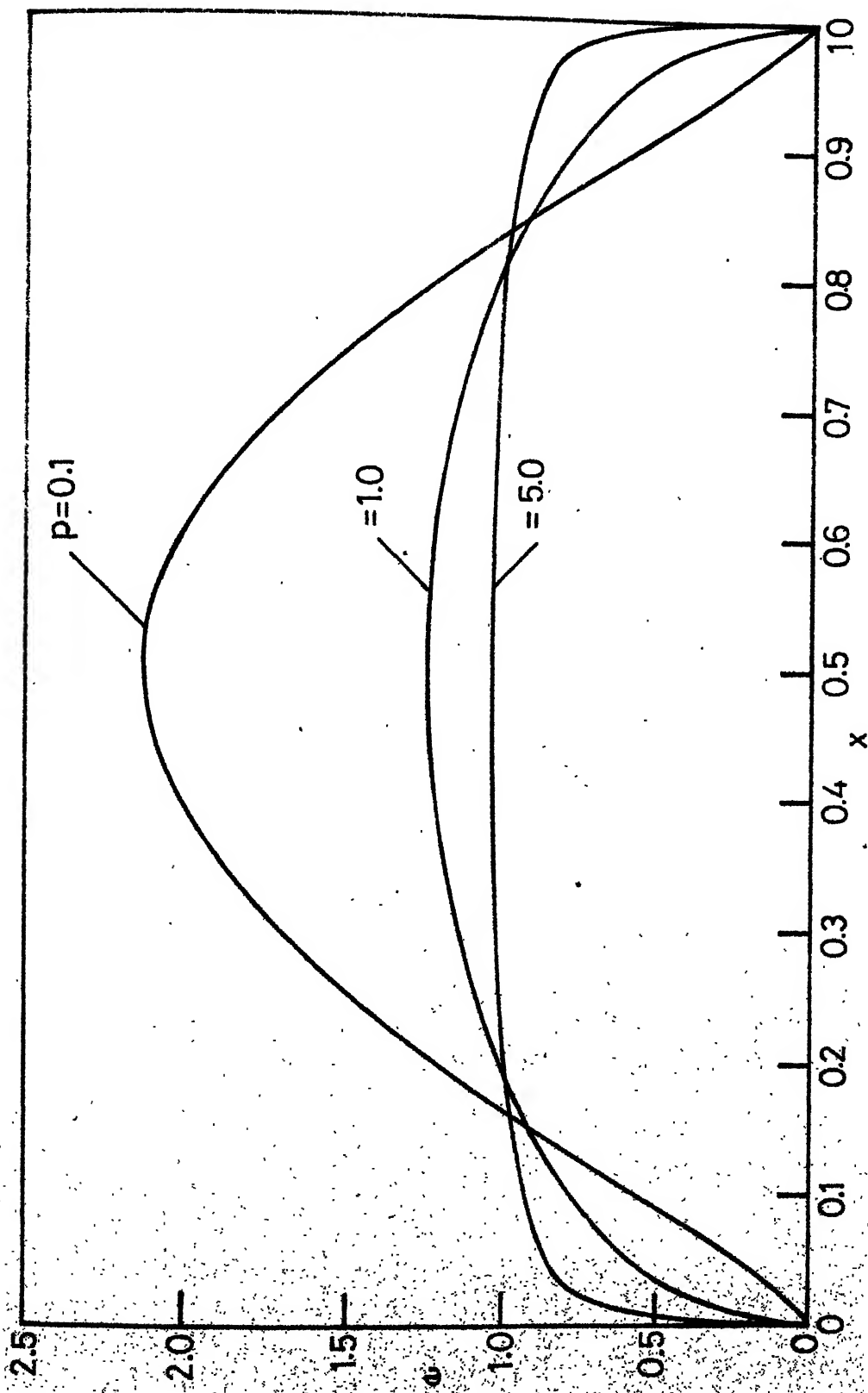


FIG.5.5b. VARIATION OF  $e$  ALONG THE  $x$  AXIS FOR HINGED - HINGED  
TAPERED COLUMNS WITH  $q=2$

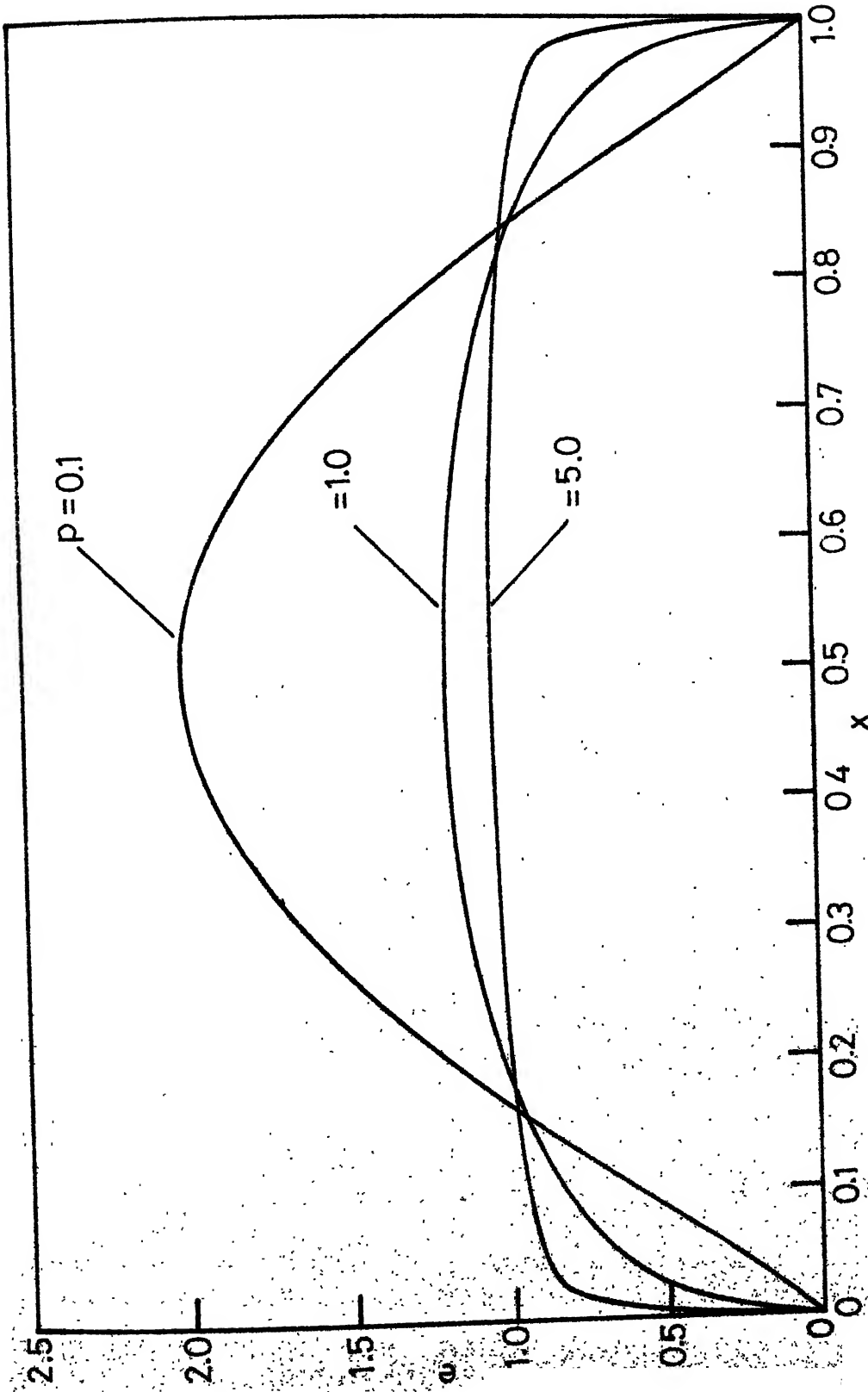


FIG. 5.5 c. VARIATION OF  $e$  ALONG THE AXIS FOR HINGED - HINGED  
TAPERED COLUMNS WITH  $q = 3$

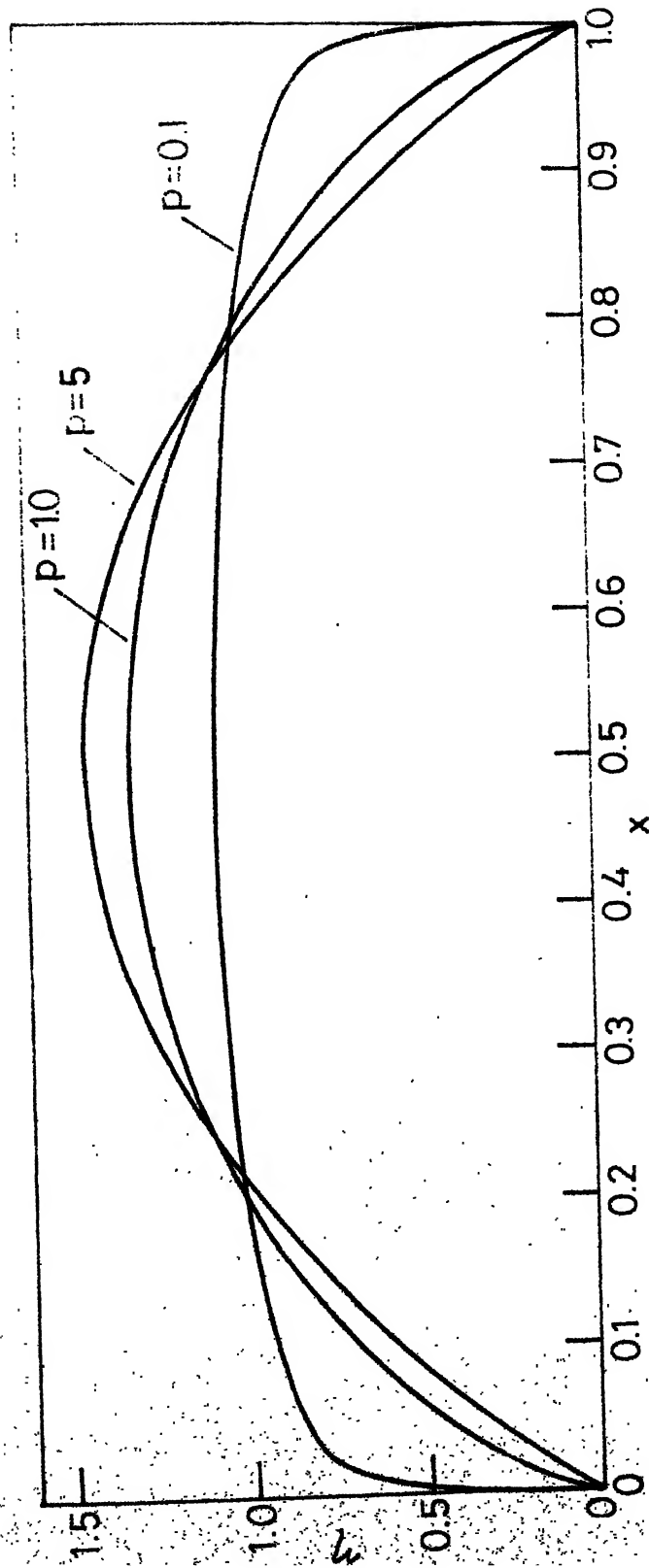


FIG. 5.6.a. VARIATION OF  $\eta$  ALONG THE AXIS FOR HINGED-HINGED TAPERED COLUMNS WITH  $q=1$

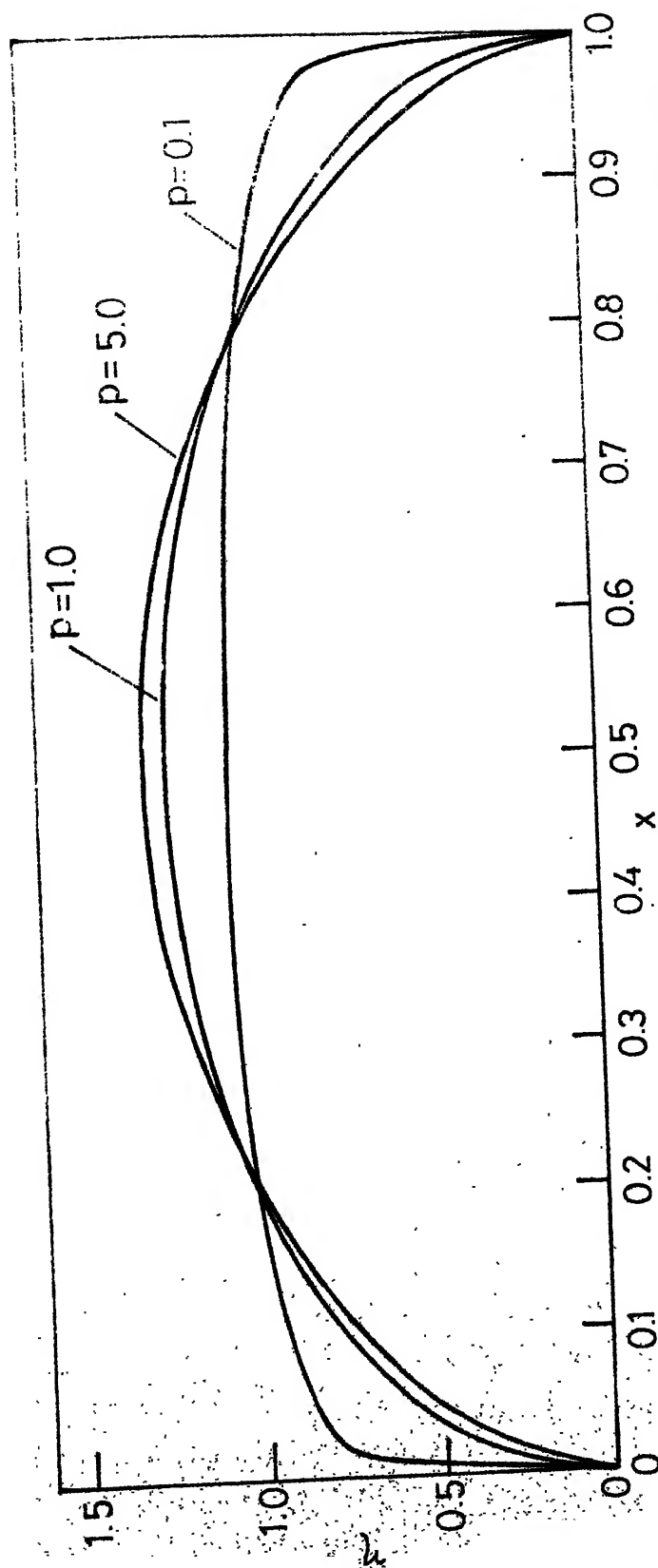


FIG 5.6b. VARIATION OF  $\eta$  ALONG THE AXIS FOR HINGED - HINGED  
TAPERED COLUMNS WITH  $q=2$

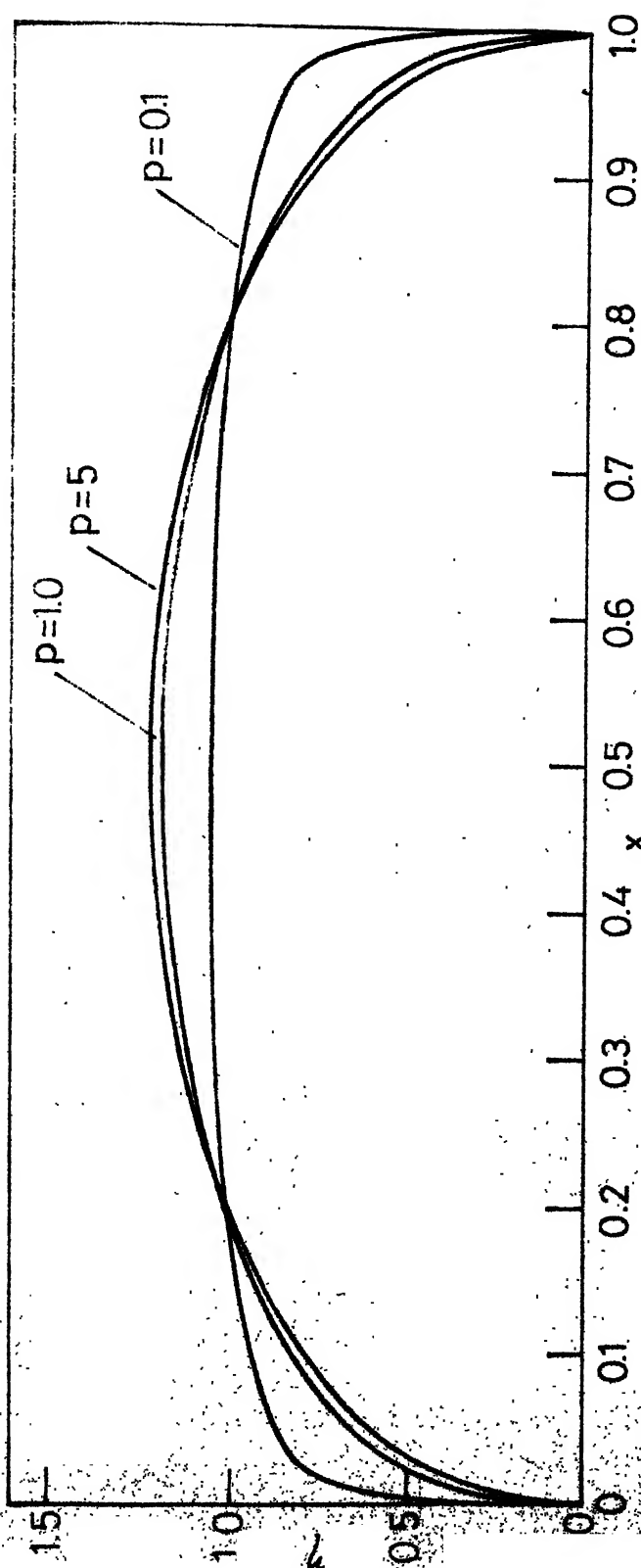


FIG 5.6 c. VARIATION OF  $\eta$  ALONG THE AXIS FOR HINGED - HINGED  
TAPERED COLUMNS WITH  $q=3$ .

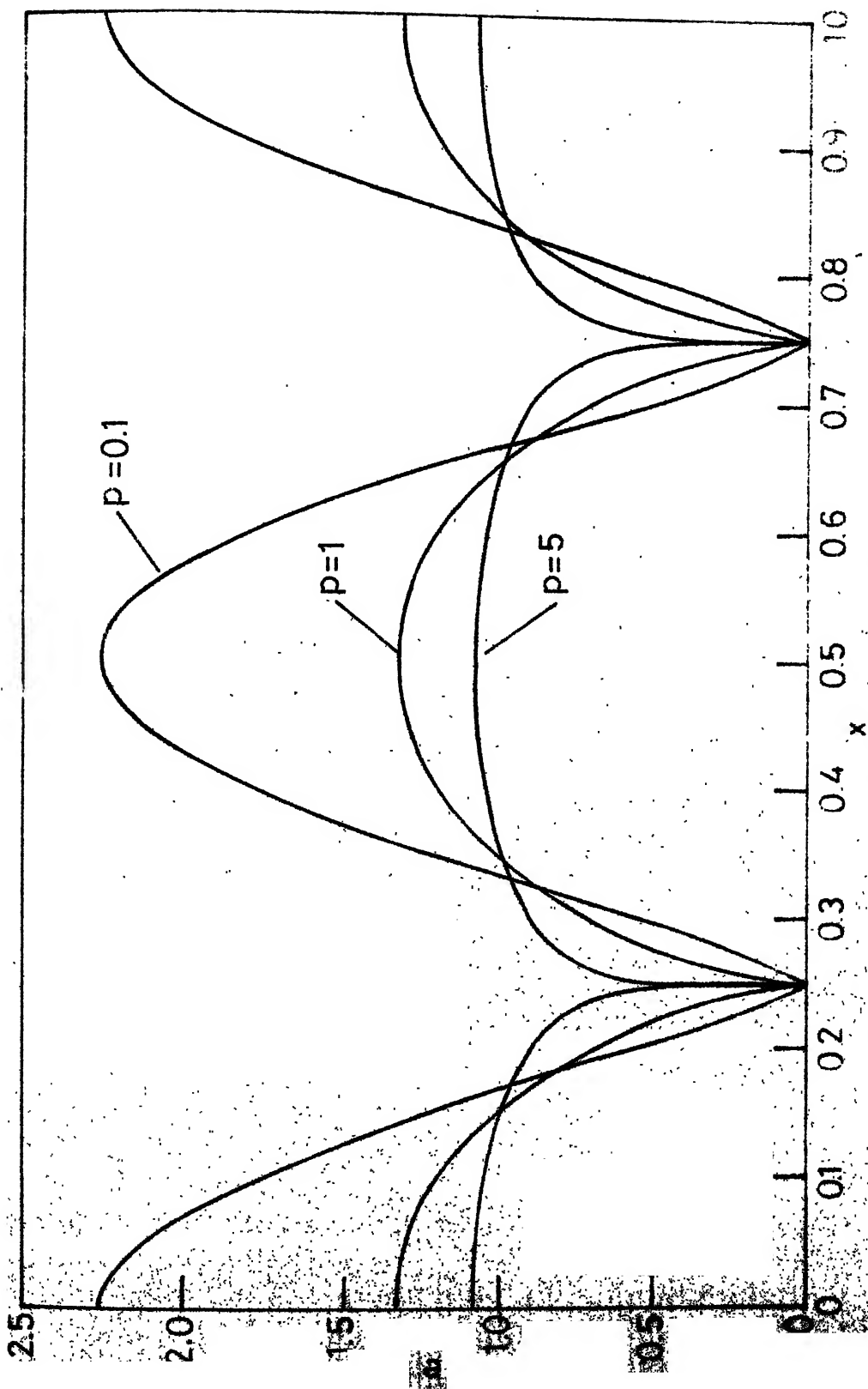


FIG 5.7a. VARIATION OF  $e$  ALONG THE AXIS FOR CLAMPED - CLAMPED TAPERED COLUMNS WITH  $q=1$

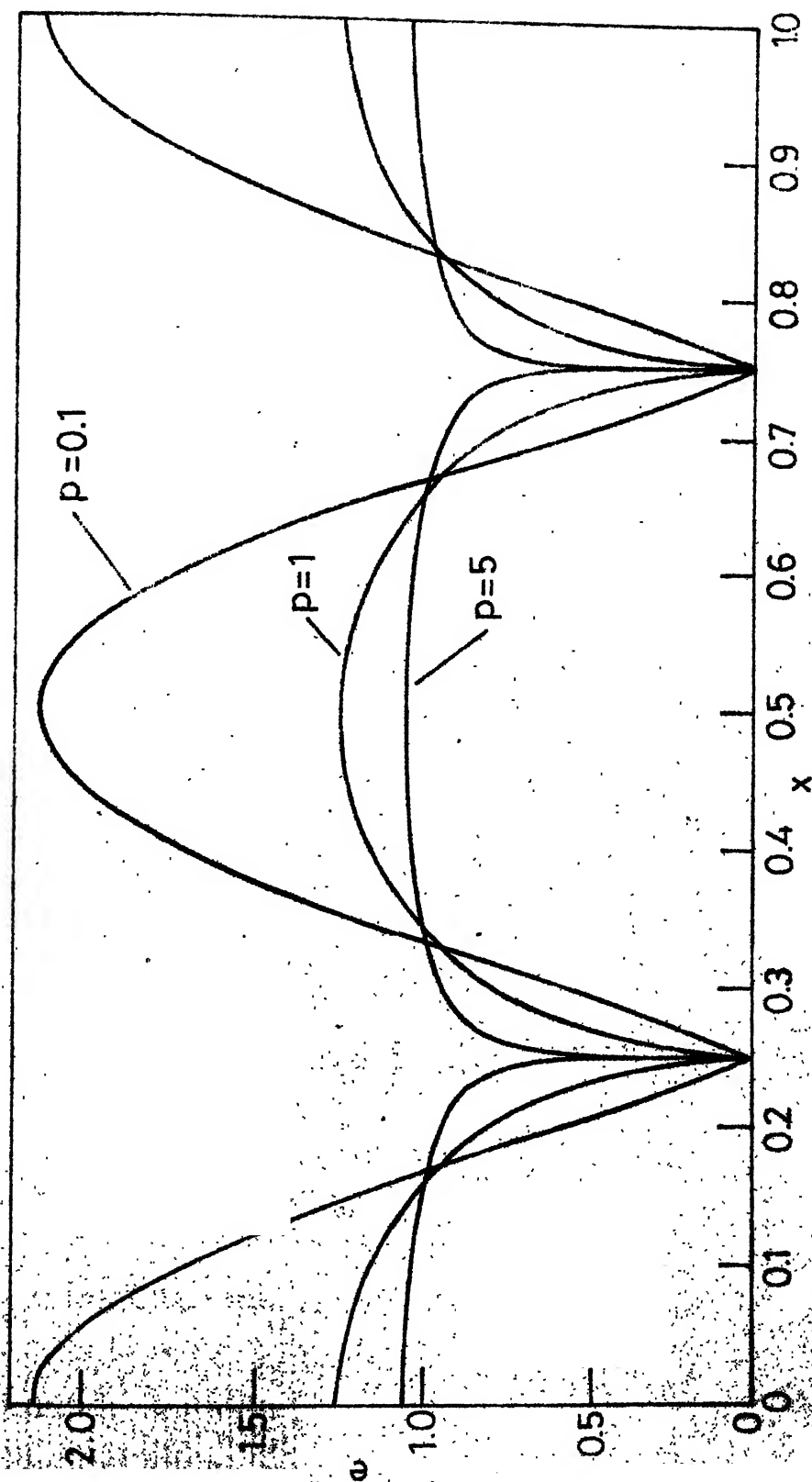


FIG. 5.7b. VARIATION OF  $e$  ALONG THE AXIS FOR CLAMPED - CLAMPED TAPERED COLUMNS WITH  $q=2$

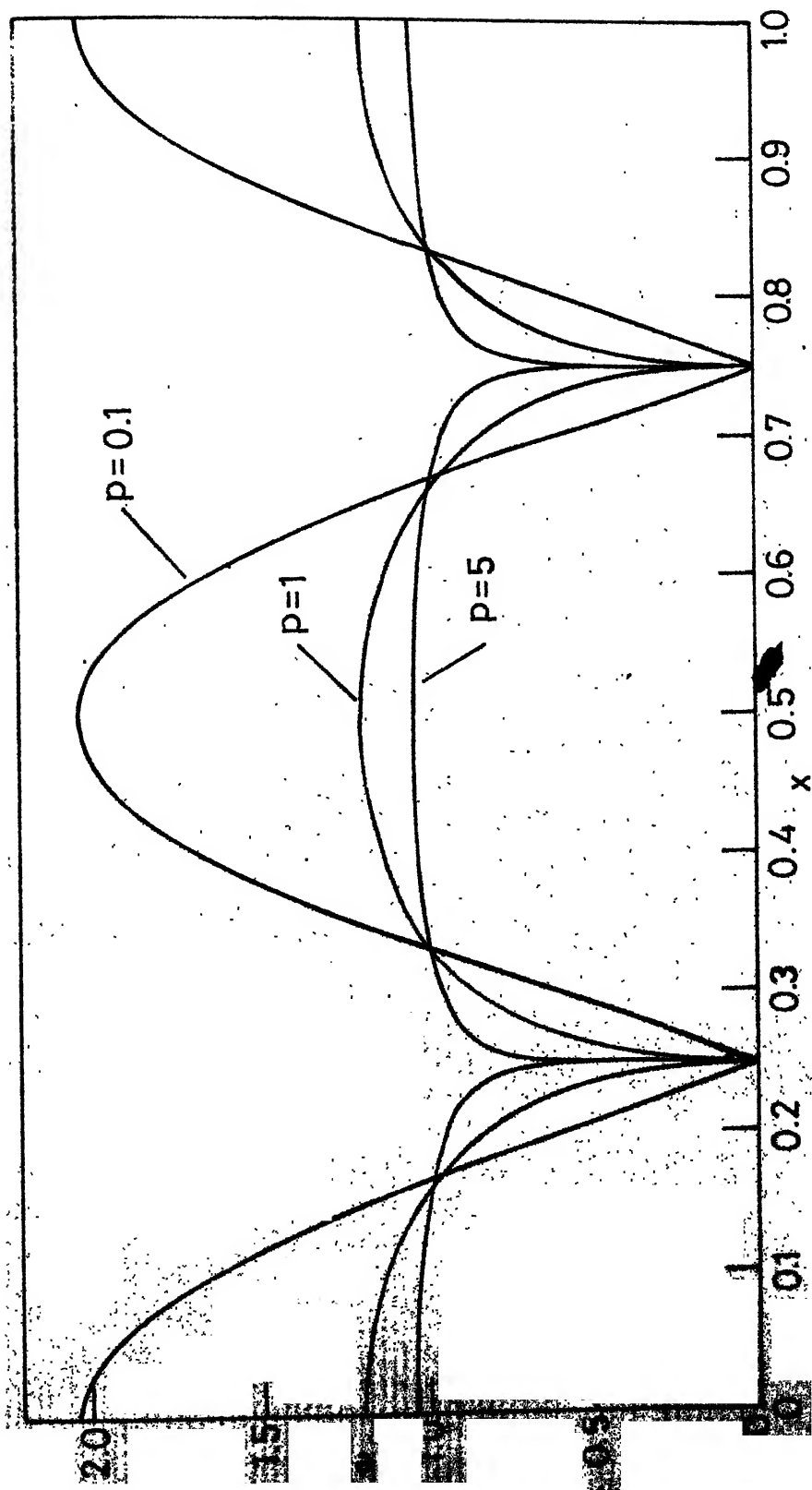


FIG. 5.7c. VARIATION OF  $e$  ALONG THE AXIS FOR CLAMPED-CLAMPED TAPERED COLUMNS WITH  $q=3$

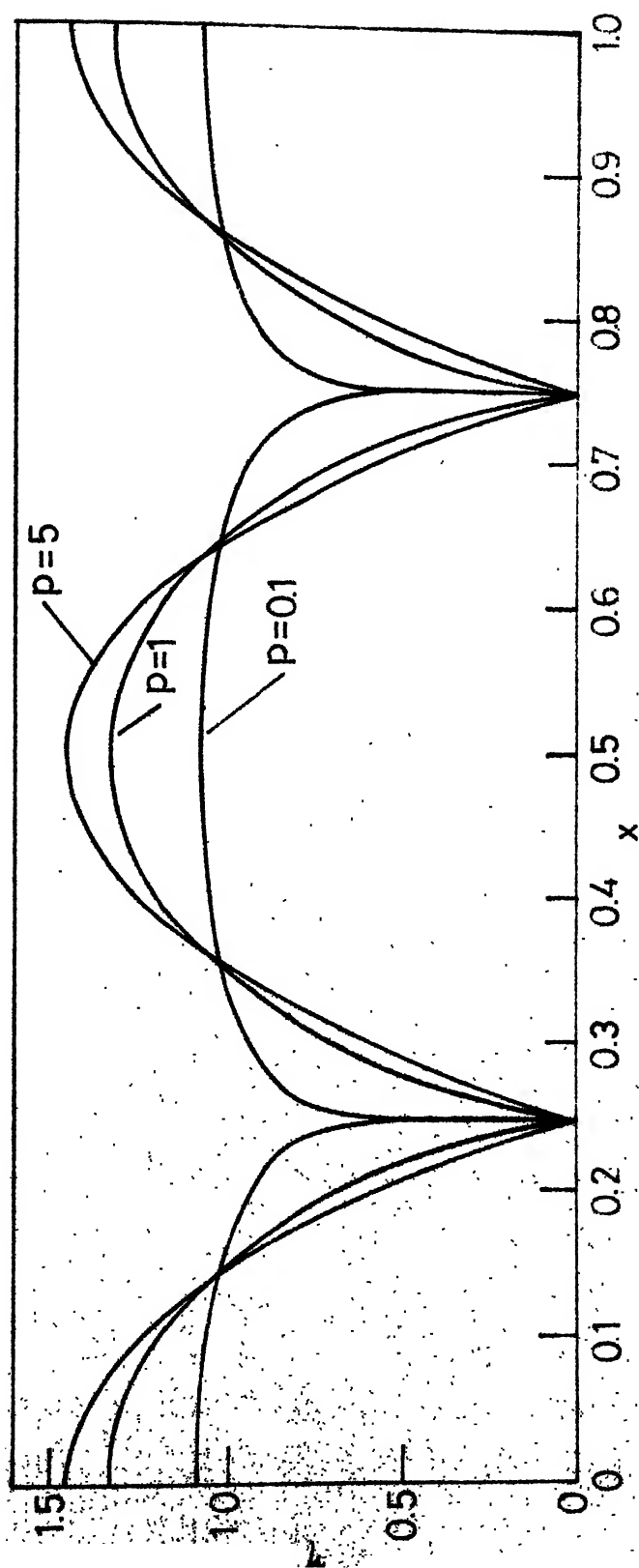


FIG 5.8a VARIATION OF  $\eta$  ALONG THE AXIS FOR CLAMPED - CLAMPED  
TAPERED COLUMNS WITH  $q=1$

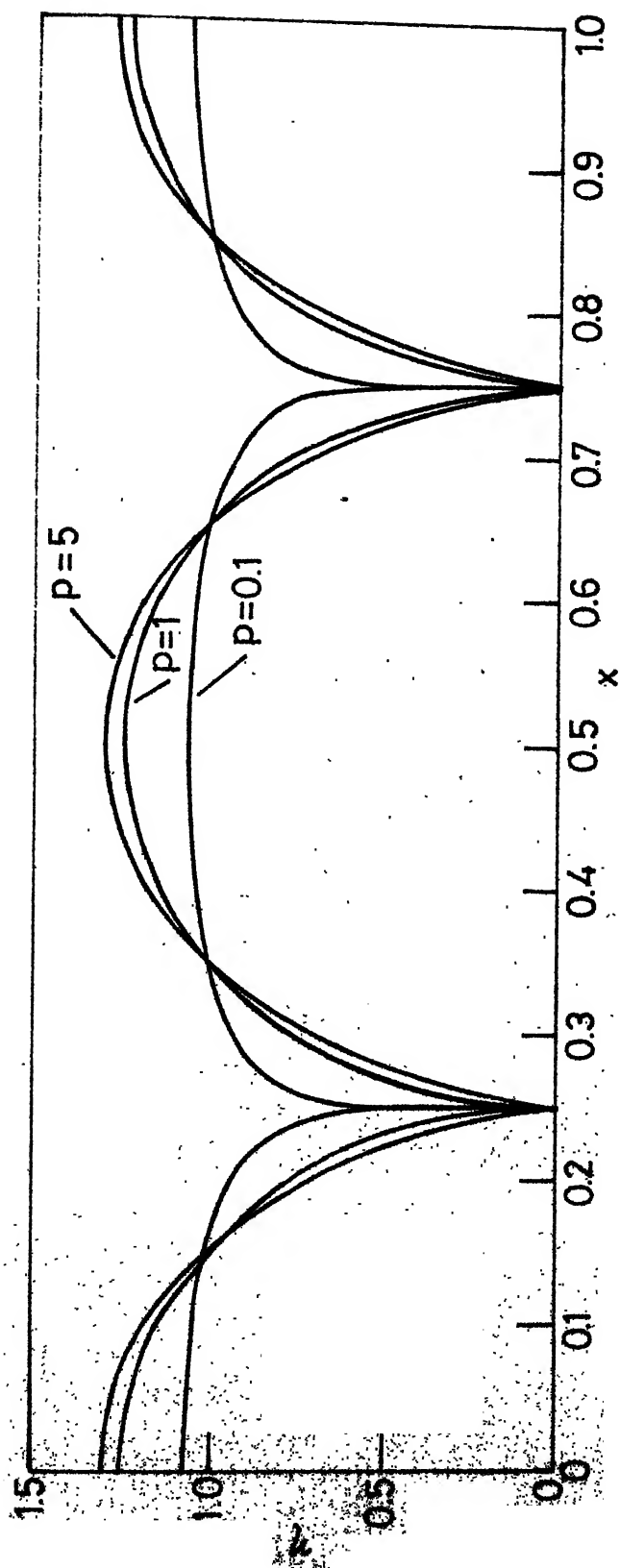


FIG 5.8b. VARIATION OF  $\eta$  ALONG THE AXIS FOR CLAMPED-CLAMPED TAPERED COLUMNS WITH  $q=2$

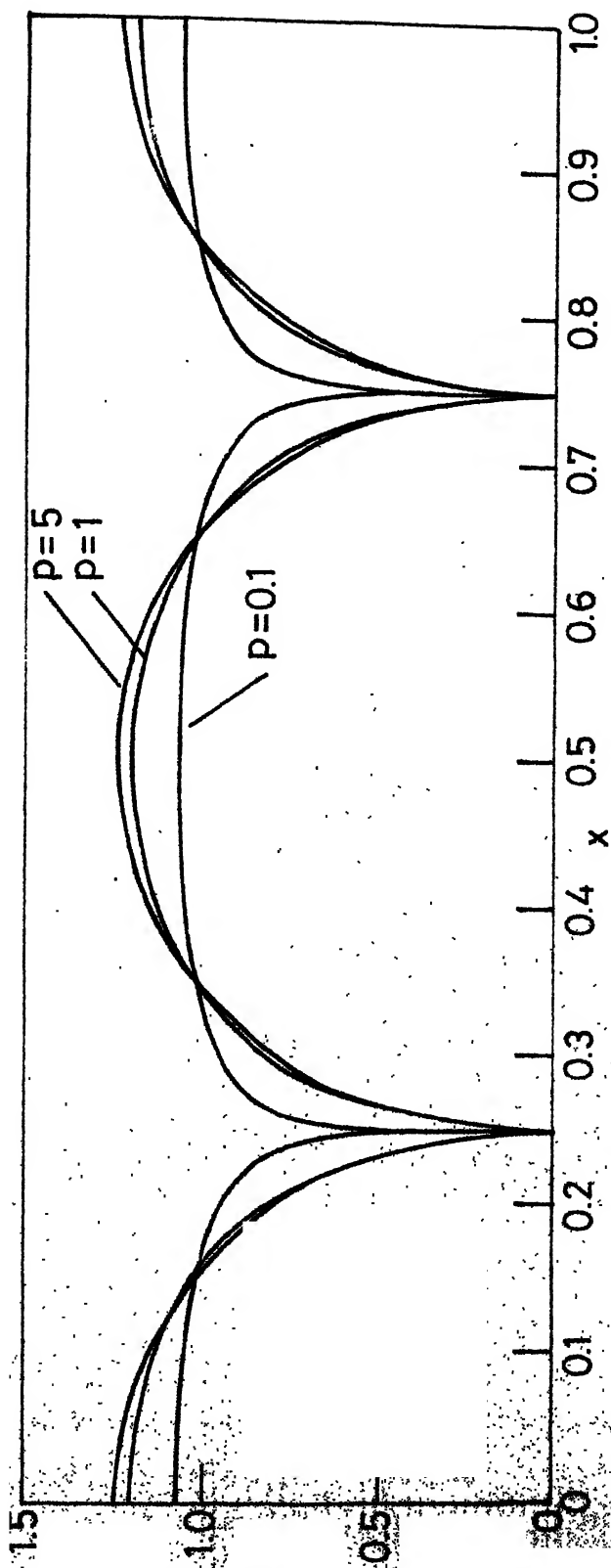


FIG 5.8c. VARIATION OF  $\eta$  ALONG THE AXIS FOR CLAMPED - CLAMPED  
TAPERED COLUMNS WITH  $q=3$

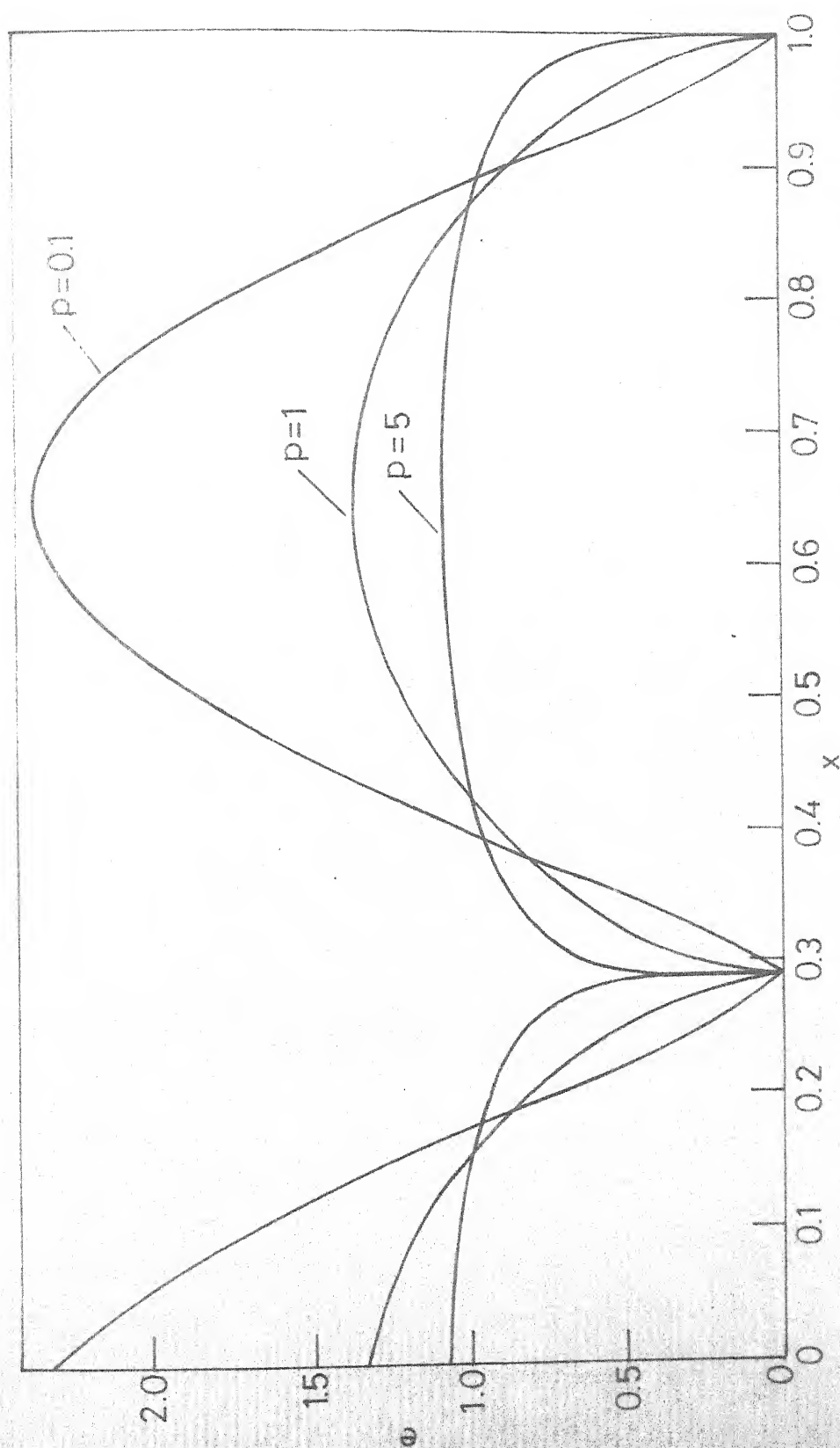


FIG. 5.9a. VARIATION OF  $e$  ALONG THE AXIS FOR CLAMPED - HINGED TAPERED COLUMNS WITH  $q=1$

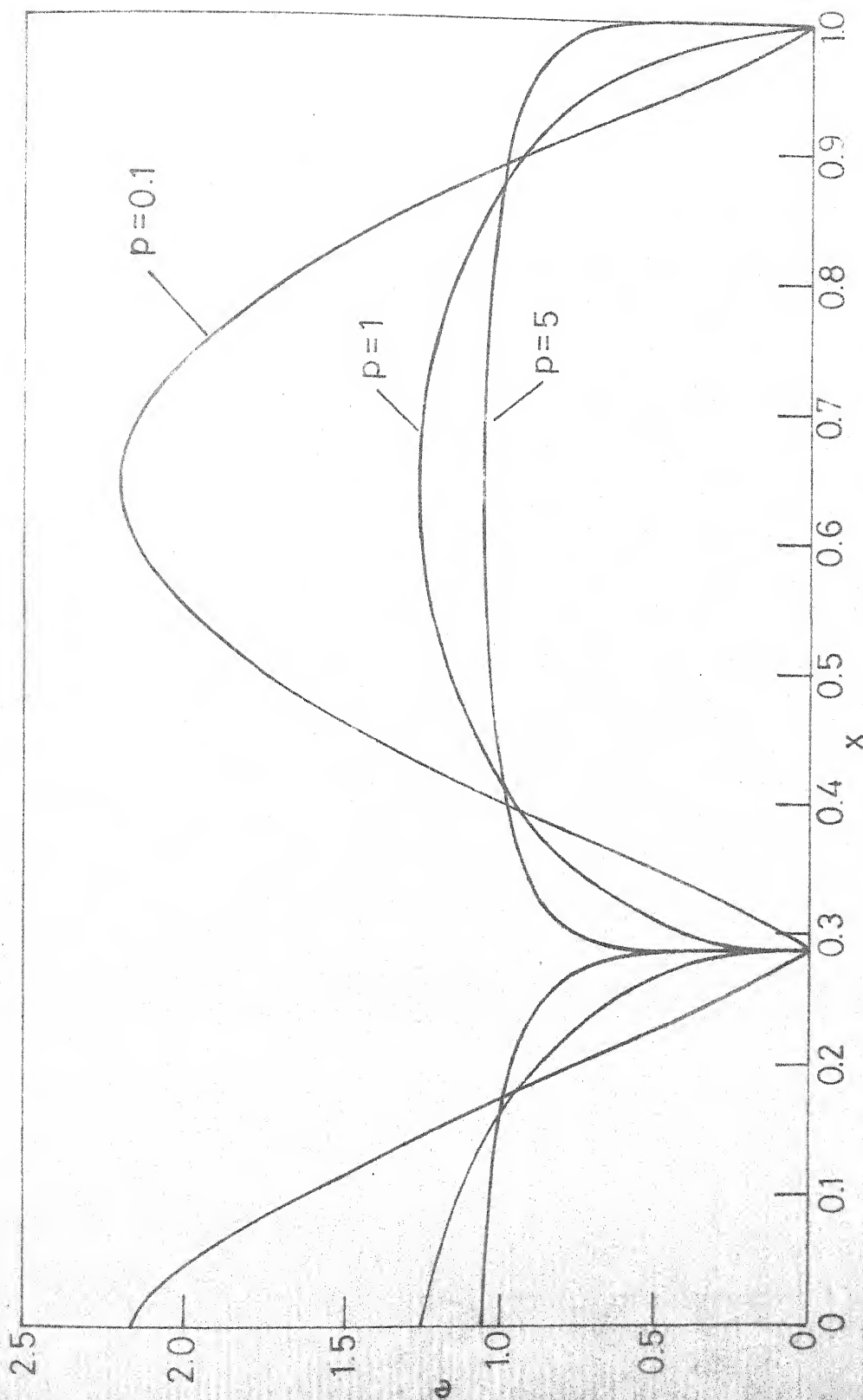


FIG.5.9b. VARIATION OF  $e$  ALONG THE AXIS FOR CLAMPED-HINGED TAPERED COLUMNS WITH  $q=2$

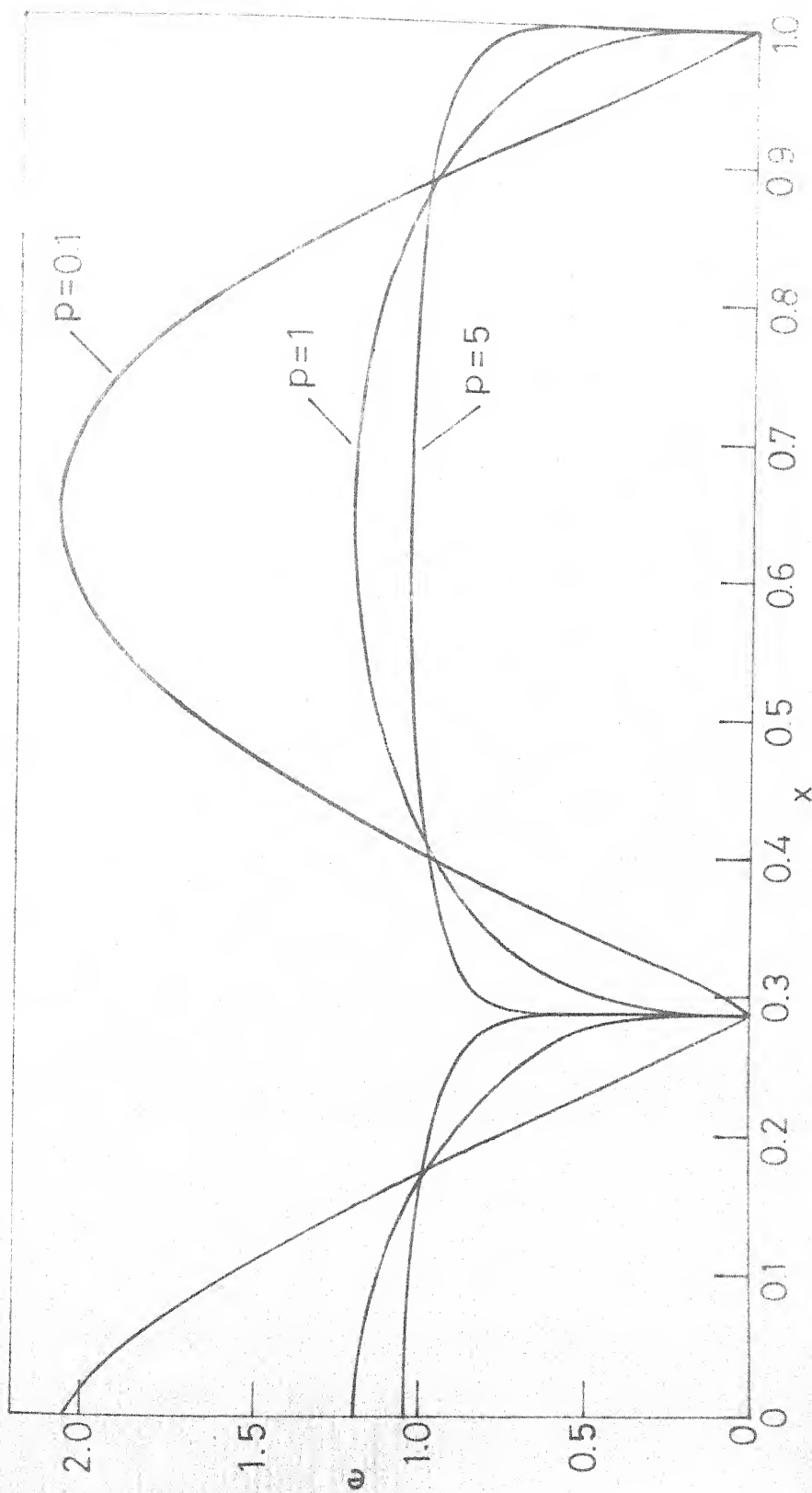


FIG. 5.9c. VARIATION OF  $e$  ALONG THE AXIS FOR CLAMPED-PINNED TAPERED COLUMNS WITH  $q=3$

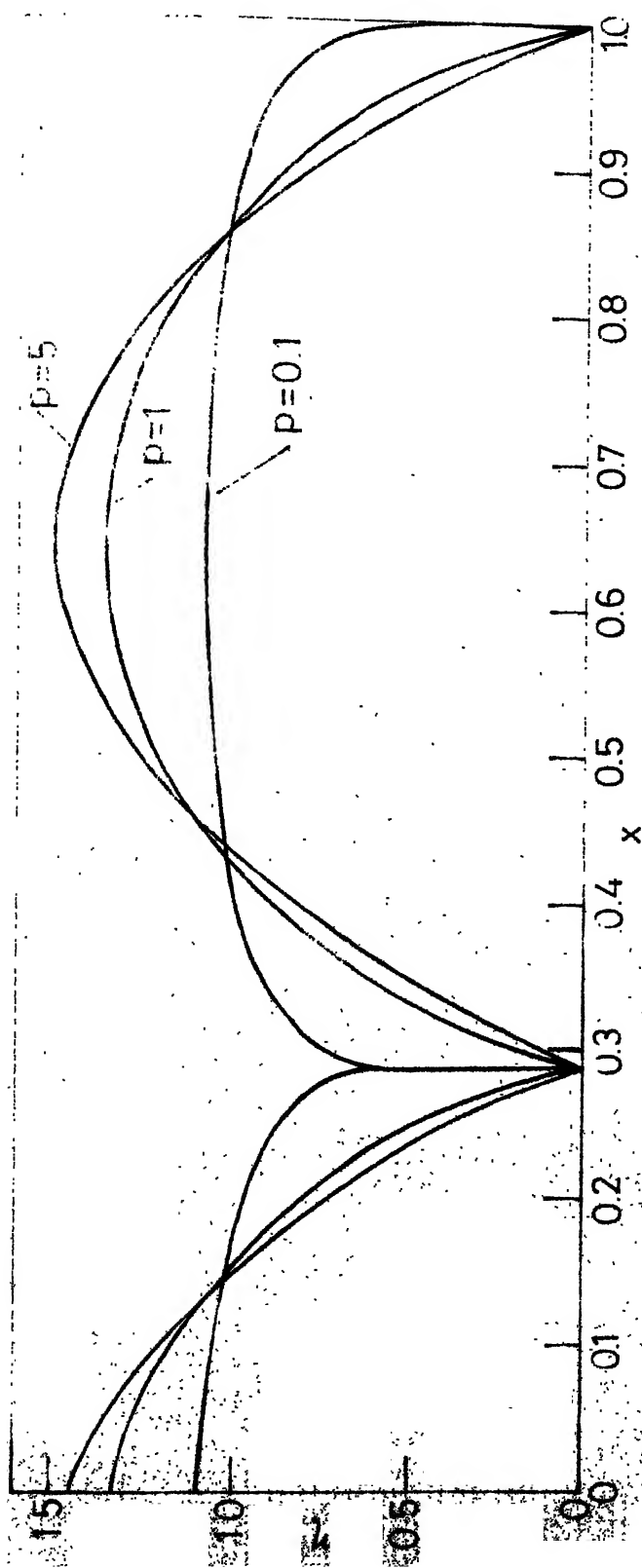


FIG 5.10a VARIATION OF  $\eta$  ALONG THE AXIS FOR CLAMPED - HINGED TAPERED COLUMNS WITH  $q=1$

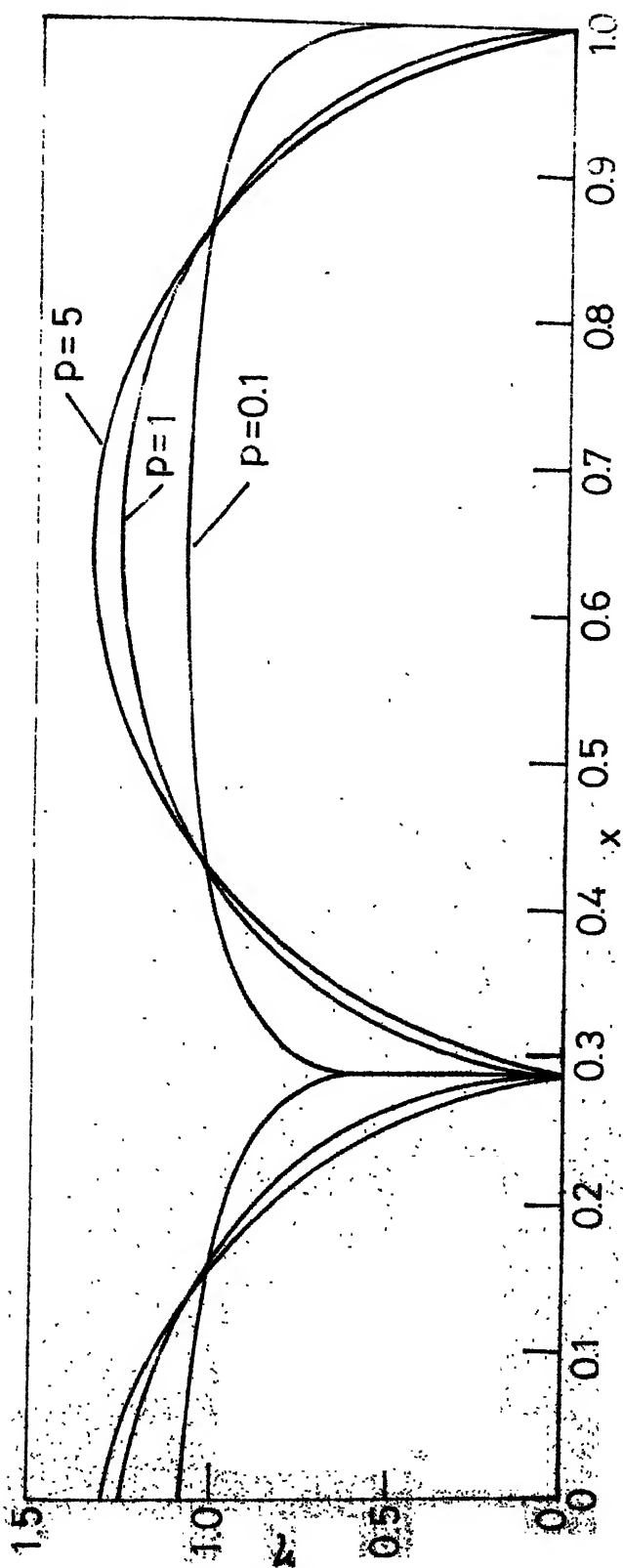


FIG 5.10b. VARIATION OF  $\eta$  ALONG THE AXIS FOR CLAMPED - HINGED TAPERED COLUMNS WITH  $q=2$

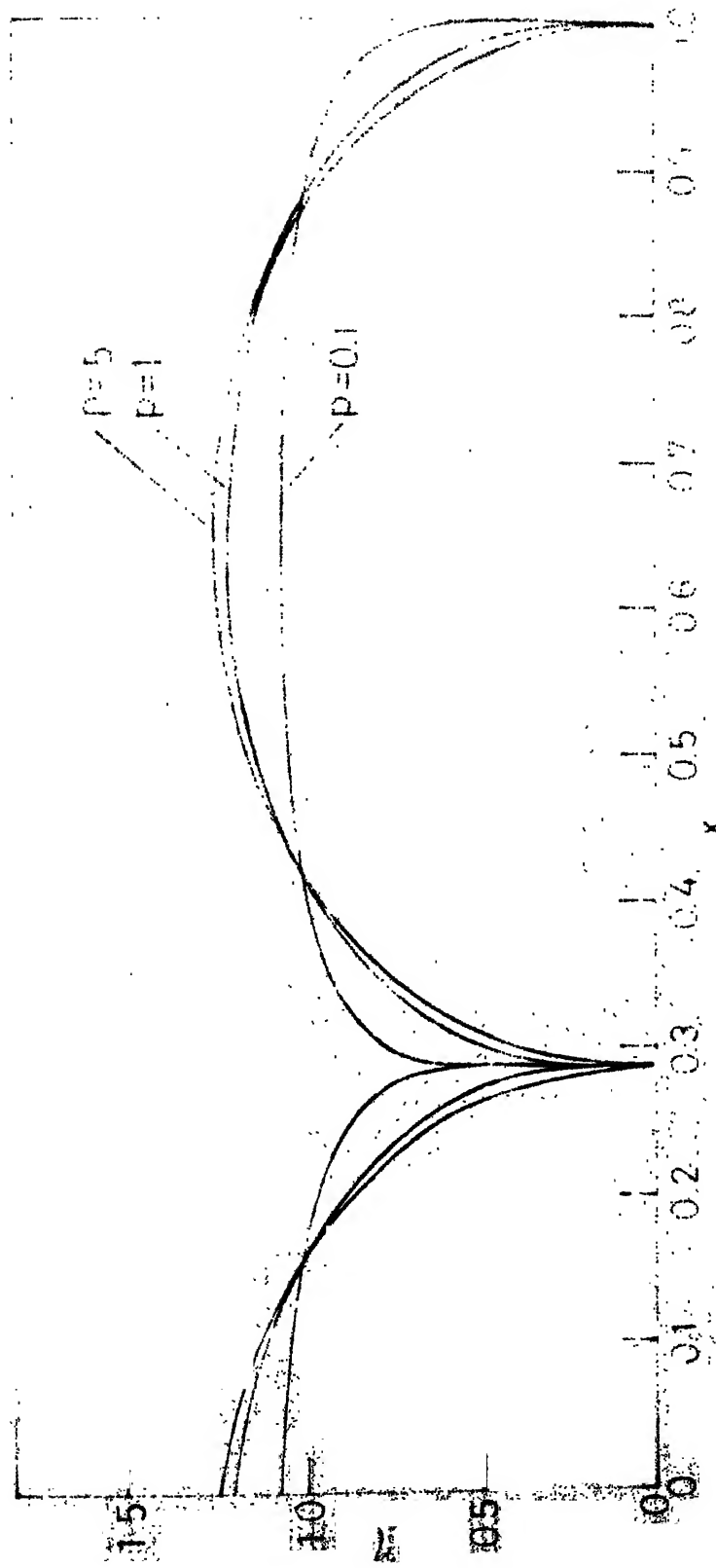


FIG. 5.10c VARIATION OF  $z$  ALONG THE AXIS FOR CLAMPED-HINGED TAPERED COLUMNS WITH  $q=3$

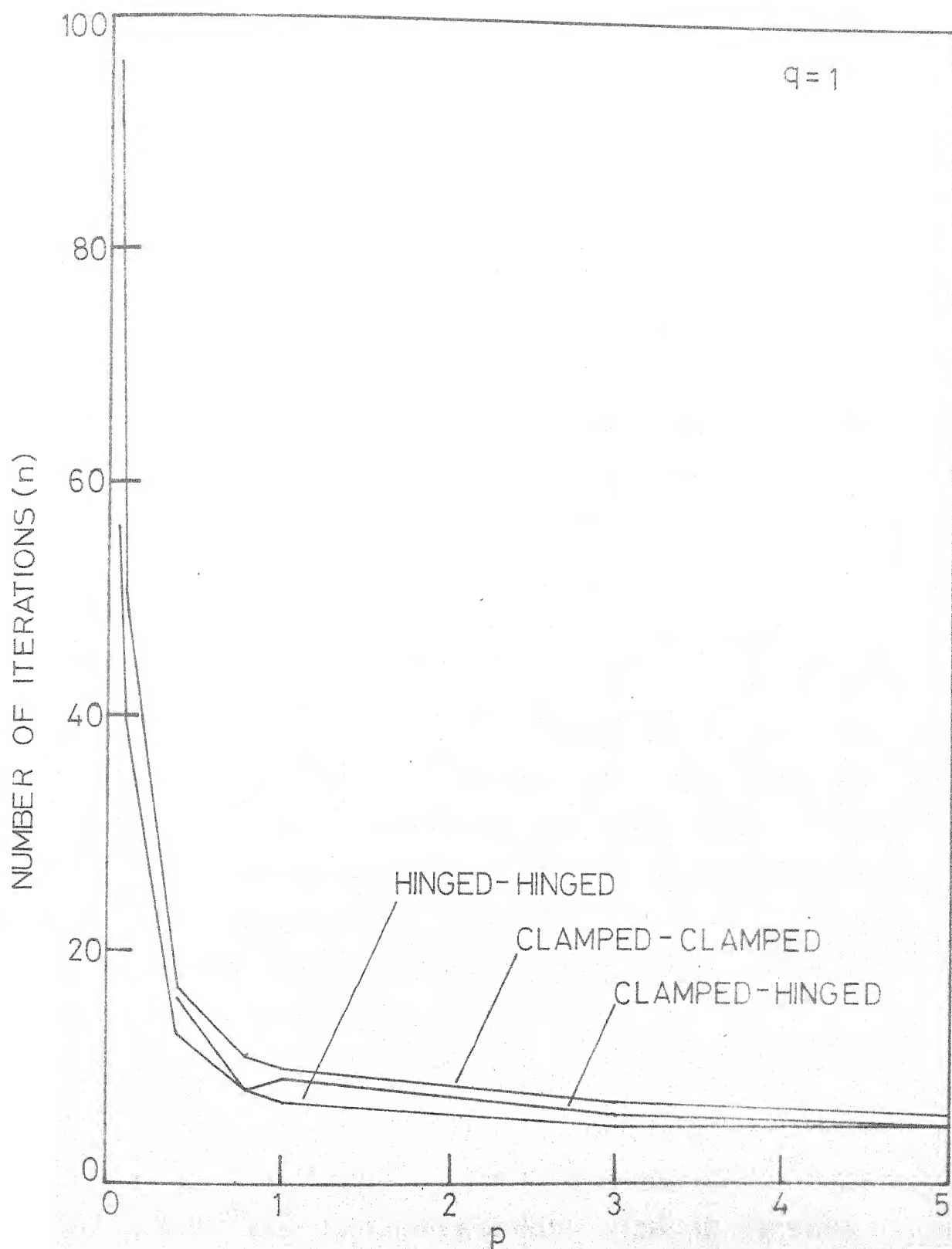


FIG.5.11. VARIATION OF NUMBER OF ITERATIONS ( $n$ ) WITH  $p$

## CHAPTER - 6

### UNIFORM-NONHOMOGENEOUS BEAMS

#### 6.1 Introduction

Problems of optimal design of vibrating elastic homogeneous elements have been thoroughly investigated in the recent past. Niordson<sup>12</sup> considered a simply supported beam with geometrically similar cross-sections ( $q = 2$ ) and determined the optimal tapering which maximizes the fundamental frequency of transverse vibrations. Brach<sup>13</sup> considered a whole group of Euler-Bernoulli beams characterized by a linear relationship between second area moment and cross-sectional area ( $q = 1$ ), and optimized their shapes with respect to fundamental frequency for all kinds of homogeneous boundary conditions. Karihaloo and Niordson<sup>14</sup> optimized the shape of a cantilever beam with respect to its fundamental frequency for  $q = 1, 2$  and  $3$ , with and without any tip mass. It was found that for  $q = 1$ , in the absence of a tip mass, the frequency is unbounded. This agrees with the similar result obtained by Brach<sup>13</sup>. Karihaloo and Niordson<sup>15</sup> further considered the problem of determining the shape of simply supported laterally vibrating beams, with  $q = 1, 2$  and  $3$ , that have the highest possible value of the first

fundamental frequency under a given axial compressive load. They concluded that for  $q = 1$  and in the absence of any compressive load, no increase in the fundamental frequency over that of a uniform beam is possible. This agrees with the result obtained by Brach<sup>13</sup>.

All the above mentioned investigations have been conducted for elastic homogeneous beams with a prescribed modulus. As stated in Chapter 1, an attempt is made here to investigate the possible increase in frequency by a proper variation of modulus along the axis of the beams with uniform and tapered cross-sections. The investigation in this chapter is, however, confined to uniform-nonhomogeneous elements. A study of tapered-nonhomogeneous beams is presented in Chapter 7.

In these studies, modulus and area variations are constrained by the relations (3.2.8) and (3.3.26) respectively. Because of the limitations stated in Chapters 1 and 3, number of design variables is restricted to two ( $e$  and  $\eta$ ) for the tapered and to one ( $e$ ) for the uniform beam. It is, therefore, as in the case of a column, assumed that uniform beam is made of a material having a constant density and variable modulus.

In Section 6.2, the Eqn. of equilibrium and boundary conditions, for H-H, F-C, C-C, and C-H end conditions

for the general case of a tapered-nonhomogeneous beam are derived. These are then specialized for the uniform beam in Section 6.2.2. The optimal problem is stated in Section 6.3 and governing equation and the optimality condition are derived in Section 6.4. These are solved for different types of end conditions in Sections 6.5 and 6.6 for  $p = 1$  and  $p \neq 1$  respectively. Comments on the numerical computations are presented in Section 6.7. Results are finally presented and discussed in Section 6.8.

## 6.2 Equation of Equilibrium for Transverse Vibrations of a Tapered-Nonhomogeneous Beam

From classical vibration theory, it is well-known that a linearly elastic beam can vibrate harmonically in anyone (or linear combination) of its infinite number of natural modes. The differential equation governing the motion is easily written as:

$$\frac{d^2}{d\xi^2} \left( EI \frac{d^2 w}{d\xi^2} \right) = \omega^2 \rho A w \quad (6.2.1)$$

where  $\omega$  is natural frequency and all other variables are defined in Section 3.2. Using the dimensionless variables defined in Eqn. (3.2.7), above equation easily reduces to:

$$(e^{\eta^q} y'')'' = \lambda \eta y \quad (6.2.2)$$

where  $\lambda$  is the dimensionless square of the frequency

$$\lambda = \frac{\rho_0^q L^{3+q} \omega^2}{\alpha E_0 m_0^{q-1}} \quad (6.2.3)$$

### 6.2.1 Boundary conditions

Solution of Eqn. (6.2.2) requires four boundary conditions for each set of end-conditions considered in this chapter. These are stated below.

#### Hinged-Hinged

$$y(0) = e\eta^q y'' \Big|_{x=0} = (e\eta^q y'')' \Big|_{x=1/2} = y'(1/2) = 0 \quad (6.2.4)$$

#### Free-Clamped

$$e\eta^q y'' \Big|_{x=0} = (e\eta^q y'')' \Big|_{x=0} = y(1/2) = y'(1/2) = 0 \quad (6.2.5)$$

#### Clamped-Clamped

$$y(0) = y'(0) = y'(1/2) = (e\eta^q y'')' \Big|_{x=1/2} = 0 \quad (6.2.6)$$

#### Clamped-Hinged

$$y(0) = y'(0) = y(1) = e\eta^q y'' \Big|_{x=1} = 0 \quad (6.2.7)$$

It may be noted that the conditions of symmetry have been used in stating (6.2.4) and (6.2.6), as the fundamental mode shapes are expected to be symmetric in the case of hinged-hinged and clamped-clamped beams. Besides, it is worth mentioning that the quantities  $e \eta^q y''$  and  $(e \eta^q y'')'$  respectively, are proportional to the bending moment and the shear force at any station  $x$ .

### 6.2.2 Equilibrium equation and B.C.'s for uniform beam

Uniform beam, as in the case of column, is assumed to be made of a material allowing a prescribed variation of modulus but having constant density. This makes

$$\eta = \tilde{\rho} a = 1 \quad (6.2.8)$$

$$e = \frac{\tilde{E}}{\tilde{\rho}^q} = a^q \tilde{E} \quad (6.2.9)$$

where both  $\tilde{\rho}$  and  $a$  are constants. Equilibrium Eqn. (6.2.2) and the B.C.'s (6.2.4) - (6.2.7), now reduce to

$$(e y'')'' = \lambda y \quad (6.2.10)$$

$$y(0) = (e y'')_{x=0} = y'(1/2) = (e y'')'_{x=1/2} = 0 \quad (\text{H-H}) \quad (6.2.11)$$

$$(e y'')_{x=0} = (e y'')'_{x=0} = y(1) = y'(1) = 0 \quad (\text{F-C}) \quad (6.2.12)$$

$$y(0) = y'(0) = y'(1/2) = (ey'')'_{x=1/2} = 0 \quad (\text{C-C}) \quad (6.2.13)$$

$$y(0) = y'(0) = y(1) = (ey'')_{x=1} = 0 \quad (\text{C-H}) \quad (6.2.14)$$

### 6.3 Statement of the Problem of Optimisation

The optimization problem can be stated as the determination of modulus distribution such that the frequency of transverse vibrations for the fundamental mode of a uniform beam of given mass and geometry, is a maximum. Following the arguments in Section 3.5, analytically, the problem may be restated as:

Minimize

$$\bar{e} = \int_0^1 e^p dx ; \quad p > 0 \quad (6.3.15)$$

such that

$$(ey'')'' = \lambda y \quad (6.2.10)$$

$$g_i = 0, \quad i = 1, 2, 3, 4 \quad (6.3.16)$$

It may be noted that equation of equilibrium (6.2.10) is treated as a constraint and  $g_i$  represent boundary conditions, stated in each of the equations (6.2.11) - (6.2.14).

#### 6.4 Necessary Conditions and the Governing Equations

Necessary conditions for the problem stated in Section 6.3 will now be obtained by applying the equations (2.3.12) to (2.3.18). The problem is, therefore, cast in the format of control theory. Defining

$$y_1 = y \quad (6.4.17)$$

$$y_2 = y' \quad (6.4.18)$$

$$y_3 = ey'' = M(x) \quad (6.4.19)$$

$$y_4 = (ey'')' = V(x) \quad (6.4.20)$$

Equation (6.2.10), which is of fourth order, can be represented by the following four first order equations.

$$\dot{y}_1 = y_2 = f_1 \quad (6.4.21)$$

$$\dot{y}_2 = \frac{y_3}{e} = f_2 \quad (6.4.22)$$

$$\dot{y}_3 = y_4 = f_3 \quad (6.4.23)$$

$$\dot{y}_4 = \lambda y_1 = f_4 \quad (6.4.24)$$

Functional  $\bar{J}$ , defined in Eqn. (2.2.8) is now easily written as:

$$\bar{J} = \sum_{i=1}^4 \gamma_i g_i + \int_0^1 [\lambda_0 e^p + \sum_{i=1}^4 \lambda_i(x)(y_i' - f_i)] dx \quad (6.4.25)$$

This yields following expressions for the functions G and H, defined in (2.3.9) and (2.3.10).

$$G = \gamma_1 g_1 + \gamma_2 g_2 + \gamma_3 g_3 + \gamma_4 g_4 \quad (6.4.25)$$

$$H = \sum_{i=1}^4 \lambda_i f_i - \lambda_0 e^p = \lambda_1 y_2 + \lambda_2 \frac{y_3}{e} + \lambda_3 y_4 + \lambda_4 \lambda y_1 - \lambda_0 e^p \quad (6.4.27)$$

Application of Eqn. (2.3.12) yields the following adjoint equations for the multipliers  $\lambda_i(x)$ .

$$\lambda_1' = -\lambda_4 \lambda \quad (6.4.28)$$

$$\lambda_2' = -\lambda_1 \quad (6.4.29)$$

$$\lambda_3' = -\frac{\lambda_2}{e} \quad (6.4.30)$$

$$\lambda_4' = -\lambda_3 \quad (6.4.31)$$

Simple algebraic manipulation of these equations gives:

$$\lambda_3 = -\lambda_4' \quad (6.4.32)$$

$$\lambda_2 = e \lambda_4'' \quad (6.4.33)$$

$$\lambda_1 = -(e \lambda_4'')' \quad (6.4.34)$$

and

$$(e \lambda_4'')'' - \lambda \lambda_4 = 0 \quad (6.4.35)$$

Thus the adjoint Eqns. (6.4.28) to (6.4.31), reduce to a single fourth order Eqn. (6.4.35) in the multiplier  $\lambda_4$ .

Equations (6.4.32) to (6.4.34) express other multipliers ( $\lambda_1, \lambda_2, \lambda_3$ ) in terms of  $\lambda_4$  and enable the boundary conditions on  $\lambda_i$ 's to be written in terms of  $\lambda_4$ . These can be easily obtained by applying Eqn. (2.3.15) to different end conditions. Procedure for each of the end conditions being the same, the steps are presented in detail for the H-H beam only.

#### Hinged-Hinged

Inserting  $\eta = 1$  in (6.2.4), function  $G$  defined in (6.4.26) reduces to:

$$G = \gamma_1 y_1(0) + \gamma_2 y_3(0) + \gamma_3 y_2(1/2) + \gamma_4 y_4(1/2) \quad (6.4.36)$$

Applying (2.3.15a) and (2.3.15b) to  $G$  in (6.4.36), one gets

$$\gamma_1 - \lambda_1(0) = 0 \quad (6.4.37)$$

$$0 - \lambda_2(0) = 0 \quad (6.4.38)$$

$$\gamma_2 - \lambda_3(0) = 0 \quad (6.4.39)$$

$$0 - \lambda_4(0) = 0 \quad (6.4.40)$$

$$0 + \lambda_1(1/2) = 0 \quad (6.4.41)$$

$$\gamma_3 + \lambda_2(1/2) = 0 \quad (6.4.42)$$

$$0 + \lambda_3(1/2) = 0 \quad (6.4.43)$$

$$\gamma_4 + \lambda_4(1/2) = 0 \quad (6.4.44)$$

Equations (6.4.38), (6.4.40), (6.4.41) and (6.4.43) provide the B.C.'s on  $\lambda_i$ 's which easily reduce to:

$$\lambda_4(0) = (e\lambda_4'')_{x=0} = \lambda_4'(1/2) = (e\lambda_4'')'_{x=0} = 0 \quad (6.4.45)$$

Equations (6.4.37), (6.4.38), (6.4.42) and (6.4.44) determine the constant multipliers  $\gamma_1, \gamma_2, \gamma_3$  and  $\gamma_4$  respectively. It is easily seen that if  $\lambda_4$  is not identically zero, all these multipliers will not be zero simultaneously.

#### Free-Clamped

$$G = \gamma_1 y_3(0) + \gamma_2 y_4(0) + \gamma_3 y_1(1) + \gamma_4 y_2(1) \quad (6.4.46)$$

$$\lambda_1(0) = \lambda_2(0) = \lambda_3(1) = \lambda_4(1) = 0 \quad (6.4.47)$$

or

$$(e\lambda_4'')_{x=0} = (e\lambda_4'')'_{x=0} = \lambda_4'(1) = \lambda_4(1) = 0 \quad (6.4.48)$$

#### Clamped-Clamped

$$G = \gamma_1 y_1(0) + \gamma_2 y_2(0) + \gamma_3 y_2(1/2) + \gamma_4 y_4(1/2) \quad (6.4.49)$$

$$\lambda_3(0) = \lambda_4(0) = \lambda_1(1/2) = \lambda_3(1/2) = 0 \quad (6.4.50)$$

or

$$\lambda_4(0) = \lambda_4'(0) = \lambda_4'(1/2) = (e\lambda_4'')'_{x=0} = 0 \quad (6.4.51)$$

Clamped-Hinged

$$G = \gamma_1 y_1(0) + \gamma_2 y_2(0) + \gamma_3 y_3(1) + \gamma_4 y_1(1) \quad (6.4.52)$$

$$\lambda_3(0) = \lambda_4(0) = \lambda_2(1) = \lambda_4(1) = 0 \quad (6.4.53)$$

or

$$\lambda_4(0) = \lambda_4'(0) = \lambda_4(1) = (e\lambda_4'')_{x=1} = 0 \quad (6.4.54)$$

Expressions determining  $\gamma_i$ 's for F-C, C-C and C-H beams are not written, as it will be seen later that their magnitude is not involved in determining the solutions.

Now, a comparison of the conditions (6.4.45), (6.4.48), (6.4.51) and (6.4.54) on  $\lambda_4$  with the corresponding conditions (6.2.11) to (6.2.14) on  $y$ , reveals that the boundary conditions on  $\lambda_4$  and  $y$  are identical. Besides, it is evident from the equations (6.2.10) and (6.4.35) that  $\lambda_4$  and  $y$  are governed by the same differential equation. This is a fortunate situation which permits writing of the solution for the multipliers in terms of the state variable  $y$ . This was observed in the case of columns also.

Evidently  $\lambda_4$  and  $y$  are related through the following expression.

$$\lambda_4 = -Ky ; \quad K > 0 \quad (6.4.55)$$

Introduction of -ve sign in (6.4.55) will be clear while deriving the optimality condition.

### Optimality condition

Now application of the Eqn. (2.3.13) to the function H defined in (6.2.27), yields:

$$\frac{\partial H}{\partial e} = -\frac{\lambda_2 y^3}{e^2} - \lambda_0 p e^{p-1} = 0 \quad (6.4.56)$$

Equations (6.4.19), (6.4.33), (6.4.55) along with (6.4.56), give:

$$e^{1-p} y^2 = \frac{\lambda_0 p}{K} \quad (6.4.57)$$

Left hand side of Eqn. (6.4.57) must be positive as  $e \geq 0$  and  $y^2 \geq 0$ . Since  $\lambda_0$  and  $p$  are positive,  $K > 0$ . This explains the particular form of  $\lambda_4$  and  $y$  relationship in (6.4.55).

Equation (6.4.57) establishes a relationship between the control variable  $e$  and the state variable  $y$  and hence may be interpreted as the optimality condition. Besides it is evident that  $e$  and  $y$  are related through (6.4.57) only for  $p \neq 1$ . When  $p$  equals 1, it reduces to:

$$y = \pm \left( \frac{\lambda_0}{K} \right)^{1/2} \quad (6.4.58)$$

In other words, optimality condition is independent of the control variable and requires mode shape to be such that the magnitude of curvature remains constant. Similar

condition was obtained for the uniform column also, and is reported by Prager and Taylor<sup>9</sup> for a homogeneous element with  $q = 1$ . Mathematically, the problem considered by them and the one considered here are equivalent.

Equation (6.4.58) will determine the mode shape and equation (6.4.10) then provides the optimum modulus distribution.

For  $p \neq 1$ , equation (6.4.57) determines  $e$  in terms of  $y''$  which when substituted in (6.4.10) yields an equation in  $y$ , which has to be solved for prescribed boundary conditions. It is, thus, evident that separate solutions have to be obtained for  $p = 1$  and  $p \neq 1$ .

## 6.5 Solution for $p = 1$

A study of the relevant equations easily reveals that the problem essentially involves five unknowns -  $e$ ,  $y$ ,  $\lambda_0$ ,  $K$  and  $\lambda$ . The number of available equations to determine these is only three - (3.3.26), (6.4.10) and (6.4.58). It appears, therefore, that the available equations are not sufficient. This is not, however, true as explained below.

Assuming the problem to be a normal one,  $\lambda_0$  can be assigned any positive value. Besides  $\lambda$  is an eigen value of the Eqn. (6.4.10) and so  $y$  can be determined

uniquely only within a scalar multiplier. This means that among the five unknowns, two are arbitrary constants and the solution must not depend on them. Identifying  $\lambda_0$  and  $K$  as these constants, and defining  $u$  as another displacement function:

$$u = y \left( \frac{\lambda_0}{K} \right)^{-1/2} \quad (6.5.59)$$

where it is assumed that  $K \neq 0$ . Equation (6.4.58) reduces to:

$$u'' = \pm 1 \quad (6.5.60)$$

Now defining

$$\tilde{e} = \frac{e}{\lambda} \quad (6.5.61)$$

equation (6.4.10), therefore, reduces to

$$\tilde{e}'' = \pm u \quad (6.5.62)$$

It may be noted that  $u$  in (6.4.59), unlike  $y$ , is a unique displacement function for a particular set of boundary conditions. Besides, if a plus (minus) sign is used in (6.5.60) then plus (minus) sign is to be used in (6.5.62) also.

#### Expressions for $\lambda$ and $e$

The relationship (3.3.26), determines following expression for  $\lambda$ .

$$\bar{e} = \int_0^1 e^p dx = \lambda \int_0^1 \tilde{e} dx = 1 \quad (6.5.63)$$

or

$$\lambda = \frac{1}{\int_0^1 \tilde{e} dx} \quad (6.5.64)$$

The distribution of  $e$  is then easily determined from (6.5.61)

$$e = \lambda \tilde{e} \quad (6.5.65)$$

It is, thus, evident that Eqns. (6.5.60), (6.5.62), (6.5.64) and (6.5.65) provide the relevant set of equations, which have to be solved for different end conditions.

#### 6.5.1 Hinged-Hinged beam

The mode shape of a H-H beam does not permit any change in the sign of curvature along the axis. Only plus (+) sign is to be used in Eqns. (6.5.60) and (6.5.62).

$$u'' = 1 \quad (6.5.66)$$

$$\tilde{e}'' = u \quad (6.5.67)$$

Now, boundary conditions being homogeneous and  $u''$  being unity, Eqn. (6.2.11) provides the following B.C.'s on  $u$  and  $\tilde{e}$ .

$$u(0) = u'(1/2) = \tilde{e}(0) = \tilde{e}'(1/2) = 0 \quad (6.5.68)$$

Integration of Eqns. (6.5.66) and (6.5.67) is very simple. Doing this for the B.C.'s stated in (6.5.68) and using (6.5.64) and (6.5.65), following solution is easily obtained.

$$u = \frac{1}{2}x(x - 1) \quad (6.5.69)$$

$$\tilde{e} = \frac{1}{24} (x^4 - 2x^3 + x) \quad (6.5.70)$$

$$\lambda = \frac{1}{2 \int_0^{1/2} \tilde{e} dx} = 120 \quad (6.5.71)$$

$$e = 5(x^4 - 2x^3 + x) \quad (6.5.72)$$

Defining dimensionless frequency  $\omega_0$  as the square root of  $\lambda$ , one gets

$$\omega_0 = (\lambda)^{\frac{1}{2}} = (120)^{\frac{1}{2}} = 10.96 \quad (6.5.73)$$

Frequency  $\omega_E$  for the corresponding uniform-homogeneous beam being  $\pi^2$ , this gives

$$\frac{\omega_0}{\omega_E} = \frac{10.96}{\pi^2} = 1.1104 \quad (6.5.74)$$

Modulus variation thus results in 11.04 percent increase in frequency. The required  $e$  distribution is provided by Eqn. (6.5.72). It is easily seen that  $e$  increases gradually from zero at the hinged end to the maximum ( $e_{\max} = 1.5625$ ) at the middle of the beam. The variation, graphically, is shown in Figure 6.2.

### 6.5.2 Free-Clamped beam

Integration of Eqns. (6.5.66) and (6.5.67) for the boundary conditions

$$u(1) = u'(1) = \tilde{e}(0) = \tilde{e}'(0) = 0 \quad (6.5.75)$$

obtained from Eqn. (6.2.12), easily yields the following solution.

$$u = \frac{x^2}{2} - x + \frac{1}{2} \quad (6.5.76)$$

$$\tilde{e} = \frac{1}{24}(x^4 - 4x^3 + 6x^2) \quad (6.5.77)$$

$$\lambda = \frac{1}{\int_0^1 \tilde{e} \, dx} = 20 \quad (6.5.78)$$

$$e = \frac{5}{6}(x^4 - 4x^3 + 6x^2) \quad (6.5.79)$$

$$\omega_0 = \sqrt{\lambda} = 4.47 \quad (6.5.80)$$

$$\frac{\omega_0}{\omega_E} = \frac{4.47}{3.52} = 1.2693 \quad (6.5.81)$$

$$e_{\max} = e(1) = 2.5 \quad (6.5.82)$$

Thus modulus variation results in an increase of 26.93 percent in frequency. The desired modulus distribution is determined by the Eqn. (6.5.79). Variation of  $e$  is shown in Figure 6.3. It is seen that  $e$  gradually increases from zero at the free end to maximum value,  $e_{\max} = 2.5$ , at the clamped end.

### 6.5.3 Clamped-Clamped beam

Mode shape for a C-C beam is characterized by an inflexion point at  $x = x_0$ . Region of integration ( $0 \leq x \leq 0.5$ ) is, therefore, divided into two parts represented by the subscripts 1 and 2. Since the magnitude of curvature is constant, + sign in (6.5.60) and (6.5.62) is used for the region 1 and - sign for the region 2. Considering continuity conditions at  $x_0$ , following appropriate equations and boundary conditions can be easily stated.

$$u_1'' = 1 \quad (6.5.83)$$

$$\tilde{e}_1'' = u_1'' \quad ; \quad 0 \leq x_1 \leq x_0 \quad (0 \leq x \leq x_0) \quad (6.5.84)$$

$$u_2'' = -1 \quad (6.5.85)$$

$$\tilde{e}_2'' = -u_2'' \quad ; \quad 0 \leq x_2 \leq 0.5 - x_0 \quad (x_0 \leq x \leq 0.5) \quad (6.5.86)$$

$$u_1(0) = u_1'(0) = 0 \quad (6.5.87)$$

$$\tilde{e}_1(x_0) = \tilde{e}_2(0) = 0 \quad (6.5.88)$$

$$\tilde{e}_1'(x_0) + \tilde{e}_2'(0) = 0 \quad (6.5.89)$$

$$u_2(0) = u_1(x_0) \quad (6.5.90)$$

$$u_2'(0) = u_1'(x_0) \quad (6.5.91)$$

$$u_2'(0.5 - x_0) = \tilde{e}_2'(0.5 - x_0) = 0 \quad (6.5.92)$$

It may be noted that  $x_1$  and  $x_2$  are the running coordinates in regions 1 and 2 respectively. Equations (6.5.88) to (6.5.91) state continuity conditions on moment, shear, deflection and slope respectively at the inflexion point. Moment at  $x_0$  is zero because of the change in sign of curvature at this point.

It is simple to determine the solution of Eqns. (6.5.83) to (6.5.92) and so the details are omitted here. The solution obtained is:

$$x_0 = 0.25 \quad (6.5.93)$$

$$u_1 = \frac{1}{2} x_1^2 \quad (6.5.94)$$

$$\tilde{e}_1 = \frac{x_1^4}{24} - \frac{x_1}{64} + \frac{23}{6144} \quad ; \quad 0 \leq x_1 \leq 0.25 \quad (0 \leq x \leq 0.25) \quad (6.5.95)$$

$$u_2 = -\frac{x_2^2}{2} + \frac{x_2}{4} + \frac{1}{32} \quad (6.5.96)$$

$$\tilde{e}_2 = \frac{x_2^4}{24} - \frac{x_2^3}{24} - \frac{x_2^2}{64} + \frac{5}{384} x_2 \quad ; \quad 0 \leq x_2 \leq 0.25 \quad (0.25 \leq x \leq .5) \quad (6.5.97)$$

Now using (6.5.64) and (6.5.65)

$$\lambda = \frac{1}{2 \left[ \int_0^{1/4} \tilde{e}_1 dx_1 + \int_0^{1/4} \tilde{e}_2 dx_2 \right]} = \frac{15360}{23} = 667.8 \quad (6.5.98)$$

$$e_1(x_1) = \lambda \tilde{e}_1 = 667.8 \left( \frac{x_1^4}{24} - \frac{x_1}{64} + \frac{23}{6144} \right) \quad (6.5.99)$$

$$e_2(x_2) = \lambda \tilde{e}_2 = 667.8 \left( \frac{x_2^4}{24} - \frac{x_2^3}{24} - \frac{x_2^2}{64} + \frac{5x_2}{384} \right) \quad (6.5.100)$$

$$\omega_0 = V_\lambda = 25.84 \quad (6.5.101)$$

$$\frac{\omega_0}{\omega_E} = \frac{25.84}{22.4} = 1.1537 \quad (6.5.102)$$

$$e_{1_{\max}} = e_1(0) = 2.5 \quad (6.5.103)$$

$$e_{2_{\max}} = e_2(1/4) = 1.196 \quad (6.5.104)$$

Equations (6.5.99) and (6.5.100) provide optimum  $e$  variation along the axis. This results in an increase of 15.37 percent in frequency over the corresponding uniform-homogeneous beam, for which frequency  $\omega_E$  is 22.4. Figure 6.4 shows variation of  $e$  graphically. It easily reveals that the maximum value  $e_{\max}$  is 2.5 at the clamped end. From 2.5, it reduces to zero at the inflexion point and then gradually increases to 1.196 at the mid point ( $x = 1/2$ ).

#### 6.5.4 Clamped-Hinged beam

Mode shape for this beam is also characterized by an inflexion point  $x_0$ , whose location is to be determined from the solution. It is easily seen that Eqns. (6.5.83) to (6.5.91) of Section 6.5.3, are applicable in this case also. Only the Eqn. (6.5.92) is to be replaced by

$$u_2(1 - x_0) = \tilde{e}_2(1 - x_0) = 0 \quad (6.5.105)$$

It may be mentioned that the region 2 here corresponds to  $0 \leq x_2 \leq 1-x_0$ .

Equations (6.5.83) to (6.5.91) together with (6.5.105) yield the solution after some simple algebraic manipulations. The equation obtained to determine  $x_0$  is:

$$2x_0^2 - 4x_0 + 1 = 0 \quad (6.5.106)$$

This gives

$$x_0 = \frac{2 - \sqrt{2}}{2} = 0.2929 \quad (6.5.107)$$

The solution for  $u$  and  $\tilde{e}$  can be easily written as:

$$u_1 = \frac{1}{2} x_1^2 \quad ; \quad 0 \leq x_1 \leq x_0 \quad (0 \leq x \leq x_0) \quad (6.5.108)$$

$$\tilde{e}_1 = \frac{1}{24}(x_1^4 - x_0^4) - C_1(x_0 - x_1) \quad (6.5.109)$$

$$u_2 = \frac{1}{2} (x_0^2 - x_2^2) + x_2 x_0 ;$$

$$0 \leq x_2 \leq 1-x_0 \quad (x_0 \leq x \leq 1-x_0) \quad (6.5.110)$$

$$\tilde{e}_2 = \frac{x_2^4}{24} - \frac{x_0 x_2^3}{6} - \frac{x_0^2 x_2^2}{4} + C_2 x_2 \quad (6.5.111)$$

where  $C_1$  and  $C_2$  are constants of integration having the following values.

$$C_2 = \frac{1}{24} (1 - x_0)(x_0^2 + 6x_0 - 1) = 0.02484 \quad (6.5.112)$$

$$C_1 = -\left(C_2 + \frac{x_0^3}{6}\right) = -0.02903 \quad (6.5.113)$$

The above relations now give

$$\lambda = \frac{1}{\int_0^{x_0} \tilde{e}_1 dx_1 + \int_0^{1-x_0} \tilde{e}_2 dx_2} = 305.05 \quad (6.5.114)$$

$$\omega_0 = V\lambda = 17.465 \quad (6.5.115)$$

$$\frac{\omega_0}{\omega_E} = \frac{17.465}{15.421} = 1.1326 \quad (6.5.116)$$

Using Eqns. (6.5.109) and (6.5.111) for  $\tilde{e}_1$  and  $\tilde{e}_2$  and  $\lambda$  from (6.5.114), Eqn. (6.5.65) easily provides  $e$  ( $e_1$  and  $e_2$ ) variation. Computations reveal

$$e_{1_{\max}} = e(0) = 2.5 \quad (6.5.117)$$

$$e_{2_{\max}} = e(0.63) = 1.405 \quad (6.5.118)$$

The solution, thus, indicates an increase of 13.26 percent in frequency. Distribution of  $e$  required to produce this is shown in Figure 6.5. It is easily seen that the maximum  $e$  required, as for C-C beam, is 2.5 at the clamped end.

It may also be noted that the inflexion point location for C-C and C-H uniform-nonhomogeneous beams is the same as that for the corresponding columns in Chapter 3. This should be expected because the optimality condition, both for columns and beams, requires a deflection mode shape with constant magnitude of curvature.

## 6.6 Solution for $p \neq 1$

Defining the displacement function  $v$  as

$$w = y \left( \frac{\lambda_0 p}{K} \right)^{-1/2} \quad (6.6.119)$$

Equation (6.4.57) reduces to:

$$e = (v''^2)^{1/p-1} \quad (6.6.120)$$

Here,  $e$  is written in this form to ensure that  $e \geq 0$  irrespective of  $v''$  being positive or negative. Substituting  $e$  in terms of  $v''$ , Eqn. (6.2.10) gives a single equation in  $v$ .

$$\left[ v''^{\frac{p+1}{p-1}} \right]'' = \lambda v \quad (6.6.121)$$

Now making the transformation

$$u = \lambda^{\frac{p-1}{2}} v \quad (6.6.122)$$

Equations (6.6.120) and (6.6.121) reduce to:

$$e = \lambda (u''^2)^{\frac{1}{p-1}} \quad (6.6.123)$$

$$\left[ \frac{u''}{(u''^2)^{\frac{1}{1-p}}} \right]'' = \left[ u''^{\frac{p+1}{p-1}} \right]'' = u \quad (6.6.124)$$

Integrating (6.6.123) between the limits  $x = 0$  to  $x = 1$  and using (3.3.26),  $\lambda$  can be determined as:

$$\lambda = \frac{1}{\int_0^1 (u''^2)^{\frac{1}{p-1}} dx} \quad (6.6.125)$$

The problem thus reduces to the solution of Eqn. (6.6.124) for a prescribed set of boundary conditions. A unique solution, specifying mode shape, is obtained. Equations (6.6.125) and (6.6.123), then, determine the eigen value  $\lambda$  and the corresponding  $e$  distribution.

Governing Eqn. (6.6.124) being nonlinear, its solution is obtained numerically by the method of successive iterations for the four end conditions, like H-H, F-C, C-C and C-H, considered in Section 6.6. The solution is determined in Sections 6.6.2 to 6.6.5.

### 6.6.1 Singular behaviour

Form of Eqn. (6.6.124) suggests that  $(u'')^{\frac{p+1}{p-1}}$  represents bending moment. Since bending moment vanishes at hinged and free ends and at the points of inflexion, these points for  $p < 1$  are obviously characterized by a

singularity in the curvature  $u''$ . Numerical integration of (6.6.121) reveals that the knowledge of exact analytical behaviour of  $u$  around the singularity is very important, not only for reaching the convergence but also for arriving at any meaningful results.

Study of the singular behaviour is done, as in the case of columns in Section 4.2, by following the approach used by Niordson<sup>12</sup>. Defining  $s$  by

$$s = -\frac{1+p}{1-p} \quad (s < 0 \text{ for } p < 1) \quad (6.6.126)$$

Equation (6.6.124) can be written in alternate expanded form.

$$s(u'')^{s-1} u^{iv} + s(s-1)(u'')^{s-2} u'''^2 - u = 0 \quad (6.6.127)$$

Now, displacement function  $u$  is expanded in a power series around the singularity, as:

$$u \sim a_0 + a_1 x + a_2 x^t + a_3 x^2 + \dots \quad (6.6.128)$$

Here  $t$  is a fraction which is expected to lie between 1 and 2, thereby making  $u''$  singular at  $x = 0$ . Since only the term involving  $t$  is of importance, one can write

$$u \sim x^t \quad (6.6.129)$$

Derivatives of  $u$  can, then, be written as:

$$u' \sim t x^{t-1} \quad (6.6.130)$$

$$u'' \sim t(t-1) x^{t-2} \quad (6.6.131)$$

$$u''' \sim t(t-1)(t-2) x^{t-3} \quad (6.6.132)$$

$$u^{iv} \sim t(t-1)(t-2)(t-3) x^{t-4} \quad (6.6.133)$$

Substituting these in (6.6.127), collecting the coefficients of the leading term  $x^{st-2s-2}$ ,  $t$  is determined from the relation:

$$st - 2s - 1 = 0 \quad (6.6.134)$$

$$\text{or } t = 2 + \frac{1}{s} = 1 + \frac{2p}{1+p} = \frac{1+3p}{1+p} \quad (6.6.135)$$

It is thus clear, that for  $p < 1$ ,  $1 < t < 2$ , which makes  $u''$  singular. For  $p > 1$ , it is evident that  $t > 2$  and hence curvature  $u''$  will vanish at  $x = 0$ . Curvature  $u''$ , therefore, being singular for  $p < 1$  and zero for  $p > 1$ , Eqn. (6.6.123) gives  $e = 0$  at the points where bending moment is zero. In the absence of any constraint on the minimum value of modulus, this is expected physically also.

#### Contribution $\Delta$ due to the peak

Effect of peak due to singularity, while numerically integrating (6.6.124), cannot be ignored. It is determined by approximating the  $u''$  curve near the singularity by

$$u'' = ax^{t-2} = ax^{\frac{p-1}{p+1}} \quad (6.6.136)$$

where  $a$  is a constant, which can be approximated by matching  $u''$  at  $x = h$ . During numerical computation,  $h$  is taken to be the spacing between successive divisions. The value of  $a$ , thus, determined is

$$a = \frac{u''(h)}{h^{\frac{p-1}{p+1}}} \quad (6.6.137)$$

The area ( $\Delta$ ) under  $u''$  curve between  $x = 0$  and  $x = h$  is easily determined by integrating (6.6.136).

$$\Delta = a \int_0^h x^{\frac{p-1}{p+1}} dx = \left(\frac{p+1}{2p}\right) h u''(h) \quad (6.6.138)$$

### 6.6.2 Hinged-Hinged beam

Equation (6.6.124) is to be solved for the boundary conditions (6.2.11) which are restated here in terms of the variable  $u$ .

$$u(0) = u'(1/2) = 0 \quad (6.6.139)$$

$$\left[u''^{\frac{p+1}{p-1}}\right]_{x=0} = 0 \quad (6.6.140)$$

$$\left[u''^{\frac{p+1}{p-1}}\right]_{x=1/2} = 0 \quad (6.6.141)$$

condition (6.6.140) implies:

$$u''(0) = \infty \quad \text{for } p < 1 \quad (6.6.142)$$

$$u''(0) = 0 \quad \text{for } p > 1 \quad (6.6.143)$$

Integration of (6.6.124) between the limits  $x$  to  $1/2$ , along with the condition (6.6.140), gives:

$$V(x) = [u''^{\frac{p+1}{p-1}}]_x^{1/2} = - \int_x^{1/2} u \, dx \quad (6.6.144)$$

where  $V(x)$  represents shear force. Integrating (6.6.144) between the limits 0 to  $x$  and employing the condition (6.6.140),  $u''$  is determined from:

$$u'' = \left[ - \int_0^x \int_x^{1/2} u \, dx^2 \right]^{\frac{p-1}{p+1}} \quad (6.6.145)$$

Integration of  $u''$  between the limits  $x$  to  $1/2$  gives  $u'$ , which when integrated in turn between the limits 0 to  $x$ , yields  $u$ . Performing this and using (6.6.139),  $u'$  and  $u$  are determined from:

$$u' = - \int_x^{1/2} u'' \, dx \quad (6.6.146)$$

$$u = - \int_0^x \int_x^{1/2} u'' \, dx^2 \quad (6.6.147)$$

$$\text{or } u = - \int_0^x \int_x^{1/2} \left[ - \int_0^x \int_x^{1/2} u \, dx^2 \right]^{\frac{p-1}{p+1}} dx^2 \quad (6.6.148)$$

To establish an iterative scheme to determine  $u$ , Eqn. (6.6.148) can be rewritten as:

$$u_{n+1} = - \int_0^x \int_x^{1/2} \left[ - \int_0^x \int_x^{1/2} u_n \, dx^2 \right]^{\frac{p-1}{p+1}} dx^2 \quad (6.6.149)$$

Here, subscript  $n$  represents to the particular stage of iteration.

#### Steps in iteration

- i) Choose some initial function  $u$ , which may or may not satisfy the boundary conditions. It was chosen such that  $u'' = 1$ .
- ii) Using Eqns. (6.6.144) to (6.6.148), determine  $V(x)$ ,  $u''$ ,  $u'$  and  $u$  respectively. The solution obtained after the first iteration, may not satisfy the governing Eqn. (6.6.124), but satisfies all the boundary conditions. It may be mentioned that function  $u$  at every stage of iteration was kept negative, as  $u''$  was selected to be positive, which implies negative  $u$ .
- iii) Using the function  $u$  thus determined, repeat the step (ii) until there is no appreciable change in  $u$ .

after two successive iterations. To avoid any premature termination, convergence is obtained on the value of  $\lambda$ , which is determined at every stage of iteration from Eqn. (6.6.125). Once the convergence is reached,  $e$  distribution is then easily determined from Eqn. (6.6.123).

Region of integration is divided into 100 equal parts. Integration, in double precision, is done by trapezoidal rule. Though the convergence is quite rapid, still the number of iterations varies with the value of  $p$ .

The solution is obtained for several values of  $p$ , varying from 0.08 to 10. For  $p < 0.1$ , the results are of theoretical interest only, as the obtained  $e$  distributions may not be achieved practically. Curve of percent increase in frequency versus  $p$  (Figure 6.1) is monotonic, frequency increasing with decreasing  $p$ . Variation of  $e$  along the axis with  $p$  as a parameter is shown in Figure 6.2. Curves are, however, drawn only for three values,  $p = 0.08, 1$  and  $10$ , indicating the general trends. All the results are presented in Table 6.2.

### 6.6.3 Free-Clamped beam

Governing Eqn. (6.6.124), in this case, is to be solved for the boundary conditions (6.2.12). These are restated here, in terms of  $u$ .

$$\left[ u''^{\frac{p+1}{p-1}} \right]_{x=0} = \left[ u''^{\frac{p+1}{p-1}} \right]_{x=1} = u(1) = u'(1) = 0 \quad (6.6.150)$$

First of the four conditions in (6.6.150), implies

$$u''(0) = \infty \quad \text{for } p < 1 \quad (6.6.142)$$

$$u''(0) = 0 \quad \text{for } p > 1 \quad (6.6.143)$$

Following the steps of Section 6.6.2, Eqn. (6.6.124) along with the conditions in (6.6.150), easily give the following expressions.

$$\left[ u''^{\frac{p+1}{p-1}} \right]' = \int_0^x u \, dx \quad (6.6.151)$$

$$u'' = \left[ \int_0^x \int_0^x u \, dx^2 \right]^{\frac{p-1}{p+1}} \quad (6.6.152)$$

$$u' = - \int_x^1 u'' \, dx \quad (6.6.153)$$

$$u = \int_x^1 \int_x^1 u'' \, dx^2 = \int_x^1 \int_x^1 \left[ \int_0^x \int_0^x u \, dx^2 \right]^{\frac{p-1}{p+1}} dx_2 \quad (6.6.154)$$

Iterative solution for  $u$  is obtained in a manner similar to that described in Section 6.6.2. The details, therefore, are omitted. Initial function in this case also, is taken as  $u'' = 1$ .

Having determined  $u$  and  $\lambda$  from the iterative process,  $e$  distribution is obtained from (6.6.125). The solution is obtained for the values of  $p$  selected in Section 6.6.2.

Variation of percent increase in frequency over the corresponding uniform-homogeneous beam is monotonic, and is shown in Figure 6.1. Variation of  $e$  along the axis is shown in Figure 6.3, for  $p = 0.6, 1$ , and  $10$ . Complete results are presented in Table 6.3.

#### 6.6.4 Clamped-Clamped beam

Mode shape in this case is characterized by the existence of an inflexion point at  $x = x_0$ , whose location is also to be determined. Since curvature  $u''$  changes sign at  $x = x_0$ , the region of integration, as in Section 6.5.3, is divided into two parts, represented by subscript 1 and 2. Besides, the conditions (6.2.13), the solution has to satisfy the continuity conditions at the inflexion point. The relevant equations and conditions, therefore, are:

$$\left[ u_i'' \frac{p+1}{p-1} \right]'' = u_i, \quad i = 1, 2 \quad (6.6.155)$$

$$u_1(0) = u_1'(0) = 0 \quad (6.6.156)$$

$$u_1'' \frac{p+1}{p-1} \Big|_{x_1 = x_0} = u_2'' \frac{p+1}{p-1} \Big|_{x_2 = 0} = 0 \quad (6.6.157)$$

$$\left[ u_1'' \frac{p+1}{p-1} \right]'_{x_1 = x_0} = \left[ u_2'' \frac{p+1}{p-1} \right]'_{x_2 = 0} \quad (6.6.158)$$

$$u_1(x_0) = u_2(0) \quad (6.6.159)$$

$$u_1'(x_0) = u_2'(0) \quad (6.6.160)$$

$$u_2'(0.5-x_0) = \left[ u_2'' \frac{p+1}{p-1} \right]'_{x_2 = 0.5-x_0} = 0 \quad (6.6.161)$$

Equations (6.6.156) to (6.6.159) state continuity conditions at  $x = x_0$ . The two regions (1 and 2) are described by the running coordinates  $x_1$  and  $x_2$ .

Integration of (6.6.155) for  $i = 1$ , twice with respect to  $x_1$  and use of (6.6.156), easily gives:

$$V - \left[ u_1'' \frac{p+1}{p-1} \right]' = \int_x^{x_0} u_1 dx_1 \quad (6.6.162)$$

$$u_1'' = \left[ \int_{x_1}^{x_0} \int_{x_1}^{x_0} u_1 dx_1^2 - V(x_0 - x_1) \right]^{\frac{p-1}{p+1}} \quad (6.6.163)$$

where

$$V = \left[ u_1''^{\frac{p+1}{p-1}} \right]'_{x_1 = x_0} \quad (6.6.164)$$

Integrating now (6.6.155) for  $i = 2$ , once with respect to  $x_2$  and using continuity of shear (6.6.157) at the inflexion point, one gets:

$$\left[ u_2''^{\frac{p+1}{p-1}} \right]' - V = \int_0^{x_2} u_2 dx_2 \quad (6.6.165)$$

Application of zero shear condition (6.6.161) at the middle point determines  $V$ .

$$V = - \int_0^{0.5-x_0} u_2 dx_2 \quad (6.6.166)$$

Integrating (6.6.165) and using condition (6.6.157) of zero moment at  $x_0$ , one gets:

$$u_2'' = \left[ \int_0^{x_2} \int_0^{x_2} u_2 dx_2^2 + Vx_2 \right]^{\frac{p-1}{p+1}} \quad (6.6.167)$$

Expressions for  $u_1''$  and  $u_2''$  are now rewritten after inserting expression (6.6.166) for  $V$ .

$$u_1'' = \left[ \int_x^{x_0} \int_x^{x_0} u_1 dx_1^2 + (x_0 - x_1) \int_0^{0.5-x_0} u_2 dx_2 \right]^{\frac{p-1}{p+1}} \quad (6.6.168)$$

$$u_2'' = - \left[ - \int_0^{x_2} \int_0^{x_2} u_2 dx_2^2 + x_2 \int_0^{0.5-x_0} u_2 dx_2 \right]^{\frac{p-1}{p+1}} \quad (6.6.169)$$

It may be noted that  $u_2''$  is put in the above form to ensure that  $u_2''$  is always negative in every iteration. Besides, this makes the quantity within brackets always positive, to avoid encountering the problem of a negative quantity being raised to a fractional power  $(\frac{p-1}{p+1})$ .

Integration of (6.6.168) and (6.6.169) along with (6.6.156) and continuity conditions (6.6.159) and (6.6.160), yields expressions to determine deflection  $u$  and slope  $u'$ .

$$u_1' = \int_0^{x_1} u_1'' dx_1 \quad (6.6.170)$$

$$u_1 = \int_0^{x_1} \int_0^{x_1} u_1'' dx_1^2 \quad (6.6.171)$$

$$u_2' = \int_0^{x_2} u_2'' dx_2 + u_1'(x_0) \quad (6.6.172)$$

$$u_2 = \int_0^{x_2} \int_0^{x_2} u_2'' dx_2^2 + x_2 u_1'(x_0) + u_1(x_0) \quad (6.6.173)$$

It may be noted that while carrying out the integrations in (6.6.170) and (6.6.172), effect of singularity for  $p < 1$  is to be accounted, properly.

Equations derived so far, determine the solution for a particular value of  $x_0$ . This is determined from the condition of zero slope (6.6.161) at  $x = 1/2$ . This gives:

$$F(x_0) = \int_0^{0.5-x_0} u_2'' dx_2 + \int_0^{x_0} u_1'' dx_1 = 0 \quad (6.6.174)$$

### Steps in iteration

- (1) Choose some initial value of  $x_0$ ;  $x_0 = 0.25$  provides a good starting point.
- (2) Select initial functions for  $u_1$  and  $u_2$ . These were taken such that  $u_1$  and  $u_2$  are positive, whereas  $u_1''$  is positive and  $u_2''$  is negative. This is important for the proper working of the iterative process.

(3) Defining

$$F_1(x_1) = \int_{x_1}^{x_0} u_1 dx_1 \quad (6.6.175)$$

$$FI_1(x_1) = \int_{x_1}^{x_0} \int_{x_1}^{x_0} u_1 dx_1^2 \quad (6.6.176)$$

$$F_2(x_2) = \int_0^{x_2} u_2 dx_2 \quad (6.6.177)$$

$$FI_2(x_2) = \int_0^{x_2} \int_0^{x_2} u_2 dx_2^2, \quad (6.6.178)$$

determine  $F_1(x_1)$ ,  $FI_1(x_1)$ ,  $F_2(x_2)$  and  $FI_2(x_2)$ .

(4) Determine  $V$  from (6.6.166). In terms of function  $F_2$ , it is given by:

$$V = -F_2(0.5 - x_0) \quad (6.6.179)$$

(5) Equations (6.6.168) and (6.6.169), now, provide  $u$  distribution. Equations (6.6.170) to (6.6.173), then, determine variation of slope and deflection along the axis.

(6) Deflection function  $u$  ( $u_1$  and  $u_2$ ) obtained in step 5, satisfies all the boundary conditions except (6.6.174). Using this, repeat the iterations from step 3 onwards till the solution converges. To avoid any premature

$$e_1(x_1) = \lambda (u_1'')^{\frac{1}{p-1}} ; \quad 0 \leq x_1 \leq x_0 \quad (0 \leq x \leq x_0) \quad (6.6.182)$$

$$e_2(x_2) = \lambda (u_2'')^{\frac{1}{p-1}} ; \quad 0 \leq x_2 \leq 0.5 - x_0 \quad (x_0 \leq x \leq 1/2) \quad (6.6.183)$$

Solution reveals that, unlike columns, inflexion point location ( $x_0$ ) does change with the parameter  $p$ . This is presented in Table 6.1c.

Percentage increase in frequency, increases monotonically with decreasing  $p$ . It is shown in Figure 6.1. Variation of  $e$  along the axis is shown in Figure 6.4 for  $p = 0.6, 1$ , and  $10$ . Complete results are presented in Table 6.4.

#### 6.6.5 Clamped-Hinged beam

Mode shape in this case is also characterized by an inflexion point at  $x = x_0$ , whose location is to be determined from the solution. The problem, here, being similar to that in Section 6.6.4, most of the details are, therefore, omitted.

Equations (6.6.155) to (6.6.160) are valid here also. Conditions in (6.6.161) are to be replaced by

$$u_2(1 - x_0) = [u_2'']^{\frac{p+1}{p-1}}_{x_2 = 1-x_0} = 0 \quad (6.6.184)$$

Developing the equations for iterative solution, it is easily seen that Eqns. (6.6.162) to (6.6.165), and (6.6.167) are applicable in this case also.  $V$  is then determined by applying the condition (6.6.184) of zero moment, at the hinged end. The relation obtained is:

$$V = - \frac{1}{(1-x_0)} \int_0^{1-x_0} \int_0^{x_2} u_2 dx_2^2 \quad (6.6.185)$$

Inserting  $V$  from (6.6.185) into (6.6.167),  $u_2''$  can be determined from:

$$u_2'' = - \left[ \left( \frac{x_2}{1-x_0} \right) \int_0^{1-x_0} \int_0^{x_2} u_2 dx_2^2 - \int_0^{x_2} \int_0^{x_2} u_2 dx_2^2 \right]^{\frac{p-1}{p+1}} \quad (6.6.186)$$

Power  $\frac{p-1}{p+1}$  in the above expression for  $u_2''$  being a fraction, it can be used only when the quantity within brackets (say  $G(x_2)$ ) is positive. As  $G(x_2)$  is the difference of two positive quantities ( $u_2 > 0$ ), it became negative. The above expression, therefore, cannot be used. An alternative expression for  $u_2''$  was found. Using this,  $G(x_2)$  always remained positive during iterations.

#### Alternative expression for $u_2''$

Integration of (6.6.165) between the limits  $x_2$  to  $(1-x_0)$ , along with the zero moment condition (6.6.184) at the hinged end, gives:

$$u_2'' \frac{p+1}{p-1} = -[(1 - x_0 - x_2)V + \int_{x_2}^{1-x_0} \int_0^{x_2} u_2 dx_2^2] \quad (6.6.187)$$

Satisfaction of the condition of zero moment at  $x_2 = 0$  in (6.6.187), gives an expression for  $V$ , which is the same as the relation (6.6.185). Expression for  $u_2''$ , then, becomes:

$$u_2'' = -\left[ \int_{x_2}^{1-x_0} \int_0^{x_2} u_2 dx_2^2 - \left( \frac{1 - x_0 - x_2}{1 - x_0} \right) \int_0^{1-x_0} \int_0^{x_2} u_2 dx_2^2 \right] \left( \frac{p-1}{p+1} \right) \quad (6.6.188)$$

It is evident that the quantity within brackets in Eqn. (6.6.188), is always positive for  $u_2(x_2) < 0$ . Slope  $u'$  and deflection  $u$ , can now be determined from Eqns. (6.6.170) to (6.6.171). The equations thus developed, satisfy the governing equation and all the boundary conditions, except the condition (6.6.184) of zero deflection at the hinged end. It is to be used to determine  $x_0$ . The following termination criterion, to determine  $x_0$ , was used.

$$\frac{u(1)}{u(0.50)} < \epsilon \quad (6.6.189)$$

Since the magnitude of maximum  $u$  is not known apriori, and it varies considerably with the value of  $p$ , the above criterion avoids premature termination. Value  $u(0.50)$  (deflection at  $x = 0.50$ ) was used, as maximum deflection occurs around this value.

The iteration follows, virtually, the same steps as stated in Section 6.6.4. Eigen value  $\lambda$  and modulus  $e$  distributions, are determined from:

$$\lambda = \frac{1}{\int_0^{x_0} (u_1'')^{\frac{1}{p-1}} dx_1 + \int_0^{1-x_0} (u_2'')^{\frac{1}{p-1}} dx_2} \quad (6.6.190)$$

$$e_1(x_1) = \lambda (u_1'')^{\frac{1}{p-1}} ; \quad 0 \leq x_1 \leq x_0 \quad (0 \leq x \leq x_0) \quad (6.6.191)$$

$$e_2(x_2) = \lambda (u_2'')^{\frac{1}{p-1}} ; \quad 0 \leq x_2 \leq 1-x_0 \quad (x_0 \leq x \leq 1) \quad (6.6.192)$$

Solutions are obtained for different values of  $p$ . Percent increase in frequency, as in other cases, increases monotonically with decreasing  $p$ , and is shown in Figure 6.1. The corresponding distributions of  $e$  for  $p = 0.6, 1$  and  $10$ , are shown in Figure 6.5. All the results, however, are presented in Table 6.5.

## 6.7 Comments on the Method of Successive Iterations

A convergence study is made to study the efficiency of the method for various end conditions. It is found that the convergence takes place in few iterations, if  $p$  is around one. Number of iterations  $n$  increases with a decrease or increase in the value of  $p$ ; increase in  $n$

being sharp for high or low values of  $p$ . For instance in the case of H-H beams,  $n$  for  $p = 0.7$  is 7 and for  $p = 0.08$ , it is 58. It is further found that for a particular value of  $p$ , number of iterations is virtually the same for all types of end conditions. A curve of  $n$  versus  $p$  is, therefore, presented in Figure 7.6 for the H-H beam only.

Determination of solution for different values of  $p$  can be done in two ways. One can either choose any initial starting function  $u(x)$  for each  $p$ , or the function  $u(x)$  obtained for a particular value of  $p$  can be used as the initial starting function for the next value of  $p$ . Since in the latter case, initial function satisfies all the boundary conditions of the problem (specially in H-H and F-C cases), and is expected to be a closer approximation to the actual function, number of iterations required is expected to be less. Experience, however, reveals that in both the cases convergence requires same number of iterations.

Some numerical difficulties are encountered in the case of C-C and C-H beams, where a singularity occurs at the inflexion point, whose location is also to be determined along with the solution. Experience shows, that while approximating contributions  $\Delta_1$  and  $\Delta_2$  due to the peak at the inflexion point (Figure 4.1)  $\epsilon_1$  and  $\epsilon_2$  should be nearly of the same magnitude. If it is not so, it may

become difficult to satisfy the termination criterion, and there is a danger of encountering numerical instability. So the region to the left as well as to the right of  $x_0$  is separately divided into 100 equal divisions for numerical integration, and then the solution is obtained by the iterative schemes presented in Sections 6.6.4 and 6.6.5. This works nicely, and  $x_0$  can be determined to a fair degree of accuracy. However, the distribution of  $e$  obtained is not convenient to represent, as one would like to specify the value of  $e$  along the axis at equidistant points, whereas the above scheme prescribes  $e$  at equidistant points, in each of the regions before and after the inflexion point.

In order to overcome this difficulty, an alternative scheme is followed. Inflexion point location  $x_0$ , is first determined accurately in the manner explained above. In the C-C case, interval  $0 \leq x \leq 1/2$  is divided into 200 equal parts and  $x_0$  is, then, approximated to the nearest mesh size ( $h = 0.0025$ ). This enables one to keep  $\varepsilon_1 = \varepsilon_2 = h$ . With this approximate location of  $x_0$ , the solution is determined. The results obtained are fairly accurate, as the frequency does not seem to be very sensitive to the small approximations in the location of  $x_0$ .

A similar approach could not be used in the case of C-H beams, even though the mesh size after dividing the interval  $0 \leq x \leq 1$  into 200 parts, is 0.005. Approximation of  $x_0$  even within this accuracy of  $h$ , introduces a large approximation. So the region  $h$  within which  $x_0$  lies, is further subdivided into 10 equal parts, and then  $x_0$  is determined within the accuracy of  $h/10$ , i.e., 0.0005. Location  $x_0$ , thus determined, satisfies termination criterion to a reasonable accuracy. The results presented in this thesis, are obtained by the scheme just presented.

## 6.8 Results and Discussion

The solutions obtained in this chapter are presented in the form of tables and curves. Variation of percent increase in the frequency with  $p$  for H-H, F-C, C-C and C-H end conditions is presented in Table 6.1, and is shown in Figure 6.1. The corresponding  $e$  distributions, are given in Tables 6.2 to 6.5, and are shown in Figures 6.2 to 6.5. Computations are restricted to only those small values of  $p$ , which yield meaningful values of  $e$ , as it will be impractical to achieve very high values of the modulus.

A study of tables and curves reveals that variation of percent increase in frequency with  $p$ , as in

the case of columns for all end conditions is monotonic, frequency increasing with decreasing  $p$ . Theoretically, any increase in frequency can be achieved, but this is restricted by the fact that the corresponding modulus distributions desired to achieve it become impractical ( $e_{\max}$  tends to be very high). Still, modulus variation offers the possibility of a substantial increase in frequency. For example in a H-H beam an increase of 33.97 percent in frequency can be achieved with a physically realizable value of  $e_{\max} = 3.230$ . This increase, however, is only 6.6 percent<sup>12</sup> in the case of homogeneous tapered beam, with similar cross-sections.

The general nature of the curves of  $e$  variation along the axis, for all end conditions, is similar to that of the bending moment variation, with  $e_{\max}$  and  $e_{\min}$  occurring at the stations, where bending moment is a maximum or a minimum. Thus  $e_{\max}$  occurs either at the clamped end or at the point of symmetry (H-H case), and  $e_{\min}$ , (which is zero here) occurs at the ends which are hinged or free, and at the points of inflexion. Location of inflexion point (Table 6.1c and 6.1d), for both C-C and C-H end conditions, varies with  $p$ . It is seen that with increasing values of  $p$ , there is a decrease in the value of  $x_0$ , i.e., inflexion point shifts to the left. This general trend saves computer time in numerical determination of  $x_0$ .

It can be further noted that there is hardly any difference in the general nature of the curves of  $e$  distribution for different values of  $p$ , except that there is a sharp variation in  $e$  and  $e_{\max}$  with decreasing  $p$ . In all the cases, as  $p$  tends to be large,  $e$  curves become flat with values approaching almost unity, i.e., the beam tends to become an Euler beam. Similar result was obtained in the case of columns also.

An interesting observation can be made, here, regarding the location and magnitude of  $e_{\max}$  in the case of F-C, C-C and C-H end conditions. It is found that in all these cases,  $e_{\max}$  has the same value and occurs at the clamped end for a particular value of  $p$ .

Finally, it is appropriate to make few comments on the physical realizability of the obtained  $e$  distributions. As already stated in Section 6.2.2,  $\eta$  is unity and  $\tilde{\rho}$  and  $a$  are constants for the uniform beam under consideration. In such a case one can achieve the desired  $e$  distributions, either by keeping  $\tilde{\rho}$  and  $a$  equal to unity or such that their product equals one. If  $\tilde{\rho} = 1$ , one needs to develop a material with the desired  $e$  distributions and a constant density, which should be the same as that of the corresponding Euler beam. From physical standpoint, this may be difficult to achieve. Designer in such a case can

choose  $a > 1$ , i.e., cross-sectional area of the non-homogeneous beam being larger than that of the Euler beam. This from Eqn. (6.2.8) requires  $\tilde{\rho} < 1$ , which from (6.2.9) implies  $\tilde{E} < e$ . This appears to be physically meaningful and one should be able to meet the requirements on actual modulus distributions given by  $\tilde{E}$ , rather than  $e$ . Specially in the case of beams with  $q > 1$ , by keeping  $a > 1$  one can considerably reduce  $\tilde{E}$  for the same  $e$ . In other words one can hope for, still, higher increases in frequency than what are presented here by performing the computations for smaller values of  $p$ .

Possibility of  $a < 1$ , perhaps, will be detrimental because it requires for the same  $e$ ,  $\tilde{\rho} > 1$  and  $\tilde{E} > e$ . Though increased density is favourable, but  $\tilde{E}$  is definitely limited, because of the limitation on specific moduli of the available fibers.

Table 6.1: Variation of frequency ( $\omega$ ), percent increase in  $\omega$  and inflexion point location  $x_0$  with  $p$

a) for hinged-hinged beams

$p$	0.08	0.2	0.4	0.7	1	3	10
$\omega$	13.22	12.46	11.79	11.25	10.96	10.31	9.995
percent increase	33.97	26.25	19.42	14.03	11.04	4.48	1.27

Table 6.1: Continued

b) for free-clamped beams

$p$	0.6	0.8	1.0	1.5	3	5	10
$\omega$	4.934	4.658	4.470	4.196	3.880	3.739	3.624
percent increase	40.35	32.49	27.0	19.35	10.36	6.35	3.09

Table 6.1: Continued

c) for clamped-clamped beams

$p$	0.6	0.8	1.0	1.5	3	5	10
$\omega$	27.33	26.46	25.84	24.90	23.68	23.25	22.75
percent increase	22.02	18.11	15.37	11.18	5.72	3.80	1.59
$x_0$	0.2625	0.2550	0.250	0.2425	0.2350	0.2300	0.2275

Table 6.1: Concluded

d) for clamped-hinged beams

$p$	0.6	0.8	1.0	1.5	3	5	10
$\omega$	18.28	17.80	17.46	16.90	16.28	16.03	15.46
percent increase	18.55	15.45	13.26	9.61	5.58	3.97	0.25
$x_0$	0.3060	0.2985	0.2929	0.2850	0.2750	0.2700	0.2700

Table 6.2: Variation of  $e$  along the axis for hinged-hinged uniform beams

$x$	$p=0.08$	$p = 0.2$	$p = 0.4$	$p = 0.7$	$p = 1$	$p = 3$	$p = 10$
0	0	0	0	0	0	0	0
0.05	0.1141	0.1254	0.1541	0.2017	0.2488	0.4822	0.7624
0.10	0.3973	0.3868	0.4055	0.4479	0.4905	0.6775	0.8628
0.15	0.7979	0.7268	0.6980	0.7016	0.7188	0.8207	0.9253
0.20	1.268	1.105	1.002	0.9468	0.9280	0.9333	0.9697
0.25	1.761	1.490	1.297	1.172	1.113	1.023	1.003
0.30	2.232	1.848	1.562	1.368	1.270	1.094	1.028
0.35	2.643	2.155	1.785	1.528	1.396	1.147	1.046
0.40	2.961	2.390	1.952	1.646	1.488	1.185	1.058
0.45	3.162	2.536	2.055	1.718	1.544	1.207	1.065
0.50	3.230	2.587	2.090	1.743	1.563	1.215	1.068

Table 6.3: Variation of  $e$  along the axis for free-clamped uniform beams

$x$	$p = 0.6$	$p = 0.8$	$p = 1$	$p = 1.5$	$p = 3$	$p = 5$	$p = 10$
0	0	0	0	0	0	0	0
0.1	0.0260	0.0355	0.0468	0.0802	0.1957	0.3316	0.5436
0.2	0.1328	0.1527	0.1747	0.2315	0.3808	0.5172	0.6931
0.3	0.3314	0.3467	0.3667	0.4210	0.5551	0.6654	0.7954
0.4	0.6173	0.6058	0.6080	0.6333	0.7183	0.7907	0.8742
0.5	0.9797	0.9171	0.8854	0.8582	0.8706	0.8995	0.9382
0.6	1.406	1.268	1.188	1.089	1.012	0.9952	0.9916
0.7	1.883	1.649	1.507	1.320	1.143	1.080	1.037
0.8	2.398	2.049	1.835	1.547	1.265	1.156	1.076
0.9	2.944	2.462	2.167	1.770	1.377	1.223	1.110
1	3.512	2.884	2.500	1.987	1.481	1.285	1.141

Table 6.4: Variation of  $e$  along the axis for clamped-clamped uniform beams

$x$	$p = 0.6$	$p = 0.8$	$p = 1$	$p = 1.5$	$p = 3$	$p = 5$	$p = 10$
0	3.514	2.884	2.500	1.986	1.483	1.284	1.141
0.05	2.663	2.236	1.978	1.637	1.309	1.179	1.088
0.10	1.867	1.610	1.459	1.269	1.108	1.051	1.021
0.15	1.144	1.016	0.9489	0.8798	0.8675	0.8862	0.9281
0.20	0.5255	0.4762	0.4576	0.4585	0.5461	0.6309	0.7633
0.25	0.0660	0.0314	0	0.1098	0.3483	0.5416	0.7290
0.30	0.2389	0.3332	0.4054	0.5298	0.7005	0.8037	0.8907
0.35	0.6131	0.6900	0.7402	0.8136	0.8917	0.9344	0.9645
0.40	0.9298	0.9698	0.9897	1.009	1.011	1.012	1.007
0.45	1.137	1.147	1.144	1.125	1.078	1.055	1.029
0.50	1.209	1.207	1.196	1.164	1.100	1.068	1.036

Table 6.5: Variation of  $e$  along the axis for clamped-hinged uniform beams

$x$	$p = 0.6$	$p = 0.8$	$p = 1$	$p = 1.5$	$p = 3$	$p = 5$	$p = 10$
0	3.508	2.887	2.500	1.987	1.481	1.284	1.141
0.1	2.092	1.797	1.616	1.384	1.169	1.093	1.045
0.2	0.8726	0.7921	0.7494	0.7201	0.7496	0.8014	0.8825
0.3	0.0222	0.0703	0.0535	0.1698	0.4171	0.5894	0.7464
0.4	0.6024	0.6705	0.7200	0.7907	0.8805	0.9244	0.9544
0.5	1.213	1.196	1.180	1.143	1.087	1.058	1.028
0.6	1.534	1.451	1.392	1.292	1.165	1.105	1.053
0.7	1.493	1.405	1.345	1.250	1.136	1.085	1.043
0.8	1.119	1.082	1.059	1.029	1.002	0.9961	0.9972
0.9	0.5364	0.5600	0.5838	0.6371	0.7408	0.8131	0.8940
1.0	0	0	0	0	0	0	0

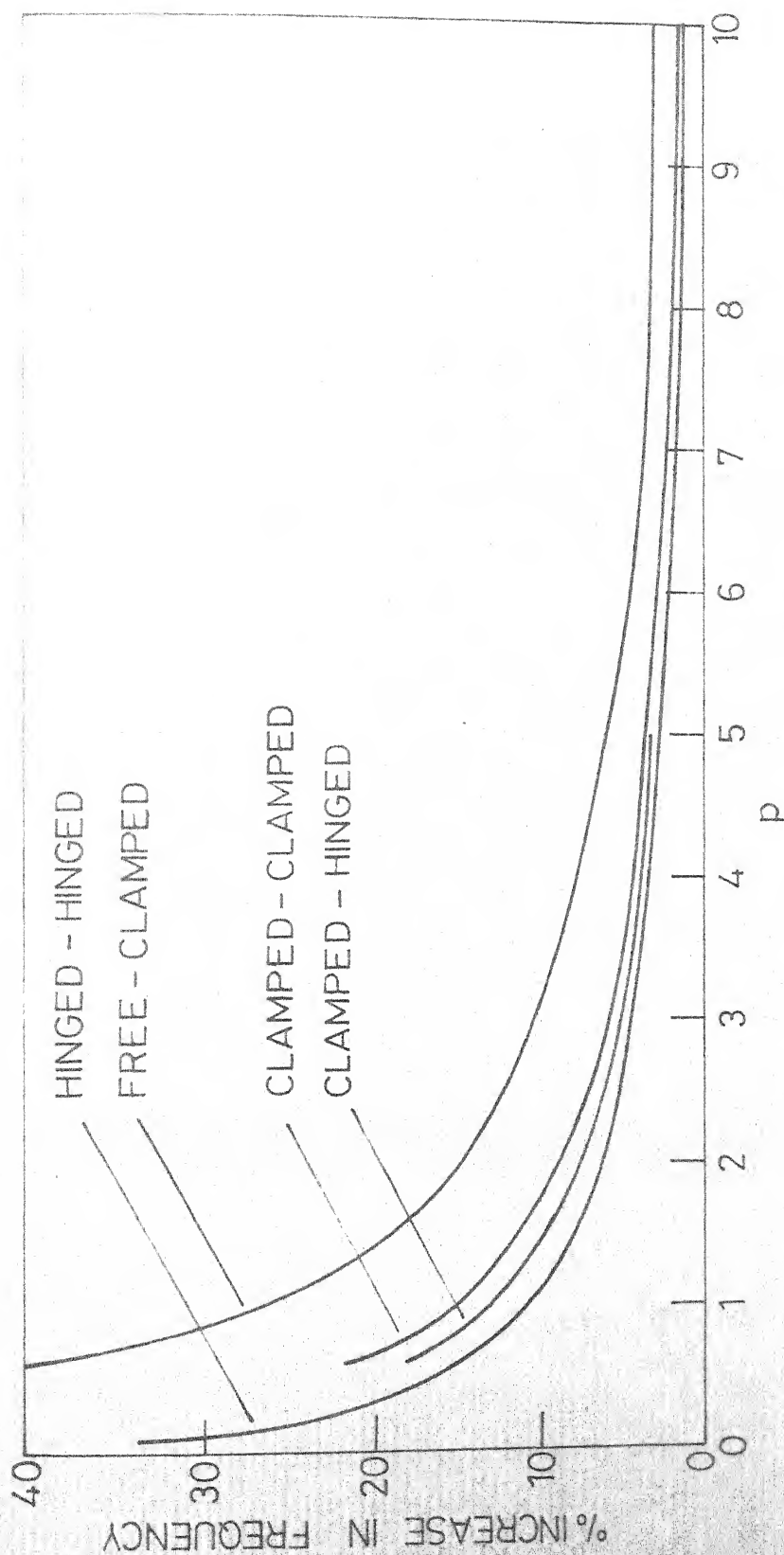


FIG.6.1. VARIATION OF PERCENT INCREASE IN FREQUENCY WITH  $p$  FOR UNIFORM BEAMS

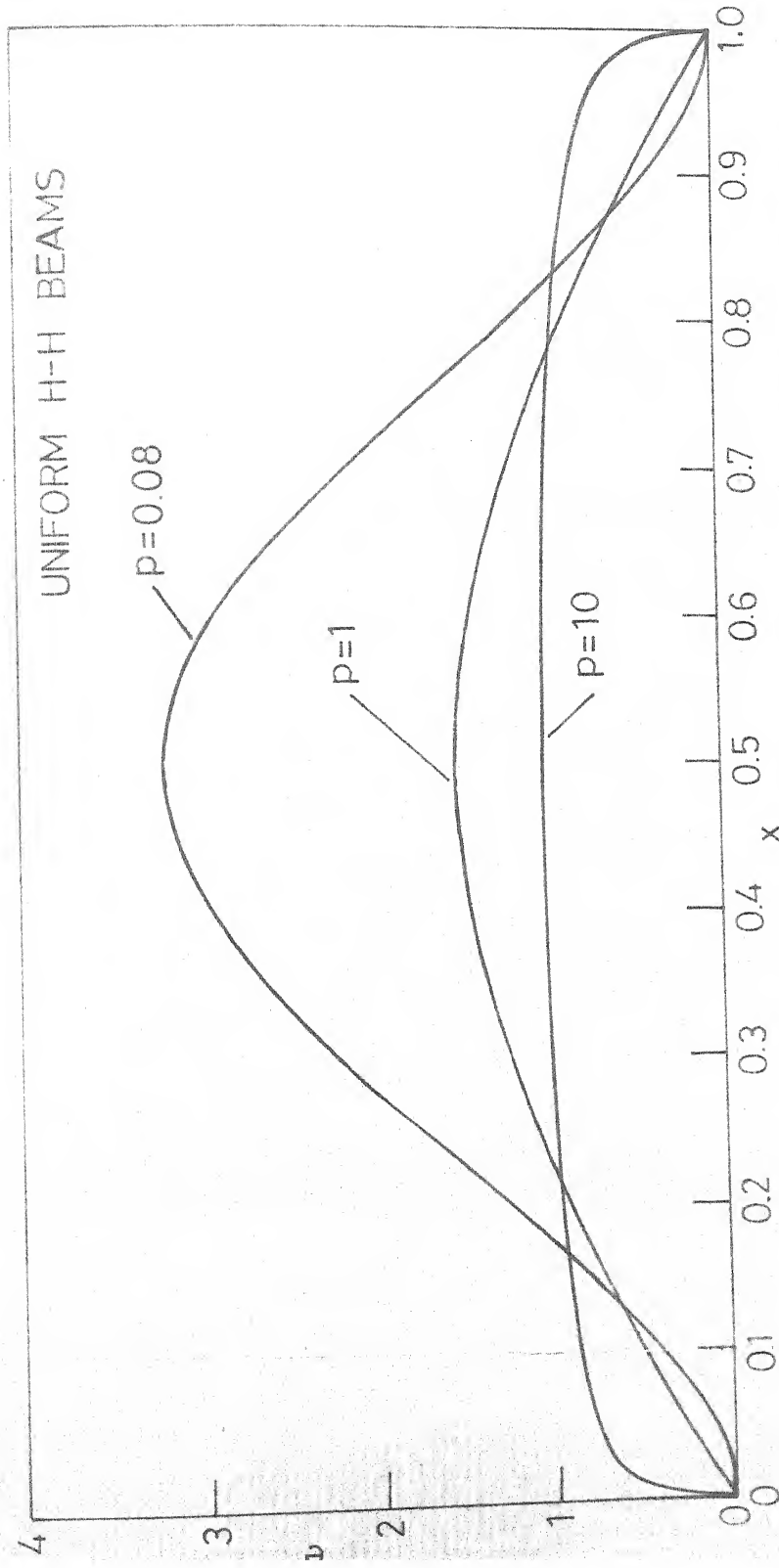


FIG. 6.2. VARIATION OF  $e$  ALONG THE AXIS FOR HINGED - HINGED UNIFORM BEAMS

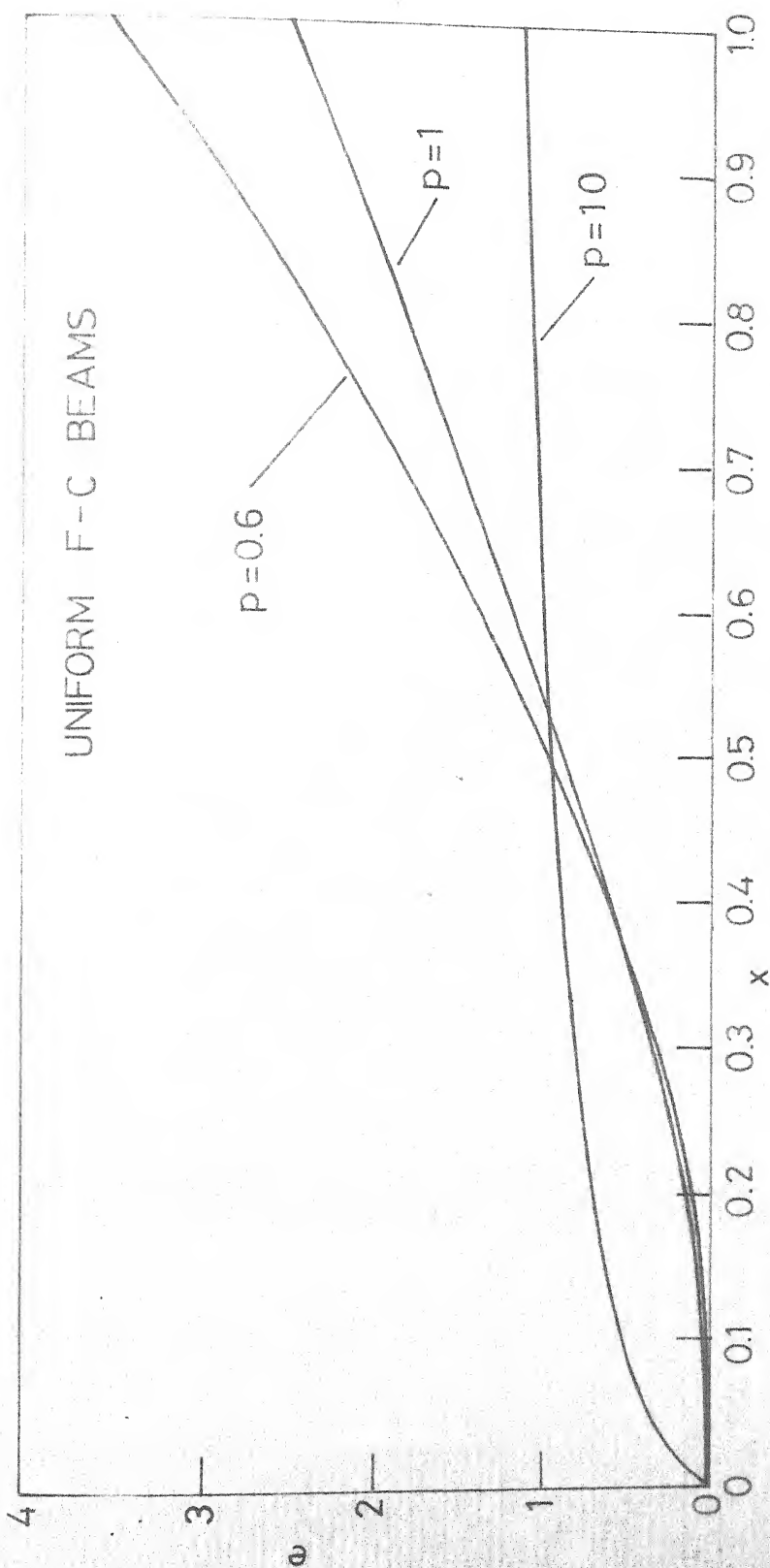


FIG. 6.3. VARIATION OF  $\omega$  ALONG THE AXIS FOR FREE - CLAMPED UNIFORM BEAMS

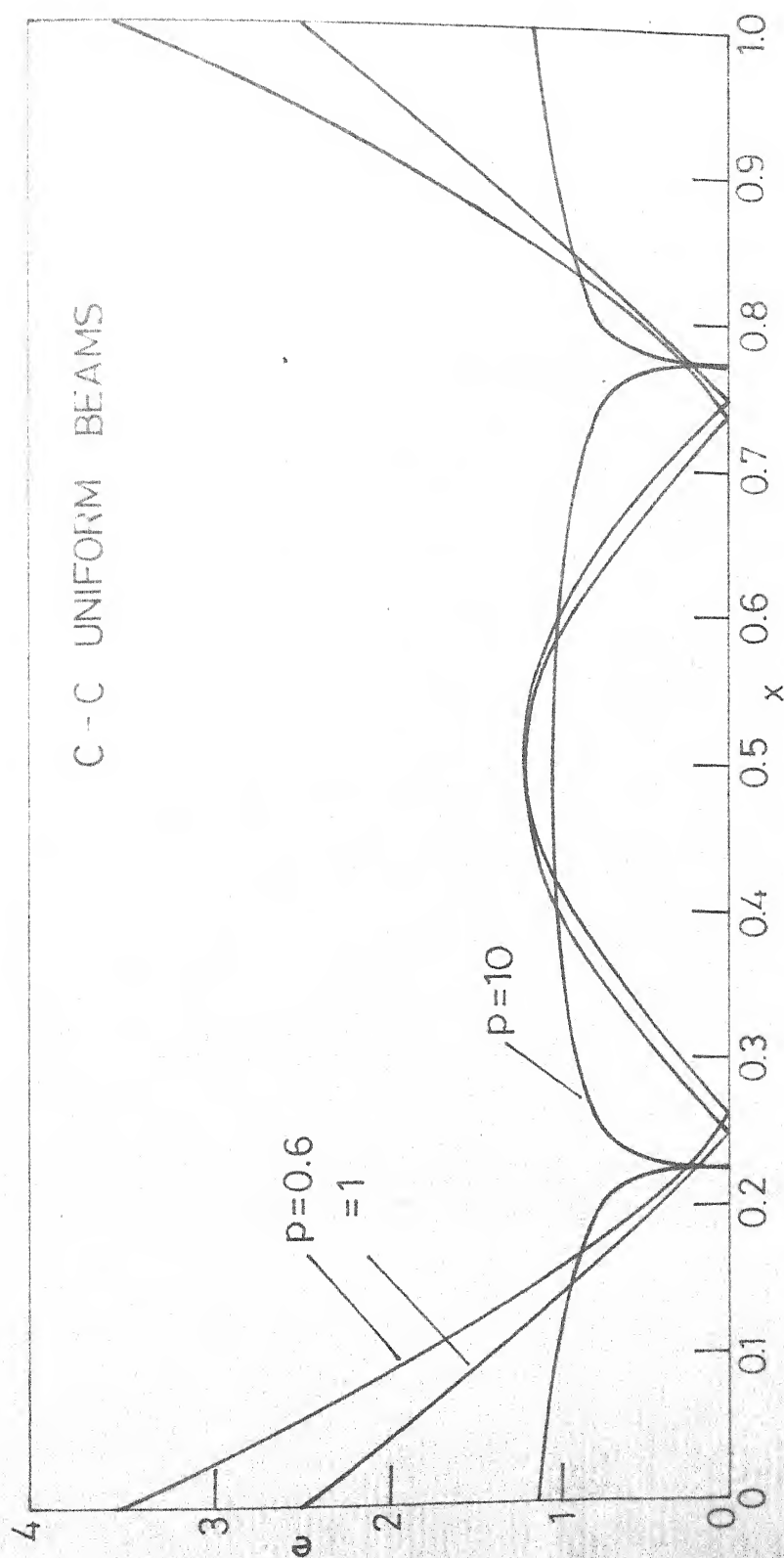


FIG. 6.4. VARIATION OF  $e$  ALONG THE AXIS FOR CLAMPED - CLAMPED UNIFORM BEAMS

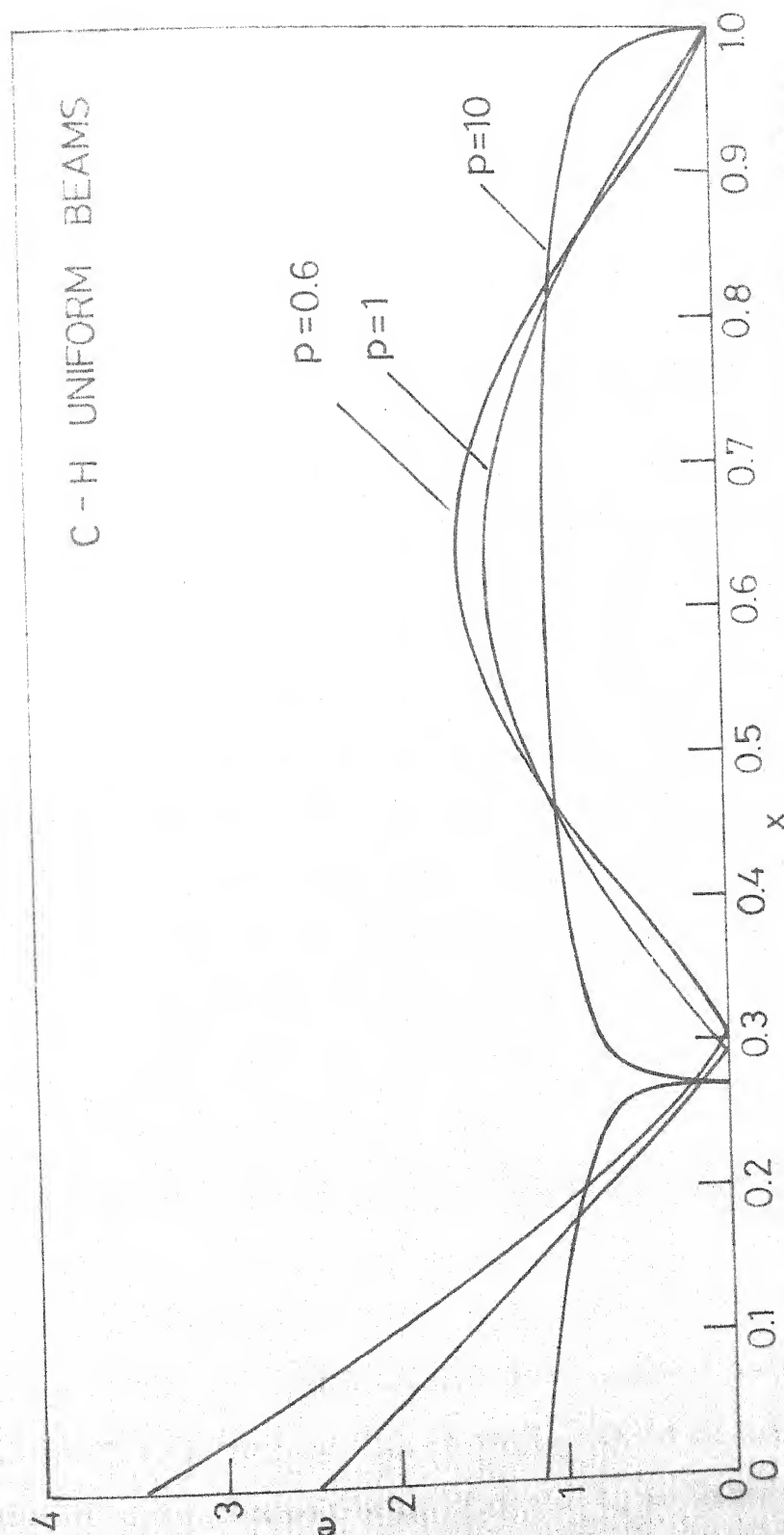


FIG. 6.5. VARIATION OF  $e$  ALONG THE AXIS FOR CLAMPED - HINGED UNIFORM BEAMS

## CHAPTER - 7

### TAPERED-NONHOMOGENEOUS BEAMS

#### 7.1 Introduction

Problem of optimal design of tapered-nonhomogeneous beams is considered in this chapter. Modulus, cross-sectional area and density are treated as design variables. However, because of the limitations stated in Chapter 3, simultaneously all these are not assumed to vary independently. Rather, only two ( $e$  and  $\eta$ ) independent design variables are considered in the present investigation. Equation of equilibrium and the boundary conditions in terms of these variables, are stated in Section 6.2. Essentially speaking, present problem differs from the problem investigated in Chapter 6, only in an additional ~~constraint~~, specifying the given mass of the beam, and a design variable  $\eta$ . General approach is therefore going to be the same as that in Chapter 6.

Besides the parameter  $p$ , general formulation involves another integer parameter  $q$ , which is introduced to incorporate a variety of cross-sectional shapes. Solution is obtained for hinged-hinged and free-clamped boundary conditions for  $q$  varying from 1 to 3. It is found that in the case of free-clamped beam, for  $q = 1$ , no meaningful solution exists.

Corresponding problems for homogeneous beams have been investigated by Niordson<sup>12</sup>, Brach<sup>13</sup> and Karihaloo and Niordson<sup>14</sup>. It is found that results obtained, here, for large values of  $p$ , which amounts to constant modulus, asymptotically approach to those obtained by Niordson.

Optimization problem is stated in Section 7.2. Corresponding necessary conditions and the governing equations are derived in Section 7.3. Governing equation is singular at points where bending moment is zero. Singular behaviour is, therefore, analytically investigated in Section 7.4. Governing equation is, then, solved numerically in Sections 7.5 and 7.6 for hinged-hinged and free-clamped end conditions.

## 7.2 Statement of the Problem

Problem requires the determination of  $e(x)$  and  $\eta(x)$  such that the frequency of transverse vibrations for the fundamental mode, for a beam of given geometry, cross-sectional shape and mass, is a maximum. Considering equation of equilibrium as a constraint, equivalently as in the case of column in Chapter 5, the problem can be restated as:

Minimize the dimensionless mass

$$\bar{\eta} = \int_0^1 \eta \, dx \quad (7.2.1)$$

such that

$$\int_0^1 e^p dx = 1 \quad (7.2.2)$$

$$(e\eta^q y'')'' = \lambda \eta y \quad (7.2.3)$$

$$g_i = 0, \quad i = 1, 2, 3, 4 \quad (7.2.4)$$

Variables used in the above equations are defined in Section 6.2 and  $g_i$  represent boundary conditions.

### 7.3 Necessary Conditions and Governing Equations

It is convenient to work in terms of the variables  $s$ ,  $\eta$  and  $y$  instead of  $e$ ,  $\eta$  and  $y$ , where  $s$  is given by

$$s(x) = e\eta^q \quad (7.3.5)$$

$$\text{or} \quad e = \frac{s}{\eta^q} \quad (7.3.6)$$

Physically  $s$  may be interpreted as the stiffness. Equations (7.2.2) and (7.2.3) then reduce to:

$$\int_0^1 \frac{s^p}{\eta^{pq}} dx = 1 \quad (7.3.7)$$

$$(sy'')'' = \lambda \eta y \quad (7.3.8)$$

Necessary conditions will now be obtained by applying the Eqns. (2.3.12) to (2.3.18). Problem is, therefore, cast in the format of control theory. Defining

$$y_1 = y \quad (7.3.9)$$

$$y_2 = y' \quad (7.3.10)$$

$$y_3 = sy'' = M(x) \quad (7.3.11)$$

$$y_4 = (sy'')' = V(x) \quad (7.3.12)$$

Equation (7.3.8) which is of fourth order, reduces to the following four first order equations.

$$y_1' = y_2 = f_1 \quad (7.3.13)$$

$$y_2' = \frac{y_3}{s} = f_2 \quad (7.3.14)$$

$$y_3' = y_4 = f_3 \quad (7.3.15)$$

$$y_4' = \lambda \eta y_1 = f_4 \quad (7.3.16)$$

Functional  $\bar{J}$ , defined in (2.3.8) can now be easily written as:

$$\bar{J} = \sum_{i=1}^4 \gamma_i g_i + \int_0^1 [\lambda_0 \eta + \sum_{i=1}^4 \lambda_i(x)(y_i' - f_i) + \gamma_5 (\frac{s^p}{\eta^{pq}} - 1)] dx \quad (7.3.17)$$

This yields following expressions for the functions G and H, defined in (2.3.9) and (2.3.10)

$$G = \gamma_1 g_1 + \gamma_2 g_2 + \gamma_3 g_3 + \gamma_4 g_4 \quad (7.3.18)$$

$$H = \sum_{i=1}^4 \lambda_i f_i - \lambda_0 \eta - \gamma_5 (\frac{s^p}{\eta^{pq}} - 1) \quad (7.3.19)$$

or

$$H = \lambda_1 y_2 + \frac{\lambda_2 y_3}{s} + \lambda_3 y_4 + \lambda_4 \lambda \eta y_1 - \lambda_0 \eta - \gamma_5 \left( \frac{s^p}{\eta^{pq}} - 1 \right) \quad (7.3.20)$$

Application of Eqn. (2.3.12) to the function  $H$ , easily gives an equation in  $\lambda_4$  which has the same form as Eqn. (7.3.8). It can be further seen by applying Eqn. (2.3.15) to function  $G$  for the homogeneous boundary conditions - H-H, F-C, C-C and C-H - that  $\lambda_4$  satisfies the same conditions as those by  $y$ . Details are omitted here, as they can be seen in Section 6.4. Solution for  $\lambda_4$ , therefore, can be written in terms of  $y$ :

$$\lambda_4 = -Ky \quad (7.3.21)$$

where  $K$  is a positive constant.

Applying the necessary conditions (2.3.13) for the control variables  $s$  and  $\eta$ , following relations are obtained.

$$\frac{\partial H}{\partial s} = -\frac{\lambda_2 y_3}{s^2} - \gamma_5 \frac{p \cdot s^{p-1}}{\eta^{pq}} = 0 \quad (7.3.22)$$

$$\frac{\partial H}{\partial \eta} = \lambda_4 \lambda y_1 - \lambda_0 + \gamma_5 pq \frac{s^p}{\eta^{pq+1}} = 0 \quad (7.3.23)$$

Since  $\lambda_2$  from (6.4.33), which is valid here also provided  $e$  is replaced by  $s$ , is known in terms of  $\lambda_4$ , Eqns.

(7.3.22) and (7.3.23) easily reduce to:

$$K_y''^2 = \gamma_{5^p} \frac{s^{p-1}}{\eta^{pq}} \quad (7.3.24)$$

$$\lambda K_y^2 + \lambda_0 = \gamma_{5^{pq}} \frac{s^p}{\eta^{pq+1}} \quad (7.3.25)$$

These equations can be rewritten as:

$$\frac{s^{p-1}}{\eta^{pq}} = \frac{K_y''^2}{\gamma_{5^p}} \quad (7.3.26)$$

$$\frac{s}{\eta} = \frac{\lambda_0 + \lambda K_y^2}{K_{qy}''^2} \quad (7.3.27)$$

Equations (7.3.26) and (7.3.27) determine  $s$  and  $\eta$  in terms of the state variable  $y$  and therefore can be interpreted as the optimality conditions. Now as stated in Section 6.5, the present problem will also have two undetermined constants. The solution must not depend on the values of these constants. Assuming the optimal problem to be a normal problem,  $\lambda_0$  and  $K$  can be identified as the undetermined constants. Making the transformation

$$u = \left( \frac{\lambda K}{\lambda_0} \right)^{1/2} y \quad (7.3.28)$$

equations (7.3.26) and (7.3.27) are rewritten as:

$$\frac{s^{p-1}}{\eta^{pq}} = \left( \frac{\lambda_0}{p \gamma_{5^p} \lambda} \right) u''^2 \quad (7.3.29)$$

$$\frac{s}{\eta} = \frac{\lambda}{q} \left( \frac{1+u^2}{u^{2p}} \right) \quad (7.3.30)$$

Simple algebraic manipulation of (7.3.29) and (7.3.30) gives:

$$\frac{s^p}{\eta^{pq+1}} = \left( \frac{\lambda_0}{\gamma_{5pq}} \right) (1+u^2) \quad (7.3.31)$$

$$\eta = \left[ \left( \frac{\lambda}{q} \right)^p \left( \frac{\gamma_{5pq}}{\lambda_0} \right) \frac{(1+u^2)^{p-1}}{(u^{2p})^p} \right]^{\frac{1}{pq+1-p}} \quad (7.3.32)$$

Equation (7.3.32) gives  $\eta$  in terms of  $u$ . Since  $s$  and  $\eta$  are related through (7.3.30), Eqn. (7.2.3) can, therefore, be written in terms of the state variable  $u$  only. The equation obtained is:

$$\left[ \left\{ \frac{(1+u^2)^{pq}}{(u^{2p})^{1+pq}} \right\} u \right]^{\frac{1}{1+pq-p}} = q \left[ \frac{(1+u^2)^{p-1}}{(u^{2p})^p} \right]^{\frac{1}{1+pq-p}} u \quad (7.3.33)$$

It may be noted that  $u$  in Eqns. (7.3.32) and (7.3.33) is put in a particular form shown above, to ensure that  $\eta$  and  $s$  are positive and changes in the sign of  $u$  at inflexion point are properly accounted for.

It is convenient to rewrite the Eqn. (7.3.33) as:

$$\left[ \frac{(1+u^2)^a}{u^b} \right]^{\frac{1}{c}} = q \left[ \frac{(1+u^2)^c}{u^d} \right]^{\frac{1}{e}} u \quad (7.3.34)$$

where

$$a = rpq \quad (7.3.35)$$

$$b = 2r(1 + pq) - 1 \quad (7.3.36)$$

$$c = r(p - 1) \quad (7.3.37)$$

$$d = 2rp \quad (7.3.38)$$

and

$$r = \frac{1}{1 + pq - p} \quad (7.3.39)$$

### Expressions for $e$ , $\eta$ and $\lambda$

Eigen value  $\lambda$  is to be determined for  $\bar{\eta} = 1$ , so that mass of the tapered-nonhomogeneous beam and the corresponding Euler beam **is** the same. Integration of (7.3.32) with respect to  $x$  between the limits 0 to 1 gives:

$$\left(\frac{\gamma_5 pq}{\lambda_0}\right) \left(\frac{\lambda}{q}\right)^p = \left[ \frac{1}{\int_0^1 \eta_0(x) dx} \right]^{(pq+1-p)} \quad (7.3.40)$$

where

$$\eta_0(x) = \left[ \frac{(1+u^2)^{p-1}}{(u^{1/2})^p} \right]^{\frac{1}{pq+1-p}} \quad (7.3.41)$$

Defining

$$I_1 = \int_0^1 \eta_0(x) dx \quad (7.3.42)$$

relation (7.3.40) and (7.3.32) reduce to:

$$\left(\frac{\gamma_{5^{pq}}}{\lambda_0}\right)\left(\frac{\lambda}{q}\right)^p = \left[\frac{1}{I_1}\right]^{(pq+1-p)} \quad (7.3.43)$$

$$\eta(x) = \frac{\eta_0(x)}{I_1} = \frac{1}{I_1} \left[ \frac{(1+u^2)^{p-1}}{(u^2)^p} \right]^{\frac{1}{pq+1-p}} \quad (7.3.44)$$

Now, Eqns. (7.3.5) and (7.3.31) yield following relationship for  $e$ .

$$e^p = \eta\left(\frac{\lambda_0}{\gamma_{5^{pq}}}\right)(1+u^2) \quad (7.3.45)$$

$$\text{or } e^p = \left(\frac{\lambda_0}{\gamma_{5^{pq}I_1}}\right) \left[ \frac{(1+u^2)^{pq}}{(u^2)^p} \right]^{\frac{1}{(pq+1-p)}} \quad (7.3.46)$$

Now, defining

$$e_0(x) = \left[ \frac{(1+u^2)^{pq}}{(u^2)^p} \right]^{\frac{1}{(pq+1-p)}} \quad (7.3.47)$$

$$\text{and } I_2 = \int_0^1 e_0(x) dx, \quad (7.3.48)$$

integration of (7.3.46) between the limits 0 to 1 gives:

$$\left(\frac{\lambda_0}{\gamma_{5^{pq}}}\right)\left(\frac{I_2}{I_1}\right) = \int_0^1 e^p dx = 1 \quad (7.3.49)$$

$$\text{or } \frac{I_2}{I_1} = \frac{\gamma_{5^{pq}}}{\lambda_0} \quad (7.3.50)$$

Equations (7.3.43) and (7.3.50), now, give an expression for  $\lambda$

$$\left(\frac{\lambda}{q}\right)^p \left(\frac{I_2}{I_1}\right) = \left(\frac{1}{I_1}\right)^{pq+1-p} \quad (7.3.51)$$

or

$$\lambda = \frac{q}{I_2^{1/p} I_1^{q-1}} \quad (7.3.52)$$

Eliminating  $(\gamma_5/\lambda_0)$  from (7.3.46) and (7.3.50),  $e$  is determined from:

$$e(x) = I_2^{-\frac{1}{p}} \left[ \frac{(1+u^2)^q}{u^{n^2}} \right]^{\frac{1}{(1+pq-p)}} \quad (7.3.53)$$

Optimization problem thus reduces to the solution of the governing equation (7.3.34), for a prescribed set of boundary conditions. Eigen value  $\lambda$  is then determined by the Eqn. (7.3.52), and the corresponding  $\eta(x)$  and  $e(x)$  distributions are obtained from (7.3.44) and (7.3.53). It is quite evident that the solution does not depend on the magnitude of the constants  $\lambda_0$  and  $K$ .

Numerical solution of Eqn. (7.3.34) will, now, be obtained by the method of the successive iterations for the hinged-hinged and free-clamped beams.

#### 7.4 Singular Behaviour

Dimensionless bending moment  $M(x)$  at any station can be expressed in terms of the variable  $u$ , with the help of expressions (7.3.30) and (7.3.44).

$$M(x) = s u'' \sim \left[ \frac{(1 + u^2)^{pq}}{(u'')^{2(1+pq)}} \right]^{\frac{1}{1+pq-p}} \quad (7.4.54)$$

Since  $\frac{1+pq}{1+pq-p} \geq 1$ ,  $u''$  is  $\infty$  at points where bending moment is zero. Singularities are, therefore, encountered at the hinged and free ends while integrating (7.3.34). Numerical experience reveals that, exact knowledge of the analytical behaviour of  $u$  around singularity is crucial to get any convergence to the meaningful results. Before attempting any solution of Eqn. (7.3.34), it is, therefore, important to investigate the singular behaviour. The general approach is discussed in detail in Section 6.6.1.

Equation (7.3.34), after some algebraic manipulation, can be rewritten in the following expanded form:

$$b A(x) + [2b u^2 A(x) + 2a B(x) - q u u''^3] + u^2 [b u^2 A(x) + 2a C(x) - q u u''^3] = 0 \quad (7.4.55)$$

where

$$A(x) = -u'' u^{iv} + (b+1) u''^2 \quad (7.4.56)$$

$$B(x) = u u''^3 - 2b u u' u'' u''' + u'^2 u''^2 \quad (7.4.57)$$

$$C(x) = u u''^3 - 2b u u' u'' u''' + (2a-1)u'^2 u''^2 \quad (7.4.58)$$

Terms in Eqn. (7.4.55), have been arranged in such a manner that the terms containing like powers of  $x$ , when  $u$  is represented by a series expansion around the singularity, are put together. Essentially it consists of three terms, each containing several terms having the same powers of  $x$ , power being different for individual major terms.

To investigate the singularity, which without any loss in generality is assumed to be at  $x = 0$  for convenience,  $u$  is expanded in the form (6.6.128). Function  $u$  can then be approximated around the singularity by

$$u \sim x^t \quad (6.6.129)$$

where  $t$  could be a positive fraction or a negative fraction or a negative integer. Depending on the value of  $t$ , following possibilities exist.

- (i)  $t > 2$ , none of the quantities,  $u$ ,  $u'$  and  $u''$  is singular
- (ii)  $1 < t < 2$ , only  $u''$  is singular
- (iii)  $0 < t < 1$ ,  $u'$  and  $u''$  are singular
- (iv)  $t < 0$ ,  $u$ ,  $u'$  and  $u''$  are singular

These possibilities, while they existed even in Section 6.6, the recognition of these as such becomes

important, here, in view of the three terms A, B, C, which were not present in the earlier case. One would, now, like to determine  $t$ , to investigate the nature of singularity. From (6.6.129), derivatives of  $u$  can be approximated as:

$$u' \sim t x^{t-1} \quad (7.4.59)$$

$$u'' \sim t(t-1)x^{t-2} \quad (7.4.60)$$

$$u''' \sim t(t-1)(t-2)x^{t-3} \quad (7.4.61)$$

$$u^{iv} \sim t(t-1)(t-2)(t-3)x^{t-4} \quad (7.4.62)$$

Now any one of the three terms in Eqn. (7.3.55) could become a leading term, depending upon the behaviour of  $u$ ,  $u'$  and  $u''$ . Each of them is, therefore, investigated for the singular behaviour.

### First term

Substituting for  $u$  and its derivatives in terms of  $x$ , first term gives:

$$b A(x) = b t^2(t-1)^2(t-2)(bt + 1 - 2b)x^{2t-6} \quad (7.4.63)$$

Equating the coefficient of  $x^{2t-6}$  to zero,  $t$  is determined as:

$$t = 2 - \frac{1}{b} \quad (7.4.64)$$

Writing  $b$  in terms of the constants  $p$  and  $q$ , (7.3.64) reduces to:

$$t = 1 + \frac{2p}{1 + pq + p} \quad (7.4.65)$$

Since  $p > 0$  and  $q \geq 1$ , it is evident that  $1 < t < 2$ . Hence, if first term is going to be the leading term of (7.4.55), only  $u''$  is then singular.

It may be mentioned here, that positive integer values of  $t$  are of no interest, as they cannot lead to singularities in  $u$  or  $u'$  or  $u''$ .

### Second term

This term can be written as:

$$\begin{aligned} & 2b u^2 A(x) + 2a B(x) - q u u''^3 \\ &= t^2(t-1)^2 [(2b^2 + 4a - 4ab - q)t^2 + \\ & \quad (2b - 8b^2 + 8ab - 2a + q)t - 4b(1 - 2b)] x^{4t-6} \end{aligned} \quad (7.4.66)$$

Equating the coefficient of  $x^{4t-6}$  to zero,  $t$  is determined from the following quadratic equation.

$$\begin{aligned} & (2b^2 + 4a - 4ab - q)t^2 + (2b - 8b^2 + 8ab - 2a + q)t - \\ & 4b(1 - 2b) = 0 \end{aligned} \quad (7.4.67)$$

Computations for all possible values of  $p$  and  $q$ , reveal that  $t$  in (7.4.67) does not have any real roots. Thus, the second term is hardly of any interest.

Third term

This term can be written as:

$$\begin{aligned}
 & u^2 [b u^2 A(x) + 2a C(x) - q u u^3] \\
 &= t^2(t-1)^2 [\{ b^2 + 4a(a-b) - q \} t^2 + \{ b(1-4b) + 2a(4b-1) \\
 &\quad + q \} t - 2b(1-2b)] x^{6t-6} \quad (7.4.68)
 \end{aligned}$$

Equating coefficient of  $x^{6t-6}$  in (7.4.68) to zero,  $t$  is determined from the following quadratic equation.

$$\begin{aligned}
 & [b^2 + 4a(a-b) - q]t^2 + [b(1-4b) + 2a(4b-1) + q]t \\
 & - 2b(1-2b) = 0 \quad (7.4.69)
 \end{aligned}$$

Numerical values for the two roots of  $t$  are computed for various values of  $p$ , with  $q = 2$  and  $q = 3$ . It is found that among the two roots, one is negative and the other is positive in all the cases. Negative root, however, does not seem to be affected by the value of  $p$ . It can, then, be easily concluded that:

$$t = -2 \quad \text{for} \quad q = 2 \quad (7.4.70)$$

$$t = -1 \quad \text{for} \quad q = 3 \quad (7.4.71)$$

Besides, it is further seen that positive root in all the cases is found to be greater than  $1 + \frac{2p}{1+p+pq}$ , the value determined in (7.4.65). Thus negative root only is of any interest, and it is clearly reflected that nature

of the singularity in this case, depends only on  $q$ . The values in (7.4.70) and (7.4.71), therefore agree with those obtained by Karihaloo and Niordson<sup>14</sup>.

It may be commented that the powers of  $x$  being  $2t-6$ ,  $4t-6$  and  $6t-6$  for three possible leading terms, it is evident after dividing the Eqn. (7.4.55) by  $x^{2t-6}$ , that the first term becomes the leading term for  $t > 0$ . Similarly division by  $x^{6t-6}$ , reveals that the third term is the leading term for  $t < 0$ . In both cases, Eqn. (7.4.55) remains satisfied at  $x = 0$ . If  $t$  is given by the first term, second and third terms are zero at  $x = 0$ , and if it is given by the third term, then the first and second terms vanish at  $x = 0$ . Thus, second term does not provide any information about the singularity. This explains the existence of only imaginary roots of Eqn. (7.4.67).

For  $q = 1$  and any  $p$ , it is interesting to note that the coefficient of  $t^2$  in Eqn. (7.4.69) vanishes, as shown below.

Relations (7.3.35) to (7.3.39) for  $q = 1$  give:

$$a = p \quad (7.4.72)$$

$$b = 1 + 2p \quad (7.4.73)$$

which yield:

$$b^2 + 4a(a-b) - q = (1+2p)^2 + 4p(p-1-2p) - 1 = 0 \quad (7.4.74)$$

Equation (7.4.69), then determines  $t$  as:

$$t = \frac{2b(1-2b)}{b(1-4b) + 2a(4b-1) + q}$$

$$= 1 + 2p > 1 \quad (7.4.75)$$

Since  $1 + 2p > 1 + \frac{2p}{1 + 2p}$ ,  $t$  determined from (7.4.75), is more than the value obtained from (7.4.65). Thus for  $q = 1$ , nature of the singularity is provided by the first term of (7.4.55). This result appears to be surprising, as the effect of end fixities has not been considered so far. For example, if for a free-clamped beam for  $q = 2$  and  $3$ ,  $t$  is negative, then for  $q = 1$  it is positive. In other words, while  $u$ ,  $u'$  and  $u''$  are simultaneously singular for  $q = 2$  and  $3$ , only  $u''$  can be singular for  $q = 1$ . Cross-sectional shape, thus changing the character of singularity, is surprising in a physical sense, even though, mathematically, this is possible since the form of the differential equation changes with  $q$ .

This behaviour does not preclude an optimal solution for any set of boundary conditions. However, it is surprising, as stated later in Section 7.6, that the case of free-clamped beam does not have an optimal solution for  $q = 1$ .

### 7.5 Hinged-Hinged Beam

Equation (7.3.34) is to be solved for the boundary conditions, stated in (6.2.14). These can be rewritten in terms of the variable  $u$ . Equation, along with the B.C.'s, is stated here for convenience.

$$\left[ \frac{(1+u^2)^a}{u^{1/b}} \right]'' = q \left[ \frac{(1+u^2)^c}{u^{1/d}} \right] u \quad (7.3.34)$$

$$u(0) = \left[ \frac{(1+u^2)^a}{u^{1/b}} \right]_{x=0} = u'(1/2) = \left[ \frac{(1+u^2)^a}{u^{1/b}} \right]'_{x=1/2} = 0 \quad (7.5.76)$$

Following the steps in Section 6.6.2, following relationships are easily obtained.

$$V(x) = \left[ \frac{(1+u^2)^a}{u^{1/b}} \right]' = -q \int_x^{1/2} \frac{(1+u^2)^c}{u^{1/d}} u \, dx \quad (7.5.77)$$

$$M(x) = \frac{(1+u^2)^a}{u^{1/b}} = -q \int_0^x \int_x^{1/2} \frac{(1+u^2)^c}{u^{1/d}} u \, dx^2 \quad (7.5.78)$$

$$u'' = \left[ - \frac{(1+u^2)^a}{q \int_0^x \int_x^{1/2} \frac{(1+u^2)^c}{u^{1/d}} u \, dx^2} \right]^{1/b} \quad (7.5.79)$$

$$u' = - \int_x^{1/2} u'' \, dx \quad (7.5.80)$$

$$\begin{aligned}
 u &= - \int_0^x \int_x^{1/2} u'' dx^2 \\
 &= - \int_0^x \int_x^{1/2} \left[ - \frac{(1+u^2)^a}{q \int_0^x \int_x^{1/2} \frac{(1+u^2)^c}{u''^d} u dx^2} \right]^{1/b} dx^2 \quad (7.5.81)
 \end{aligned}$$

Iterative solution of  $u$ , is obtained in a similar manner as outlined in Section 6.6.2. Once  $u$  is determined,  $\lambda$ ,  $\eta$  and  $e$  are easily obtained from (7.3.52), (7.3.44) and (7.3.53) respectively. Solution is obtained for several values of  $p$ , varying from 0.05 to 10. For  $q = 1$ , computations are performed from  $p = 0.05$  to 5 and for  $q = 2$  and 3,  $p$  varies from 0.1 to 10.

#### 7.5.1 Comments on numerical computations

Initially, computations were done by dividing the interval  $0 \leq x \leq 1/2$  into 100 equal parts. Integration is done, in double precision, by trapezoidal rule. To account for the effect of singularity at  $x = 0$ , while integrating  $u''$  to get  $u'$ , contribution  $\Delta$  due to the peak is computed by an expression similar to Eqn. (6.6.138). Results indicate a peculiar distribution of  $\eta$ . It is found that, specially for  $q = 1$  and small  $p$ ,  $\eta$  reaches from zero to a very high maximum value at a point, which is close to the hinged end.

and then drops to the minimum value at  $x = 1/2$ . At the outset, this looks strange as one expects  $\eta$ , which represents mass per unit length (cross-sectional area), to be zero at the hinged end and maximum at the middle, as in Ref.[12]. In any case, requirement of large  $\eta_{\max}$  near the hinged end is hard to believe. One, therefore, suspects some kind of error in the numerical approximation around the singularity. In order to safeguard against such a possibility, a detailed investigation was carried out.

Mesh size ( $h$ ) was reduced to  $h/2$  by increasing the number of divisions from 100 to 200. It is found that except for  $p < 0.1$  and  $q = 1$ , which is hardly of any practical interest, the difference in results for 100 and 200 divisions is insignificant. Even for  $p < 0.1$ , it is found that the difference in the increase in frequency is less than 2 percent. Since the computer time required with 200 divisions is more, computations are performed with 100 divisions only. Besides, it may be mentioned that the number of iterations required for the convergence in both the cases, is the same.

In order to check any error involved in the approximation of  $\Delta$ , contribution due to peak, which is obtained by matching  $u''$  at  $x = h$ , the region  $0 \leq x \leq h$  is further subdivided into 10 parts. Matching of  $u''$  is done

at  $x = h/10$ . Computations reveal that in the case of  $q = 2$  and  $q = 3$ , the effect of this inflation of the region around singularity, hardly has any effect on the results. Similarly the effect on the number of iterations required for convergence is also insignificant. Since the time taken by the computer is not adversely affected, results presented in this chapter have been obtained after inflation of the singular region, as it is expected to yield better results.

In the case of  $q = 1$ , inflation does have significant effect, specially when  $p < 0.3$ . Though the increase in frequency is not significantly affected, value of  $\eta_{\max}$  does change appreciably. Actually, it is seen that the location of  $\eta_{\max}$  shifts towards  $x = 1/2$ , with increasing  $p$  (Table 7.1a). For  $p < 0.3$ , this location is at  $x < h$ . This explains the difference in  $\eta_{\max}$ , with and without inflating the region  $0 \leq x \leq h$ . For  $p > 0.3$ , results are virtually the same, whether singular region is inflated or not. This indirectly suggests that the effect of singularity has been properly accounted, without any error.

While computing the results for different values of  $p$ , an interesting observation was made. Solution can be determined in two ways. One can either choose any initial starting function  $u(x)$  for each  $p$ , or the function  $u(x)$  obtained for a particular value of  $p$  can be used as

the initial starting function for the next value of  $p$ . Computations reveal a marked difference in the speed of convergence in these two cases. For example, for  $p = 0.1$ ,  $0.3$  and  $0.5$  (with  $q = 1$ ) number of iterations required is 42, 48 and 53 respectively. However, if for  $p = 0.3$ , function  $u(x)$  determined for  $p = 0.1$  is taken as the initial function, convergence occurs in 5 iterations only. If this is followed subsequently for all the remaining values of  $p$ , it is found that in each case convergence takes place in about 5 iterations. A study of the results obtained by these two methods, shows a difference in the solutions obtained. If the difference in the solutions were negligible, the method with faster convergence is to be preferred. Besides, it is further seen in the method with faster convergence, that results depend on the initial value of  $p$ , with which computations commence. In other words, if solution for  $p = 0.7$  is obtained by starting from  $p = 0.1$  and from  $p = 0.3$ , the two solutions are different. A remarkable feature of the difference in results is, that the frequency virtually remains unaffected (difference being less than 1.5 percent). A difference of about 2 to 5 percent is observed in  $e$  distribution, the difference in  $\eta$  distributions is more and the difference in the displacement function, which as stated earlier is unique, is substantial. Because

of the possibility of getting different solutions for the same value of  $p$ , the method with faster convergence is dropped. All the results presented in this chapter, therefore, have been obtained by the first method.

Use of the function  $u$  for a particular value of  $p$ , as the initial function for the subsequent value of  $p$ , amounts to prescribing an initial function. Effect of different initial functions was also investigated. It is found that for a particular value of  $p$ , irrespective of initially chosen functions, the solution determined and the number of iterations for convergence, are the same. Only such results are reported in this chapter. It appears that the initial displacement function in the fast convergence scheme, is such that the iterative solution, is not able to reach the results presented here.

### 7.5.2 Results, discussion and comments

Solutions determined in Section 7.5 are presented in the form of tables and curves. Table 7.1 gives variation of frequency ( $\omega$ ), percent increase in  $\omega$ ,  $\eta_{\max}$  and its location ( $x^*$ ), with  $p$ . Magnitude of  $\eta_{\max}$  and its location have also been provided to appreciate the peculiar distribution of  $\eta$ , stated in Section 7.5.1. The corresponding distributions of  $e$  and  $\eta$ , for  $q$  varying from 1 to 3,

are presented in Tables 7.2-7.4. These tables contain stiffness ( $s$ ) distribution also. This is done to show that though  $\eta$  has a peculiar distribution,  $s$  distribution does not contain any anomalous character,  $s$  being zero at the hinged end and gradually reaching to maximum at the middle. This indirectly puts confidence in the obtained results.

Dimensionless area distribution ( $\eta$  for  $p = \infty$ ) for the tapered-homogeneous beams, (investigated by Niordson<sup>12</sup>, and Karihaloo and Niordson<sup>15</sup>) with  $q = 2$  and  $3$ , are also presented in Tables 7.3d and 7.4d. This has been done to show that for large values of  $p$ , nonhomogeneous-tapered beams asymptotically approach to the corresponding homogeneous beams. Since the numerical results are not available in the references [12,15], the homogeneous beam problems were reformulated by the method presented in this chapter, and the corresponding solutions were obtained.

Graphically, curves of percent increase in frequency with  $p$  for  $q = 1, 2$  and  $3$  are shown in Figure 7.1. The corresponding  $e$  and  $\eta$ , distributions are shown in Figures 7.2 and 7.3. To indicate the general trends, curves are drawn only for  $p = 0.7, 1$  and  $5$  for  $q = 1$ , and for  $p = 0.3, 1$  and  $10$  for  $q = 2$  and  $3$ .

Curves of percent increase in frequency versus  $p$  (Figure 7.1) are monotonic, frequency increasing with

decreasing  $p$ . For large values of  $p$ , the increase approaches asymptotically to that obtained for the corresponding homogeneous tapered beam<sup>12,15</sup>, which is zero, 6.6 and 11.9 percent for  $q = 1, 2$  and  $3$  respectively. Modulus variation thus offers the possibility of a considerable increase in frequency, more than 30 percent within physically feasible distributions. Theoretically,  $e$  and  $\eta$  variations permit increase in frequency in the case of  $q = 1$  also. But the obtained distributions, seem to be impractical. Thus a theoretical optimal solution does exist for  $q = 1$  but being impractical, it virtually means that Euler beam is the optimal, as reported by Brach<sup>13</sup> and Karihaloo and Niordson<sup>15</sup>. Therefore, one easily concludes that in the case of  $q = 1$ , an increase in frequency should be obtained (as in Section 6.6.2) by keeping  $\eta = 1$ , and varying the modulus only.

Distributions of  $e$ , as shown in Figure 7.2, are such that  $e$  is zero at the hinged end, and is a maximum at the middle. Since the role of  $e$  and  $\eta$  is similar in contributing to the stiffness,  $e$  distributions appear to be similar to the area distributions obtained in Ref. [6] and [15]. Increase in frequency being large for small  $p$ , value of  $e_{\max}$  also increases with decreasing  $p$ . For large values of  $p$ , as the beam tends to become the corresponding homogeneous beam, it is easily seen that  $e$  versus  $x$  curves become flat, with  $e$  being around one for the whole beam.

Similarly it is seen that for large values of  $p$ ,  $\eta$  distributions (Figure 7.3) approach the corresponding distributions for non-dimensional area for the tapered homogeneous beam<sup>12,15</sup>. This is expected, because  $\eta$  corresponds to dimensionless area if  $q = 1$ . For small values of  $p$ ,  $\eta$  curves tend to be flat,  $\eta$  being in the vicinity of one. This reflects that the large increases in frequency, which occur when  $p$  is small, are largely due to the modulus variation. This is indeed the case, as the increase in frequency due to area variation alone is small, for example 6.6 percent for  $q = 2$ .

A study of results, as already stated, shows an unexpected behaviour of  $\eta$  distribution,  $\eta$  shooting to very high values (e.g., 39.94 at  $x = 0.0005$  for  $p = 0.05$  and  $q = 1$ ) near the hinged end. It is seen, that this character is strongly reflected when  $q = 1$ . It is observed that not only  $\eta_{\max}$  has large values in the case of  $q = 1$ , but the corresponding location  $x^*$  for all values of  $p$ , lies much before the middle point. In the case of  $q = 2$  and 3,  $\eta_{\max}$  is considerably less (around 1) and occurs at  $x = 1/2$  for  $p \geq 1$  when  $q = 2$  and for  $p \geq 0.50$  when  $q = 3$ . In all the cases, it is observed that  $x^*$  shifts towards  $x = 1/2$  with increasing  $p$ . It may be mentioned here, that even though  $\eta_{\max}$  is near the hinged end for small values of  $p$  in the cases of  $q$

being 2 and 3,  $\eta$  distributions, however, are not impractical. Since  $\eta_{\max}$  is around unity, and  $\eta$  is the product of dimensionless density ( $\hat{\rho}$ ) and cross-sectional area ( $a$ ), it appears to be feasible to achieve the desired  $\eta$  distributions, practically.

A study of the convergence of the iterative scheme is presented in Figure 7.6, which shows variation of the number of iterations ( $n$ ), required for the convergence, with  $p$  for  $q = 1, 2$  and  $3$ . It is found generally that  $n$  in the case of  $q = 1$ , is much more than that for  $q = 2$  and  $3$ . Besides, it is observed that in most cases,  $n$  increases with increasing  $p$ . This behaviour is different from that observed in the case of columns and uniform beams, where  $n$  generally is more for small values of  $p$  and is the least for  $p = 1$ .

Finally, a comment may be made about the feasibility of determining the governing equation and its solution for a uniform beam, as a special case of the tapered beam, by inserting  $q = 0$  in the Eqn. (7.3.33). On doing this, one gets:

$$[u'' \frac{p+1}{p-1}]'' = 0 \quad (7.5.82)$$

Comparing this equation with the Eqn. (6.6. 124) for the uniform beam, it is evident that the two equations are

different. Hence, unlike the columns, uniform beam elements have to be treated separately, as done in Chapter 6.

## 7.6 Free-Clamped Beam

Governing equation and the boundary conditions, which are obtained from (6.2.5), for free-clamped beam are

$$\left[ \frac{(1+u^2)^a}{u^{''b}} \right]'' = q \left[ \frac{(1+u^2)^c}{u^{''d}} \right] u \quad (7.3.34)$$

$$M(0) = \left[ \frac{(1+u^2)^a}{u^{''b}} \right]_{x=0} = 0 \quad (7.6.83)$$

$$V(0) = \left[ \frac{(1+u^2)^a}{u^{''b}} \right]'_{x=0} = 0 \quad (7.6.84)$$

$$u(1) = u'(1) = 0 \quad (7.6.85)$$

### Singular behaviour

Bending moment  $(M(0))$  being zero from (7.6.83), implies that the curvature  $u''$  is singular at  $x = 0$ . However, before integration of (7.3.34) is attempted, it is important to know if deflection  $u$  and slope  $u'$  are also singular. This information is provided by the zero shear condition (7.6.84).

Expression for shear force can be written as:

$$V(x) = \left[ \frac{(1+u^2)^a}{u^{''b}} \right]' = (1+u^2)^a \left[ \frac{2a u u'}{(1+u^2)u^{''b}} - \frac{b u^{''''}}{u^{''b+1}} \right] \quad (7.6.86)$$

Defining

$$V_1(x) = \frac{u u'}{(1+u^2)u^{''b}} \quad (7.6.87)$$

$$V_2(x) = \frac{u^{''''}}{u^{''b+1}} \quad (7.6.88)$$

Condition (7.6.102), therefore, implies

$$V_1(0) = V_2(0) = 0 \quad (7.6.89)$$

Now, (7.6.89) will be checked by writing  $V_1(x)$  and  $V_2(x)$  in terms of  $x$  around  $x = 0$ , by using (6.6.129) and (7.4.59) to (7.4.62). The cases  $t > 0$  and  $t < 0$  will be examined separately.

Case (1):  $t > 0$

Since  $2 > t > 1$ ,  $u$  and  $u'$  are finite quantities.

From (7.3.36),  $b$  can be written as:

$$b = \frac{1+pq-p}{1+p+pq}, \text{ i.e., } 1 > b > 0 \quad (7.6.90)$$

Parameter  $b$  being positive,  $u$  and  $u'$  being finite, and  $u''$  being singular, evidently  $V_1(0)$  equals zero.

Since  $u'''$  and  $u''$  both are singular,  $V_2(x)$  is to be written in terms of  $x$ :

$$V_2(x) = \frac{u'''}{u''b+1} \approx \frac{x^{t-3}}{x^{(t-2)(b+1)}} = x^{t-3+(2-t)(b+1)} = x^\beta \quad (7.6.91)$$

where

$$\beta = t - 3 + (2-t)(b+1) \quad (7.6.92)$$

Substitution of  $b$  from (7.6.90) into (7.6.92), gives:

$$\beta = \frac{(1+pq-p)(1-t) - 2p}{1 + p + pq} \quad (7.6.93)$$

Inserting  $t$  from (7.4.65), following value of  $\beta$  is obtained.

$$\beta = - \frac{2p(2+pq-p)}{(1+p+pq)} < 0 \quad (7.6.94)$$

Hence

$$V_2(0) = \infty \quad (7.6.95)$$

Thus if only curvature is singular ( $2 > t > 1$ ), condition  $V_2(0) = 0$  is violated. Therefore  $t$  cannot be positive.

Case (2):  $t < 0$

In this case  $u$ ,  $u'$  and  $u''$  are singular simultaneously.  $V_1(x)$ , from (7.6.87) can be approximated as:

$$V_1(x) = \frac{u}{u^2} \frac{u'}{u''b} = x^{-[1+b(t-2)]} = x^\gamma \quad (7.6.96)$$

where

$$\gamma = -[1+b(t-2)] = -\left[1 + \frac{1+pq-p}{1+pq+p} (t-2)\right] \quad (7.6.97)$$

Since  $t < 0$  for  $q = 2$  and  $3$ , only these cases are of interest. Values of  $\gamma$  and  $\beta$  will now be determined for these cases.

Case (i):  $q = 2, t = -2$

Substituting the values of  $q$  and  $t$ , following expression for  $\gamma$  and  $\beta$  is obtained.

$$\gamma = \beta = \frac{3+p}{1+3p} > 0 \quad (7.6.98)$$

Case (ii):  $q = 3, t = -1$

Equations (7.6.97) and (7.6.93) easily yield the following expression to determine  $\gamma$  and  $\beta$ .

$$\gamma = \beta = \frac{2(1+p)}{1+4p} > 0 \quad (7.6.99)$$

It, thus, follows from (7.6.98) and (7.6.99) that the condition (7.6.89) is satisfied when  $t < 0$ . Hence,  $u$ ,  $u'$ , and  $u''$  are simultaneously singular for free-clamped beam. Nature of singularity is, thus, quite different from that for the hinged-hinged beam, for which only  $u''$  is singular.

### Solution by successive iterations

Because of the particular nature of singularity in the case of F-C beam, solution cannot be obtained by employing an iterative solution similar to that developed in Section 7.5. Thus, instead of working with  $u$ ,  $u'$  and  $u''$ , which are singular at  $x = 0$ , iterative solution is developed in terms of two functions  $z(x)$  and  $f(x)$ , which are finite and well behaved. These are obtained by suitable transformation of variables. The general approach is essentially the same, as that used by Karihaloo and Niordson<sup>14</sup>.

Introducing the transformation

$$u = x^{-m} f(x) \quad (7.6.100)$$

where

$$m = -t \quad (7.6.101)$$

$$\text{or} \quad m = 2 \quad \text{for} \quad q = 2 \quad \text{and} \quad m = 1 \quad \text{for} \quad q = 3, \quad (7.6.102)$$

$u''$  can be written as:

$$u'' = x^{-(m+2)} z(x) \quad (7.6.103)$$

where

$$z(x) = x^2 f'' - 2mx f' + m(m+1)f \quad (7.6.104)$$

As the effect of singularity is contained in the coefficients of  $f(x)$  and  $z(x)$  in (7.6.100) and (7.6.103), these functions

are well behaved and do not become unbounded, anywhere in the interval  $0 \leq x \leq 1$ .

Using the boundary conditions (7.6.85), and the relation (7.6.100), integration of (7.6.103) yields:

$$f(x) = x^m \int_x^1 \int_x^1 \frac{z(x)}{x^{m+2}} dx^2 \quad (7.6.105)$$

Similarly formal integration of (7.3.34), along with (7.6.83) and (7.6.84), yields:

$$u'' = \left[ \frac{(1+u^2)^a}{q \int_0^x \int_0^x \frac{(1+u^2)^c}{u^{d/2}} u dx^2} \right]^{1/b} \quad (7.6.106)$$

Eliminating  $u$  and  $u''$  from (7.6.106), it reduces to:

$$z(x) = \left[ \frac{x^{m(b-2a)+2b} (x^{2m} + f^2)^a}{q \int_0^x \int_0^x \frac{x^{2d+m(d-2c-1)} \cdot (x^{2m} + f^2)^c f}{z^d} dx^2} \right]^{1/b} \quad (7.6.107)$$

Relations (7.6.105) and (7.6.107) are the expressions, which determine the functions  $f(x)$  and  $z(x)$ , and hence the solution of the problem. These are determined by the method of successive iterations.

#### Steps in iteration

- i) Starting with some initial function  $z_0(x)$ , say  $z_0(x) = 1$ , which may or may not satisfy the boundary conditions,

- determine  $f(x)$  from (7.6.105) and then  $z(x)$  from (7.6.107). Functions  $f(x)$  and  $z(x)$ , obtained after the first iteration, will satisfy all the boundary conditions.
- ii) Using these functions, repeat the step (i). Iteration is continued till convergence takes place. To avoid any premature termination, convergence is sought not only for  $z(x)$  and  $f(x)$ , but also for the eigen value ( $\lambda$ ). Thus  $\lambda$  is computed in every iteration with the help of the relation (7.3.52). Corresponding distributions of  $\eta(x)$  and  $e(x)$ , are then determined from (7.3.44) and (7.3.55) respectively.

Subdividing the region of integration into 200 equal parts, integration in double precision, is done by simple trapezoidal rule. It is found that the solution is affected by the mesh length ( $h$ ), if  $h > 0.005$ . For  $h < 0.005$ , the effect is insignificant.

It may be commented here that relation (7.6.107) determines  $z(x)$  at all other stations, except  $x = 0$ . Determination of  $z(0)$  was, therefore, attempted in three different ways:

- i)  $z(0) = 0$
- ii)  $z(0) = z(h)$
- iii)  $z(0)$ , determined by extrapolation, using a second degree polynomial through the points  $x = h$ ,  $x = 2h$  and  $x = 3h$ .

Computations reveal, that the approximation in the determination of  $z(0)$  has insignificant effect on the results. It is found, that in all the above cases, convergence not only takes place in the same number of iterations, but the final result is also the same up to 6 significant figures.

### Solutions for $q = 2$ and $3$

Solutions have been obtained for  $p = 0.1, 0.4, 0.8, 1$  and  $2$ , and  $q = 2$  and  $3$ . Solutions for  $p < 0.1$  and  $p > 2$ , are hardly of any interest, as  $p < 0.1$  gives  $e$  distributions which are meaningless, and for  $p > 2$  solution approaches the solution for the corresponding homogeneous beam. Results are stated in the form of tables and curves.

Table 7.5 gives variation of  $\omega$  and percent increase in  $\omega$  with  $p$ , for  $q = 2$  and  $3$ . The corresponding,  $e$  and  $\eta$  distributions for  $q = 2$  and  $3$ , are presented in Tables 7.6 and 7.7. Besides, dimensionless area distributions ( $\eta$  for  $p = \infty$ ) for the optimum homogeneous-tapered beams, investigated in Ref. [14], are also presented in these tables. One can, thus, easily verify that the solution for nonhomogeneous beam approaches the corresponding solution for homogeneous beam, for large  $p$ .

Graphically, curves of percent increase in frequency versus  $p$  are available in Figure 7.4. The

corresponding curves for  $e$  and  $\eta$  distributions, are shown in Figures 7.4 and 7.5. These curves, are drawn for  $p = 0.4$  and 2 only, to show the general trends. It is easily seen, that for large values of  $p$ ,  $e$ -curves tend to be flat with  $e$  being around one, and  $\eta$ -curves approach to the dimensionless area distributions for the corresponding optimal homogeneous beams. Similar results were obtained in the case of columns and H-H beams also.

#### Solution for $q = 1$

As already stated in Section 7.4, only  $u''$  is singular in this case. Iterative solution, employing functions  $f(x)$  and  $z(x)$ , therefore, cannot be applied. A solution, similar to that presented in Section 6.5 for the H-H beam, was attempted. It is found that the iterative process does not proceed beyond one or two iterations, for any value of  $p$ . Iterations are divergent, with  $u$ ,  $u'$  and  $u''$  approaching infinity. In other words, it appears that the governing Eqn. (7.3.34) does not have a solution for a cantilever beam, with  $q = 1$ . This result is not surprising, as the corresponding homogeneous beam also does not have an optimal solution<sup>13,14</sup>. Since the solution for large values of  $p$ , should tend to the optimal solution for homogeneous-tapered element which in this case does not exist, one will

be really surprised to get an optimal solution for a non-homogeneous tapered cantilever beam, with  $q = 1$ .

#### 7.6.1 Comments and discussion

Theoretically, any increase in frequency is possible because of the monotonic character of the percent increase in frequency versus  $p$  curve. Though the increase in  $\omega$  is very large compared to the corresponding Euler beam, the increase relative to the corresponding tapered-homogeneous element<sup>14</sup> is marginal. Area variation alone results in an increase of 578 percent for  $q \doteq 2$ , and 325 percent for  $q = 3$ . Introduction of the modulus variation, along with the area variation, does not offer any substantial increases beyond these values. Thus, it will be highly uneconomical to design a tapered-nonhomogeneous beam. It is, therefore, recommended that large increases, over the Euler beam, should be obtained by proper tapering, and if relatively small increases are desired, then a uniform-nonhomogeneous beam may be employed (Section 6.6.3). This conclusion is further confirmed by the  $e$  distributions, shown in Figure 7.5. As in the case of the H-H beam, where  $\eta$  has a peak near the hinged end, in this case  $e$  distributions have a peak near the free end. This is a peculiar behaviour, which one, normally does not

expect. Such distributions are impractical to be reproduced physically.

Finally, some observations can be made about the efficiency of the iterative scheme used in this section. It is found that the convergence takes place in about 30 iterations in the case of  $q = 2$ , and about 10 iterations when  $q = 3$ . Variation of number of iterations ( $n$ ) with  $p$  is insignificant. It is further seen that if the termination criterion is made less stringent, convergence occurs in about 15 iterations for  $q = 2$ , and 6 iterations for  $q = 3$ . The difference in the increase in frequency due to this, is less than half percent. The iterative process, thus, seems to become slow near the optimum point.

Table 7.1: Variation of frequency ( $\omega$ ), percent increase in  $\omega$ ,  $\eta_{\max}$  and location ( $x^*$ ) of  $\eta_{\max}$  with  $p$  for hinged-tapered beams  
a) for  $q = 1$

$p$	0.05	0.1	0.3	0.5	0.7	1	2	5
$\omega$	15.59	14.59	12.68	11.85	11.38	10.96	10.36	9.886
percent increase	57.98	47.88	28.52	20.08	15.30	11.06	4.99	0.17
$\eta_{\max}$	39.94	26.35	6.201	3.555	2.553	1.920	1.306	1.090
$x^*$	0.0005	0.002	0.01	0.015	0.02	0.03	0.05	0.15

Table 7.1: Continued  
b) for  $q = 2$

$p$	0.1	0.3	0.5	0.7	1	2	5	10
$\omega$	13.29	12.15	11.68	11.41	11.19	10.88	10.67	10.59
percent increase	34.63	23.07	18.32	15.68	13.39	10.27	8.11	7.34
$\eta_{\max}$	1.360	1.116	1.083	1.089	1.120	1.191	1.244	1.265
$x^*$	0.05	0.10	0.20	0.25	0.50	0.50	0.50	0.50

Table 7.1: Concluded  
c) for  $q = 3$

$p$	0.1	0.3	0.5	0.7	1	2	5	10
$\omega$	13.16	12.23	11.87	11.69	11.53	11.31	11.16	11.11
percent increase	33.30	23.89	20.32	18.41	16.78	14.60	13.13	12.61
$\eta_{\max}$	1.127	1.060	1.092	1.126	1.158	1.201	1.233	1.244
$x^*$	0.10	0.20	0.50	0.50	0.50	0.50	0.50	0.50

Table 7.2: Variation of  $e$ ,  $\eta$  and  $s$  along the axis for hinged-hinged tapered beams with  $q = 1$

a) for  $p = 0.05$  and  $0.1$

x	p = 0.05			p = 0.1		
	e	$\eta$	s	e	$\eta$	s
0	0	0	0	0	0	0
0.05	0.0361	1.350	0.0488	0.0364	1.823	0.0663
0.10	0.2633	0.5204	0.1370	0.2421	0.7314	0.1770
0.15	0.7671	0.3095	0.2375	0.6719	0.4443	0.2985
0.20	1.530	0.2210	0.3382	1.299	0.3215	0.4177
0.25	2.471	0.1748	0.4319	2.052	0.2568	0.5270
0.30	3.473	0.1479	0.5137	2.841	0.2188	0.6215
0.35	4.413	0.1315	0.5804	3.571	0.1954	0.6979
0.40	5.177	0.1216	0.6295	4.159	0.1813	0.7539
0.45	5.675	0.1162	0.6596	4.540	0.1736	0.7881
0.50	5.847	0.1145	0.6697	4.671	0.1712	0.7996

Table 7.2: Continued

b) for  $p = 0.3$  and  $0.5$

x	p = 0.3			p = 0.5		
	e	$\eta$	s	e	$\eta$	s
0	0	0	0	0	0	0
0.05	0.0563	2.383	0.1342	0.0869	2.258	0.1963
0.10	0.2537	1.188	0.3013	0.2947	1.327	0.3911
0.15	0.5811	0.7974	0.4634	0.5850	0.9616	0.5626
0.20	0.9971	0.6133	0.6116	0.9180	0.7748	0.7113
0.25	1.453	0.5103	0.7413	1.259	0.6651	0.8372
0.30	1.900	0.4474	0.8501	1.578	0.5959	0.9404
0.35	2.296	0.4077	0.9361	1.851	0.5513	1.021
0.40	2.605	0.3832	0.9983	2.060	0.5233	1.078
0.45	2.802	0.3697	1.036	2.191	0.5078	1.112
0.50	2.869	0.3654	1.048	2.235	0.5029	1.124

Table 7.2: Continued

c) for  $p = 0.7$  and 1

x	p = 0.7			p = 1		
	e	$\eta$	s	e	$\eta$	s
0	0	0	0	0	0	0
.05	0.1226	2.046	0.2509	0.1789	1.779	0.3182
.10	0.3394	1.358	0.4609	0.4026	1.340	0.5394
.15	0.6070	1.041	0.6321	0.6448	1.092	0.7039
.20	0.8917	0.8687	0.7746	0.8828	0.9454	0.8346
.25	1.169	0.7634	0.8923	1.102	0.8520	0.9393
.30	1.420	0.6953	0.9870	1.294	0.7899	1.022
.35	1.629	0.6506	1.060	1.450	0.7483	1.085
.40	1.786	0.6222	1.111	1.564	0.7216	1.129
.45	1.884	0.6064	1.142	1.635	0.7065	1.155
.50	1.917	0.6013	1.153	1.658	0.7017	1.164

Table 7.2: Concluded

d) for  $p = 2$  and 5

x	p = 2			p = 5		
	e	$\eta$	s	e	$\eta$	s
0	0	0	0	0	0	0
.05	0.3474	1.306	0.4538	0.6197	0.9178	0.5687
.10	0.5585	1.231	0.6878	0.7607	1.079	0.8208
.15	0.7428	1.118	0.8304	0.8646	1.090	0.9425
.20	0.9011	1.035	0.9325	0.9446	1.076	1.017
.25	1.034	0.9758	1.009	1.007	1.060	1.067
.30	1.143	0.9339	1.068	1.055	1.046	1.104
.35	1.228	0.9046	1.111	1.091	1.035	1.129
.40	1.289	0.8853	1.141	1.116	1.027	1.147
.45	1.325	0.8742	1.158	1.131	1.023	1.157
.50	1.337	0.8706	1.164	1.136	1.021	1.160

Table 7.3: Variation of  $e$ ,  $\eta$  and  $s$  along the axis for hinged-hinged tapered beams with  $q = 2$

a) for  $p = 0.1$  and  $0.3$

x	p = 0.1			p = 0.3		
	e	$\eta$	s	e	$\eta$	s
0	0	0	0	0	0	0
0.05	0.0660	1.360	0.1220	0.1396	1.014	0.1435
0.10	0.2505	1.271	0.4049	0.3406	1.116	0.4245
0.15	0.5912	1.144	0.7735	0.6120	1.112	0.7572
0.20	1.099	1.033	1.174	0.9433	1.078	1.095
0.25	1.745	0.9474	1.566	1.309	1.038	1.411
0.30	2.461	0.8835	1.921	1.676	1.003	1.686
0.35	3.159	0.8378	2.217	2.009	0.9752	1.911
0.40	3.743	0.8072	2.439	2.274	0.9554	2.075
0.45	4.132	0.7897	2.576	2.444	0.9437	2.176
0.50	4.267	0.7840	2.623	2.503	0.9398	2.210

Table 7.3: Continued

b) for  $p = 0.5$  and  $0.7$

x	p = 0.5			p = 0.7		
	e	$\eta$	s	e	$\eta$	s
0	0	0	0	0	0	0
0.05	0.2163	0.8602	0.1601	0.2865	0.7749	0.1720
0.10	0.4231	1.026	0.4456	0.4905	0.9698	0.4613
0.15	0.6596	1.077	0.7655	0.7010	1.051	0.7743
0.20	0.9185	1.083	1.078	0.9164	1.081	1.072
0.25	1.183	1.072	1.360	1.126	1.089	1.335
0.30	1.434	1.057	1.602	1.317	1.087	1.557
0.35	1.651	1.043	1.795	1.479	1.082	1.732
0.40	1.819	1.031	1.935	1.601	1.077	1.859
0.45	1.926	1.024	2.020	1.678	1.074	1.935
0.50	1.962	1.022	2.049	1.704	1.073	1.961

Table 7.3: Continued

c) for  $p = 1$  and  $2$ 

x	p = 1			p = 2		
	e	$\eta$	s	e	$\eta$	s
0	0	0	0	0	0	0
0.05	0.3755	0.7013	0.1847	0.5666	0.6032	0.2061
0.10	0.5684	0.9173	0.4783	0.7167	0.8409	0.5068
0.15	0.7491	1.024	0.7851	0.8387	0.9798	0.8051
0.20	0.9225	1.076	1.069	0.9450	1.064	1.070
0.25	1.083	1.102	1.315	1.037	1.116	1.291
0.30	1.225	1.114	1.519	1.114	1.149	1.470
0.35	1.342	1.118	1.678	1.174	1.170	1.606
0.40	1.429	1.120	1.792	1.218	1.182	1.703
0.45	1.482	1.120	1.861	1.245	1.189	1.760
0.50	1.500	1.120	1.883	1.254	1.191	1.779

Table 7.3: Concluded

d) for  $p = 5$  and  $10$ 

x	p = 5			p = 10			p = $\infty$
	e	$\eta$	s	e	$\eta$	s	$\eta^*$
0	0	0	0	0	0	0	0
0.05	0.7780	0.5374	0.2246	0.8780	0.5143	0.2322	0.4909
0.10	0.8617	0.7851	0.5312	0.9255	0.7646	0.5411	0.7434
0.15	0.9228	0.9445	0.8232	0.9558	0.9308	0.8307	0.9164
0.20	0.9724	1.051	1.073	0.9850	1.045	1.075	1.039
0.25	1.013	1.123	1.277	1.006	1.125	1.273	1.126
0.30	1.045	1.173	1.437	1.023	1.181	1.426	1.189
0.35	1.070	1.206	1.557	1.035	1.220	1.540	1.233
0.40	1.088	1.228	1.641	1.044	1.245	1.619	1.263
0.45	1.099	1.240	1.690	1.049	1.260	1.665	1.280
0.50	1.102	1.244	1.707	1.051	1.265	1.681	1.286

\*  $\eta$ , recomputed for the case considered in Ref. [12].

Table 7.4: Variation of  $e$ ,  $\eta$  and  $s$  along the axis for hinged-hinged tapered beams with  $q = 3$

a) for  $p = 0.1$  and  $0.3$

x	p = 0.1			p = 0.3		
	e	$\eta$	s	e	$\eta$	s
0	0	0	0	0	0	0
0.05	0.0876	1.112	0.1205	0.1968	0.8797	0.134
0.10	0.2863	1.127	0.4102	0.4133	1.003	0.4165
0.15	0.6151	1.092	0.8015	0.6707	1.047	0.7709
0.20	1.079	1.047	1.239	0.9629	1.060	1.147
0.25	1.655	1.005	1.678	1.272	1.059	1.511
0.30	2.288	0.9691	2.082	1.575	1.052	1.836
0.35	2.903	0.9416	2.424	1.845	1.045	2.105
0.40	3.420	0.9222	2.682	2.058	1.039	2.305
0.45	3.763	0.9107	2.842	2.195	1.034	2.429
0.50	3.884	0.9069	2.897	2.242	1.033	2.470

Table 7.4: Continued

b) for  $p = 0.5$  and  $0.7$

x	p = 0.5			p = 0.7		
	e	$\eta$	s	e	$\eta$	s
0	0	0	0	0	0	0
0.05	0.2973	0.7841	0.1433	0.3804	0.7326	0.1495
0.10	0.5104	0.9421	0.4267	0.5819	0.9070	0.4341
0.15	0.7272	1.019	0.7693	0.7691	1.001	0.7707
0.20	0.9489	1.058	1.124	0.9492	1.055	1.113
0.25	1.166	1.077	1.459	1.118	1.086	1.433
0.30	1.367	1.087	1.754	1.269	1.105	1.712
0.35	1.538	1.090	1.995	1.394	1.116	1.938
0.40	1.670	1.092	2.173	1.488	1.122	2.104
0.45	1.752	1.092	2.282	1.547	1.126	2.205
0.50	1.780	1.092	2.319	1.567	1.126	2.239

Table 7.4: Continued

c) for  $p = 1$  and  $2$ 

x	p = 1			p = 2		
	e	$\eta$	s	e	$\eta$	s
0	0	0	0	0	0	0
0.05	0.4769	0.6884	0.1556	0.6598	0.6299	0.1649
0.10	0.6581	0.8755	0.4416	0.7885	0.8315	0.4533
0.15	0.8132	0.9833	0.7732	0.8866	0.9575	0.7783
0.20	0.9544	1.050	1.106	0.9692	1.042	1.097
0.25	1.081	1.093	1.412	1.039	1.101	1.386
0.30	1.191	1.121	1.677	1.097	1.141	1.632
0.35	1.281	1.139	1.890	1.143	1.169	1.828
0.40	1.347	1.150	2.046	1.176	1.188	1.970
0.45	1.387	1.156	2.140	1.195	1.198	2.056
0.50	1.401	1.158	2.172	1.202	1.201	2.085

Table 7.4: Concluded

d) for  $p = 5$  and  $10$ 

x	p = 5			p = 10			p = $\infty$
	e	$\eta$	s	e	$\eta$	s	$\eta^*$
0	0	0	0	0	0	0	0
0.05	0.8357	0.5907	0.1722	0.9120	0.5768	0.1750	0.5627
0.10	0.9018	0.8006	0.4628	0.9482	0.7894	0.4664	0.7778
0.15	0.9482	0.9383	0.7834	0.9729	0.9312	0.7854	0.9237
0.20	0.9852	1.035	1.093	0.9921	1.032	1.091	1.029
0.25	1.015	1.105	1.369	1.007	1.106	1.364	1.107
0.30	1.039	1.155	1.602	1.020	1.160	1.592	1.165
0.35	1.058	1.191	1.786	1.029	1.199	1.772	1.206
0.40	1.071	1.215	1.919	1.035	1.224	1.901	1.235
0.45	1.078	1.228	1.998	1.039	1.239	1.978	1.251
0.50	1.081	1.233	2.025	1.041	1.244	2.004	1.256

\*  $\eta$ , recomputed for the case considered in Ref. [15].

Table 7.5: Variation of frequency ( $\omega$ ) and percent increase in  $\omega$  with  $p$  for free-clamped tapered beams

p	q = 2		q = 3	
	$\omega$	percent increase	$\omega$	percent increase
0.1	24.96	609.9	15.67	345.7
0.4	24.33	592.2	15.25	333.7
0.8	24.13	586.3	15.12	330.0
1	24.08	584.8	15.09	329.2
2	23.96	581.5	15.02	327.2

Table 7.6: Variation of  $e$  and  $\eta$  along the axis for free-clamped tapered beams with  $q = 2$

$x$	$p = 0.1$		$p = 0.4$		$p = 0.8$		$p = 1$		$p = 2$		$p =$
	$e$	$\eta$	$e$	$\eta$	$e$	$\eta$	$e$	$\eta$	$e$	$\eta$	$\eta^*$
0	0	0	0	0	0	0	0	0	0	0	0
0.1	0.6507	0.0014	0.8054	0.0011	0.8787	0.0011	0.8979	0.0011	0.9431	0.0010	0.0010
0.2	0.6392	0.0219	0.7990	0.0175	0.8746	0.0160	0.8945	0.0157	0.9412	0.0150	0.0141
0.3	0.6187	0.1118	0.7862	0.0874	0.8664	0.0794	0.8875	0.0775	0.9373	0.0735	0.0690
0.4	0.6019	0.3538	0.7692	0.2745	0.8539	0.2479	0.8767	0.2417	0.9308	0.2282	0.2131
0.5	0.6348	0.8117	0.7711	0.6474	0.8506	0.5873	0.8729	0.5729	0.9274	0.5411	0.5048
0.6	0.7985	1.388	0.8389	1.196	0.8868	1.111	0.9020	1.089	0.9418	1.040	0.9795
0.7	1.197	1.845	1.023	1.759	0.9950	1.702	0.9919	1.686	0.9905	1.645	1.590
0.8	1.913	2.096	1.335	2.188	1.176	2.211	1.142	2.215	1.072	2.220	2.219
0.9	2.940	2.223	1.734	2.487	1.395	2.605	1.321	2.635	1.165	2.706	2.794
1.0	4.191	2.306	2.159	2.719	1.612	2.929	1.494	2.987	1.251	3.127	3.314

\*  $\eta$ , recomputed for the case considered in Ref. [14].

Table 7.7: Variation of  $e$  and  $\eta$  along the axis for free-clamped tapered beams with  $q = 3$

$x$	$p = 0.1$		$p = 0.4$		$p = 0.8$		$p = 1$		$p = 2$		$p =$
	$e$	$\eta$	$e$	$\eta$	$e$	$\eta$	$e$	$\eta$	$e$	$\eta$	$\eta^*$
0	0	0	0	0	0	0	0	0	0	0	0
0.1	0.5333	0.0607	0.7469	0.0515	0.8440	0.0496	0.8699	0.0479	0.9276	0.0465	0.0449
0.2	0.5015	0.2467	0.7238	0.2048	0.8284	0.1915	0.8559	0.1884	0.9200	0.1818	0.1745
0.3	0.5017	0.5426	0.7129	0.4521	0.8188	0.4222	0.8471	0.4152	0.9143	0.4000	0.3830
0.4	0.5701	0.8854	0.7395	0.7617	0.8321	0.7167	0.8576	0.7060	0.9192	0.6821	0.6547
0.5	0.7435	1.187	0.8239	1.077	0.8823	1.031	0.8993	1.019	0.9418	0.9928	0.9612
0.6	1.059	1.401	0.9738	1.349	0.9724	1.320	0.9745	1.312	0.9830	1.293	1.269
0.7	1.540	1.534	1.182	1.560	1.093	1.562	1.075	1.562	1.037	1.560	1.555
0.8	2.185	1.616	1.429	1.722	1.230	1.760	1.186	1.769	1.095	1.789	1.811
0.9	2.963	1.672	1.692	1.851	1.367	1.925	1.296	1.944	1.151	1.987	2.040
1.0	3.832	1.715	1.952	1.960	1.495	2.069	1.398	2.097	1.201	2.163	2.245

\*  $\eta$ , recomputed for the case considered in Ref. [14].

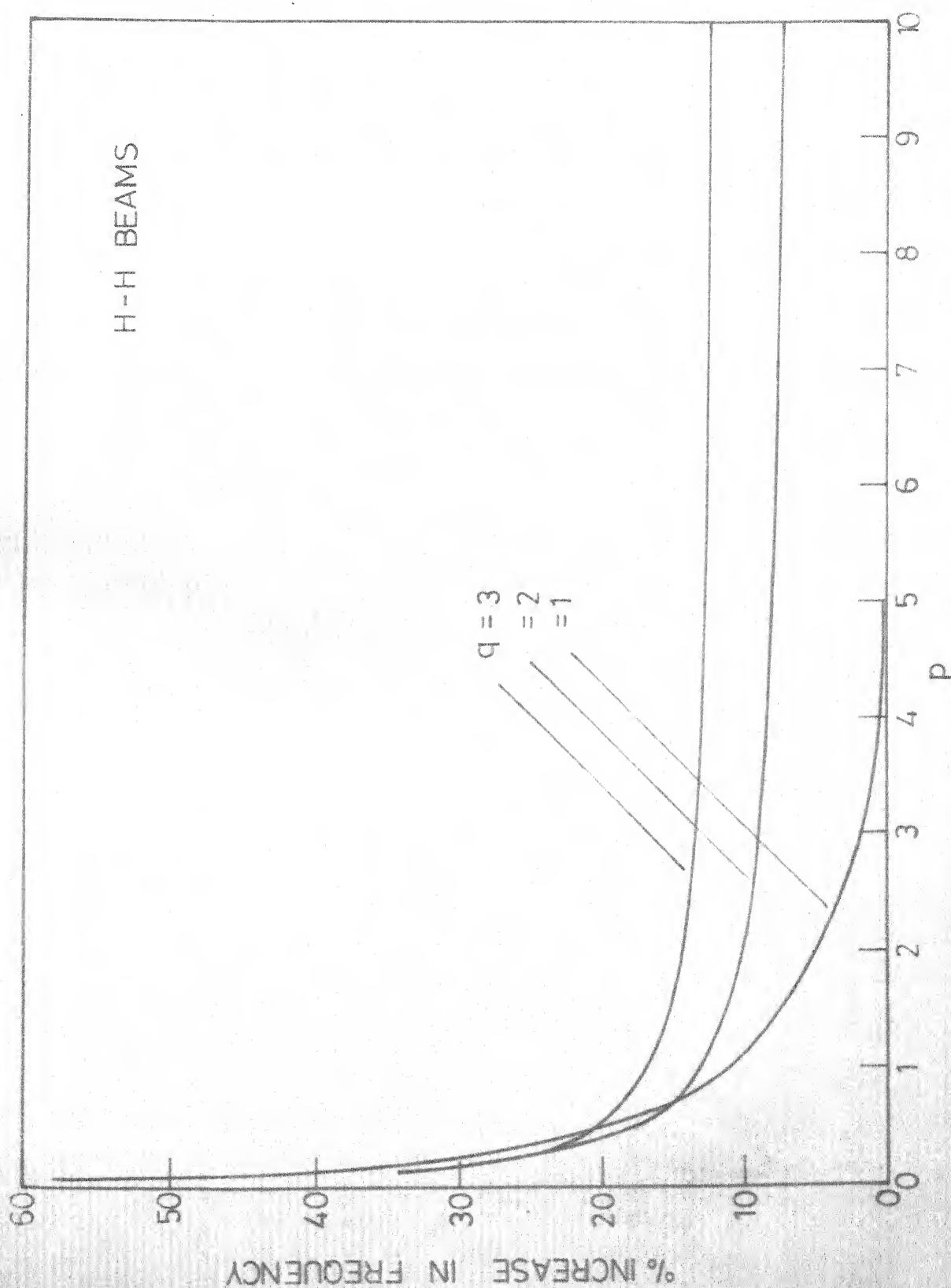


FIG.71. VARIATION OF PERCENT INCREASE IN FREQUENCY WITH  $p$  FOR  
HINGED - HINGED TAPERED BEAMS

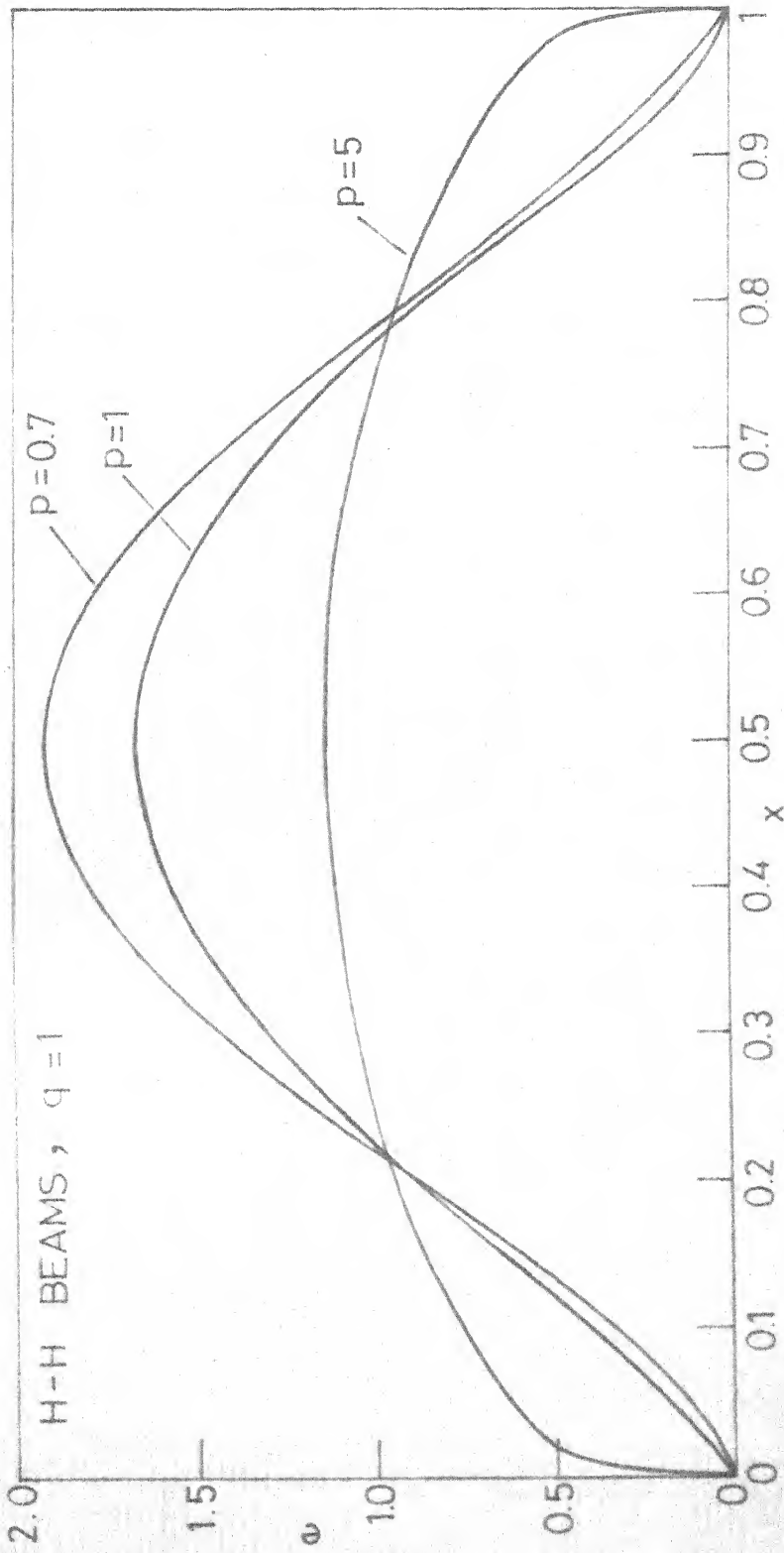


FIG.7.2a. VARIATION OF  $e$  ALONG THE AXIS FOR HINGED - HINGED TAPERED BEAMS WITH  $q=1$

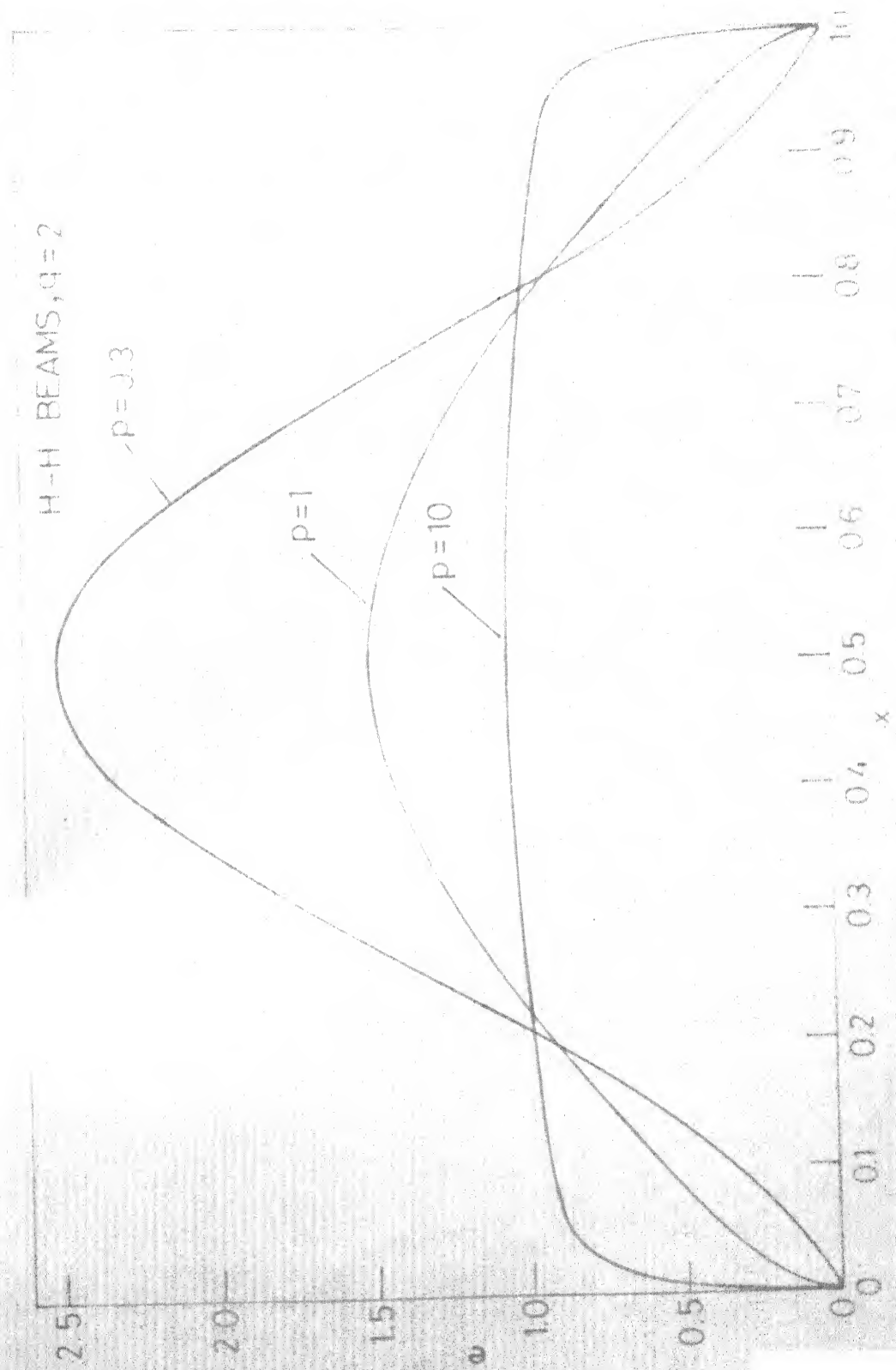


FIG 72b. VARIATION OF  $e$  ALONG THE AXIS FOR HINGED - HINGED BEAMS WITH  $q=2$

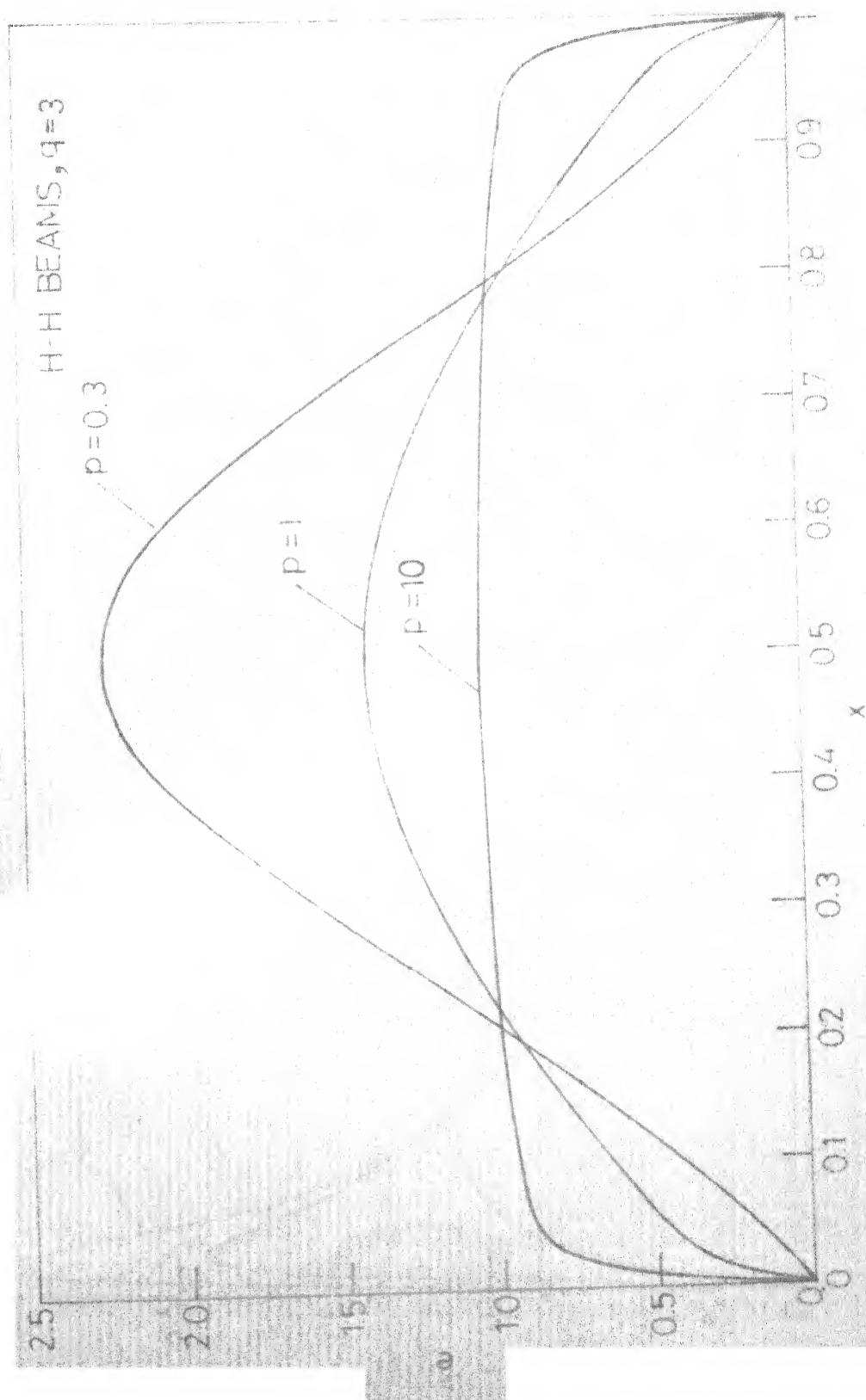


FIG 72c. VARIATION OF  $e$  ALONG THE AXIS FOR HINGED - HINGED TAPERED BEAMS WITH  $q = 3$

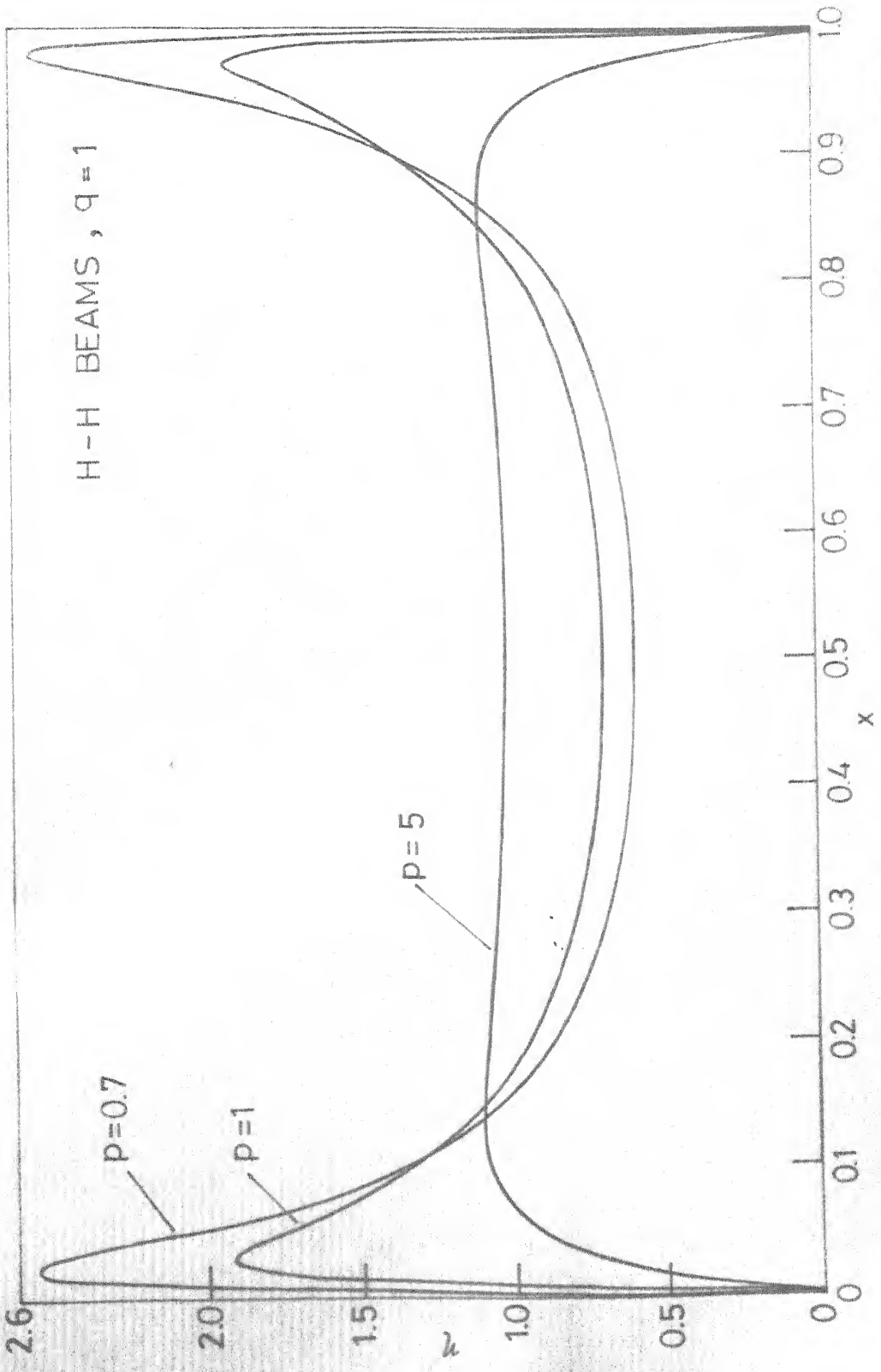


FIG.73a. VARIATION OF  $\eta$  ALONG THE AXIS FOR HINGED - HINGED TAPERED BEAMS WITH  $q=1$

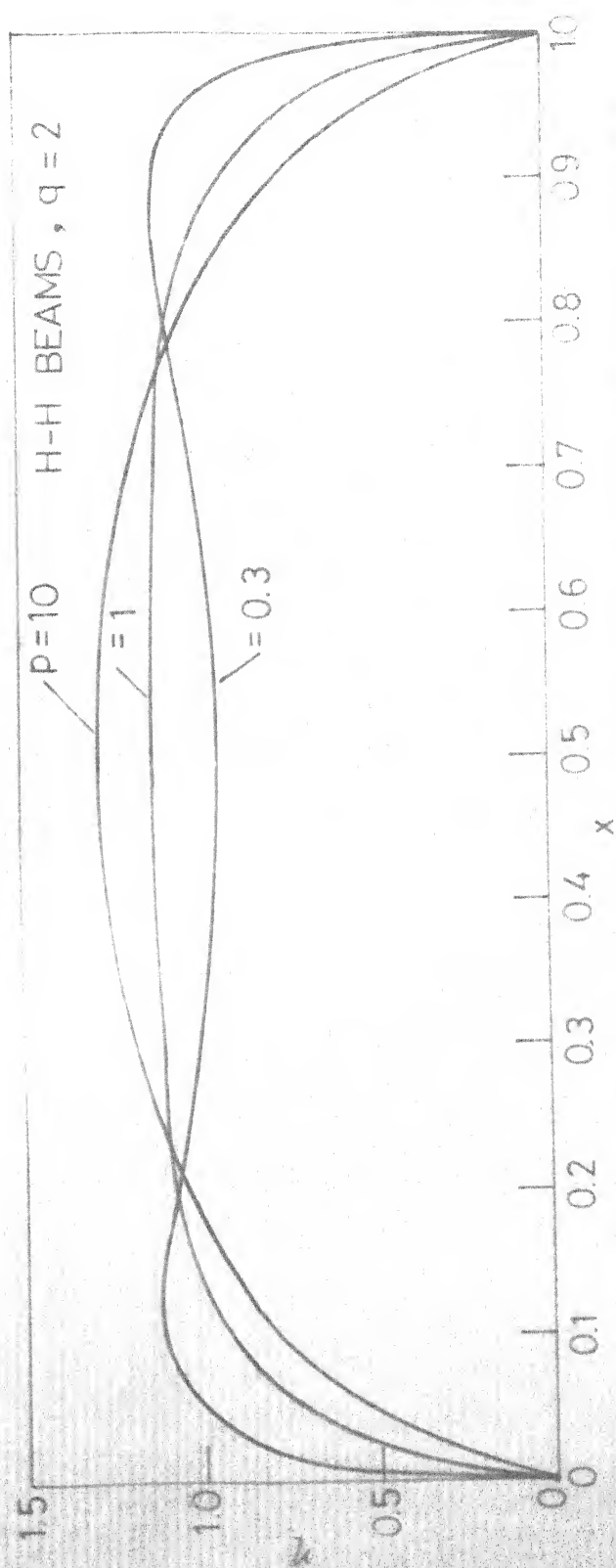


FIG. 7.3b. VARIATION OF  $\eta$  ALONG THE AXIS FOR HINGED - HINGED  
TAPERED BEAMS WITH  $q=2$

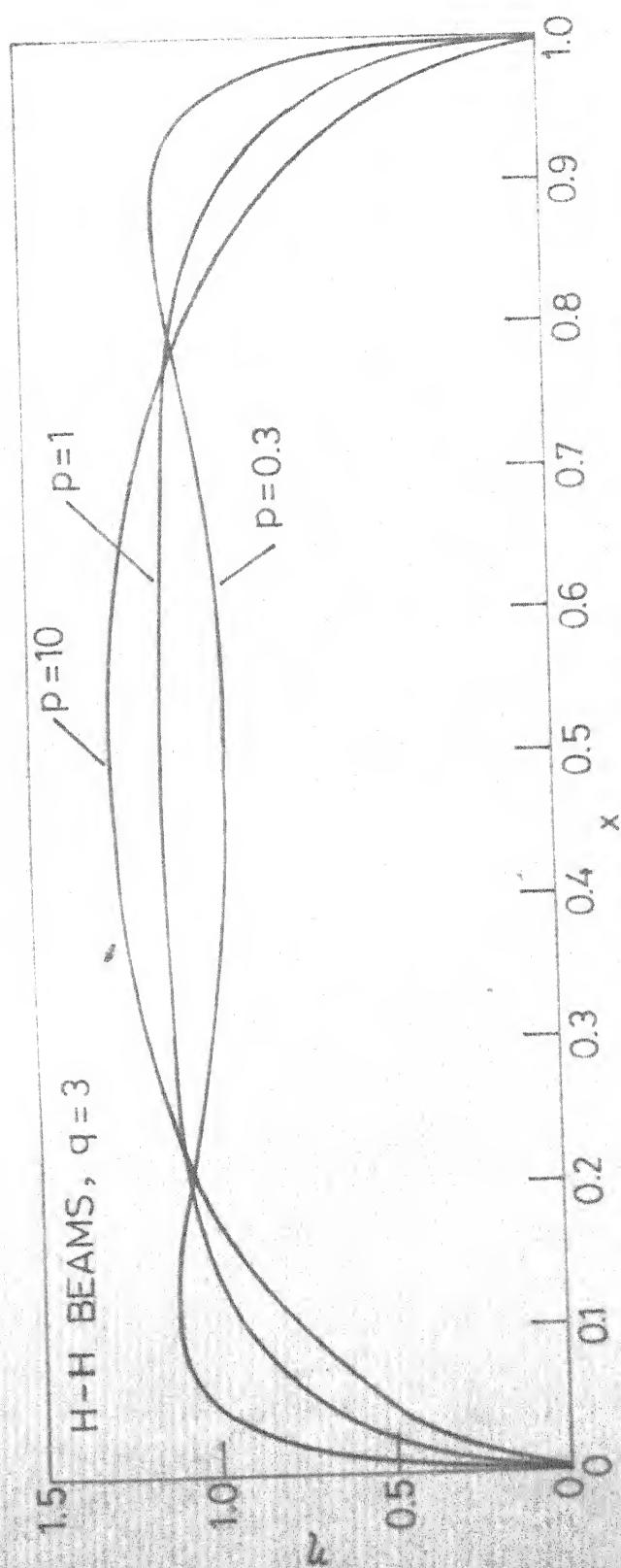
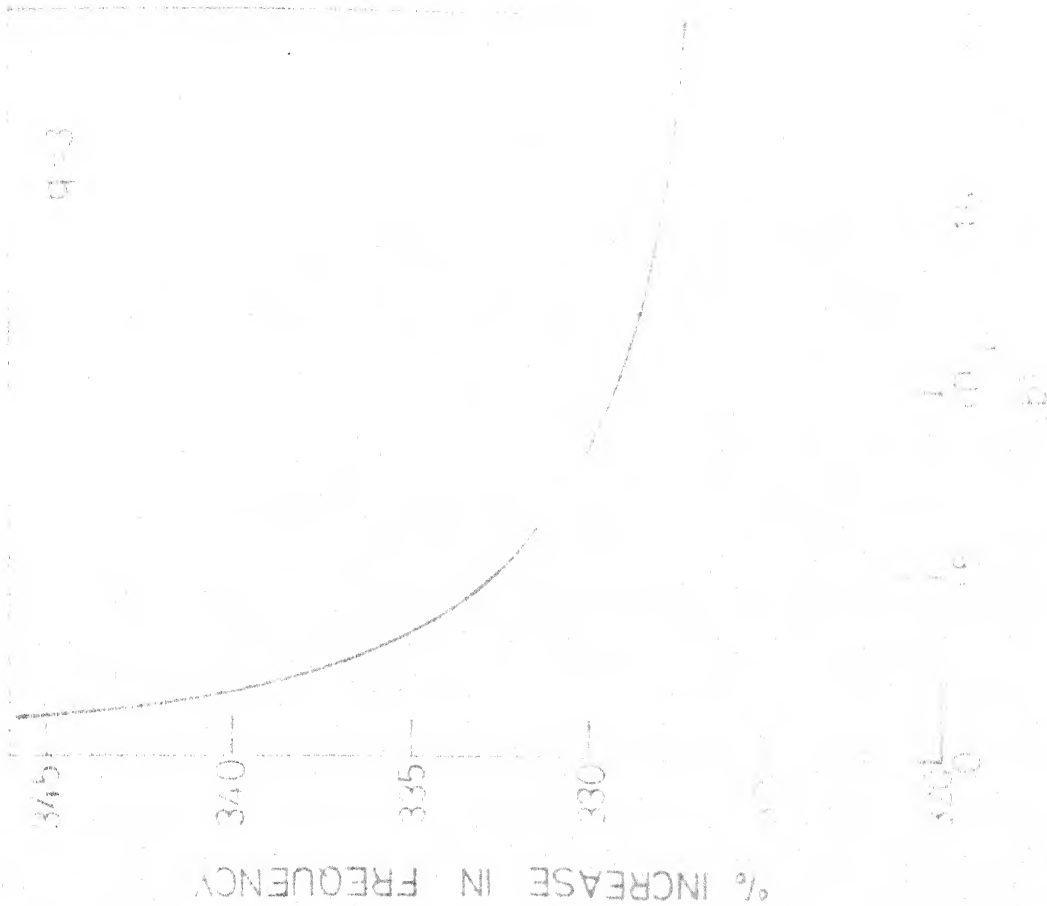
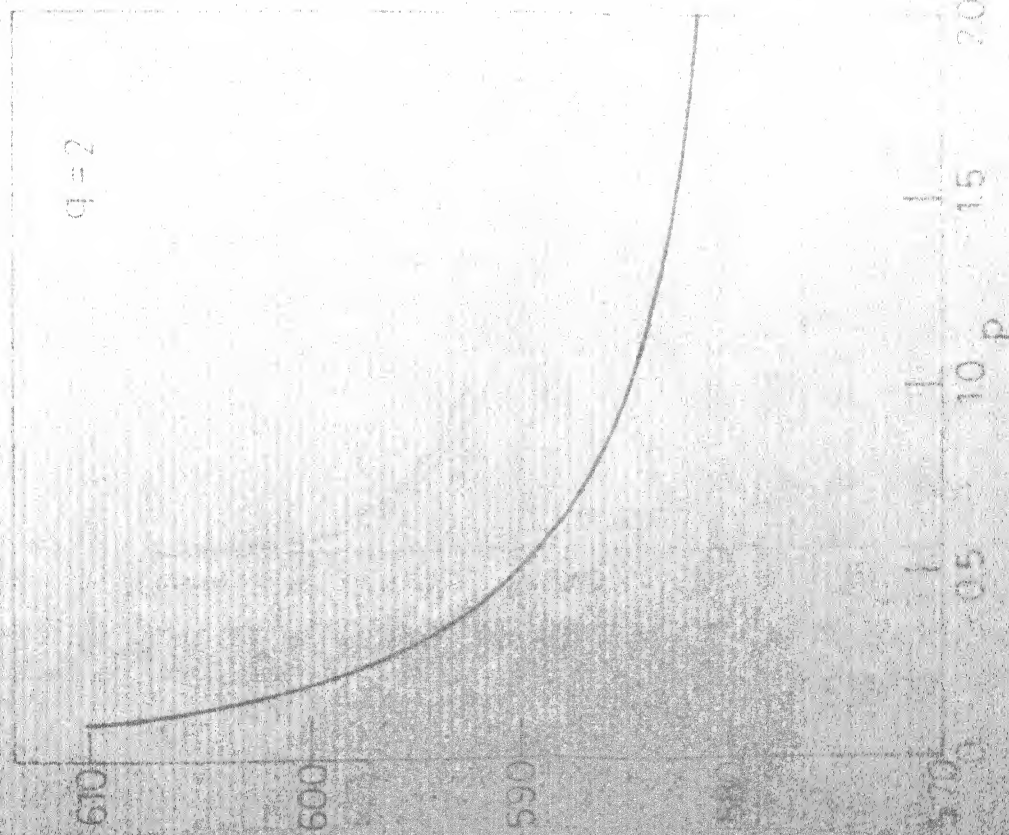


FIG.7.3c. VARIATION OF  $\eta$  ALONG THE AXIS FOR HINGED - HINGED TAPERED BEAMS WITH  $q=3$



(a)

(b)

FIG.7.4. VARIATION OF PERCENT INCREASE IN FREQUENCY WITH  $p$  FOR FREE CLAMPED TAPERED BEAMS

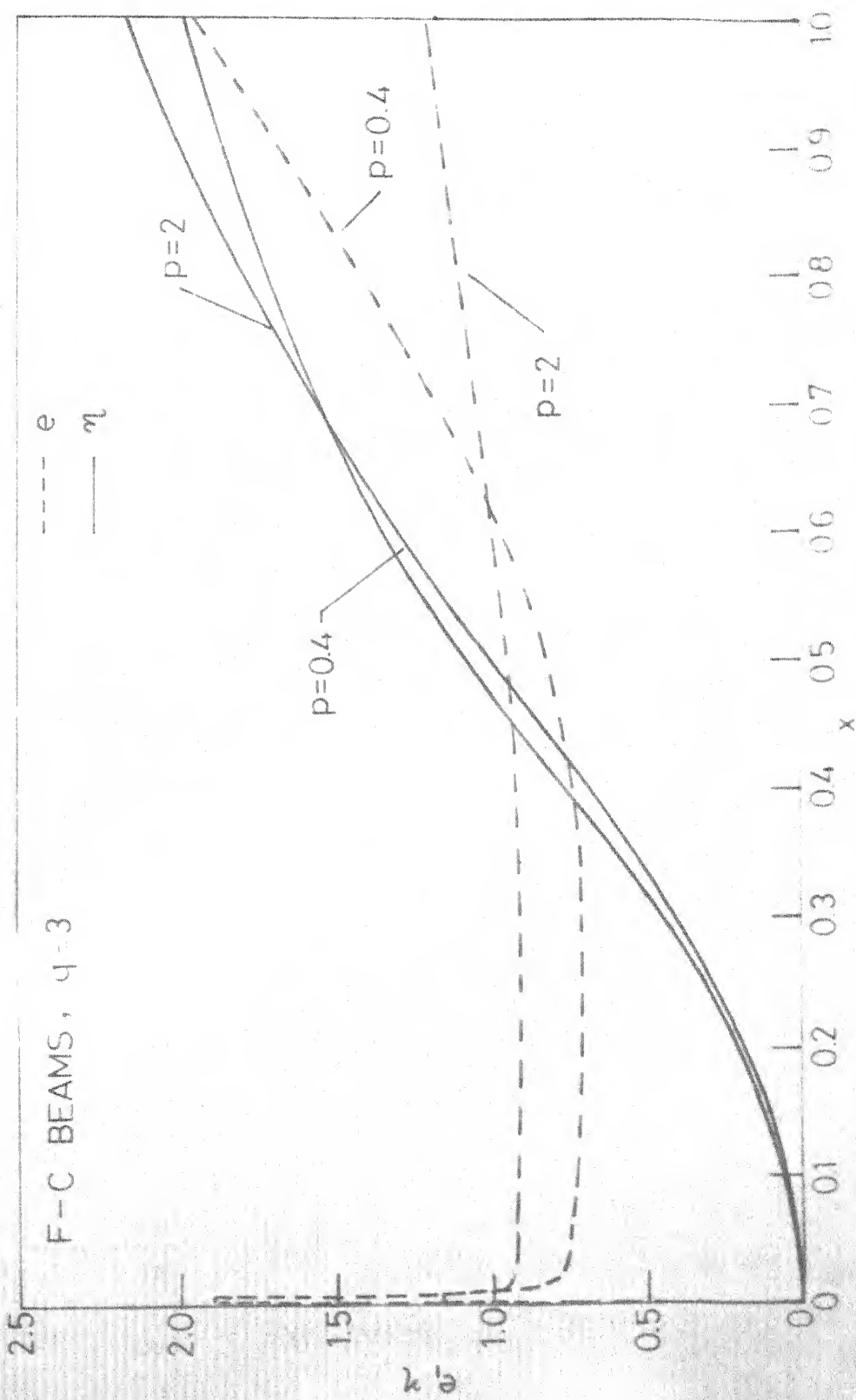


FIG 7.5b. VARIATION OF  $e$  AND  $\eta$  ALONG THE  $x$ -AXIS FOR F-C BEAMS WITH  $q=3$

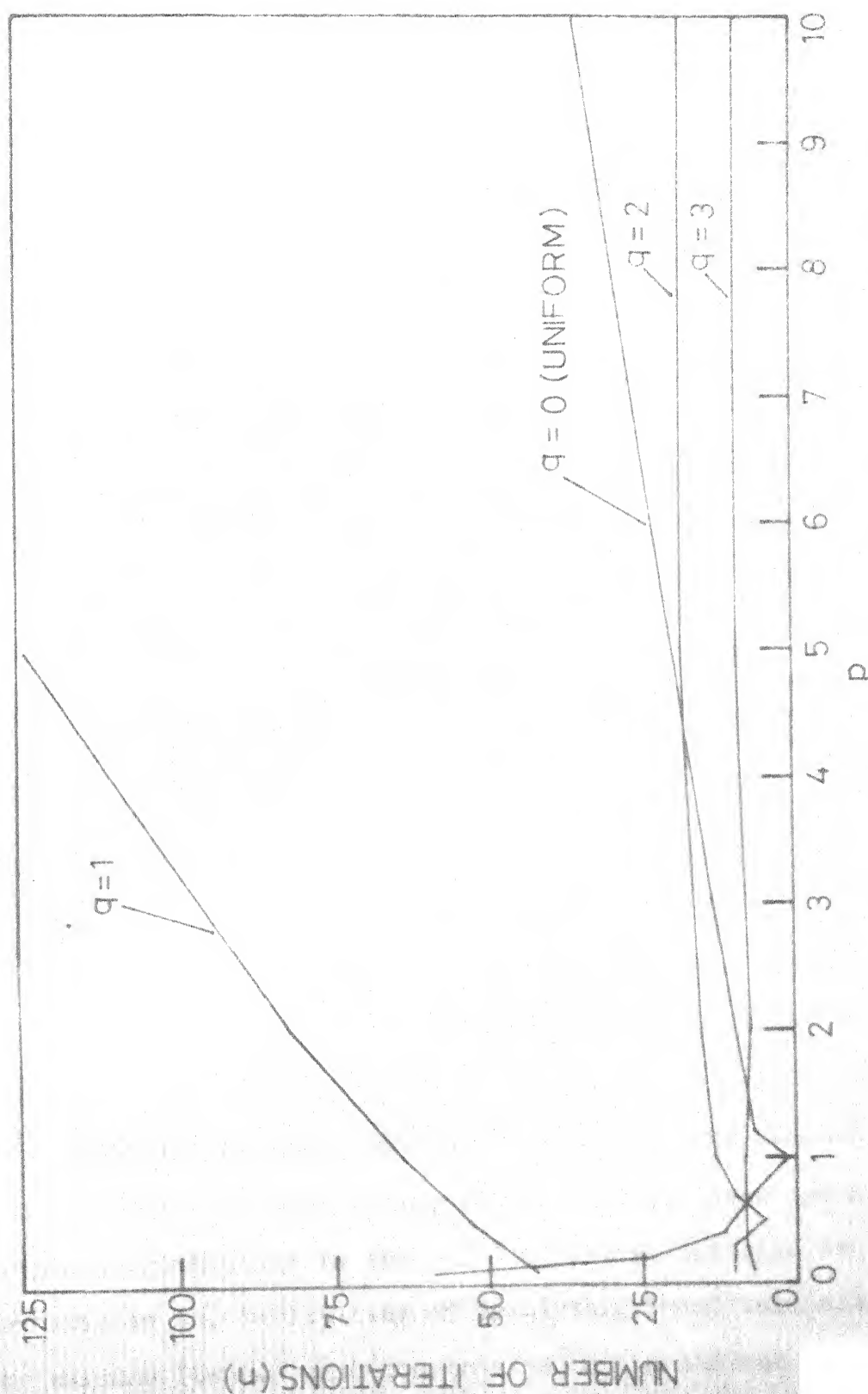


FIG.7.6. VARIATION OF NUMBER OF ITERATIONS ( $n$ ) WITH  $p$  FOR  
HINGED - HINGED BEAMS

## CHAPTER - 8

### APPROXIMATE SOLUTIONS

#### 8.1 Introduction

Exact physical realization of the distributions of  $e$  and  $\eta$ , obtained in Chapters 3, 4, 5, 6, and 7, is difficult in practice. An attempt is, therefore, made in this chapter to examine the sensitivity of the eigen values to small perturbations in the numerically-obtained distributions of the design variables. These have been approximated by simple polynomials. It is shown, by considering the particular example of the hinged-hinged columns with  $p = 1$ , which are characterized by identical distributions of  $e$  and  $\eta$ , that the effect of approximation on the eigen value (implying the critical load) is marginal. Further, an attempt is also made to predict the optimum distributions of  $e$  and  $\eta$ , for columns, with constraints on the minimum values of these variables.

#### 8.2 Approximating Polynomials and Corresponding Results

Our objective, here, is not only to determine a simple approximation to the  $e$  and  $\eta$  curves, but also to investigate the feasibility of predicting these variables for columns (beams) with constraints on the minimum values

of  $e$  and  $\eta$ . This study is made, here, by considering the particular example of the hinged-hinged columns with  $p = 1$ .

From physical considerations,  $e$  ( $\eta$ ) distribution (for a constrained hinged-hinged column) is expected to be such that it would be a constant (equal to the minimum specified  $e$ , say  $e_0$ ) up to a certain distance (which depends on  $e_0$ ) from the hinged end. It would then, gradually reach the maximum at the middle.

For the case of  $p = 1$ , the following polynomial, for approximating both  $e(x)$  and  $\eta(x)$ , which are the same for the unconstrained columns, is proposed.

$$\eta(x) = e(x) = e_0 + a_1(x-x_0) + a_2(x-x_0)^2 + a_3(x-x_0)^3 ;$$

$$x_0 \leq x \quad (8.2.1a)$$

$$\eta(x) = e(x) = e_0 ; \quad x \leq x_0 \quad (8.2.1b)$$

Here,  $e_0$  refers to the minimum specified  $e$ ,  $x_0$  refers to the distance up to which  $e(x)$  and  $\eta(x)$  remain constant, and  $a_1$ ,  $a_2$ , and  $a_3$  are the coefficients, which are to be determined, suitably. For a given  $e_0$ ,  $x_0$  is gradually increased from zero to some suitably selected value (say 0.1), and in each case, critical load  $\lambda$  is determined. The value of  $x_0$  and the associated  $e$  and  $\eta$  distributions, which yield the maximum value of  $\lambda$ , determine an approximate solution of the constrained problem.

Coefficients  $a_1$ ,  $a_2$ , and  $a_3$  in Eqn. (8.2.1a), are determined by setting the following three conditions:

- i)  $2 \int_0^{1/2} e(x) dx = 1$
- ii) symmetry of  $e(x)$ , i.e.,  $\left. \frac{de}{dx} \right|_{x=1/2} = 0$
- iii)  $e(1/2) = e_{\max}$  for the unconstrained column, thereby, approximating polynomial becoming close to e-curves obtained in Chapter 5.

The above three conditions, produce three linear equations, to determine  $a_1$ ,  $a_2$ , and  $a_3$ . Equation (8.2.1), then determines the associated  $e(x)$ , which was obtained for  $e_0$  varying from 0.1 to 0.7. In each case,  $x_0$  varied from 0 to 0.1 and  $q$  from 1 to 3.

In order to study the effect of approximations,  $x_0$  is kept 0 and  $e_0$  is suitably chosen such that the maximum value of  $\lambda$  is obtained. It is seen that in the case of  $q = 1$  and 2, a very close approximation is obtained. Increase in load for  $q = 1$ , is 32.54 percent whereas the maximum possible increase is 33.37 percent. The difference in the solution obtained by simple polynomial and the strongest column solution is, thus, marginal. The results, giving the percent increase in load and the associated value of  $e_0$ , for  $q = 1, 2$ , and 3 are presented in Table 8.1. The

corresponding  $e$ -curve is, however, shown for  $q = 1$  only in Figure 8.1.

A study for  $q = 3$  reveals that a better approximation is possible by setting  $x_0 \neq 0$ . It is found that  $x_0 = 0.005$  and  $e_0 = 0.40$ , produces an increase of 42.7 percent, in load. This result could also be interpreted as approximate solution to the constrained column with  $e_0 = 0.4$ .

Approximation to the constrained problem is studied in detail for  $q = 1$ , with  $e_0 = 0.50$ . For this value of  $e_0$ ,  $x_0$  is varied from 0 to 0.1 at suitable intervals. In each case,  $e(\eta)$  distributions (along with the associated eigen values) are determined. It is found that  $\lambda$  first increases with the increase in  $x_0$  and then starts decreasing, thereby yielding an optimum value of  $x_0$  for the given  $e_0$ . One, thus, gets an approximate solution for the constrained column with  $e_0 = 1$ . The results, giving the percent increase in load for different values of  $x_0$ , are presented in Table 8.2. Distribution of  $e$  is, however, shown only for  $x_0 = 0.05$ , for which the maximum value of the percent increase in load is obtained. For comparison, solution obtained in Chapter 5 for  $p = 1$  and  $q = 1$ , is also reproduced in Figure 8.1.

### 8.3 Comments and Discussion

A similar study can be extended to all the problems studied in this thesis. On the basis of the particular cases studied in this chapter, with a fair degree of confidence, it seems possible to approximate the numerically obtained curves for the design variables. Besides, the eigen value does not seem to be sensitive to small variations in these curves.

The simple study, conducted in this chapter, indicates the possibility of predicting approximate solutions of the constrained problems through the solutions of the unconstrained problems. This can be done, at least in the present case, by determining solutions for different values of  $e_0$  and  $x_0$ . Optimum values of  $e_0$  and the corresponding  $x_0$  can, then, be easily picked by inspection. After some experience, one can easily reduce the effort involved in determining these values.

The approximating polynomials, here, have been obtained by matching the value of  $e$  at only one point ( $x = 1/2$ ) with the value for the unconstrained column. This particular point is selected because the difference in the values of  $e_{\max}$  in the two cases, especially, for small values of  $e_0$ , is expected to be marginal. One may consider the matching at some other point and investigate the possibility of obtaining better results.

Table 8.1: Percent increase in  $\lambda$  and the associated  $e_0$  for  $x_0 = 0$ , for hinged-hinged columns with  $p = 1$

q	percent increase		$e_0$
	approximate	strongest*	
1	32.54	33.37	0.1
2	39.16	40.81	0.3
3	41.98	45.97	0.5

\* Results computed in Chapter 5.

Table 8.2: Variation of percent increase in  $\lambda$  with  $x_0$  for  $e_0 = 0.5$ , for hinged-hinged columns with  $q = 1$

$x_0$	0	0.015	0.025	0.050	0.075	0.100
percent increase	27.51	28.20	28.61	29.23	28.69	26.25

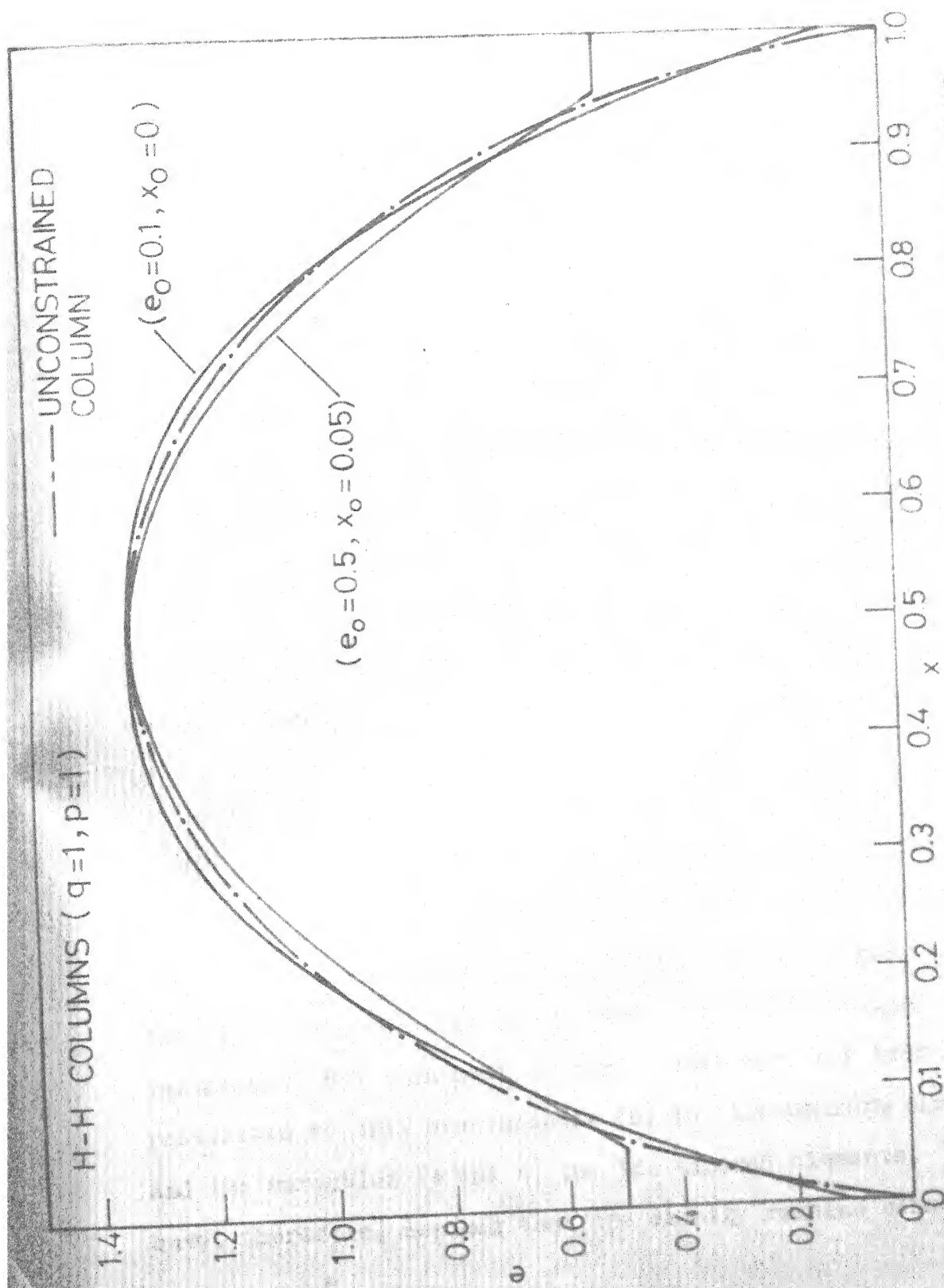


FIG. 8.1. APPROXIMATE CURVES FOR THE VARIATION OF  $e$  ALONG THE AXIS

## CHAPTER - 9

### CONCLUSIONS AND RECOMMENDATIONS

#### 9.1 Conclusions

Studies in this thesis, have established that considerable improvements in eigen values of the simple elements, such as columns and beams, is possible through suitable longitudinal variation of the modulus. Theoretically, modulus variation can result in unlimited increases in the eigen values, whereas the improvements for the corresponding homogeneous elements with optimal tapering, are limited. However, very high increases are not practically feasible because of the limitations on the specific moduli of the available materials.

Both the uniform as well as the tapered-nonhomogeneous elements have been investigated, to determine the effect of the optimum modulus distribution on the eigen values. In a general problem, though, modulus, area, and density, simultaneously can be the independent design variables, the treatment in the present work has been restricted to only one variable ( $e$ ) for the uniform elements, and two variables ( $e$  and  $\eta$ ) for the tapered elements. We have, therefore, assumed that the density remains constant

in the case of uniform elements. This assumption, seems to be realistic today because of the advancements in the composite material technology and the development of high specific modulus fibers.

A study of the strongest columns, for four classical-homogeneous boundary conditions (H-H, F-C, C-C and C-H), reveals that considerable improvements in the critical loads beyond those achieved by the optimal tapering<sup>6</sup>, are possible by suitable variations of the moduli along the axis of the columns. Furthermore, modulus variation seems to be, largely, responsible for producing higher increases in the load. Considering the fabrication aspects, use of uniform columns is to be recommended for increases beyond 65 percent. However, tapered columns may be used when only the percentage increase in load is of utmost importance.

Investigations for the uniform (H-H, F-C, C-C and C-H) and tapered (H-H and F-C) beams, reveal the existence of large increases in the fundamental frequency of transverse vibrations through optimal variation of the modulus along the axis. Though the percentage increase in the case of free-clamped tapered beams is not small, still it is marginal relative to the corresponding homogeneous-tapered beams<sup>14</sup>. Besides, it is further concluded that the tapered hinged-hinged beams ( $q = 1$ ) and the free-clamped-tapered beams are of academic interest only, because of the

numerically obtained infeasible distributions of the design variables. For  $q = 1$ , modulus variation, theoretically, offers the possibility of increasing the frequency beyond that for the corresponding Euler beam, which is the optimal<sup>13,15</sup> if only area variation is considered. For free-clamped beam with  $q = 1$ , optimal solution, as stated in references 13,14 for the homogeneous-tapered beam, does not exist.

Introduction of the parameter  $p$  in the optimization problems, investigated in the present work, offers the possibility of achieving a desired increase in the eigen value of the structural element under consideration. The corresponding desired optimum distributions of the design variables, can be predicted by determining the solution for a suitably chosen value of  $p$ .

Method of successive iterations has been employed, successfully, for determining the numerical solutions in all the cases, considered in this thesis. The method is powerful, and in most cases, convergence occurs in few iterations. However, it is also found in some cases, that the convergence is very slow. Generally, it is seen that the slow convergence is associated with extreme values of  $p$  for which the solution either asymptotically approaches to the corresponding solution for the uniform element ( $p \ll 1$ ), or to the solution for the corresponding homogeneous element ( $p \gg 1$ ).

Further, it is also seen that the convergence gets slow near the optimum. This is, normally, encountered in optimal control problems and in the solutions of the problems by using direct methods of optimization. Thus, slow convergence could be attributed to both these facts.

Governing equations, both for the columns and beams, are singular. Exact knowledge of the analytical behaviour of singularity, is very important in arriving at the correct solutions. It may be noted that the singularities in the column problems have been encountered, here, for the first time.

In all the derivations, the optimization problem, finally, reduces to the solution of a nonlinear equation in the eigen function, which has a unique solution. Eigen value and the distributions of the design variables are, then, easily obtained from the solution of this eigen function. The approach, thus, differs from that followed by Niordson<sup>12,14</sup>. He not only determines the eigen function but a **constant also**, out of the iterative process used by him. The additional relation, to determine the constant, is obtained by employing Rayleigh's quotient for the frequency. Since in an eigen value problem, displacement remains undetermined within a scalar multiplier, the determination of the constant by Niordson seems to be redundant. The problems<sup>12,14</sup>,

investigated by him, were reformulated by the method presented in this thesis, and the same results were obtained. Luckily, Niordson gets the right results for his problem, but if the similar approach is followed for the problems investigated in the present work, one gets erroneous results, e.g., for  $p = 1$  and  $q = 2$ , hinged-hinged beam solution yields an increase of 45 percent in frequency, whereas the correct result is 13.4 percent. This happens because of the fact that the scalar multiplier for the eigen function can have any value.

Since the physical reproduction of numerically obtained distributions for the design variables ( $e$  and  $\eta$ ) is difficult in practice, the effect of approximation of these curves by simple polynomials (on the eigen value) has been attempted. A study of the hinged-hinged columns ( $p = 1$ ) suggests that the eigen value is not significantly affected by small perturbations in the numerically obtained distributions of  $e$  and  $\eta$ . Besides, through the use of the solutions obtained in this thesis, it seems feasible to predict a good approximation to the solution for an element with constraints on the minimum value of the area and modulus.

## 9.2 Recommendations for Further Study

The following are some of the problems, that can be recommended for further study.

- i) Detailed study of the approximations to the numerically-obtained  $\epsilon$  and  $\eta$  distributions in all the cases, investigated in this thesis.
- ii) Optimal design of nonhomogeneous columns and beams with constraints on minimum modulus and area, and verification of the possibility of approximating these curves by employing the results for the corresponding strongest columns and the stiffest beams.
- iii) Determination of the solution in the case of tapered-nonhomogeneous beams, for clamped-clamped and clamped-hinged boundary conditions.
- iv) Proof of the stationary solutions being the optimal solutions, in the case of optimum beams.
- v) Proof of the convergence of the method of successive iterations.
- vi) Feasibility of improving the convergence in the cases, where it is very slow.

# REFERENCES

1. Edward J. Hang, Jr., Optimal Design of Structural Systems (Lecture Notes), Chapter 6.
2. Liusternik, L.A. and Sobolev, V.J., Elements of Functional Analysis, Ungar, New York, 1961.
3. Pontryagin, L.A., Boltyanskii, V.G., Gamkrelidze, R.V., and Mishchenko, E.F., The Mathematical Theory of Optimal Processes, Wiley, New York, 1962.
4. Berkovitz, L.D., "Variational Methods in Problems of Control and Programming," J. Math. Anal. Appl. Vol. 3, 145-169, 1961.
5. Keller, J.B., "The Shape of the Strongest Column," Arch. Rational Mech. Anal. 5, 275-285, 1960.
6. Keller, J.B. and Tadjbakhsh, I., "Strongest Columns and Isoperimetric Inequalities for Eigen Values," J. Appl. Mech. 29(1), 159-164, 1962.
7. Taylor, J.E., "The Strongest Column: An Energy Approach," J. Appl. Mech. 34(2), 486, 1967.
8. Taylor, J.E. and Liu, C.Y., "Optimal Design of Columns," J. Amer. Inst. Aeronaut. Astronaut. 6(8), 1497-1502, 1968.
9. Prager, W. and Taylor, J.E., "Problems of Optimal Structural Design," J. Appl. Mech. 35(1), 102-106, 1968.
10. Frauenthal, J.C., "Constrained Optimal Design of Columns Against Buckling," J. Struct. Mech. 1(1), 79-89, 1972.
11. Budiansky, B., Frauenthal, J.C., and Hutchinson, J.W., "On Optimal Arches," J. Appl. Mech. 36(4), 880-882, 1969.
12. Niordson, F.I., "On the Optimal Design of a Vibrating Beam," Q. Appl. Math. 23, 1965.

13. Brach, R.M., "On the Extremal Fundamental Frequencies of Vibrating Beams," Int. J. Solids Structures 4, 667-674, 1968.
14. Karihaloo, B.L. and Niordson, F.I., "Optimum Design of Vibrating Cantilevers," DCAMM Report No. 15, May 1971.
15. Karihaloo, B.L. and Niordson, F.I., "Optimum Design of Vibrating Beams under Axial Compression," Arch. Mech. 24(5-6), 1029-1037, 1972.
16. Timoshenko, S.P. and Gere, J.M., Theory of Elastic Stability, McGraw-Hill, 1961.